Essays on the Economics of Renewable Energy and Cross-Sectoral Decarbonization

Inauguraldissertation

zur

Erlangung des Doktorgrades

der

Wirtschafts- und Sozialwissenschaftlichen Fakultät

der

Universität zu Köln

2019

vorgelegt

von

MSc ETH Masch.-Ing. Jakob Peter

aus

Basel

Betreuer:	Prof. Dr. Felix Höffler
Referent:	Prof. Dr. Marc Oliver Bettzüge
Korreferent:	PD Dr. Dietmar Lindenberger
Tag der Promotion:	29. Mai 2019

Preface

I would like to express profound gratitude to my academic advisor, Prof. Dr. Felix Höffler, for his precise and constructive feedback, which inspired me and considerably improved my research. Also, I want to thank him for giving me the opportunity to collaborate with him on two research projects at his chair. Furthermore, I am very grateful to Prof. Dr. Marc Oliver Bettzüge for his availability to be the referee of my thesis. During my years as a doctoral student at the Institute of Energy Economics (EWI) at the University of Cologne, we had various very inspiring discussions and collaborations. Also, I want to thank PD Dr. Dietmar Lindenberger for co-refereeing my thesis and for our very professional collaboration in various projects.

I am grateful to Johannes Wagner for the outstanding collaboration in our joint research project, which I deeply enjoyed. Furthermore, I am very thankful to Simeon Hagspiel and Andreas Knaut for inspiring discussions in our joint research project. Also, I want to express my gratitude to Simeon Hagspiel for giving me the opportunity to collaborate with him on the research project he was working on as post-doctoral fellow. Furthermore, I want to thank Broghan Helgeson for all the intense and inspiring common working hours in our joint research paper. My thanks also go to Philipp Henckes, Christopher Frank and Nils Küchler, for the inspiring collaboration within our joint multi-disciplinary research project in the fields of Energy Economics, Meteorology and Geophysics.

Special thanks go to my fellow research associates at the Institute of Energy Economics for the great times we had together. I am very grateful for the good research and work environment at the institute, which was made possible by Monika Deckers, as well as the whole administration, communication and IT team. I would also like to extend my gratitude to Henrike Sommer, Andreas Fischer, Marcel Dahl and Marius Overath, who provided excellent research assistance.

An institutionally and financially stable framework has been provided by the Institute of Energy Economics and the University of Cologne, as well as by the German Research Foundation (DFG) and the Ministry of Economic Affairs, Innovation, Digitalization and Energy of the State of North Rhine-Westphalia. The work was carried out within UoC Emerging Group on 'Energy Transition and Climate Change

(ET-CC)', UoC Forum 'Market design and regulation for stochastic electricity supply chains', 'Virtual Institute - Power to Gas and Heat' (W041A), as well as 'Virtual Institute - Power to Gas and Heat' (EFRE-0400155). Funding by the DFG Zukunftskonzept (ZUK 81/1) and by the 'Operational Program for the promotion of investments in growth and employment for North Rhine-Westphalia from the European fund for regional development' (OP EFRE NRW) through the Ministry of Economic Affairs, Innovation, Digitalization and Energy of the State of North Rhine-Westphalia is gratefully acknowledged.

Finally, I am deeply thankful to Lena Ditte Nissen, Benedict Vischer, Johannes Weickenmeier, Johanna Wehkamp, Sebastian Kraus, Christina Elberg, Jacob Rohm, Enrico Orselli, Tobias Flemming as well as other friends for providing indispensable motivation throughout my time as a doctoral fellow. Also, I am very grateful to my family for supporting me. I wish to dedicate this thesis to Philippa Leonie Carlotta.

Jakob Peter Cologne, February 2019

Contents

1 Introduction

There's one issue that will define the contours of this century more dramatically than any other, and that is the urgent and growing threat of a changing climate.

Barack Obama (2014)

Climate change, resulting from rising greenhouse gas concentrations in the atmosphere, is a problem of the commons. Global commons are resources and areas, which do not fall under the sovereignty of any state. Examples include the water column beyond territorial seas, the outer space, the Antarctic and – the atmosphere (Wijkman (1982)). If each country had its own atmosphere, then self-interested countries would fulfill their climate targets, similar to their provision of education, transportation infrastructure and other public goods. But with the atmosphere being a global common, a country reducing its carbon emissions receives only a fraction of the benefits, yet carries the costs for abatement. The self-interested response is to free-ride – particularly in a globalized economy, where economic competitiveness depends, amongst others, on costs of energy (Cramton et al. (2017)). This results in the famous tragedy of the commons (Hardin (1968)). The solution to this game theoretical problem – cooperation – was concisely described by Cramton et al. (2017): "To save the commons, the users of the commons must cooperate. That requires trust, and trust requires reciprocal agreement – we will if you will, and you will if we will." Such a reciprocal agreement could be based on common commitments, e.g., a common minimum price on carbon emissions. While recognizing the great diplomatic success of adopting the Paris Agreement (United Nations (2015)), one main criticism from an economic perspective has been its focus on collective goals rather than on common commitments and the resulting difficulties in verification. A prioritization of negotiations on a reciprocal common commitment like global carbon pricing is expected to ease the way to cooperation in future climate diplomacy.

From the perspective of welfare economics, climate change is a negative externalities problem. Taxing the negative externality with a Pigouvian tax, i.e. a tax on carbon emissions equal to the social cost of carbon, aims at correcting the undiserable and inefficient market outcome. Yet, real world progress on carbon pricing still

lacks ambition, with only 20 % of global carbon emissions being covered by carbon pricing initiatives. In 2018, carbon prices ranged from 0.8 - 112 EUR/tCO_2e, while 46 % of carbon emissions covered are priced below 8 EUR/tCO_2e – considerably below current estimates of social costs of carbon (World Bank (2018)).[1] Yet, carbon pricing continues to gain traction and an increasing number of organizations are using internal carbon pricing to mitigate climate-related financial risks and innovate for the transition to a low-carbon economy.

To counteract climate change, game theory and welfare economics thus both proclaim carbon pricing, i.e. a minimum price on carbon emissions serving as a natural comparison standard for abatement efforts. Its advantages can be summarized as follows (Cramton et al. (2017)): It simplifies negotiations by focusing on a single minimum price variable and facilitates reciprocity; it reduces countries' risks and makes it easier to account for "common but differentiated responsibilities"; and it is compatible with (supra-)national climate policies such as carbon taxes, emission trading systems or command and control policies, which are typically applied to regulate sectors.

Within the fields of energy and climate economics, this thesis focuses on the electricity and transport sectors. With 25 % and 14 % of global greenhouse gas emissions, respectively, both sectors are prominent targets for effective regulation to combat climate change (IPCC (2014b)). Moreover, despite the electricity sector still being the largest single contributor to greenhouse gas emissions, it has been identified as a key enabler for deep decarbonization scenarios limiting global warming to 1.5 °C above pre-industrial levels, as envisaged by the Paris Agreement. With technologies for decarbonization of the electricity sector being readily available, decarbonized electricity can be used for electrification of energy end use and decarbonization of other fuels via power-to-x processes. In enabling the decarbonization of other sectors, the electricity sector is projected to double its electricity supply by 2050, reaching a 3.5 to 6-fold increase by 2100 in 1.5 °C-consistent pathways (IPCC (2018a)). The transition towards decarbonized electricity systems is expected to be largely based on variable renewable energies in light of recent cost reductions, particularly for wind and solar PV, in combination with increasing awareness and regulation of environmental externalities (e.g., Ueckerdt et al. (2017), IPCC (2018c), IEA (2017)). However, electricity systems based on variable renewable energy generators need to be designed for the specific characteristics of these generators, such

[1] Multilateral Development Banks, such as the World Bank, Asian Development Bank or European Investment Bank, use social cost of carbon estimates for project evaluation ranging from 29 - 65 EUR/tCO_2e for 2020 and 40 - 81 EUR/tCO_2e for 2030 (World Bank (2018)).

as low short-run cost, variability, uncertainty and location constraints, to name a few (IEA (2014)). Therefore, designing a regulatory framework guiding this transition in an economic efficient way while keeping the pace required for climate change mitigation is of utmost importance.

In light of this apparent need for a regulatory framework, this thesis investigates the transformation towards deep decarbonization of the electricity and road transport sectors. The integration of variable renewable energies into electricity systems requires an understanding of their contribution to security of supply. Moreover, flexibility needs and decarbonization will lead to a significant coupling between sectors. Therefore, this thesis contributes to the academic debate on security of supply and cross-sectoral decarbonization based on four papers that are contained in Chapters 2 - 5. Three of the four chapters are joint work with co-authors, who contributed equally to all parts of the corresponding paper.

Chapter 2: Reliability in Multi-Regional Power Systems – Capacity Adequacy and the Role of Interconnectors (with Simeon Hagspiel and Andreas Knaut).
EWI Working Paper Series, No. 17/07 (Hagspiel et al. (2017)). Published in *The Energy Journal*, Vol. 39 (5), 2018 (Hagspiel et al. (2018)).

Chapter 3: Optimal Allocation of Variable Renewable Energy Considering Contributions to Security of Supply (with Johannes Wagner).
EWI Working Paper Series, No. 18/02 (Peter and Wagner (2018)). Revised and resubmitted to *The Energy Journal*.

Chapter 4: How Does Climate Change Affect Optimal Allocation of Variable Renewable Energy?
EWI Working Paper Series, No. 19/03 (Peter (2019)). Forthcoming in *Applied Energy*.

Chapter 5: The Role of Electricity in Decarbonizing European Road Transport – Development and Assessment of an Integrated Multi-Sectoral Model (with Broghan Helgeson).
EWI Working Paper Series, No. 19/01 (Helgeson and Peter (2018)). In revision at *Applied Energy*.

The remainder of the introduction is structured as follows: Section 1.1 gives an outline of the four chapters. Building on that, Section 1.2 critically discusses the methodology and gives an outlook for further research. Section 1.3 concludes.

1.1 Outline of the thesis

In my thesis, I investigate several aspects of the economics and regulatory design of the electricity and transport sectors. All chapters focus on systems with high shares of variable renewable energies (VRE), characterized by time-varying and interdependent temporal and spatial distributions of electricity supply and electricity demand. While Chapters 2 and 3 analyze the implications on security of supply, Chapter 4 investigates the impact of climate change on electricity systems in general and VRE in particular. Chapter 5 assesses, how the electricity and road transport sector can optimally be decarbonized, accounting for synergies in supply and demand when coupling the two sectors via electrification and power-to-x processes. In the following, the chapters will be outlined in more detail.

Chapter 2 deals with the question, how reliability targets can efficiently be reached considering the firm capacity provision of VRE and interconnectors. While interconnections with neighboring regions have proven an effective means to foster reliability of supply in power systems, it is often considered an issue of national interest from a political perspective. For instance in capacity mechanisms, reliability contributions of interconnectors and VRE are often included in a very simplified manner, or even excluded explicitely. This inevitably results in market distortions and economic inefficiencies.

Against this background, this paper develops, based upon probabilistic reliability metrics, an optimization model to determine the efficient amount and location of firm generation capacity to achieve reliability targets in multi-regional electricity systems. A particular focus lies on the representation and contribution of interconnector capacities as well as VRE. The model is calibrated with a comprehensive dataset for Europe. Results show that there are substantial benefits from regional cooperation. The amount of firm generation capacity to meet a perfectly reliably system could be reduced by 36.2 GW (i.e., 6.4 %) compared to an isolated regional approach, which translates to savings of 14.5 bn Euro. Interconnectors contribute in both directions, with capacity values up to their technical maximum of close to 200 %, while wind power contributions are in the range of 3.8 - 29.5 %. Furthermore, the paper finds that specific reliability targets heavily impact the efficient amount and distribution of reliable capacity as well as the contribution of individual technologies.

These results provide empirical evidence that a consistent analysis of multi-regional systems with restricted interconnector capacities is crucial for reliability of supply analyses. In practice, the approach could thus be used for the improved design

of capacity mechanisms by providing an approach to consider interdependencies with physically connected neighbors. Moreover, the large differences between the first-best and isolated results provide strong arguments to achieve reliability targets efficiently in a cooperative manner, e.g., by means of joint capacity mechanisms.

Chapter 3 picks up the approach developed in Chapter 2 and develops a framework, which allows to apply it in combination with a large-scale investment and dispatch model for electricity markets. VRE are typically less correlated on a wider geographical scope, which enables balancing effects because of imperfectly correlated supply and demand patterns at different locations. Moreover, the capacity value of VRE, i.e. their contribution to security of supply, is characterized by decreasing returns to scale. Against this background, it is ex-ante unclear, how the optimal mix and allocation of VRE capacity should be organized in order to benefit from balancing effects both in generation and contribution to security of supply while reaching an envisaged reliability target.

This paper aims at closing this research gap by developing a new methodology to endogenously determine the capacity value of VRE in large-scale investment and dispatch models for electricity markets. The framework allows to account for balancing effects due to the spatial distribution of generation capacities and interconnectors. The practical applicability of the methodology is shown with an application for wind power in Europe. The paper finds that wind power can substantially contribute to security of supply in a decarbonized European electricity system in 2050, with regional capacity values ranging from 1 - 40 %. Analyses, which do not account for the temporal and spatial heterogeneity of the contribution of wind power to security of supply therefore lead to inefficient levels of dispatchable back-up capacity. Applying a fixed wind power capacity value of 5 % results in an overestimation of firm capacity requirements in Europe by 66 GW in 2050. This translates to additional firm capacity provision costs of 3.8 bn EUR per year in 2050, which represents an increase of 7 %.

The results suggest that capacity mechanisms should allow for participation of generation capacities based on VRE resources as well as cross-border contributions. However, the assigned capacity values should be determined based on careful assessments of the statistical properties of the VRE generators and need to be regularly updated in order to account for changes in the system configuration. Finally, the results show that market integration by increasing interconnections between different countries increases the potential of variable renewable energy sources to contribute to security of supply.

Chapter 4 investigates impacts of strong climate change on electricity systems. The analysis focuses on climate change scenario RCP8.5, the most extreme scenario used in the latest IPCC reports, which is associated with a likely range of global average temperature increase by the end of century of 3.2 - 5.4 °C compared to pre-industrial levels. For Europe, most important are effects on variable renewable energy resources (both availability and gradients), hydro power availability, cooling water availability for thermal power plants and electricity consumption. Each of these effects may work differently in size, direction and transmission mechanism. Hence, it is not only important to understand the total effects, i.e., how much welfare may be gained when accounting for climate change impacts in all dimensions, but also to disentangle various effects in terms of their marginal contribution to the potential welfare loss. This may be particularly relevant when accounting for uncertainties in climate change scenarios and discussing policy reactions and priorities.

In this paper, a two-stage modeling framework is applied to assess RCP8.5 climate change impacts on the European electricity system. Thereby, the performance of two electricity system design strategies – one based on no anticipation of climate change and one anticipating impacts of climate change – is studied under a variety of climate change impacts. Impacts on wind and solar resources are found to cause the largest system effects in 2100. Combined climate change impacts increase system costs of a system designed without climate change anticipation due to increased fuel and carbon permit costs. Applying a system design strategy with climate change anticipation increases the cost-optimal share of VRE based on additional wind offshore capacity in 2100, at a reduction in nuclear, wind onshore and solar PV capacity. Compared to a no anticipation strategy, total system costs are reduced.

Our results imply that impacts of climate change show non-negligible effects on electricity systems with system cost increases up to 12 % when climate change impacts are not anticipated. Ramping up climate ambition to comply with the Paris Agreement and designing mitigation measures to avoid drastic climate change impacts should therefore be treated with highest priority in order to limit economic damage in a world beyond 1.5 °C global warming, compared to a world with 1.5 °C. However, in order to be prepared for futures beyond 2 °C – which are likely given today's climate ambition level – and considering the long technical lifetime of certain assets like hydro and nuclear power plants, as well as grid infrastructure, long-term electricity system planning should consider impacts of climate change. Thereby, in particular allocation effects in optimal wind onshore and wind offshore capacity should be accounted for. Next to impacts on VRE, the regulator is advised to take

into consideration constraints in cooling water availability when setting the regulatory framework for cost-optimal power plant investments, including the choice of cooling technology.

Chapter 5 takes a closer look at the European road transport sector, where progress on decarbonization is challenging in view of a 22 % increase in emissions since 1990. Decarbonization via electrification is expected to play an important role, as electricity as an energy carrier can be used for fueling both electric vehicles and power-to-x systems to produce synthetic power-to-x fuels. Yet, decarbonizing the road transport sector via electricity results in the road transport and electricity sectors being coupled, i.e. supply and demand become linked across sectors. This has a range of implications. On the one hand, increased electricity consumption from road transport and power-to-x systems requires additional electricity generation, which must obey to its own emission reduction regulations. On the other hand, linking the road transport and electricity sectors provides system flexibility since, e.g., electric vehicles or power-to-x systems may serve as energy storage capacities for the electricity sector.

To understand the economic implications of increased coupling of the road transport and electricity sectors, this paper develops an integrated multi-sectoral partial-equilibrium investment and dispatch model for the European electricity and road transport sectors, linked by an energy transformation module to endogenously account for, e.g., increasing electricity consumption and flexibility provision from electric vehicles and power-to-x systems. The model is applied to analyze the effects of sector-specific CO_2 reduction targets on the vehicle, electricity and power-to-x technology mix as well as trade flows of power-to-x fuels in European countries from 2020 to 2050. The results show that, by 2050, the fuel shares of electricity and power-to-x fuels in the European road transport sector reach 37 % and 27 %, respectively, creating an additional electricity demand of 1200 TWh in Europe. To assess the added value of the integrated modeling approach, an additional analysis is performed in which all endogenous ties between sectors are removed. The results show that by decoupling the two sectors, the total system costs are significantly overestimated and the production costs of power-to-x fuels are inaccurately approximated, which affects the merit order of decarbonization options.

Regulatory practice often does not yet account for the implications of decarbonization via coupled sectors. In order to reach cost-optimal allocation of power-to-x systems, the regulator may design a market environment focusing on transparent price signals, e.g., via nodal pricing. Also, the current regulatory design of levies

and taxes is creating inefficiencies and market distortions. It should be adjusted in anticipation of an energy system characterized by a considerable increase in electricity consumption and flexibility needs due to coupled sectors and cross-sectoral decarbonization.

1.2 Discussion of methodological approaches

The four essays of this dissertation focus on different aspects of electricity and transport systems. Depending on the specific research questions of each chapter, suitable methodological approaches are chosen and developed. Thereby, economic models are solved by means of numerical methods. Assumptions are made in view of keeping the analysis tractable without loosing relevant aspects for the respective research question. Nevertheless, as each choice of methodology or assumptions implicates a loss in generality, such issues will be critically discussed in the following, complemented with hints for promising fields of future research.

As discussed in Section 1.1, the aspects of security of supply investigated in Chapters 2 and 3 stem from the interdependent temporal and spatial distribution of supply, in particular from VRE, and demand. The developed probabilistic optimization problem, which enables us to endogenously derive the efficient amount of required equivalent firm capacity to reach a certain reliability target, is analytically hardly solvable. Thus we formulate the deterministic equivalent of the probabilistic problem, resulting in a linear program. The idea is to replace probabilities and random variables by their deterministic counterpart, which may then be calibrated based on data covering a large range of possible outcome. We apply the so-called hindcast approach, i.e. we calibrate the model using a large number of historical joint observations. In order to better represent the joint probability space, we combine historical observations from load and wind. Thereby, we assume stochastic independence between wind and load distributions. With a mean correlation between wind and load over all European countries of 0.08 (median 0.06), this assumption can be justified. In further research, the developed methodology could be applied to solar power. In doing so, the stochastic independence between solar and load distributions should, however, be further investigated.

While Chapter 2 introduces the probabilistic optimization program, Chapter 3 develops a novel iteration framework, where the probabilistic optimization program is combined with a partial-equilibrium investment planning model for electricity markets. The iterative solution approach is chosen to integrate the non-linear contribu-

tion of wind power to security of supply in a linear model framework for investment planning. Thereby, the non-linear properties of the capacity value of wind is successively linearized by iteratively solving two corresponding linear problems. However, as the non-linearity of the underlying problem remains, we can only numerically check for the existence and uniqueness of a global optimum without formal proof. Further research could focus on this aspect of the problem. To keep long-term investment planning models computationally tractable, they commonly apply a reduced temporal resolution (time slices). Thereby, relevant properties of wind and solar generation as well as load have to be captured, despite the reduced resolution. In order to do so, Chapter 3 implements a two-stage spatial and temporal clustering algorithm to derive time slices, which represent the characteristics of the original dataset. Future research could further investigate, how the number of spatial and temporal clusters affects the results.

Chapter 4 is based on a two-stage modeling framework building on a partial equilibrium investment planning model for electricity markets. In the first stage, the model is run in a long-term investment planning mode. Hereby, analogous to Chapter 3, a reduced temporal resolution based on time slices derived via clustering is applied. In the second stage, the model is run in a high-resolution dispatch mode with fixed power plant capacities from the first stage, representing a full year in hourly resolution, which is also derived via clustering. While the historical load data is available on a hourly basis, the data for wind speeds and solar irradiation, taken from climate projections within the EURO-CORDEX project, is only available in three-hourly resolution. Further research could therefore – as soon as data with higher temporal resolution is available – apply hourly data also for wind and solar. It is important to keep in mind that the data for wind and solar, which is used throughout this dissertation, is based on meteorological models. Obviously, model data is not equivalent to measured wind speed and solar irradiation data. However, measurements with the required spatial resolution (Europe, on a 6 - 12 km grid) for historical time periods of 20 years are not available. Therefore, either so-called gridded data, based on interpolation between measurement points, or model-based data are typically applied. Model-based data may particularly in regions with sparse measurement data have advantages and are, e.g., in the case of reanalysis models, calibrated with measurements. It is therefore certainly a promising research direction to further validate and calibrate the data used in the context of electricity market models.

Chapter 5 develops a model framework, in which a partial equilibrium invest-

ment planning model for the electricity sector is coupled to a partial equilibrium investment planning model for the road transport sector. The latter is a novel model framework developed in this paper. Furthermore, as a link between the two sectors, an energy transformation module is developed, representing fuel conversion technologies such as power-to-x processes. The resulting multi-sectoral model framework allows to endogenously account for supply and demand effects when coupling different sectors. Thereby, interaction effects between the sectors due to, e.g., decarbonization or technology adoption constraints, can be endogenously analyzed, resulting in endogenous price reactions. Promising research extensions hereby include endogenous charging of electric vehicles, which in this analysis are represented by exogenous average charging profiles.

Complex model frameworks dealing with increasingly large datasets have to be kept computationally tractable, e.g. by formulation as linear programs. Under certain assumptions, non-linear welfare maximization problems can be transformed to linear problems and solved via cost minimization: Electricity demand is assumed to be inelastic, except for the demand endogenously covered by the model, e.g., from storage or power-to-x processes. Market participants are assumed to behave fully rational and have perfect foresight. Furthermore, the assumption of perfect competition implies that conditions such as perfect information, no transaction costs, no externalities and no market entry or exit barriers are met. While these assumptions are common in literature, they have to be kept in mind when interpreting the results. Electricity demand is, especially in the short-term, still rather inelastic, mainly due to large shares of consumers not being exposed to short-term price variations in the wholesale market. This is, however, expected to change in light of the expected large-scale deployment of smart devices linked to, e.g., industry appliances, homes or electric vehicles. While partly accounted for in this thesis by endogenous electricity demand from storage or power-to-x processes, this aspect could certainly be further investigated in future work. The issue of perfect foresight is often addressed by using stochastic modeling. Keeping large-scale stochastic models computationally tractable, however, often represents a challenge, leading to trade-offs between complexity vs. accounting for stochasticity. While the assumption of perfect competition in liberalized electricity markets is not uncommon in light of the large amount of market participants with to their best knowledge rational behaviour, it can certainly be questioned for the road transport sector, in particular when it comes to private vehicles. The results of Chapter 5 should therefore be interpreted from a social planner perspective who strives for an optimal joint decarbonization of the electricity and road transport sectors.

1.3 Concluding remarks

The necessity of decarbonized electricity and transport will shape future energy systems. Thereby, the topics analyzed in this thesis will gain importance. Both the contribution of VRE to security of supply and interdependencies between sectors in coupled energy systems will be highly relevant for the efficient operation of decarbonized energy systems. Also, the chance that future systems will have to deal with impacts of drastic climate change like the RCP8.5 scenario analyzed in this thesis is not unrealistic, given today's climate ambition level.

Most studies on energy markets – including this thesis – take climate targets as politically defined external boundary conditions. Moreover, the focus mostly lies on estimating and comparing the costs of different climate change mitigation instruments. Recognizing this, concerns with this practice need to be mentioned: With political decisions being, amongst others, based on such economic studies, we as scientists informing politics should never get tired of constrasting the costs with the benefits from climate change mitigation, in order for the politicians to have a balanced decision basis. Global warming, currently at about 1 °C above pre-industrial levels, will have and already has severe impacts on various aspects of life all over the world. Extreme events, such as cold temperature extremes, heat waves, droughts, heavy precipitation events and storm surges are more likely with climate change (Mann et al. (2017), Kharin et al. (2018), IPCC (2014a)). Armed-conflict risks are enhanced by climate-related disasters (Schleussner et al. (2016), Burke et al. (2015), IPCC (2014a)). Global sea level rises with climate change, affecting inhabitated coastal areas (Schuerch et al. (2018), Hauer et al. (2016)). Migration increases due to armed-conflicts, sea level rise and changes in crop yield (Abel et al. (2019), Feng et al. (2010)). Ocean acidification increases with strong impacts on marine ecosystems (IPCC (2014a)). Naturally, translating such consequences into measurable economic figures, which can be compared to abatement costs, is inherently difficult. Yet, scientific evidence increases that a world beyond 1.5 °C global warming implies larger economic damage, compared to a world with 1.5 °C (Burke et al. (2018), IPCC (2018b)). The imagination of a higher frequency in events like the 2018 drought in Europe, with low Rhine river flows resulting in logistics and production shortfalls and losses for large corporations such as BASF and COVESTRO adds anecdotal evidence to such projections (FAZ (2018), SPIEGEL (2018)).

The long lifetime of greenhouse gases in the atmosphere make climate change a cumulative problem, where delayed action requires stronger action to reach the

same outcome. However, as societal transformation processes take time, there is a limit to the pace of delayed strong action. Therefore, decisions to ramp up climate ambition in line with the Paris Agreement and to design robust mitigation measures are crucial for stabilizing the climate and need to be taken within the next two decades in order to have a chance of limiting global warming to 1.5 °C (IPCC (2018b)).

Most importantly, as a society, we should keep in mind that such economic considerations often fall short of accounting for ethical aspects of global inequality and justice, which are at the very core of the climate change crisis. I am thinking of aspects like the distribution and correlation of historical emissions and wealth, the disproportionately higher risk of adverse climate change consequences for disadvantaged populations, and the prolongation of existing and creation of new poverty traps. The Philosopher Hans Jonas observed that technology has introduced human actions of such novel scale that a whole new dimension of ethical relevance has opened up. He thus suggested, in dependence on Kant's categorical imperative, a new imperative accounting for the novel scale and time horizon of human action: 'Act so that the effects of your action are compatible with the permanence of genuine human life' (Jonas (1973)).

Profound comprehension of the implications of a RCP8.5 climate change outlook should make us run to ring the alarm bells in all our communities and demand bold climate ambition from our political leaders. Ultimately, I believe that successful climate change mitigation will depend on economic and political commitment. The main obstacles will in large parts not be technical issues, but a lack in political ambition to guide the necessary transformation. As the global political community tries to define and enforce measures to reach commonly shared goals, we face a race against time, as climate change is a process following its own physical laws. Designing economic frameworks that account for these political constraints, both on a supranational and national level, will therefore be key. While pursuing efforts to reach economic first-best solutions, it seems reasonable to consider economic second- or third-best solutions that reconcile economic efficiency and political feasibility. This is what makes our task as economists particularly interesting. And, combined with the impressive dynamics of recent technological innovations and resulting economic opportunities, this is what helps me remain optimistic and makes me looking forward to contributing to climate change mitigation in my future career.

2 Reliability in Multi-Regional Power Systems – Capacity Adequacy and the Role of Interconnectors

Based upon probabilistic reliability metrics, we develop an optimization model to determine the efficient amount and location of firm generation capacity to achieve reliability targets in multi-regional electricity systems. A particular focus lies on the representation and contribution of transmission capacities as well as variable renewable resources. Calibrating our model with a comprehensive dataset for Europe, we find that there are substantial benefits from regional cooperation. The amount of firm generation capacity to meet a perfectly reliably system could be reduced by 36.2 GW (i.e., 6.4 %) compared to an isolated regional approach, which translates to savings of 14.5 bn Euro. Interconnectors contribute in both directions, with capacity values up to their technical maximum of close to 200 %, while wind power contributions are in the range of 3.8 - 29.5 %. Furthermore, we find that specific reliability targets heavily impact the efficient amount and distribution of reliable capacity as well as the contribution of individual technologies.

2.1 Introduction

Due to its high economic value, reliability of supply has always been a major concern in electricity systems. The topic has been subject to extensive scientific research effort, both from a technical as well as an economic perspective (see, e.g., Billinton (1970) or Telson (1975) for early contributions in the two fields). However, new challenges are currently arising due to the large-scale deployment of renewable energies to avoid greenhouse gas emissions and combat climate change. The reason lies in the variable nature of many renewable energy resources, such as wind and solar, and the possible risk of recurring unavailability during times of stress (e.g., Cramton et al. (2013)).

In order to foster reliability of supply in power systems, interconnections with neighboring regions have proven an effective means. As such, balancing effects in

supply and demand may be lifted, and better overall reliability levels be reached (e.g., Cepeda et al. (2009) or Hagspiel (2017)). In fact, enhanced reliability of supply was the main reason to create large interconnected electricity systems, such as the European or the North-American one. In the context of renewable energy integration, large-scale systems gain further importance due to the fact that renewable energy resources are typically more diverse on a wide geographical scope. Hence, cooperative actions with respect to reliability gain further importance to account for balancing effects (both in load and generation) and to reach envisaged reliability levels at lower costs compared to an isolated approach.

From a political perspective, however, reliability of supply is often considered an issue of national interest. As a consequence, assessments and measures to ensure reliability often have a narrow spatial scope, e.g., bounded by national borders.[1] For instance, capacity mechanisms have been put into place in many power systems worldwide, with the aim to reach a certain level of reliability within national borders (e.g., Joskow (2008)). In this context, interconnectors with neighboring countries are often included in a very simplified manner, or even excluded explicitly. This inevitably results in market distortions and economic inefficiencies (e.g. Newbery (2015)). As a countermeasure, the European Union has recently required member states to account for cross-border trade within capacity mechanisms (European Commission (2016c)). Benefits shall thus be lifted by means of cooperative considerations and actions. However, it so far lacks stringent approaches to investigate reliability in multi-regional power systems with capacity-constrained interconnectors to ensure security of supply in highly meshed and interdependent electricity systems (Newbery (2015)). At the same time – as we will show in this paper – cross-regional effects and interconnectors have a major impact on reliability assessments. Especially, they largely drive the overall amount and distribution of generation capacity needed to ensure reliability. Therefore, misspecifications may entail substantial economic inefficiencies and distributive effects.

As a simple intuitive example, consider two systems A and B: In an isolated system-state, A and B both require 5 units of reliable capacity to achieve a certain reliability target. It is clear that the overall amount of reliable capacity might be decreased to less than 10 units when these systems interconnect, for instance due to statistical balancing in load. However, determining the optimal overall amount of reliable

[1] This is particularly relevant for the European context where energy policy is largely driven by idiosyncratic yet interconnected and interdependent nation states. Note that this is in contrast to other more integrated systems, such as – for instance – the multi-state approach of the PJM independent system operator in the Eastern interconnection (U.Ss) controlled by the Federal Energy Regulatory Commission (a single policy maker).

capacity Z and its best locational shares Z_A, Z_B for reliable capacities requires a consistent analysis of the entire system, including the joint probability distribution of load and generation as well as limited interconnection capacities. Naturally, the extension to $N > 2$ interconnected systems further complicates the problem and constitutes a complex multivariate probabilistic optimization problem.

Against this background, this paper provides a comprehensive framework to investigate reliability in power systems consisting of multiple technologies and multiple interconnected regions. We first review well-known probabilistic metrics to determine the level of reliability in isolated one-regional power systems as well as the contribution of individual generators (known as capacity value[2]). Subsequently, we extend this literature which typically neglects capacity-constrained transmission infrastructure. In contrast to (stochastic) simulation techniques, we propose a novel approach based on a comprehensive optimization model that flexibly accounts for multi-regional settings and multiple generation technologies, including dispatchable power plants and variable renewable energies, as well as capacity-constrained transmission lines. The main innovative strength of this model lies in its ability to quantify the economically efficient amount and distribution of reliable capacity in each region within a consistent optimization framework. Furthermore, it may also be used to determine the capacity value of individual technologies in a system context. Our paper therefore incurs some noticeable difference compared to papers or reports that assess adequacy for a given or assumed system state, such as the report of the PLEF on system adequacy (Pentalateral Energy Forum (2018)) or ENTSO-E's Seasonal Outlook (ENTSO-E (2017)). While these latter assessments take generation capacities as exogenous input to derive reliability metrics, our approach tackles the issue from the opposite side: we take reliability metrics as given and endogenously optimize the firm capacity levels across interconnected regions to achieve these targets.

After a general description of our methodology, we introduce the comprehensive numerical dataset used to calibrate our model for different European case studies. The focus of the data lies on system properties incorporating large-scale variations – such as infeed from wind and solar power – to replicate the (joint) probability of various possible system outcomes. As direct observations are missing (due to a rapid system development with respect to the deployment of variable renewable energies), we build our optimization on a synthetic dataset created from 20 years of hourly reanalysis data with a high level of spatial resolution. In contrast, we abstract from a full representation of other existing generators in the system to be

[2] Capacity value is also often referred to as capacity credit. Throughout this paper we will, however, stick to the term capacity value.

in line with our objective to endogenously determine the amount of equivalent firm capacity needed to serve load at some level of reliability.

In a first step, we illustrate our approach based on two two-regional systems (namely France - Germany and France - Great Britain). Specifically, we depict how an interconnector can contribute to reliability, dependent on its size as well as the joint probability of load levels and capacity availability. Second, we apply the model to the entire European electricity system in order to quantify the efficient amount and location of firm generation capacity to achieve reliability targets as well as the contribution of wind power and interconnectors in a realistic case study. Compared to an isolated region-by-region approach, cooperation by means of an efficient usage of interconnectors would allow to reduce the overall necessary amount of reliable generation capacity by 32.4 GW (i.e., 6.1 %) on a European level to ensure perfect reliability, also impacting the distribution of capacities. In this cooperative solution, several interconnectors contribute in both directions, with up to their technical maximum of close to 200 % of their nominal capacity.[3] In contrast, due to its variability, the contribution of wind power is only in the range of 3.8 - 29.5 %. These results provide empirical evidence that a consistent analysis of multi-regional systems with restricted interconnector capacities is crucial for reliability of supply analyses. In practice, our approach could thus be used for the improved design of capacity mechanisms by providing an approach to consider interdependencies with physically connected neighbors. Moreover, the large differences between the first-best and isolated results provide strong arguments to achieve reliability targets efficiently in a cooperative manner, e.g., by means of joint capacity mechanisms.

As an additional insight, we find that specific reliability targets heavily impact the efficient amount and distribution of reliable capacity as well as the contribution of individual technologies. In practice, policymakers and system engineers should therefore choose reliability targets for power systems with care to avoid inefficiencies from excessively high (or low) capacity levels.

The rest of this paper is structured as follows: In Section 2.2, we introduce our methodology. The data are discussed in Section 2.3, while our results are comprised in Section 2.4. Section 2.5 concludes.

[3] In our calibration, we will assume a directional transmission efficiency $<100\,\%$, such that the capacity value is slightly reduced.

2.2 Methodology

Different methodologies have been proposed to determine generation adequacy and the capacity value of individual technologies in settings with one region only (i.e., without considering grid restrictions). The Loss-of-Load-Expectation ($LOLE$) and the Expected-Energy-Unserved (EEU) are two well established measures to depict the ability of a system to cover expected load levels (e.g., Allan and Billinton (1996)). After having determined the total system's adequacy, one may derive the contribution of individual technologies – typically referred to as capacity value or capacity credit (e.g., Keane et al. (2011), Madaeni et al. (2013)). Different approaches exist, but the equivalent firm capacity (EFC) is often recommended due to its ability to provide consistent results (Amelin (2009)).

In the following, we will first revise the well-known $LOLE$, EEU and EFC measures, valid for a one-region one-technology setting. We will then present an alternative formulation based on an optimization problem, before we extend our analysis to generation adequacy and the capacity value in a multi-region multi-technology context.

2.2.1 Notation

We will use the notation as listed in Table 2.1 in Appendix 2.6. Unless noted differently, we will use capital letters for random variables, bold capital letters for sets, and lower case letters for parameters, and bold lower case letters for nominal optimization variables.

2.2.2 Reliability metrics for one region only

In a self-contained system without transmission constraints, we follow Allan and Billinton (1996) and define the loss-of-load probability at a specific instant in time t as

$$LOLP_t = P(X_t^e < L_t), \tag{2.1}$$

i.e., as the probability that the available existing capacity X^e is smaller than load L_t. X_t^e will typically represent the availability of multiple power generators in the system, each characterized by its nominal capacity $\bar{x}_i^e$ and its capacity availability $X_{i,t}^e \in [0,1]$, such that $X_t^e = \sum_{i \in \mathbf{I}} \bar{x}_i^e X_{i,t}^e$. Note that in the above equation, we implicitly assume that load is inelastic with no adjustment when capacity is scarce, e.g.,

due to the lack of real time pricing. Consequently, in a market environment, there may be situations where all capacities are running at maximum availability without being able to serve the level of load, i.e., market clearing cannot be guaranteed even if there are high price levels.

Summing up probabilities over some time-period T yields the well-known reliability level measure Loss-of-Load-Expectation

$$LOLE = \sum_{t \in \mathbf{T}} LOLP_t. \tag{2.2}$$

A straightforward extension of the $LOLE$ is the reliability measure EEU, weighting the $LOLPs$ with the expected load level that cannot be served (therefore indicating the severity of these situations):

$$EEU = \sum_{t \in \mathbf{T}} E(L_t - X_t^e) * LOLP_t. \tag{2.3}$$

To determine the contribution of individual technologies, we determine their equivalent firm capacity. I.e., we derive the amount of equivalent firm capacity $\mathbf{z}^y$ by which X_t^e can be reduced when installing some new capacity $\bar{y}$ with availability $Y_t \in [0,1]$ whose capacity value shall be determined, such that the initial (target) reliability level EEU is achieved. To this end, the modified equation that needs to be solved for $\mathbf{z}^y$ writes as

$$EEU = \sum_{t \in \mathbf{T}} E(L_t - (X_t^e + \bar{y} Y_t - \mathbf{z}^y)) * P(X_t^e + \bar{y} Y_t - \mathbf{z}^y < L_t). \tag{2.4}$$

Due to the fact that $\bar{y} > 0$ and $0 \leq Y_t \leq 1$, it must hold that $\mathbf{z}^y \geq 0$. The capacity value of a technology with capacity $\bar{y}$ is then defined as

$$\nu = \frac{\mathbf{z}^y}{\bar{y}}, \tag{2.5}$$

with $0 \leq \nu \leq 1$.

Note that the above equations for the capacity value are typically solved by means of numerical iteration. Loosely speaking, after $\bar{y}$ has been added to the system, in each step $\mathbf{z}^y$ is increased by some small amount until the target EEU is reached. Due to the convexity of the problem, this approach is guaranteed to yield the desired result.

2.2.3 The effect of interconnections

In contrast to the self-contained system considered before (say, system m), let us now study the effect of system interconnections. For illustration, assume m is interconnected with system n by means of a line with maximum transfer capacity $\bar{k}$. In this case, the $LOLP$ of m needs to be extended by several terms:[4]

$$\begin{aligned} LOLP_{m\leftarrow n} = P(&X_m < L_m \text{ and} && \text{(2.6a)}\\ &[X_n < L_n \text{ or} && \text{(2.6b)}\\ &(X_n > L_n \text{ and } L_m - X_m > X_n - L_n) \text{ or} && \text{(2.6c)}\\ &(X_n > L_n \text{ and } L_m - X_m < X_n - L_n \text{ and } L_m - X_m > \bar{k})]). && \text{(2.6d)} \end{aligned}$$

The above equations state that a capacity shortage $X_m < L_m$ in system m may be relieved by means of an interconnection with system n. However, this does not hold if there is no spare capacity in n (Equation (2.6b)), if the spare capacity is not large enough to cover the shortage in m (Equation (2.6c)), or if the transfer capacity is not sufficient to cover the shortage in m (Equation (2.6d)). We will illustrate the meaning of these four terms for a numerical example in Section 2.4.

Note that comparing Equation (2.6) with Equation (2.1) reveals that it must hold that $LOLP_{m\leftarrow n} \leq LOLP_m$, i.e., that an interconnected system m is at least as reliable as if it was isolated. Consequently, interconnections will have a neutral or a lowering effect on the level of equivalent firm capacity needed to serve load at some predefined level of reliability in the respective systems.

This beneficial effect may also be seen in an alternative formulation for the $LOLP$ of m being interconnected with n, where capacity imports are contained in a lump-sum variable $K_{m\leftarrow n}$:

$$LOLP_{m\leftarrow n} = P(X_m + K_{m\leftarrow n} < L_m) \tag{2.7}$$

Due to the fact that only imports are considered, K is positive. From above, K is bounded by the import capacity $\bar{k}$, such that the support of $K_{m\leftarrow n}$ is $[0, \bar{k}]$. Of course – as stated above – if K is positive, it must be that $LOLP_{m\leftarrow n} \leq LOLP_m$. Or, conversely, that the amount of equivalent firm capacity needed may be smaller in an interconnected system to reach a fixed target reliability.

[4] For better readability, we skip the subscript t and superscript e here.

Unfortunately, beyond the statement that interconnections must yield positive effects, this theoretical analysis does not allow to derive further details regarding the size of the effect. This is due to the fact that the specific system's $LOLP$ (and thus, its $LOLE$, too) depends on the specific statistical characteristics of the random variables involved, i.e., their joint distributions. In fact, even if assuming independent variables in the above equations, the joint distributions and inequalities can – if at all – analytically only be tackled by means of upper and lower bounds (e.g., by applying Hoeffding's or Bennett's inequality). The case is further complicated when considering dependent variables which naturally occur in our area of application, such as load and wind profiles in neighboring countries.

Because of these inherent analytical complexities, we will continue our analysis by presenting a framework to endogenously determine the level of equivalent firm capacity which we can calibrate with numerical data to derive further insights into the generation adequacy of multi-regional interconnected systems.

2.2.4 A framework for endogenous equivalent firm capacity

The above introduced reliability metrics typically build upon *exogenous* systems, characterized by the availability of existing capacities X_t^e and (expected future) demand levels L_t. In contrast, we suggest an approach to *endogenize* the level of equivalent firm capacity. Similar to the concept of equivalent firm capacity described in Equation (2.4), we strive for a probabilistic optimization program minimizing the equivalent firm capacity $\mathbf{z}$ that needs to be added to (or removed from) the system to achieve the target reliability level EEU. For notational simplicity, let us drop the capacity additions $\bar{y}$ and aggregate all capacities exogenously given to the system by their nominal capacities $\bar{x}_i^e$ and their capacity availabilities $X_{i,t}^e$. The program to solve for one region can be written as follows (2.8):

$$\min \mathbf{z} \tag{2.8a}$$

$$\text{s.t.} \quad \sum_{t \in \mathbf{T}} E(L_t - (\sum_{i \in \mathbf{I}} \bar{x}_i^e X_{i,t}^e + \mathbf{z})) * P(\sum_{i \in \mathbf{I}} \bar{x}_i^e X_{i,t}^e + \mathbf{z} < L_t) \leq EEU \tag{2.8b}$$

Due to the fact that the above probabilistic problem is hardly solvable for the general case, we formulate its deterministic equivalent which is a linear program. The idea is to replace probabilities and random variables by their deterministic counter-

part, which may then be calibrated based on data covering a large range of possible outcomes. The validity and consistency of the result obtained may then be justified by the central limit theorem (Zachary and Dent (2012)).

For one single region (or market), the objective function (2.9a) minimizes the equivalent firm capacity $\mathbf{z}$ in this region subject to two constraints: First, the adequacy constraint (2.9b) states that the equivalent firm capacity should be greater or equal to the region-specific and time-varying demand l_t minus the load curtailment variable $\mathbf{u}_t$ minus the sum of the exogenously given technologies' available capacity at every instant in time t. And second, the reliability constraint (2.9c) requires the sum of load curtailment activities $\mathbf{u}_t$ not to exceed a certain reliability target, specified as expected energy unserved EEU within the considered period of time T.[5]

$$\min \mathbf{z} \tag{2.9a}$$

$$\text{s.t.} \quad \mathbf{z} \geq l_t - \mathbf{u}_t - \sum_{i \in \mathbf{I}} \bar{x}_i^e x_{i,t}^e \qquad \forall t \tag{2.9b}$$

$$\sum_{t \in \mathbf{T}} \mathbf{u}_t \leq EEU \tag{2.9c}$$

Note that the load curtailment variable $\mathbf{u}_t$ allows for a relaxation of the load serving requirement in Equation (2.9b). If EEU is set to zero, only one of the hourly constraints (2.9b) is binding, namely the hour of peak residual demand (given that all residual demand levels are distinct).[6] With EEU increasing, the peaks are increasingly shaved off by the load curtailment variable $\mathbf{u}_t$.

Solving roblem (2.9) yields $\mathbf{z}^*$, i.e., the equivalent firm capacity required to obtain the requested level of reliability in one region. In order to determine the capacity value of technology $i = i'$, we simply need to set $\bar{x}_{i'}$ to zero and resolve the model, thus yielding $\mathbf{z}^+$. Equivalent to the difference in equivalent firm capacity depicted

[5] Note that it is straightforward to reformulate the problem when reliability targets are based on the $LOLE$ measure. Specifically, Equations (2.9b) and (2.9c) need to be modified using $\mathbf{s}_t$ as the load shedding (binary) variable:

$$\mathbf{z} \geq l_t \mathbf{s}_t - \sum_i \bar{x}_i^e x_{i,t}^e \quad \forall t$$

$$\sum_t (1 - \mathbf{s}_t) \leq LOLE$$

Note that for the case of $LOLE$, the problem becomes a mixed integer optimization.

[6] Residual demand $= l_t - \sum_i \bar{x}_i^e x_{i,t}^e$.

in Equation (2.5), the technology and region-specific capacity value can then be calculated by Equation (2.10).

$$\nu = \frac{\mathbf{z}^{+} - \mathbf{z}^{*}}{\bar{x}_{i'}} \tag{2.10}$$

2.2.5 Extension to interconnected regions

Extending Problem (2.9) to multiple interconnected regions while assuming cooperation with respect to reliability, the planning problem becomes an integrated optimization. The objective function (2.11a) aims at minimizing the sum of required equivalent firm capacity $\mathbf{z}_m$ over all regions, subject to four constraints: First, the adequacy constraint (2.11b) states that the required equivalent firm capacity should be greater or equal to the region-specific and time-varying load $l_{m,t}$ minus the load curtailment variable $\mathbf{u}_{m,t}$, minus the sum of the additional technologies' available capacity, and plus electricity exchanges $\mathbf{k}_{m,n,t}$ from region m to region n at every instant in time t. We charge electricity imports with an efficiency loss $\eta_{m,n}$ in order to account for transmission losses. The reliability constraint (2.11c) remains unchanged compared to the one-region optimization above. Note that by Equation (2.11c), a specific target reliability shall be reached within each region. Additionally, however, we now need an electricity exchange constraint (2.11d) limiting $\mathbf{k}_{m,n,t}$ to the installed transmission capacity $\bar{\mathbf{k}}_{m,n}$.[7]

$$\min \sum_{m \in \mathbf{M}} \mathbf{z}_m \tag{2.11a}$$

$$\text{s.t.} \quad \mathbf{z}_m \geq l_{m,t} - \mathbf{u}_{m,t} - \sum_{i \in \mathbf{I}} \bar{x}^{e}_{i,m} x^{e}_{i,m,t} + \sum_{n \in \mathbf{M}} \mathbf{k}_{m,n,t} - \sum_{n \in \mathbf{M}} \eta_{m,n} \mathbf{k}_{n,m,t} \qquad \forall m, t, m \neq n \tag{2.11b}$$

$$\sum_{t \in \mathbf{T}} \mathbf{u}_{m,t} \leq EEU_m \qquad \forall m \tag{2.11c}$$

$$\mathbf{k}_{m,n,t} \leq \bar{k}_{m,n} \qquad \forall m, n, t, m \neq n \tag{2.11d}$$

Solving Problem (2.11) yields $\mathbf{z}^{*}_{m}$. In order to determine the capacity value of technology $i = i'$ in region $m = m'$ with respect to the entire system, we set the

[7] Again, reformulation to represent the $LOLE$ measure is straightforward.

corresponding capacity $\bar{x}^e_{i',m'}$ to zero and resolve the model, which yields $\mathbf{z}^+_m$. Based on the result we can calculate $v_{m',i'} = \frac{\sum_{m \in \mathbf{M}} \mathbf{z}^+_m - \mathbf{z}^*_m}{\bar{x}^e_{i',m'}}$. In contrast, if we aim at the capacity value of technology $i = i'$ in region $m = m'$ with respect to its own isolated region m', we solve the problem for isolated systems and calculate $v_{m',i'} = \frac{\mathbf{z}^+_{m'} - \mathbf{z}^*_{m'}}{\bar{x}^e_{i',m'}}$. Analogously, we can determine the capacity value of a specific transmission capacity $\bar{k}_{m',n'}$ between region $m = m'$ and $n = n'$ by setting the capacity to zero and solving for capacity levels $\mathbf{z}^+_m$.

2.3 Data

The data required to calibrate our model can be classified into three areas: First, we need region- and time-specific load levels ($l_{m,t}$). Second, information is required for capacity availabilities of existing generators, i.e., installed nominal capacity levels $\bar{x}^e_{i,m}$ as well as their corresponding availabilities $x^e_{i,m,t}$. Third, we need data on the transmission capacities $\bar{k}_{m,n}$.

Common to all data will be the regional coverage: We aggregate data on a national level, and cover the following European regions: Austria (AT), Belgium (BE), Bulgaria (BG), Switzerland (CH), Czech Republic (CZ), Germany (DE), Denmark (DK), Estonia (EE), Spain (ES), Finland (FI), France (FR), Great Britain (GB), Greece (GR), Croatia (HR), Hungary (HU), Ireland (IE), Italy (IT), Lithuania (LT), Luxembourg (LU), Latvia (LV), Netherlands (NL), Norway (NO), Poland (PL), Portugal (PT), Romania (RO), Sweden (SE), Slovenia (SI), Slovakia (SK).

Recall that load $l_{m,t}$ and generation availability $x^e_{i,m,t}$ need to be calibrated with a large amount of possible outcomes to replicate the characteristics of the corresponding random variables L_t, X^e_t. To this end, we will deploy the so-called hindcast approach, i.e., we calibrate the model using a large number of historical joint observations (for details, the reader is referred to Zachary and Dent (2012) and Keane et al. (2011)). Furthermore, we combine historical observations in order to better represent the joint probability space. Specifically, we focus our attention on load and wind capacity availability, which are the system properties with the largest variation.

Load data are taken from ENTSO-E (ENTSO-E (2016a)) for the years 2010 - 2015. They depict the national vertical load, i.e., the amount of electricity consumed, on an hourly basis. It should be noticed that these historical measurements were a result of a functioning electricity system and may include some price responsiveness of consumers or load shedding. To calibrate our model, however, we need to assume

that the observed load data is price inelastic. Meanwhile, historical load data is the best proxy available for the fluctuating electricity demand over time, and price responsiveness during times of scarcity was indeed found to be fairly low (Lijesen, 2007).

Our hourly wind generation profiles are based on wind speeds from reanalysis data in COSMO-REA6 provided by the Hans Ertel Centre for Weather Research (HErZ) (Bollmeyer et al., 2014). Energy output has been calculated for the existing wind parks in 2014 using data from *The Wind Power*[8] with the methodology explained in Henckes et al. (2018). The total dataset consists of 20 years with hourly wind production levels from 1995 - 2014. In contrast to wind power, solar power could not be included due to the lack of sufficiently disaggregated data with respect to installed capacities.

We combine each load year with each wind year available in order to get a good representation of the joint probability space. Noticeably, we implicitly assume there is no causal relationship between wind and load.[9] This leads us to a total of 120 years with hourly load and wind data. Note that the amount of data used in our analysis is well beyond the requirements identified by Hasche et al. (2011), and can hence be expected to yield consistent results. In order to reduce the computational burden, we focus our analysis on the relevant, most extreme conditions. This was done by sorting and filtering the data at a threshold of 0.1 % of the highest residual load cases being relevant for system adequacy.[10]

In contrast to the detailed representation of load and wind, we abstract from a full representation of other existing generators in the system. This is mainly due to three reasons: First, detailed information about installed capacities of individual generators and their capacity availabilities is difficult to obtain (i.e., for thermal and hydro power plants, but also for other renewable technologies, such as PV). Second, abstraction allows to circumvent the need to derive a probability function for the availability of capacity X, usually depicted via a Capacity Outage Probability Table (COPT) and calculated via convolution.[11] Third, and most importantly, abstraction is in line with our objective to determine the amount of equivalent firm capacity

[8] www.thewindpower.net

[9] The average correlation over all countries between wind and load is 0.08 with a median of 0.06. Therefore we assume no causal relation between both.

[10] We tested up to which point the filtering had an effect on the results and found that while increasing the threshold from 0.1 % to 0.2 % had no effect, a further reduction to 0.07 % indeed influenced the results.

[11] Note that implicitly, we thus also circumvent the need to further reflect on fundamental policy differences between countries that might affect the entire argument of a more efficient Europe, such as substantial differences in nuclear or renewable policies, for instance.

needed to serve load at some level of reliability. Therefore, our model can be seen as a way to endogenously determine the amount of equivalent firm capacity that needs to enter the system while other system characteristics are fixed. For instance, the expansion of renewable energies is typically driven by support schemes and hence largely exogenous.

Data on transmission capacities are based on publications by ENTSO-E in the Ten Year Network Development Plan (ENTSO-E, 2016c). We make use of Net Transfer Capacity (NTC) values to represent average transmission capacities between countries in 2016. NTC is the maximum exchange program between two areas compatible with security standards applicable in both areas and taking into account the technical uncertainties on future network conditions ETSO (2011).

2.4 Results

We present our results in two main steps: first, we consider the illustrative case of two-regional systems to gain insights into the general problem characteristics and model outcomes. Second, we deploy our complete dataset for the entire European continent for more comprehensive and realistic results.

2.4.1 Two-regional system

Isolated regions

For illustration, we parametrise our isolated region model (i.e., Problem (2.9)) with one year of data from France, Germany and Great Britain. Figure 2.1 shows scatter plots of residual load (i.e., load - wind power) for the region combinations Great Britain - France (left) and Germany - France (right).

The dashed lines represent the level of equivalent firm capacity ($\mathbf{z_m}$) required in the respective region when they strive for reliability in an isolated approach.[12] We apply here a typical reliability benchmark of 3 hours per year which is often used in theory (e.g., Keane et al. (2011)) as well as in practice (e.g., in the capacity markets in Great Britain or by the ISO New England). Therefore, the scatter plots depict

[12] Recall from the previous sections that this level of equivalent firm capacity relates to the overall system needs and does not distinguish existing power generation units, except for wind power. Nevertheless, for deriving further practical implications, one may compare these figures with (derated) existing capacities present in today's power system. We will do so in Section 2.4.2.

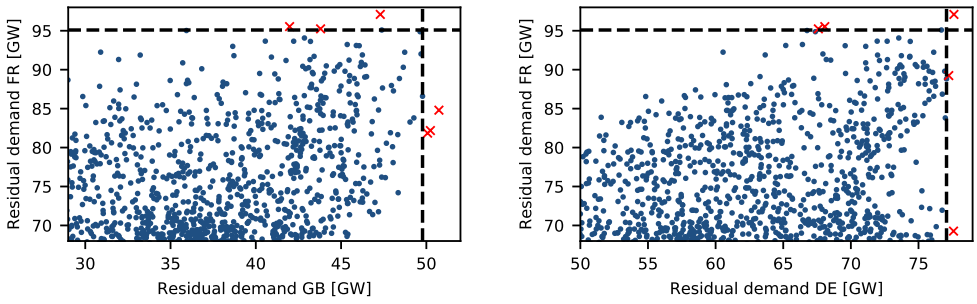

(a) Great Britain - France

(b) Germany - France

Figure 2.1: Critical residual demand in the isolated two-regional systems Great Britain (GB) - France (FR) and Germany (DE) - France (FR) for $LOLE = 3\,\mathrm{h/y}$.

residual load levels exceeding the necessary level of equivalent firm capacity during 3 hours in each region. In our methodology section, this would have been depicted by an expected value of 3 in Equation (2.2). Naturally, tightening the reliability target shifts the required equivalent firm capacity lines outwards, up to a perfectly reliable system ($LOLE = 0$) where the dotted lines cover all residual load levels and no load shedding is allowed to occur.

Note that in the right hand side figure, there is one situation where residual load cannot be met in both regions at the same time (indicated by the dot in the rectangle in the upper right corner). In contrast, the data in the left hand side figure show no coincidental load shedding. This is crucial for benefits from cooperation, as demonstrated in Equation (2.6) and discussed in the subsequent section.

Cooperating regions

In case of cooperation, regions take into account interconnections with neighbors to reach their envisaged reliability target while solving the integrated problem (2.11). Therefore, they take full advantage of balancing effects on the supply as well as on the demand side.

Requirements for equivalent firm capacity For illustration, in Figure 2.2 we recapture the region combinations Great Britain - France and Germany - France. Again, the thicker dashed lines depict the necessary equivalent firm capacity level per region which can now be reduced due to gains from cooperation (corresponds to term (2.6a) in Equation (2.6)). The thinner dotted lines represent the sum of equivalent

firm capacity plus transmission capacity (2 GW for GB - FR and 1.2 GW for FR - DE), derated by a transfer efficiency of 0.95.[13] Thus, all points in between the dashed and dotted lines – indicated by green triangles – can be covered by capacity exchange between the two regions.

Noticeably, interconnectors can only contribute to system adequacy if there is sufficient generation in the adjacent region to be exported. This is the case as long as the point of interest does not lie above the sloped dotted line in the top right corner which limits the interconnector's contribution to system adequacy (depicted by terms (2.6b)-(2.6d) in Equation (2.6)). Interestingly, as the critical situations change due to the interconnection, there are now two situations in the right hand side figure where residual load cannot be met in both regions simultaneously (indicated by the two crosses in the upper right corner). Also in the left hand side figure, there is now one simultaneous load curtailment situation. This explains the reduced number of crosses compared to Figure 2.1.

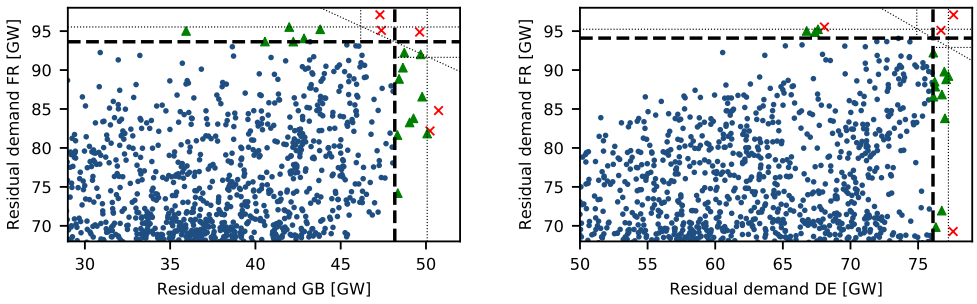

(a) Great Britain - France

(b) Germany - France

Figure 2.2: Critical residual demand in the cooperating two-regional systems Great Britain (GB) - France (FR) and Germany (DE) - France (FR) for $LOLE = 3\,\mathrm{h/y}$.

The capacity value of wind power Figure 2.3 shows the capacity value of wind power derived from Equation (2.10)) and the full dataset for isolated and cooperating two-regional systems. The graph depicts the capacity value of increasing wind capacities ranging from 0 - 80 GW in the respective region, while in the cooperation case the installed wind capacity in the interconnected region is held constant at its installed capacity in 2014, as listed in Table 2.3 in Appendix 2.6. In general, our

[13] The directional efficiency factors of transmission capacities are hard to quantify and break down to one single number. In reality they depend on line length and the topology of the grid. As our model is focused on gaining first insights based on the methodology proposed we use a value of 0.95 as an estimate.

results confirm that the capacity value decreases with increasing capacity installations due to decreasing returns to scale (e.g., see numerical evidence by Hasche et al. (2011) or Keane et al. (2011), or theoretical analyses by Zachary and Dent (2012) or Hagspiel (2018)). For perfectly reliable systems ($LOLE = 0$), the problem reduces to the analysis of the hour with peak residual load. Due to the stochastic nature and at times low output of wind power, this approach yields low and rather flat capacity values in a perfectly reliable system (Figures 2.3(a), 2.3(b)). Flat capacity values arise when peak residual load is reduced at a constant rate with increasing wind capacity. Relaxing the reliability constraint to $LOLE = 3$ (Figures 2.3(c), 2.3(d)) and the corresponding EEU (Figures 2.3(e), 2.3(f)) increases the capacity value of wind, due to the fact that wind is then allowed to deliver its contribution within a longer (i.e., relaxed) period.[14] Note that this results from the shaved off peaks due to load curtailment. Thus we observe that setting a low reliability level EEU results in flat capacity values for wind power which in turn increases equivalent firm capacity requirements and thereby total system costs.

Figure 2.3 also shows how the capacity value of wind is affected by cooperation, i.e., a change in the reference system the wind may contribute to. For $LOLE = 0$, wind in Great Britain and France does not benefit from cooperation, as the interconnector is used to its full capacity during peak load, irrespective of the installed wind capacity in the two regions (Figures 2.3(a), 2.3(b)). In contrast, the usage of German interconnectors during peak load increases with increasing wind capacity, thus reducing the equivalent firm capacity requirements of the interconnected system, and resulting in improved wind capacity values (Figure 2.3(b)).

Interestingly, at relaxed reliability levels and wind capacities >10 GW in Great Britain, the capacity value of wind for cooperating regions is (slightly) lower than for isolated regions. This at first counter-intuitive result can be explained by the observation that, in contrast to wind capacities <10 GW, the critical residual load situations switch to hours where the interconnectors with France and Great Britain are congested, resulting in higher equivalent firm capacity requirement.

Even though the EEU reliability target is directly derived from $LOLE = 3$, capacity values are different (Figures 2.3(e), 2.3(f)). Especially, the capacity value of wind in France for capacities <10 GW is not constant as for $LOLE = 3$, but decreases starting from a higher value. This is due to the fact that the EEU target allows to distribute the energy unserved to an arbitrary amount instead of only a restricted amount of

[14] The EEU has been derived from Equation (2.3) with a $LOLE = 3$ in isolated regions, resulting in EEU values amounting to GB 3.72 GWh, FR 6.17 GWh, and DE 2.43 GWh.

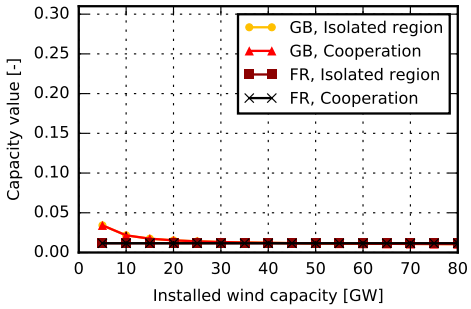

(a) Wind power in GB and FR, respectively, for two-region system GB - FR | $LOLE = 0$

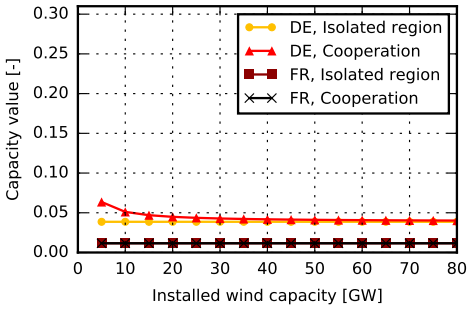

(b) Wind power in DE and FR, respectively, for two-region system DE - FR | $LOLE = 0$

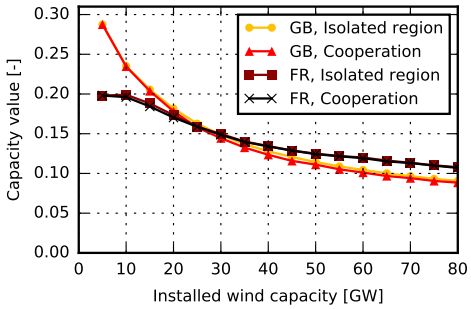

(c) Wind power in GB and FR, respectively, for two-region system GB - FR | $LOLE = 3$

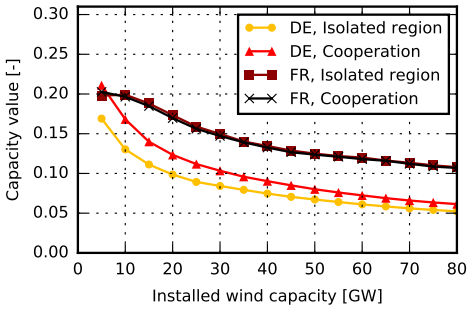

(d) Wind power in DE and FR, respectively, for two-region system DE - FR | $LOLE = 3$

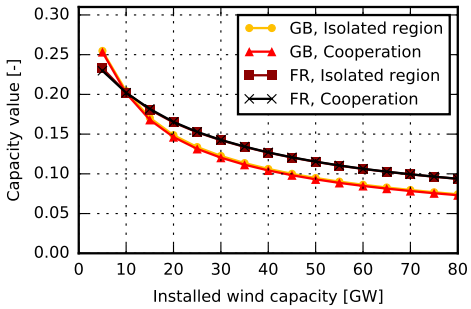

(e) Wind power in GB and FR, respectively, for two-region system GB - FR | EEU

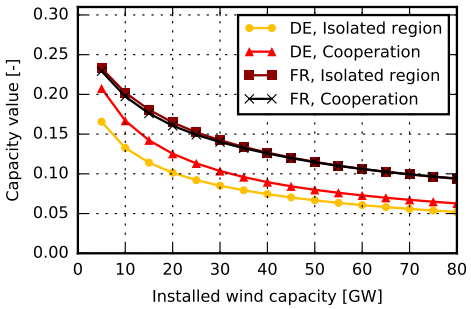

(f) Wind power in DE and FR, respectively, for two-region system DE - FR | EEU

Figure 2.3: Capacity value of wind power for isolated and cooperating two-region systems Great Britain (GB) - France (FR) and Germany (DE) - France (FR) with different reliability targets. Upper graphs: $LOLE = 0$, middle graphs: $LOLE = 3$, lower graphs: corresponding EEU (GB 3.72 GWh, FR 6.17 GWh, DE 2.43 GWh).

hours.

The capacity value of interconnectors Figure 2.4 shows the capacity value of the interconnectors for cooperating two-regional systems. Noticeably, values can exceed 100 % due to its utilisation in two directions. Thus, they are limited by 200 % in a world without transmission losses, and by 190 % when taking into account directional efficiency factors of $\eta = 0.95$.

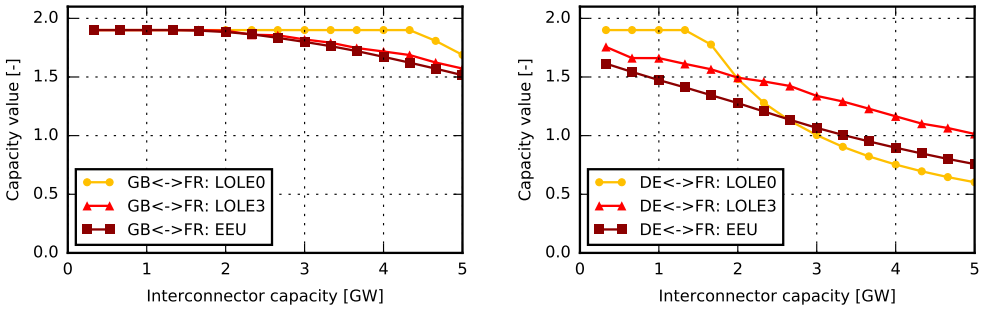

(a) Great Britain - France

(b) Germany - France

Figure 2.4: Capacity value of interconnectors for cooperating two-region systems Great Britain (GB) - France (FR) and Germany (DE) - France (FR) with different reliability targets: $LOLE = 0$, $LOLE = 3$, and corresponding EEU: GB 3.72 GWh, FR 6.17 GWh, and DE 2.43 GWh.

The interconnector between Great Britain and France is found to be highly beneficial, contributing its technical maximum to both regions at low capacity levels. This implies that peak load hours are mutually exclusive. Capacity values begin to drop slightly after 4.3 GW for $LOLE = 0$, and after 2 GW for relaxed reliability targets.

Looking at the two-region system Germany - France with $LOLE = 0$, the interconnector capacity value is at its maximum up to an interconnector capacity of 1.3 GW, followed by a sharp decrease. Relaxing the reliability level to $LOLE = 3$ or EEU leads to new peak residual demand situations where the interconnector capacity is not fully utilized anymore. This results in lower values for small capacities, but also much slower decrease (such that the curves intersect with the one for $LOLE = 0$). Essentially, this is due to the shape of the residual demand curve as compared to the peak residual load.

2.4.2 European system

We will now investigate efficiency gains through cooperation on a European level. More specifically, we look at minimum required equivalent firm capacity in each region considering all system interactions under the assumption of cooperation, and compare it to the results in isolated regions. Moreover, we calculate the reliability contributions of individual technologies.

Requirements for equivalent firm capacity The equivalent firm capacity aggregated over Europe as a function of the reliability target EEU for isolated regions and cooperating regions is shown in Figure 2.5. Recall that for the case of isolated regions, Problem (2.9) is solved for each country individually, and the firm capacity requirements are summed up to obtain the red line, while the yellow line results from an integrated optimization including interconnection (i.e., Problem (2.11)).

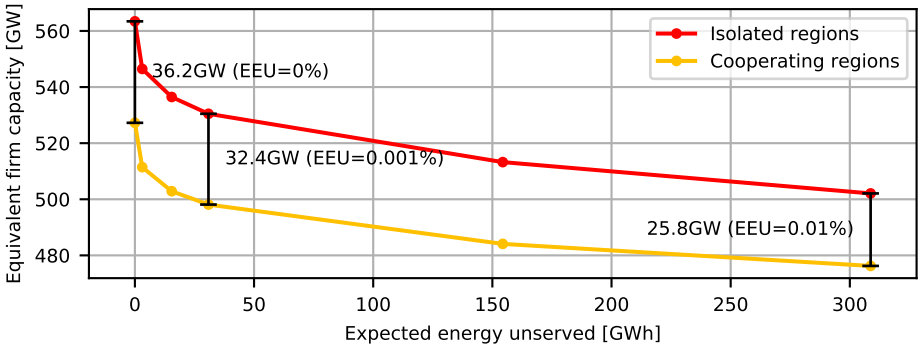

Figure 2.5: Capacity requirements aggregated over Europe as a function of EEU with the respective gains from cooperation (marked in black).

We observe that – as expected – relaxing the reliability target reduces the required level of equivalent firm capacity. While capacity requirements are reduced more significantly when moving away from an EEU of zero, reductions become smaller for further relaxations of the reliability target. The capacity savings induced by European cooperation (compared to isolated efforts) are significant and range from 36.2 GW for $EEU = 0\,\%$ to 25.8 GW for $EEU = 0.01\,\%$. This corresponds to a relative reduction of 6.4 %-5.1 %. When valuing the reduced capacity needs with 400 EUR/kW (i.e., typical investment costs of an open-cycle gas turbine which can be regarded as safe back-up capacity), the gains from cooperation amount to 10.3 - 14.5 bn EUR.

Even though capacity requirements are generally decreased with relaxed targets,

region-specific gains from cooperation are more diverse (Figure 2.6). For instance, in Denmark, at a reliability level of $EEU = 0.001\,\%$ of annual load, the reduction in equivalent firm capacity is lower than for $EEU = 0.01\,\%$. Therefore, cooperation not only affects efficiency (i.e., the overall amount of capacity needed), but also entails distributive effects. The region-specific capacity savings for $EEU = 0.001\,\%$, which corresponds roughly to $LOLE = 3$, range from 82 to 6430 MW. Comparing to the market size in the respective countries, we find relative capacity savings of 1.6 % - 30.7 % with respect to the region-specific peak load.

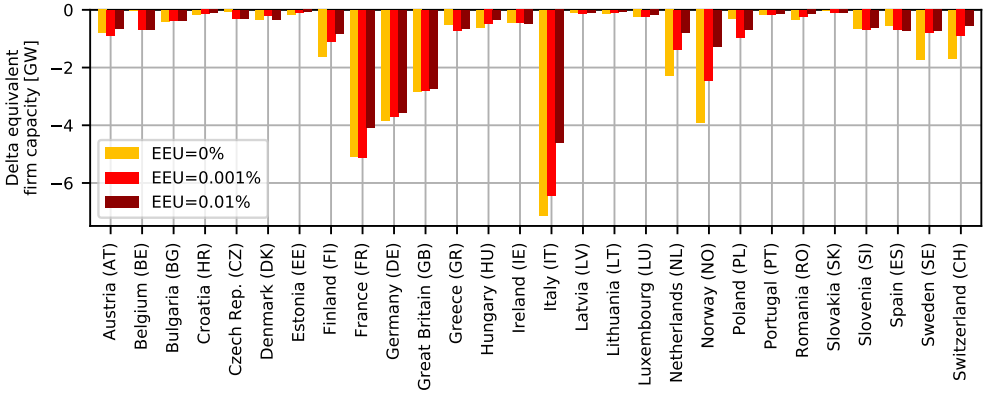

Figure 2.6: Gains from cooperation: Reduction in equivalent firm capacity with cooperation of total system (EU), compared to isolated regions.

Comparison of firm capacity requirements to European generation capacities
To put the above results into context, statistical data on installed generation capacities in Europe as well as their derating factors (i.e., technical availabilities) were collected in order to obtain derated capacities installed in each country which can be compared to our results for an optimized system.[15] Net generation capacities were obtained for the year 2016 from ENTSO-E (2016b), while historical derating factors are available in VGB and Eurelectric (2012) and dena (2010). Wind power was derated according to the results which will be presented hereafter. Meanwhile, two comments are noteworthy: First, the comparison builds on systems with different levels of reliability: it is predefined in our model results, but endogenous in the real system. And second, summing up the derated capacities across Europe can only be directly compared to the case of isolated regions, but not to the firm capac-

[15] Note that this approach is not meant to be a full-fledged adequacy assessment of the European power system. Especially, the capacity derating builds on the simplification that generation capacities are sufficiently small and outages statistically independent. Moreover, derating factors are assumed to be constant throughout the year, including times of scarcity.

ity requirements in the cooperating regions case. This is due to that in our model we consider transmission constraints between countries, while the summation of European derated capacities would assume a copper plate.

From these data, the derated installed capacity for each country can be derived. Aggregated over Europe, it amounts to 650 GW and is considerably higher than the equivalent firm capacity resulting from our optimization. Specifically, even for the case of $EEU = 0$, the derated capacity is 87 GW higher than in our optimized isolated regions, and 123 GW higher than for our interconnected and cooperating regions. Even though this gives a clear indication that Europe as a whole might have a conservative level of installed capacities, the picture needs to be complemented with a more detailed analysis on a more disaggregated regional level. This is done in Figure 2.7, where the equivalent firm capacity for isolated and cooperating regions is compared to the 2016 derated capacities in the respective region, for a reliability level of $EEU = 0.001$ % of annual load. As expected from the Pan-European comparison, the derated capacity typically exceeds the equivalent firm capacity requirements in most regions (most significant overcapacities are observed for Germany, Italy and Spain). However, there are also cases for which the derated capacity is lower than the equivalent firm capacity requirements, namely in Finland, France, Lithuania and Luxembourg, basically reflecting a strong need to import electricity during times of peak demand. Indeed, these findings are in line with recent adequacy assessments (e.g., ENTSO-E (2017)).

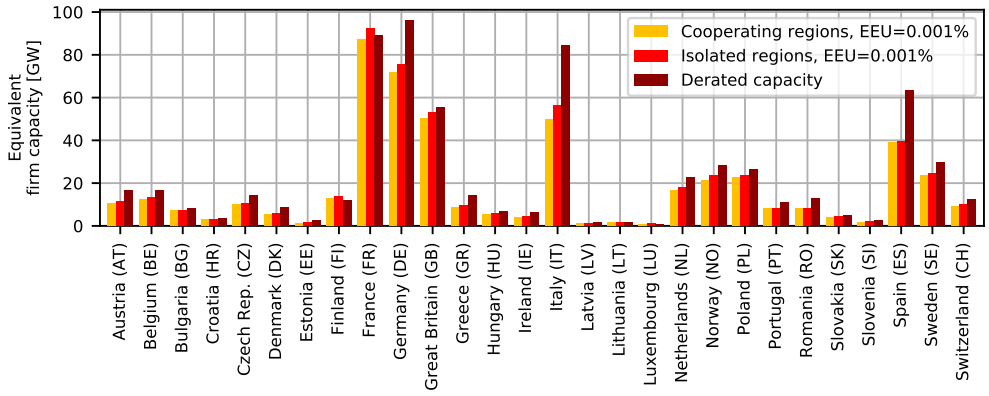

Figure 2.7: Equivalent firm capacity for isolated and cooperating regions compared to existing derated capacities.

The capacity value of wind power Figure 2.8 shows the region-specific capacity value of wind power in 2014 with respect to two different system boundaries. It

ranges broadly from 3.2 % to 25.5 % in isolated, and from 3.8 % to 29.5 % in cooperating regions (i.e., on a European level).[16] Noticeably, changing the system boundaries from isolated to cooperating entails increasing capacity values for some of the regions (e.g., for wind in Germany), but also adverse effects (e.g., for wind in France). This is due to the fact that the load profile wind power needs to match is changed, while it is unclear a priori whether this is facilitating or complicating the task.

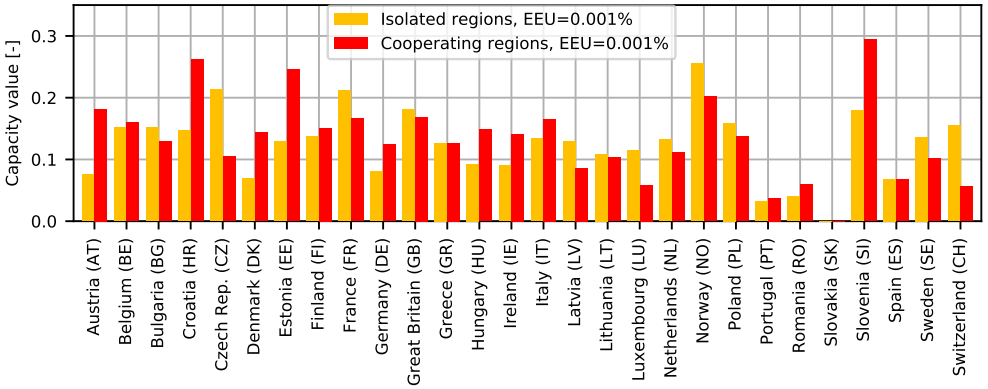

Figure 2.8: Region-specific capacity value of wind power with respect to total system (EU) for isolated and cooperating regions.

The influence of the reliability level on the capacity value of wind power (in case of cooperation on an EU level) is shown in Figure 2.9. We observe that in tendency, lower reliability levels have an increasing effect on the capacity value of wind. For perfectly reliable systems ($EEU = 0\%$), the analysis is limited to the peak residual demand hour, and thus very sensitive. Therefore, the capacity values vary considerably depending on the respective generation level in that particular hour.

Besides the optimized values, our modeling framework also allows to determine marginal capacity values of technologies. This is done by substituting the nominal capacity parameters with variables and adding additional constraints fixing the variables to the nominal capacity parameters. This seemingly cumbersome formulation helps us to derive the marginal capacity value via the Lagrange multiplier. We find that for wind power, marginal values are smaller but close to the actual values, due to decreasing returns to scale. Thus, marginal values differ most for regions with large amounts of wind power being installed, such as Germany or Denmark, for instance. The detailed results can be found in Appendix 2.6.

[16] Note that Slovakia (SK) is not shown in this figure due to missing wind power data for that region.

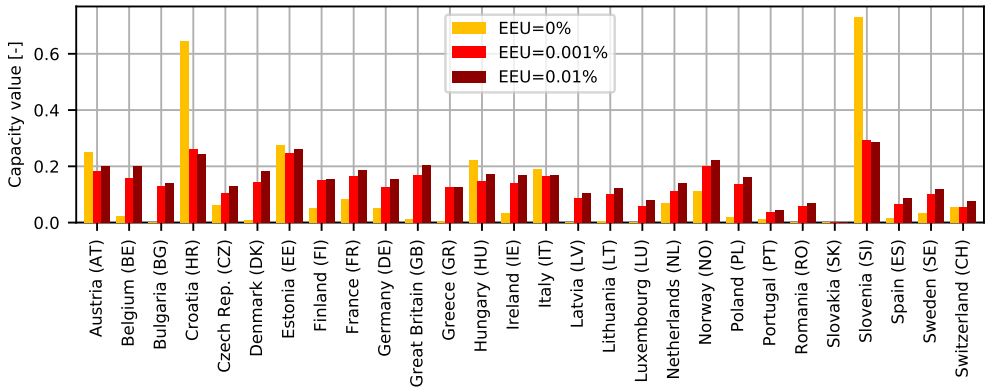

Figure 2.9: Region-specific capacity value of wind power with respect to total system (EU) for different reliability levels EEU.

The capacity value of interconnectors Figure 2.10 shows the capacity values of the existing interconnector capacities in 2016 with respect to the total system for different reliability levels EEU. Results are driven by the difference in demand and generation profiles, as well as their correlation. Some less embedded regions take particular advantage when being interconnected, i.e., Great Britain, Italy, and Romania. The interconnector from/to the Iberian Peninsula (FR-ES) is also highly beneficial to ensure reliability of supply in an efficient way. Marginal values are again shown in Appendix 2.6.

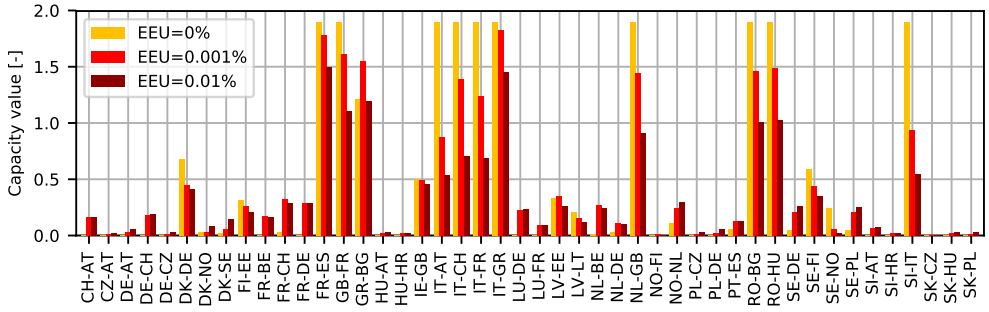

Figure 2.10: Capacity values of interconnectors between two regions with respect to total system (EU).

2.5 Conclusions

Reliability of supply is of key importance in any power system. In order to achieve reliability targets efficiently, balancing effects and gains from cooperation may be

deployed by means of large-scale interconnected systems. In practice, however, reliability is often considered on a narrow spatial scale (e.g., national). Furthermore, it lacks consistent approaches to consider interdependencies with other regions along with scarce transmission capacities.

In this paper, we have therefore developed a comprehensive computational framework to determine the efficient amount and location of firm generation capacity needed to achieve reliability targets in multi-regional systems with constrained transmission capacities. In addition, the model allows to value the contribution of individual technologies to reliability, such as wind power in a particular region or specific interconnectors.

Calibrated with a detailed dataset for Europe, our calculations show that there are indeed large benefits from cooperation: compared to an isolated region-by-region approach, the amount of firm capacity to meet a perfectly reliably system may be reduced by 36.2 GW (i.e., 6.4 %) when considering reliability in an cooperative manner, which translates to 14.5 bn Euro when valued with typical investment costs of an open-cycle gas turbine. Individual countries could reduce their amounts by up to 31.8 %. In this cooperative solution, some interconnectors contribute substantially – in both directions – with up to their technical maximum. Especially valuable are the interconnectors from/to Great Britain, Italy, and Romania, as well as the interconnector between France and Spain. Capacity expansions at those borders would therefore help most to further reduce the need for firm generation capacity. Despite its fluctuations, wind power in European countries would in the cooperative solution be able to contribute with 3.8 - 29.5 % of its nominal capacity to the reduction of necessary firm generation capacity, compared to a capacity value of 3.2 - 25.5 % when considering reliability in isolated countries.

As an additional key insight, we find that the amount and distribution of reliable capacity as well as the contribution of individual technologies strongly depend on the specific reliability target required from the system. For instance, pushing the target from an Expected Energy Unserved of 0.001 % of annual load to perfect reliability requires 29.1 GW of additional firm capacity in a coordinated European solution, and 33.0 GW for isolated target fulfillment. Therefore, targets should be carefully revisited and chosen to avoid substantial economic inefficiencies.

Based on our model, we are able to show that cooperation can lead to significant reductions of firm capacity and costs (36.2 GW, 14.5 bn Euro). Nevertheless, it has to be kept in mind that the values are based on a zonal model accounting for NTCs. This means the numbers are based on a high abstraction of the real network

by introducing NTCs and not accounting for internal network congestion within the zones. On the one hand, this may lead to an overestimation of the potential benefit if internal network congestions are the limiting factor. On the other hand, if the possible flows between zones are higher than the NTCs it may lead to an underestimation. Besides technical feasibility, countries need also be open to cooperate to provide a secure supply of electricity. While a reduction in costs for end consumers seems to be a promising incentive to do so there may be national motivations that hinder cooperation.

Therefore, our paper could be extended in several directions: The network infrastructure could be represented in more detail, e.g., by means of full-fledged load flow equations in our optimization framework. Strategic interactions between regions could be considered to investigate (and eventually, facilitate) the process of cooperative actions. The model could also be extended to tackle the problem of optimal reliability targets by a more detailed and endogenous representation of the supply, transmission and demand side including their cost structures.

Acknowledgments

The authors thank Felix Höffler, Marc Oliver Bettzüge and three anonymous referees for their helpful comments, Marius Overath for his support, and the participants of the workshops '15. Wind Integration Workshop' (Vienna, 2016) and 'Transition to power systems with weather-dependent generation' (Cologne, 2016) for valuable discussions. The work was carried out within the UoC Emerging Group on 'Energy Transition and Climate Change (ET-CC)' as well as within the UoC Forum 'Market design and regulation for stochastic electricity supply chains'. Funding by the DFG Zukunftskonzept (ZUK 81/1) is gratefully acknowledged. This article first appeared in The Energy Journal, Vol. 39, No. 5, 2018, DOI: http://dx.doi.org/10.5547/01956574.39.5.shag - Reproduced by permission of the International Association for Energy Economics (IAEE).

2.6 Appendix

Nomenclature and abbreviations

Sets	
$i \in \mathbf{I}$	Existing generators
$m, n \in \mathbf{M}$	Regions
$t \in \mathbf{T}$	Time slices
Random variables	
L	Load
X^e	Availability of existing capacity
Y	Availability of extra capacity
K	Availability of import capacity
Parameters	
$LOLP$	Loss of load probability
$LOLE$	Loss of load expectation
EEU	Expected energy unserved
$\bar{x}^e$	Nominal capacity of existing generator
x^e	Availability of existing generator
$\bar{y}$	Nominal capacity of extra generator
v	Capacity value of extra capacity $\bar{y}$
l	Load
$\bar{k}$	Transmission capacity
η	Transmission efficiency
Optimization variables	
$\mathbf{z}$	Overall equivalent firm capacity needed
$\mathbf{z}^y$	Equivalent firm capacity of extra capacity $\bar{y}$
$\mathbf{u}$	Load curtailment
$\mathbf{k}$	Capacity exchange

Table 2.1: Model sets, parameters and variables.

AT	Austria	FI	Finland	NL	Netherlands
BE	Belgium	FR	France	NO	Norway
BG	Bulgaria	GB	Great Britain	PL	Poland
CH	Switzerland	GR	Greece	PT	Portugal
CZ	Czech Republic	HR	Croatia	RO	Romania
DE	Germany	HU	Hungary	SE	Sweden
DK_E	Eastern Denmark	IE	Ireland	SI	Slovenia
DK_W	Western Denmark	IT	Italy	SK	Slovakia
EE	Estonia	LT	Lithuania		
ES	Spain	LV	Latvia		

Table 2.2: Country codes.

a	Years
bn	Billion
COPT	Capacity Outage Probability Table
CO_2	Carbon dioxide
ENTSO-E	European Network of Transmission System Operators for Electricity
EUR	Euro
GW	Gigawatt
$MtCO_2$	Million tons of CO_2
MW	Megawatt
NTC	Net transmission capacity
OCGT	Open-cycle gas turbine
PJM	Pennsylvania-New Jersey-Maryland Interconnection
PLEF	Pentalateral Energy Forum
PV	Photovoltaics
t	Ton
TWh	Terawatt hour
VRE	Variable renewable energy

Table 2.3: Abbreviations.

Input parameters

In Table 2.4, installed wind capacities per region in 2014 are depicted.

Austria (AT)	2.01 GW	Belgium (BE)	1.83 GW	Bulgaria (BG)	0.59 GW
Switzerland (CH)	0.06 GW	Czech Republic (CZ)	0.30 GW	Germany (DE)	35.19 GW
Denmark (DK)	4.64 GW	Estonia (EE)	0.29 GW	Spain (ES)	22.24 GW
Finland (FI)	0.52 GW	France (FR)	9.14 GW	Great Britain (GB)	12.08 GW
Greece (GR)	1.40 GW	Croatia (HR)	0.22 GW	Hungary (HU)	0.51 GW
Ireland (IE)	2.00 GW	Italy (IT)	8.80 GW	Lithuania (LT)	0.20 GW
Luxembourg (LU)	0.06 GW	Latvia (LV)	0.05 GW	Netherlands (NL)	3.14 GW
Norway (NO)	0.84 GW	Poland (PL)	3.24 GW	Portugal (PT)	4.68 GW
Romania (RO)	2.55 GW	Sweden (SE)	3.17 GW	Slovenia (SI)	0.01 GW
Slovakia (SK)	0.01 GW				

Table 2.4: Installed wind capacities in 2014.

Additional results

The marginal capacity value of wind power in case of cooperation is shown in Figure 2.11 for different reliability targets EEU. One can observe that a higher reliability level has no clear directional influence on the capacity value of wind power.

Figure 2.12 shows the marginal capacity values of interconnectors. As expected, in line with the capacity values derived in Figure 2.10, the marginal capacity values of the interconnectors of little interconnected regions are highest. This points to the insight that an expansion of these interconnectors would be most beneficial with respect to system reliability in case of cooperation.

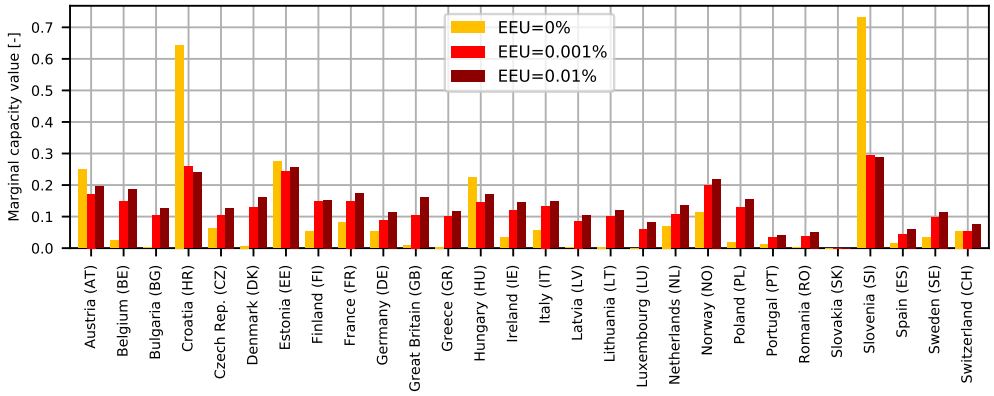

Figure 2.11: Region-specific marginal capacity value of wind power with respect to total system for different reliability levels EEU.

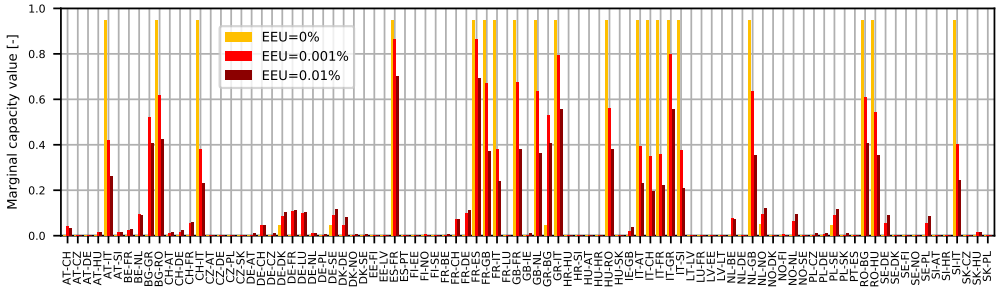

Figure 2.12: Marginal capacity values of interconnectors between two regions with respect to total system (EU).

3 Optimal Allocation of Variable Renewable Energy Considering Contributions to Security of Supply

Electricity markets are increasingly influenced by variable renewable energy such as wind and solar power with a pronounced weather-induced variability and imperfect predictability. As a result, the evaluation of the capacity value of variable renewable energy, i.e. its contribution to security of supply, gains importance. This paper develops a new methodology to endogenously determine the capacity value in large-scale investment and dispatch models for electricity markets. The framework allows to account for balancing effects due to the spatial distribution of generation capacities and interconnectors. The practical applicability of the methodology is shown with an application for wind power in Europe. We find that wind power can substantially contribute to security of supply in a decarbonized European electricity system in 2050, with regional capacity values ranging from 1 - 40 %. Analyses, which do not account for the temporal and spatial heterogeneity of the contribution of wind power to security of supply therefore lead to inefficient levels of dispatchable back-up capacity. Applying a fixed wind power capacity value of 5 % results in an overestimation of firm capacity requirements in Europe by 66 GW in 2050. This translates to additional firm capacity provision costs of 3.8 bn EUR per year in 2050, which represents an increase of 7 %.

3.1 Introduction

The Paris Agreement aims at holding global warming to well below 2 degrees Celsius (United Nations (2015)), creating the need for a deep decarbonization of the global electricity sector. Recent cost reductions suggest that the optimal pathway will to a substantial part be based on variable renewable energy sources (VRE). As a consequence, global electricity markets are increasingly influenced by generation technologies based on VRE such as wind and solar energy. Electricity generation from VRE differs from dispatchable power generation in its pronounced dependency on weather conditions. These weather-induced variations show spatial dependencies

and are not perfectly predictable. Accordingly, there arise important implications for reliability of supply in power systems as electricity is only storable at comparatively high cost and the supply-demand balance has to be maintained at all times in order to prevent outages.

Reliability of supply has always been a major concern in electricity systems as outages incur high economic losses. With increasing shares of VRE, reliability issues gain further importance due to the variability, spatial dependency and imperfect predictability of electricity generation based on VRE and the resulting risk of unavailability during times of stress (e.g. Cramton et al. (2013)). VRE resources are typically less correlated on a wider geographical scope, which reduces fluctuations because of imperfectly correlated generation patterns at different locations. Subsequently, this will be referred to as balancing effects. Hence, markets can benefit from these balancing effects via interconnections and cross-border cooperation. Envisaged reliability levels can thereby be reached at lower costs compared to reliability measures restricted to national borders (e.g., Cepeda et al. (2009) and Hagspiel (2017)). Against this background, the following research question arises: What is the optimal mix and allocation of VRE capacity in order to benefit from balancing effects both in generation and contribution to security of supply to reach an envisaged reliability target?

Assessing the contribution of VRE to security of supply is complex, because of the stochasticity of electricity generation based on weather-dependent resources. The ability of an additional VRE generation unit to provide secure capacity depends on the correlation of its electricity generation with electricity demand and with electricity generation from other units. To give intuition for this dependency, consider a simple example for wind energy: An electricity system has an off-peak demand of one and a peak demand of two with off-peak periods being more frequent compared to peak demand situations. Additionally, there are two possible sites A and B for investment into wind capacities. Wind generation at site A is perfectly correlated with off-peak demand and wind generation at site B is perfectly correlated with peak demand hours. In this setting, wind capacities at site A generate more electrical energy because off-peak situations are more frequent. Nevertheless, wind investments at site B can be preferable because wind generation capacities at site B generate electricity in the critical peak demand situations. Thus, one unit of wind capacity at site B reduces the need for one unit of dispatchable capacity and therefore contributes to security of supply. Now consider the situation where there is already one unit of wind capacity in place at site B, which generates one unit of electricity

in peak demand hours. The remaining residual demand, which must be supplied by dispatchable generation capacity, is one in off-peak and one in peak demand periods. As a result, installing one additional unit of wind capacity at site B cannot contribute to security of supply because firm capacity is still required in the off-peak demand period and thus cannot be substituted. However, if there were wind capacities of one unit installed at both sites, investing in one additional unit of wind capacity at site B would indeed contribute to security of supply.

The highly stylized example clarifies that the marginal contribution to security of supply from additional generation capacities based on VRE depends on all existing installed capacities within the system, because these capacities and their weather-dependent generation determine the critical residual demand situations. Typically, generation patterns of wind and solar power plants at different locations are positively correlated. Therefore, the ability of one unit of VRE generation capacity to substitute firm capacity, which is referred to as its capacity value (or capacity credit)[1], declines as the share of VRE in total generation increases.[2] Nevertheless, economic long-term simulation models for electricity markets, which are widely used in scientific and political practice, often assign fixed exogenous capacity values to wind and solar generation and neglect cross-border effects for reasons of simplification and computational tractability. Similarly, adequacy studies and capacity mechanisms often do not or only crudely allow for participation of VRE and are often confined to national borders.[3]

Against the described backdrop, this paper develops a new methodology to endogenously determine the contribution of VRE to security of supply in a long-term partial equilibrium model for electricity markets. The proposed methodology builds on an iterative approach, which captures the non-linear dependency of the capacity value of VRE on installed capacity and its spatial distribution considering cross-border cooperation via interconnectors. The methodology therefore determines cost-minimal investment into power plants taking into account electricity generation as well as provision of security of supply of VRE, while keeping computational tractability in a large-scale application. After introducing our methodology, we apply it in a

[1] In literature, capacity value and capacity credit are used as synonyms. Throughout this paper we will stick to the term capacity value. It is important not to confuse a technologyÂ´s capacity value with its capacity factor describing its yearly average capacity utilization.

[2] See IRENA (2017) for an overview of empirical studies showing this decreasing return to scale effect.

[3] See e.g. Cepeda et al. (2009) and Hobbs and Bothwell (2017) for a discussion. An overview on how U.S. and European capacity mechanisms credit VRE contributions to reliability is given in Byers et al. (2018) and European Commission (2016a). Furthermore, there are efforts to coordinate European adequacy assessments and foster cross-border cooperation (European Commission (2016c)).

first step to a simple two-country example. Building on that, we extend it to the European electricity system to determine an optimal decarbonization pathway until the year 2050, starting from the existing power plant fleet. Our analysis focuses on wind power, however the presented approach can be applied to all VRE technologies. We build the analysis on a new dataset, which is based on meteorological reanalysis data featuring a high spatial and temporal resolution. The data is therefore well suited to optimally capture the stochastic properties of wind generation and the resulting contribution to security of supply.

We show that the proposed methodology is capable to endogenously determine the capacity value of wind power in large-scale investment and dispatch models for electricity markets. The results of the large-scale application imply that wind power can substantially contribute to security of supply in a decarbonized European electricity system cooperating with respect to reliability, with an average wind power capacity value of 13 % in 2050. Additionally the results show that the capacity value of wind power is heterogeneous across different regions and years, which is a result of varying wind conditions as well as increasing total installed capacities and technological innovation over time. Existing modeling approaches, which typically assign constant exogenous capacity values for wind power, therefore result in inefficient levels of dispatchable capacities, which are required to guarantee security of supply in electricity systems with high shares of VRE. In our application for the European electricity system, the additional yearly costs for firm capacity provision[4] when applying exogenous fixed wind power capacity values of 5 % compared to endogenous capacity values amount to 1.5 and 3.8 bn EUR in 2030 and 2050, respectively, which represents additional costs of 3 % and 7 %. Finally our results suggest that European market integration can substantially improve the contribution of wind power to security of supply due to cross-border balancing effects.

Our paper is mainly related to two streams of literature. The first relevant stream examines system adequacy and reliability of supply in electricity systems. Reliability of supply in electricity systems has been subject to extensive scientific research effort, both from a technical as well as an economic point of view.[5] In particular, the contribution of individual technologies to system adequacy, i.e. the capacity value, has been a focus of interest. The probability theory of the capacity value of additional generation for the cases of statistical independence and dependence is presented in

[4] The yearly costs to provide firm capacity are calculated by summing the annuitized investment costs and the fixed operation and maintenance costs of all dispatchable power plants. Thereby, the fixed costs to hold available dispatchable capacity are represented.

[5] Early contributions in the two fields include e.g. Billinton (1970) and Telson (1975).

Zachary and Dent (2012). Based on these theories, various contributions investigate empirical methods to evaluate the capacity value of wind power in electricity systems.[6] Cepeda et al. (2009) investigate the positive implications of connecting different electricity systems on reliability and ways to internalize cross-border effects in a two-zone model. Hagspiel et al. (2018) introduce a comprehensive framework to investigate reliability in power systems consisting of multiple technologies and interconnected regions. All the mentioned studies focus on static analyses for given power systems. Consequently, the capacity value is not evaluated within a dynamic model, which determines the optimal future structure of an electricity system. This research gap is filled in this work by developing a dynamic framework, which builds on the framework introduced by Hagspiel et al. (2018) and combines it with an investment planning model through an iterative process.

The second relevant literature stream focuses on the analysis of electricity systems with high shares of VRE based on long-term dynamic partial equilibrium models. Typical research questions within this literature are optimal decarbonization pathways for electricity systems or optimal allocation of renewable generation capacites. However, the contribution of VRE to security of supply is often only crudely accounted for by assigning fixed exogenous capacity values.[7] Grave et al. (2012) address this issue by varying the capacity value of wind power exogenously in order to determine sensitivities in the resulting amount of required dispatchable back-up capacity. The endogenous dependency of the capacity value on total installed capacity of VRE and the impact of interconnections are not accounted for. Welsch et al. (2015) integrate a stepwise linear function for the capacity value into an optimization model. As a result, the capacity value declines endogenously. However, balancing effects of imperfectly correlated wind power generation in different geographical areas and technological innovation over time are not captured by this approach. Hobbs and Bothwell (2017) use a market equilibrium model for the ERCOT system to endogenously assess the capacity value of wind and solar power. However, they apply a greenfield approach with a limited regional representation of wind and solar power generation. The scalability of the applied methodology to more complex models with various years and a higher geographical resolution is computationally limited.

In summary, our contribution with respect to the above mentioned literature is

[6] See e.g. Keane et al. (2011) for a discussion of different methodologies including capacity value approximation techniques and Milligan et al. (2017) for a recent review of research into the capacity value of wind power.

[7] See for example Hagspiel et al. (2014) or Fürsch et al. (2013).

to (i) endogenously evaluate the capacity value of wind power within a dynamic investment and dispatch model for electricity markets, while (ii) accounting for the statistical properties of wind power in interconnected systems and (iii) keeping computational tractability in a large-scale application.

The remainder of the paper is structured as follows. Section 3.2 introduces our methodology. Section 3.3 illustrates the proposed approach based on a simple example with two countries. Section 3.4 discusses a large-scale application for the European electricity system. Section 3.5 concludes.

3.2 Methodology

In order to develop a consistent economic framework to investigate the system adequacy of future electricity systems and the contribution of VRE generation to reliability, we will start with a brief revision of the reliability metrics, in particular the well-known loss of load expectation, expected energy unserved and equivalent firm capacity measures, and a definition of the capacity value (Section 3.2.1). We will then revisit a framework to calculate the contribution of a single supplier to reliability, i.e. its capacity value, based on an optimization problem introduced by Hagspiel et al. (2018) (Section 3.2.2) Subsequently, we will introduce the optimization problem for planning and operation of power systems in order to show, how the capacity value of individual technologies is typically accounted for in long-term investment and dispatch models (Section 3.2.3). Finally, we will discuss how the two economic modeling frameworks are linked by means of an iteration procedure developed in this work (Section 3.2.4).

We will use the notation as listed in Table 3.2 in Appendix 3.6. Unless noted differently, we will use capital letters for random variables, bold capital letters for sets, lower case letters for parameters and bold lower case letters for optimization variables.

3.2.1 Reliability metrics

The reliability measure expected energy unserved (EEU) is often applied to depict the ability of a system to cover expected load levels (Allan and Billinton (1996)). The contribution of individual technologies to system adequacy, i.e. their capacity value, has been investigated using different approaches, whereof the most commonly used

are the effective load carrying capability ($ELCC$) and the equivalent firm capacity (EFC) approaches (Keane et al. (2011), Madaeni et al. (2013), Zachary and Dent (2012)). Following Hagspiel et al. (2018), we apply the EFC approach.[8] Note that the EFC approach provides consistent results with the $ELCC$ approach (Amelin (2009)).

In the following, we will briefly revisit the derivation of the well-known EEU measure applied in this analysis. We define the loss of load probability ($LOLP$) at a specific instant in time t as

$$LOLP_t = P(X_t < L_t), \tag{3.1}$$

i.e., as the probability that the available existing capacity X_t is smaller than load L_t (Allan and Billinton (1996)).[9] To calculate the expected energy unserved EEU, the $LOLPs$ are then weighted with the expected load level that cannot be served:[10]

$$EEU = \sum_{t \in \mathbf{T}} E(L_t - X_t) * LOLP_t. \tag{3.2}$$

The contribution of individual technologies is then determined by applying the EFC approach. Our focus of interest is the amount of equivalent firm capacity $\mathbf{z}^y$ by which the available existing capacity X_t can be reduced when installing some new capacity $\bar{y}$ with availability $Y_t \in [0,1]$, such that the initial (target) reliability level EEU is achieved. Thus, by replacing X_t by its equivalent $(X_t + \bar{y}Y_t - \mathbf{z}^y)$ and applying Equation (3.1), the modified equation that needs to be solved for $\mathbf{z}^y$ then writes as

$$EEU = \sum_{t \in \mathbf{T}} E(L_t - (X_t + \bar{y}Y_t - \mathbf{z}^y)) * P(X_t + \bar{y}Y_t - \mathbf{z}^y < L_t). \tag{3.3}$$

Based on the resulting $\mathbf{z}^y$, the capacity value v of a technology with capacity $\bar{y}$ can be calculated according to

$$v = \frac{\mathbf{z}^y}{\bar{y}} \tag{3.4}$$

[8] Amelin (2009) define the equivalent firm capacity of a generating unit as the capacity of a fictitious 100 % reliable unit, which results in the same loss of load probability decrease as the respective unit.

[9] Note that in Equation (3.1), we implicitly assume that load is inelastic with no adjustment when capacity is scarce, e.g., due to the lack of real-time pricing.

[10] For completeness and comparability for the interested reader, the definition of the loss of load expectation is also revisited: $LOLE = \sum_{t \in \mathbf{T}} LOLP_t$.

with $0 \leq \nu \leq 1$.

In practice, Equation (3.3) is typically solved by means of numerical iteration: after $\bar{y}$ has been added to the system, in each iteration step $\mathbf{z}^y$ is increased by some small amount until the reliability target EEU is reached.

The above equations describe a self-contained system without interconnections to neighboring systems. In interconnected systems, the $LOLP$ and $LOLE$ depend on the statistical characteristics of the random variables involved, i.e. their joint distributions. If we consider dependent stochastic variables such as load and wind profiles in neighboring countries, the problem becomes analytically highly complex and thus not tractable in a large-scale application.[11] Thus we apply a framework that endogenously determines the level of equivalent firm capacity by means of numerical optimization, as described in the following section.

3.2.2 A framework for endogenous equivalent firm capacity in multiple interconnected markets

In the following, the optimization framework introduced by Hagspiel et al. (2018) is briefly revisited, being a crucial component of the iteration algorithm developed in this study (Section 3.2.4).[12] In contrast to the above introduced reliability metrics, which typically build upon *exogenously* given existing capacities X_t and demand levels L_t, the framework at hand *endogenizes* the level of equivalent firm capacity by minimizing the firm capacity $\mathbf{z}$ that needs to be available in the system to achieve the target reliability level EEU. The framework is based on Problem (3.3), with the probabilistic problem being transformed to its deterministic equivalent and extended to multiple interconnected regions.[13]

The general idea of the optimization framework is the following: A central authority (social planner) minimizes the required firm capacity over all markets to reach

[11] See Zachary and Dent (2012) for a thorough discussion of the probability theory of the capacity value of additional generation considering independent and dependent variables.

[12] The reader is referred to Hagspiel et al. (2018) for a comprehensive derivation of the methodology. While Hagspiel et al. (2018) introduce the capacity value framework, the contribution of this analyis consists in combining the framework with an investment planning model through an iteration algorithm in order to endogenize the capacity value of VRE and applying it in a large scale application to derive allocation effects.

[13] The deterministic equivalent of a probabilistic problem is obtained by replacing probabilities and random variables by their deterministic counterpart based on data covering a large range of possible outcomes, which is typically referred to as hindcast approach in the literature. Hereby, the probability measure P models the distributions of the random variables, approximated via sums over historic time series. The validity of the hindcast approach may be justified by the central limit theorem (Zachary and Dent (2012)).

a certain market-specific target reliability level EEU, taking into consideration load, solar and wind characteristics as well as interconnection constraints.[14] Alternatively, the social planner problem can be interpreted as a representation of multiple interconnected markets, which perfectly cooperate with respect to reliability. The resulting planning problem can then be formulated as the integrated optimization problem (3.5).[15]

The objective function (3.5a) minimizes the sum of firm capacity $\mathbf{z}_m$ over all markets, subject to four constraints: The adequacy constraint (3.5b) states that the required firm capacity has to be greater or equal to the market-specific and time-varying load $l_{m,t}$ minus the load curtailment variable $\mathbf{u}_{m,t}$, minus the sum of the available generation capacity, plus the sum over electricity exchanges $\mathbf{k}_{m,n,t}$ and $\mathbf{k}_{n,m,t}$ between market m and market n at every instant of time t. Thereby, we charge electricity imports with an efficiency loss $\eta_{m,n}$ in order to account for transmission losses. The reliability constraint (3.5c) requires the sum of load curtailment activities $\mathbf{u}_t$ not to exceed a certain reliability target, specified as expected energy unserved EEU within the considered period of time T. Hence, the load curtailment variable $\mathbf{u}_t$ allows for a relaxation of the load serving requirement (Equation (3.5b)) by shaving off load peaks until the reliability level EEU is reached. And finally, the electricity exchange constraint (3.5d) limits $\mathbf{k}_{m,n,t}$ to the installed transmission capacity $\bar{k}_{m,n}$.

$$\min \sum_{m} \mathbf{z}_m \tag{3.5a}$$

$$\text{s.t.} \quad \mathbf{z}_m \geq l_{m,t} - \mathbf{u}_{m,t} - \sum_{i \in \mathbf{I}} \bar{x}_{i,m} x_{i,m,t} + \sum_{n \in \mathbf{M}} \mathbf{k}_{m,n,t} - \sum_{n \in \mathbf{M}} \eta_{m,n} \mathbf{k}_{n,m,t} \qquad \forall m, t, m \neq n \tag{3.5b}$$

$$\sum_{t} \mathbf{u}_{m,t} \leq EEU_m \qquad \forall m \tag{3.5c}$$

$$\mathbf{k}_{m,n,t} \leq \bar{k}_{m,n} \qquad \forall m, n, t, m \neq n \tag{3.5d}$$

[14] It is straightforward to reformulate the problem for reliability targets based on the $LOLE$ measure instead of EEU (see Hagspiel et al. (2018)). Note however, that, as this approach includes binary load shedding variables, the problem becomes a mixed integer optimization problem as opposed to the linear program optimization at hand.

[15] Note that for notational simplicity, the capacity additions $\bar{y}$ in Equation (3.3) were dropped and all capacities exogenously given to the system were aggregated by their nominal capacities $\bar{x}_i$ and their capacity availabilities $x_{i,t}$.

for $i \in \mathbf{I}, m, n \in \mathbf{M}, t \in \mathbf{T}$.

Solving Problem (3.5) yields the required firm capacity in each market $\mathbf{z}_m^+$ to reach the specified level of reliability, assuming cooperation with respect to reliability. In order to determine the capacity value of technology i in market n under perfect cooperation, we set the corresponding capacity $\bar{x}_{i,n}$ to zero and resolve the model, which yields the required firm capacity $\mathbf{z}_{i,n,m}^-$.

Based on the result we then calculate the technology- and region-specific capacity value under perfect cooperation according to

$$v_{i,n,m} = \frac{\mathbf{z}_{i,n,m}^- - \mathbf{z}_m^+}{\bar{x}_{i,n}} \qquad \forall i, m, n. \tag{3.6}$$

This framework can be applied to derive the local capacity value $v_{i,m,m}$ of technology i with capacity $\bar{x}_{i,m}$ with respect to market m where the technology is located ($n = m$), but also to derive the cross-border capacity value $v_{i,n,m}$ of a technology $\bar{x}_{i,n}$ located in market n with respect to an interconnected neighboring market m. The cross-border capacity value $v_{i,n,m}$ describes the cross-border contribution of technology i to reliability, i.e. the change in required firm capacity ($\mathbf{z}_{i,n,m}^- - \mathbf{z}_m^+$) in an interconnected neighboring market m considering the reliability contribution of capacity $\bar{x}_{i,n}$ located in market n.

Note that in this formulation, the capacity value represents the marginal contribution of a technology to reliability, given the contribution of all other technologies. Or, framed as a coalition game, it depicts the marginal contribution of a single coalition member to the total coalition of suppliers, e.g. wind and solar generators.[16] Additionally, note that each market m can consist of more than one region for solar and wind generation to account for their spatial heterogeneity. Thereby, we implicitly assume no internal network constraints inside a market.[17]

[16] Such a coalition game, namely the allocation of the joint contribution of a set of multiple interdependent suppliers to reliability has been analysed by Hagspiel (2018). He finds that the Shapley value represents a unique additive consistent allocation rule. While the Shapley value represents the average marginal contribution of a single supplier over all possible permutations to form a coalition, our approach captures the marginal contribution of the analyzed supplier to the full coalition (see Equation (3.6)). Because of the decreasing returns to scale of the capacity value with respect to total installed capacity, our approach can be interpreted as a conservative estimate in comparison to the Shapley value.

[17] Our approach generally allows for consideration of internal network constraints. It could be extended in this direction, e.g. by applying a load flow approach with multiple nodes per market.

3.2.3 Accounting for the contribution to reliability in an investment and dispatch model

To pursue our objective of investigating allocation effects of different ways to account for contributions to reliability, we apply an investment and dispatch model based on optimization problem (3.7). The problem at hand is similar to the integrated problem for investment and operation as formulated e.g. in Turvey and Anderson (1977). By assuming inelastic demand, e.g. due to the lack of real-time pricing, and market clearing under perfect competition - which is common in electricity market modeling literature - we are able to treat the problem as a cost minimization problem. It can be interpreted as a social planner problem where a social planner with perfect foresight minimizes total system costs for investment in generation capacity and the operation of generation and transmission between markets.

$$\min \quad TC = \sum_{i,m} \delta_{i,m} \bar{\mathbf{x}}_{i,m} + \sum_{i,m,t} \gamma_{i,m,t} \mathbf{g}_{i,m,t} \tag{3.7a}$$

$$\text{s.t.} \qquad l_{m,t} = \sum_{i} \mathbf{g}_{i,m,t} + \sum_{n} \mathbf{k}_{n,m,t} \qquad \forall m,t,m \neq n \tag{3.7b}$$

$$\mathbf{g}_{i,m,t} \leq x_{i,m,t} \bar{\mathbf{x}}_{i,m} \qquad \forall i,m,t \tag{3.7c}$$

$$|\mathbf{k}_{m,n,t}| \leq \bar{k}_{m,n} \qquad \forall m,n,t,m \neq n \tag{3.7d}$$

$$\mathbf{k}_{m,n,t} = -\mathbf{k}_{n,m,t} \qquad \forall m,n,t,m \neq n \tag{3.7e}$$

$$l_{m,peak} \leq \sum_{i,n} \nu_{i,n,m} \bar{\mathbf{x}}_{i,n} \qquad \forall m \tag{3.7f}$$

$$GHG_{cap} \geq \sum_{i,m,t} \kappa_i \, \mathbf{g}_{i,m,t} / \eta_{i,m} \tag{3.7g}$$

for $i \in \mathbf{I}, m,n \in \mathbf{M}, t \in \mathscr{T}$.

The objective function (3.7a) minimizes total system costs over all markets m, technologies i and time steps t. It consists of a fixed costs term and a variable costs term. Generation capacity $\bar{\mathbf{x}}$, electricity generation $\mathbf{g}$ and transmission between markets $\mathbf{k}$ are optimization variables. Additional generation capacities can be installed at the costs of $\delta_{i,m}$ and electricity generation incurs variable costs of $\gamma_{i,m,t}$. The cost minimizing objective function is subject to various constraints: The equilibrium constraint (3.7b) states that the load level $l_{m,t}$ has to be satisfied at all times by the sum of generation in market m and electricity exchanges between markets m and n. Constraints (3.7c) and (3.7d) mirror that generation and transmission are restricted by

installed generation and transmission capacities.[18] Furthermore, electricity trades from market m to market n are necessarily equal to negative trades from market n to market m (Equation (3.7e)). The peak capacity constraint (3.7f) requires the sum of generation capacities $\bar{\mathbf{x}}_{\mathbf{i},\mathbf{n}}$ weighted with their capacity values $v_{i,n,m}$ to be greater or equal than the market-specific annual peak load $l_{m,peak}$. Note that both local capacity ($n = m$) as well as capacity from a neighboring market n can contribute to the peak constraint in market m. Finally, the decarbonization constraint (3.7g) requires the sum of yearly carbon emissions of all technologies in all markets to be lower than a yearly greenhouse gas cap. In practical applications, Problem (3.7) is usually complemented with additional constraints in order to improve the representation of technical properties of electricity systems and politically implied restrictions. These constraints include, amongst others, constraints for capacity investment and decommissioning, capacity development over time, start up, ramping and storage.[19]

The capacity value as discussed in the previous section enters Problem (3.7) via the peak capacity constraint (3.7f). This constraint is introduced in order to represent the full variability of demand and VRE supply as well as unavailabilites of dispatchable generation while optimizing over a limited set of time slices $\mathscr{T} \subset \mathbf{T}$. Especially for reliability assessments, large time periods of VRE generation and demand have to be considered in order to generate statistically robust results.[20] However, the temporal resolution in investement and dispatch models is limited in practice due to computational limitations. Consequently, Equation (3.7f) allows to integrate robust reliability measures into Problem (3.7), which is based on a representative subset of time slices $\mathscr{T}$ in order ensure computational tractability. Note that reliability measures such as EEU do not explicitly enter into Problem (3.7). However, as the capacity value $v_{i,n,m}$ is calculated based on specific EEU requirements, reliability is considered implicitly via the capacity value, which measures the share of installed capacity, which can be considerd as firm capacity. A higher reliability target would for example decrease the capacity value of VRE and therefore increase the required

[18] Note that in this formulation, we neglect a market's internal transmission constraints. Like in the capacity value framework introduced above, the model at hand could be extended to account for internal transmission constraints, e.g. by applying a load flow approach with multiple nodes per market.

[19] Such constraints are considered in this work's large-scale application for the European electricity market (Section 3.4). Note that while Problem (3.7) describes a greenfield investment model, the model applied in this analysis accounts for path dependencies in investment decisions. The interested reader is referred to Bertsch et al. (2016a) and Richter (2011) for a detailed description of the definition of additional constraints, such as constraints for investment and decommissioning decisions, capacity development over time, start up, ramping and storage.

[20] In the application presented in Section 3.4 we a use combination of 20 years of wind and solar generation and 5 years of load data resulting in a total of 100 years.

amount of firm back-up capacity in problem (3.7).

The investment and dispatch model (3.7) is formulated as a linear program. However, as discussed above, the capacity value $v_{i,n,m}$ is a function of generation capacity $\bar{x}$. Hence, if the capacity value in the peak capacity constraint (3.7f) would be formulated as a function of generation capacity $\bar{\mathbf{x}}_{i,m}$, e.g. by applying the analytical expression introduced by Voorspools and D'haeseleer (2006) for the capacity value of wind, the problem would become non-linear. While solution algorithms exist to solve non-linear problems, the applicability of non-linear problems in real-world, large-scale electricity market applications often suffers from prohibitively high solving times. Alternatively, piece-wise linearization would represent a way to deal with non-linear analytical expressions in linear problems. However, analytical expressions so far only exist for systems without interconnections and are thus not suited to address our research question. Against this background, we solve the non-linear problem by means of iteration, as discussed in the following section.

3.2.4 A framework to endogenize the capacity value in a large-scale electricity market model

In order to endogenize the capacity value of VRE in a large-scale electricity market model, we introduce the iteration algorithm depicted in Figure 3.1 and discuss its application for the example of wind power: after running the investment and dispatch model (3.7) with exogenous start values for the region-specific capacity values of wind generation, the capacity value framework (3.5) is applied based on the resulting optimal region-specific wind generation capacities. In the next iteration step, the updated capacity values $v_{i,n,m}$ calculated in Equation (3.6) are passed to the peak capacity constraint (3.7f) of the investment and dispatch problem. Subsequently, updated capacity values are calculated considering the new wind capacities. This iteration algorithm is continued until convergence is reached. Note that the iteration framework presented in Figure 3.1 decouples the integrated non-linear problem into a linear cost minimization problem and a linear capacity minimization problem. The formulation of the capacity value framework as a capacity minimization problem allows to reduce computational effort and therefore enables the optimization over large sets of historical data. Nevertheless, the results are consistent with the cost minimization problem because investment costs for back-up capacity are considered to be equal across markets. Consequently, a system with minimal back-up capacity is – ceteris paribus – also cost minimal.

The investment model is solved based on a dataset with reduced temporal resolution (time slices) in order to keep the model computationally tractable. We apply a two-stage spatial and temporal clustering algorithm in order to derive a reduced dataset, which captures the relevant properties of wind and solar generation as well as load.[21] The capacity value on the other hand is calculated based on the full temporal resolution in order to allow for a correct evaluation of security of supply.

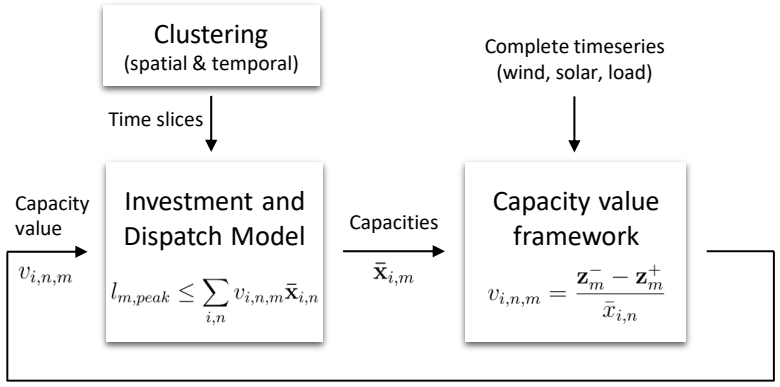

Figure 3.1: Iteration algorithm.

The procedure depicted in Figure 3.1 successively linearizes the non-linear properties of the capacity value by iteratively solving two corresponding linear problems. Hence, this novel framework allows to endogenously account for the non-linear dependency of the capacity value of wind power on the amount and spatial distribution of installed wind capacity, as well as resulting system effects via interconnectors. Building on that, effects on system costs and optimal allocation of capacities resulting from different ways of crediting the contribution of wind power to reliability can be quantified. Despite the iterative linearization, the non-linearity of the problem remains. As a result, existence and uniqueness of a global optimum can not generally be guaranteed.[22] In order to address this issue, we numerically test optimality by comparing model runs for a wide range of start values.[23]

From a practical perspective, the social planner in the presented capacity value framework can be interpreted as a central authority, e.g. the European Commission, which assesses the required firm capacity in each market in order to reach

[21] See Section 3.4.2 and Appendix 3.6 for a description of the comprehensive high-resolution data set and the clustering algorithm.

[22] Global unique optima can be guaranteed for convex minimization problems. A formal proof of the convexity of the problem is out of the scope of the paper. Nevertheless the decreasing returns to scale of the capacity value with respect to installed capacity, which is observed in empirical studies, suggest convexity.

[23] See Sections 3.3 and 3.4.

market-specific target reliability levels, taking into consideration load, solar and wind characteristics as well as interconnection constraints. This centralized assessment of market-specific required dispatchable capacity is then taken as a basis for the amount of capacity procurement in each market. Consequently, the capacity value framework determines the required quantity of dispatchable generation capacity, while the specific cost-minimal structure of back-up capacities to meet this requirement is determined in the investment and dispatch model.

In the following, we apply the presented methodology to a simple two-country system for illustrative purposes (Section 3.3), followed by a large-scale application covering the European electricity system (Section 3.4).

3.3 Illustrative example: Two-country system

In order to illustrate the basic functioning of the proposed methodology, this section presents an application to a simple case with only two countries, namely France and Germany. The example follows a greenfield approach, which optimizes the system configuration in both countries for the year 2030. For reasons of simplification, only investments into gas-fired power plants, battery storage and onshore wind power capacities are allowed with each country consisting of only one wind region. The interconnection between both countries is assumed to have a capacity of 5 GW. The remaining data assumptions for example on costs, electricity demand and CO_2 reduction targets are equivalent to the large-scale application and are described in detail in Section 3.4.2.

By solving the integrated problem (3.5), it is assumed that the two countries perfectly cooperate with respect to reliability. As such, they take full advantage of balancing effects in capacity supply and demand. In this illustrative example, for simplification, the reliability target expected energy unserved is set to perfect reliability ($EEU = 0$) in both countries, which means that load must be fully served in all hours as no peak shaving is allowed. Thus, the problem reduces to the analysis of the hour with peak residual load in each country and derives the minimally required firm capacity, considering capacity exchanges via the interconnector. The resulting firm capacity requirement is then applied as minimal capacity procurement level in the electricity market investment and dispatch model (3.7).

We start the iteration by running the investment and dispatch model with a start value of 5 % for the local capacity value of wind power and 0 % for cross-border

contributions of wind to security of supply. The resulting capacity values, installed capacities for wind power and required firm capacity as well as total system costs are depicted in Figure 3.2 for the first eight steps of the iteration. Figure 3.2(a) shows the local capacity value of wind power (e.g. 'FR in FR' for the capacity value of French wind power in France) as well as the cross-border capacity value via the interconnector from France to Germany ('FR in DE') and vice versa. In the first iteration step, the electricity market model determines the optimal wind power capacities based on the start values for the wind power capacity values. The resulting wind power capacities are then used in the capacity value framework to calculate capacity values based on actual wind infeed and load time series. As shown in Figure 3.2(a), the local capacity value of wind in Germany increases in the second iteration step, while the French capacity value slightly decreases. Moreover, the cross-border capacity values both increase to non-zero values.

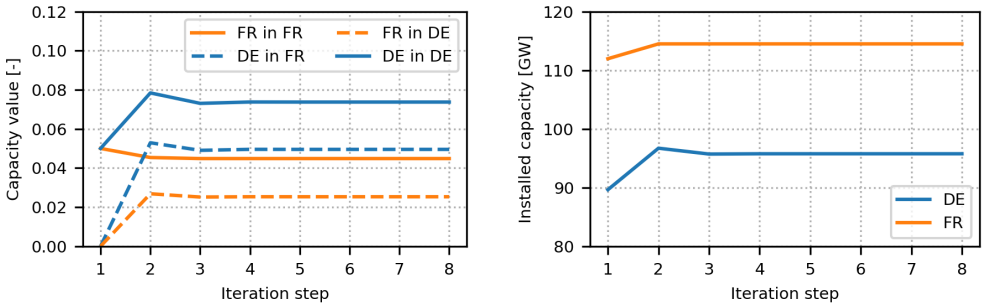

(a) Capacity value of wind power in FR and DE (national and cross-border)

(b) Installed wind power capacity in FR and DE

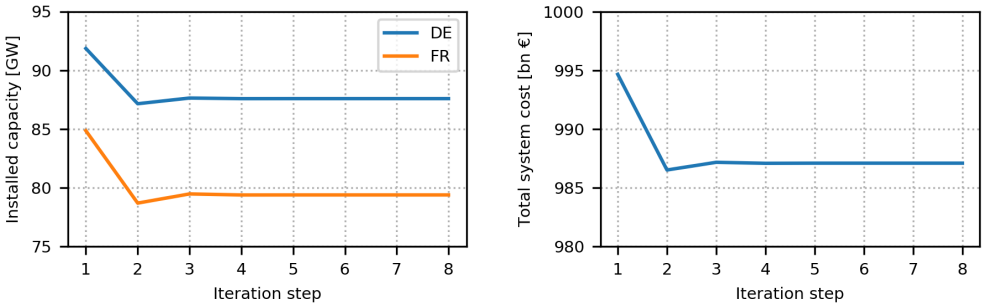

(c) Required firm capacity in FR and DE

(d) System costs for two-country system FR-DE

Figure 3.2: Iteration results in 2030 for the illustrative two-country system FR-DE.

Based on the updated capacity values the electricity market model determines new optimal wind power investment, taking into consideration the adjusted contribution to security of supply from wind power. As shown in Figure 3.2(b), optimal

wind power capacities increase in the second iteration step because of the higher capacity value. The corresponding required firm capacity to reach the reliability target decreases, as shown in Figure 3.2(c). Consequently, the required firm capacity provided by dispatchable capacities is reduced as the contribution of wind power to security of supply is increased. In the third iteration, the capacity values are slightly reduced because increased wind capacities decrease the relative contribution to security of supply. After the fifth iteration, convergence is reached and the model results remain constant in the following iterations.[24]

The two country case shows the basic interactions of the key model variables throughout the iteration process. In the following section, the methodology will be applied to a real-world large-scale application. The basic logic of the model interactions is identical to the discussion in this section.

3.4 Large-scale application: European electricity market

This section presents an application and extension of the previously developed methodology to the European electricity system. A large-scale investment and dispatch model for the European electricity market is applied in order to determine the optimal pathway to a low-carbon electricity system in 2050. Based on the presented methodology, the development of regional capacity values of wind power over time and the corresponding implications on optimal allocation of wind power capacities are assessed.

The analysis is structured as follows: Sections 3.4.1 and 3.4.2 give a brief description of the applied electricity market model as well as assumptions and data sources. Section 3.4.3 presents the model results.

3.4.1 Electricity market model and scenario definition

The applied model is a partial equilibrium model that determines the cost minimal configuration of the European electricity system, considering investment decisions as well as dispatch of power plants. Cost minimization over several years reflects perfect competition and the absence of market distortions as well as perfect foresight as fundamental model assumptions. The model is an extended version of the linear large-scale investment and dispatch model presented in Richter (2011), which has

[24] In order to test for robustness, the calculations were conducted for a wide range of start values.

been applied for example in Bertsch et al. (2016a), Bertsch et al. (2016b) and Knaut et al. (2016).

The model represents a total of 27 European countries.[25] Transmission between countries is represented by net transfer capacities (NTC), which are assumed to be extended according to the ENTSO-E Ten-Year Network Development Plan 2018 (ENTSO-E (2018)). The starting year of the model is 2015. The considered power plant technologies include wind onshore, wind offshore, photovoltaics, biomass, geothermal, hydro (run-of-river and hydro storage), pumped hydro storage, compressed air storage, battery storage, nuclear, lignite, coal, combined and open cycle gas turbines (CCGT/OCGT). Existing power plant capacities in 2015 are based on a detailed database developed at the Institute of Energy Economics at the University of Cologne, which is mainly based on the Platts WEPP Database (Platts (2016)) and constantly updated. Based on these start values, the model optimizes the european electricity system up to year 2050. Investment into nuclear power is only allowed for countries with no existing nuclear phase-out policies. Fuel costs and investment costs for new generation capacities are based on the World Energy Outlook 2017 (IEA (2017b)).[26] Yearly national electricity consumption is assumed to develop according to the ENTSO-E Ten-Year Network Development Plan 2018 (ENTSO-E (2018)). The European CO_2 reduction targets are implemented as yearly CO_2 quotas, which impose a reduction of emissions by 95 % in 2050 compared to 1990 levels. Additional reduction targets for the intermediate years are implemented with 21 % reduction in 2020 compared to 2005 and 43 % in 2030 compared to 2005. All values are based on official reduction targets formulated by the European Commission.[27] In summary, the model optimizes investments and dispatch of the European power system from 2015 to 2050, subject to CO_2 reduction constraints, exogenous interconnection capacity expansion and cost assumptions for technologies and fuels. Detailed numerical assumptions on fuel prices, costs, techno-economic parameters and development of electricity consumption are presented in Appendix 3.6.

The country-specific reliability target in the capacity value framework of the large-

[25] Austria (AT), Belgium (BE), Bulgaria (BG), Switzerland (CH), Czech Republic (CZ), Germany (DE), Denmark (DK), Estonia (EE), Spain (ES), Finland (FI), France (FR), Great Britain (GB), Greece (GR), Croatia (HR), Hungary (HU), Ireland (IE), Italy (IT), Lithuania (LT), Latvia (LV), Netherlands (NL), Norway (NO), Poland (PL), Portugal (PT), Romania (RO), Sweden (SE), Slovenia (SI), Slovakia (SK)

[26] The levelized cost of electricity generation (LCOE) of the technologies considered are a result of the optimization, as the utilization of single technologies results from the dispatch decisions of the model.

[27] See https://ec.europa.eu/clima/policies/strategies for detailed explanations.

scale application is set to an EEU, which corresponds to a loss of load expectation of 3 hours per year in every modeled country. This value is often applied in theory (e.g., Keane et al. (2011)) as well as in practice (e.g., in the capacity markets in Great Britain or by the ISO New England).[28]

3.4.2 Input data for variable renewable electricity generation and load

In addition to the assumptions described in the previous section, detailed data on weather-dependent renewable energy sources are required in order to assess contributions to security of supply of wind power generation and to generate robust estimates for the capacity value. We apply a novel dataset for wind and solar power generation based on the meteorological weather model COSMO-REA6. The data for wind power generation from existing capacities is based on Henckes et al. (2018). The wind speed data derived from the weather model is combined with a detailed dataset of European wind parks, which includes location, installed capacity, hub-height and turbine data in order to generate a consistent hourly time series of wind power generation over 20 years (1995-2014).[29]

The same methodology is extended in our application for potential future generation capacities. We assume power curves based on state-of-the-art onshore and offshore wind power plants for new capacity investment.[30] These plants are assumed to be distributed on a 24x24 km grid over whole Europe in order to determine wind generation data for potential new generation investment. Again, a consistent hourly 20 year time series of wind power generation is generated.

Even though solar power generation is not the focus of the present analysis we also use high resolution hourly time series for solar power. The data is generated based on solar irradiance data of COSMO-REA6 for the same 24x24 km grid over Europe as for wind power generation. The methodology is described in detail in

[28] In European countries, reliability targets measured in $LOLE$ generally range from 3 to 8 hours per year (Table 6 in European Commission (2016a)). Note that in case of a loss of load event, the system operator typically still has a number of options before finally resorting to selective disconnections, amongst others asking generators to exceed their rated capacity, invoking demand side balancing reserves or reducing voltage levels (Newbery (2016)). We estimate the EEU corresponding to $LOLE = 3$ in each country based on the historical ordered residual load curve in each modeled country. The resulting EEU for all markets are listed as shares of yearly demand in Table 3.6 in Appendix 3.6.

[29] A detailed statistical analysis of the weather data including correlation maps and comparisons to measured historical wind power generation data is presented in Henckes et al. (2018).

[30] The considered wind turbines are Enercon E-126 EP4 for onshore wind and Vestas V164 for offshore wind. Power curves for both turbines were determined based on technical data on the manufacturer websites.

Frank et al. (2018) and Henckes et al. (2019).

In order to keep the large-scale investment and dispatch model computationally tractable, the spatial and temporal resolution of wind and solar power generation data has to be reduced. We apply a two-step clustering approach in order to accomplish this. In a first step the spatial resolution is reduced by clustering the high resolution data into representative wind and solar regions. The number of regions for onshore wind and solar is chosen based on the surface area of each country. Additionally one offshore wind region with water depths smaller than 50 m for bottom-fixed offshore wind turbines and one region with water depths between 50 m and 150 m for floating offshore wind turbines are considered. In total the model consists of 54 representative regions both for onshore wind and solar power and 41 representative regions for offshore wind in Europe (see Table 3.10 in Appendix 3.6). A detailed description of the spatial clustering methodology is presented in Appendix 3.6.

Based on the spatially reduced data a temporal clustering is performed in order to identify time slices, which allow to reduce the temporal resolution without losing the statistical properties of weather-dependent wind and solar power generation and load. Load data is based on hourly national vertical load[31] data for all considered countries for the years 2011-2015 taken from ENTSO-E (2016a). Note that these historical measurements - being the result of a functioning electricity market - may include some price responsiveness of consumers or load shedding. However, historical load represents the best approximation available for the variable electricity demand over time. Additionally, price responsiveness during times of scarcity is low (Lijesen (2007)), which justifies the assumption of inelastic load. The historical load data is normalized and scaled based on the assumptions for total yearly future electricity demand development in order to generate consistent time series.[32] Each of the five years is then combined with the 20 years of renewable energy generation data in order to get a good representation of the joint probability space, resulting in 100 synthetic years of hourly load and renewable energy data. Hereby, we assume stochastic independence between load and wind.

Based on this dataset and the temporal clustering approach presented in Nahmmacher et al. (2016a), we generate 16 typical days for the time slices used in the

[31] i.e., national net electricity consumption plus network losses.

[32] Scaling historical load time series implies that the temporal structure of electricity demand does not change in the future. Consequently, possible changes in the demand structure as a result of increasing electrification in the mobility or heating sector are not accounted for.

investment and dispatch model.[33] As depicted in Figure 3.1, these typical days are used as input data only for the electricity market model while the capacity value calculations are based on the full temporal resolution of the data set.

3.4.3 Results and discussion

This section presents the model results, which are determined based on the described methodology and assumptions in an application for wind power. First, the resulting contribution of wind power to security of supply is presented. Based on these results, this section then discusses differences between the proposed optimization methodology and existing modeling approaches, which do not account for the endogeneity of the capacity value of wind power generation. The discussion focuses on wind power and its contribution to reliability. Additional model results for the cost-optimal development of the European power plant capacity and electricity generation until 2050 are shown in Appendix 3.6.

The applied iteration algorithm converges also in the large-scale application after only a few iterations (see Figure 3.13 in Appendix 3.6). In order to check the presented results for robustness we ran the model with a wide range of start values for the capacity value. All robustness checks showed quick convergence and merely identical results.

Contribution of wind power to security of supply

The main novelty of the presented methodology is the explicit endogenous representation of the contribution of wind power generation to security of supply in a large-scale model for electricity markets. Figure 3.3 shows the resulting aggregated average national capacity value of European wind power plants together with total installed wind power capacity in Europe for the simulated years. The presented values can be interpreted as the average share of wind power capacity in Europe that can be considered as firm capacity in the respective year, assuming cooperation with respect to reliability by means of an efficient usage of interconnectors.

The depicted results show that the contribution of wind power to security of supply is above 10 % in all considered model years. In 2015 the capacity value of wind amounts to roughly 14 % on average. Until 2020 this value only slightly decreases

[33] Nahmmacher et al. (2016a) show in their analysis that, in investment models for electricity markets, even less than 10 typical days are sufficient to obtain similar results to model runs with very high temporal resolution.

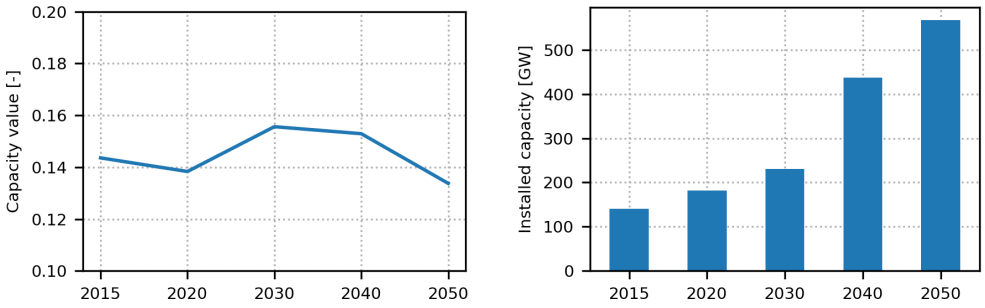

(a) Aggregated average capacity value of wind power in Europe

(b) Aggregated installed wind capacity in Europe

Figure 3.3: Average contribution of wind power to security of supply in Europe.

despite capacity additions. The reason is that interconnections between European countries are extended according to the Ten-Year Network Development Plan 2018 of ENTSO-E. As a result the decline in average capacity value, which results from additional generation capacities and decreasing returns to scale, is dampened by additional interconnectors. This dampening effect emerges because we calculate the capacity value based on the ability of wind power to provide secure capacity given the availability of interconnections to neighboring countries. Consequently, as interconnector capacities increase, the ability of wind power to provide secure capacity in combination with interconnectors also increases.

Remarkably, between 2020 and 2030 the average capacity value of European wind power increases despite continued capacity additions. This effect can be explained by technological innovation as a large share of the existing wind power plants reach the end of their technical lifetime during this time span. Consequently, many old wind power plants with relatively low rated capacities and hub heights are substituted by state-of-the-art wind turbines, which enable more stable and reliable wind power generation on average. As a result the capacity value increasing effect of technological innovation in combination with continued increased market integration outweighs the decreasing effect of decreasing returns to scale. After 2030, the two increasing effects are less pronounced because the wind power plant fleet is already to a large part renewed and the extension of interconnectors is less pronounced. Additionally total installed wind power capacity more than doubles from roughly 230 GW in 2030 to over 560 GW in 2050. Accordingly, the average capacity value of wind power decreases between 2030 and 2050.

In addition to the described average effects in Europe, the model results show a

strong heterogeneity across different regions. To illustrate this, Figure 3.4 shows the regional capacity value in 2030 and 2050, based on color-coded maps. It is shown that the capacity credit varies between 1 % and 40 % across countries and declines in most regions between 2030 and 2050. Interestingly this is not the case for all regions, for example in some regions in France and Italy as well as some offshore regions in France and Norway, the capacity value remains constant or even increases. In all mentioned regions, this can be explained by small installed wind power capacities in 2030 and no or relatively small capacity additions between 2030 and 2050. Thus, no decreasing return to scale effect arises, which would reduce the capacity value. At the same time, the temporal structure of residual load in neighboring regions changes due to wind and solar capacity additions, increasing the value of the temporal wind structure in the mentioned regions. It can be concluded that the differing temporal patterns of wind power generation as well as the differing total installed capacities, technology mixes and interconnection capacities lead to heterogeneous contributions of wind power to security of supply across countries.

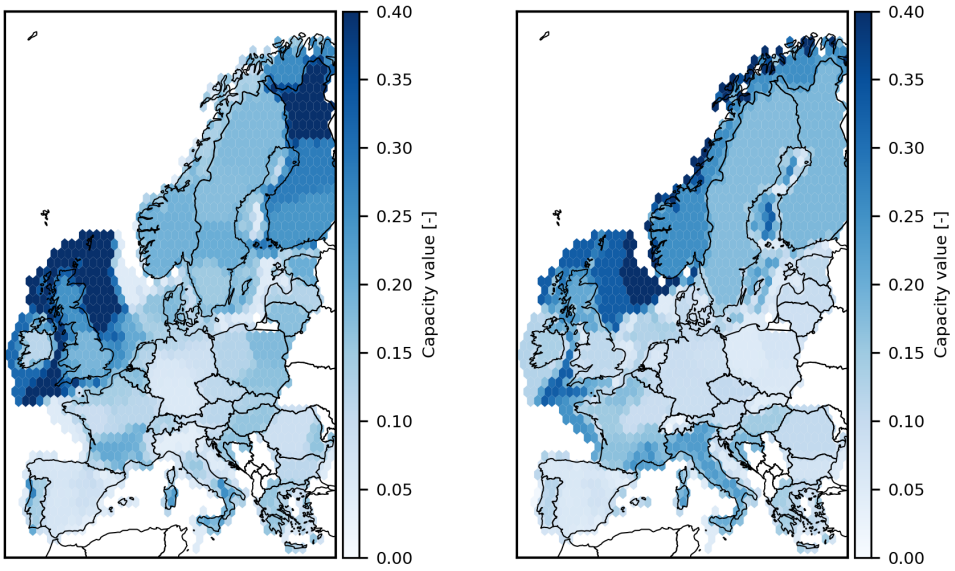

(a) Capacity value of wind power in 2030

(b) Capacity value of wind power in 2050

Figure 3.4: Regional capacity values of wind power in the European electricity system.

Based on the market-specific capacity values the equivalent firm capacity of wind power can be calculated. The results for all considered countries in 2050 are shown in Figure 3.5. It differentiates between firm capacity that is provided by wind power plants within the respective country and firm capacity that is provided cross-border

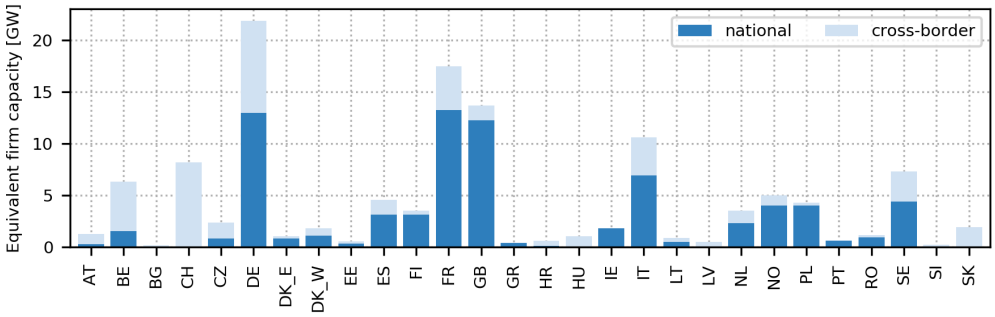

Figure 3.5: National and cross-border equivalent firm capacity provision of wind power in European countries in 2050.

via interconnections to neighboring markets, given they cooperate with respect to reliability. Again it is apparent that the contribution of wind power to security of supply varies substantially between countries depending on the capacity value and the installed capacities. In comparatively large countries such as Germany, France or Great Britain the national equivalent firm capacity of wind power amounts to more than 10 GW. Additionally, it is shown that substantial cross-border contributions are present in many countries. In Switzerland, for example, the equivalent firm capacity provided by wind in neighboring countries amounts to more than 5 GW. This is a result of increasing Swiss market integration and large installed wind power capacities in neighboring countries, especially Germany and France.

Implications on electricity system configuration

As shown in the previous section, the contribution of wind power capacities to security of supply can be substantial. Additionally the results show that the capacity value of wind power is heterogeneous across countries and varies over time depending on the installed capacity of wind power, the available transmission capacities between countries and technological innovations. In practice however, long-term scenarios of the electricity system are typically based on the assumption of a fixed exogenous capacity value (e.g. 5 % in Jägemann et al. (2013)). Because of these modeling practices we analyze in this section how the results of our proposed methodology differ from existing modeling approaches with fixed capacity values for wind power. We thereby compare our model results to equivalent model runs with fixed capacity values for wind ranging from 0 % to 20 %.

Figure 3.6 shows the difference in firm capacity requirements for European countries in 2050 for simulations applying exogenous wind power capacity values com-

pared to simulations applying endogenous capacity values, which account for their temporal and spatial heterogeneity. Positive values imply additional firm capacity requirements with exogenous capacity values. Applying fixed exogenous wind capacity values results in inefficient amounts of firm capacity provision, with an overestimation of firm capacity requirements when applying wind capacity values below 10 % for most countries. In addition, the heterogeneity of the capacity value across different countries implies that country- or even region-specific evaluations of the capacity value are necessary in order to correctly estimate the required dispatchable firm capacity.

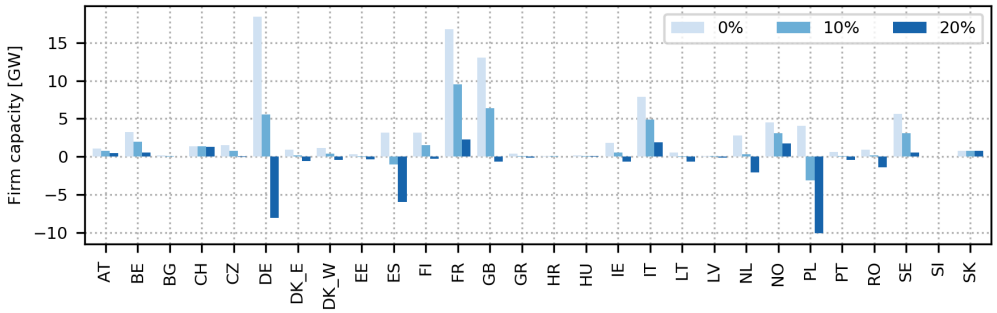

Figure 3.6: Difference in firm capacity requirements in 2050: Endogenous wind power capacity values vs. exogenous capacity values.

The requirement for additional firm capacity translates into additional yearly costs for its provision, i.e. annuitized investment costs as well as fixed operation and maintenance costs. Typically, such additional dispatchable back-up capacity is provided by low-cost open-cycle gas turbines. The absolute and relative difference in yearly costs of firm capacity provision between a model run with endgenous capacity values and model runs with exogenous capacity values ranging from 0 % to 20 % is presented in Table 3.1. The results show that costs of firm capacity provision are substantially overestimated when low exogenous capacity values are applied. For exogenous capacity values of, e.g., 5 % the difference amounts to 1.5 and 3.8 bn EUR in 2030 and 2050, respectively, which represents additional costs of 3 % and 7 %. Applying high exogenous capacity values of 20 % underestimates the required costs of firm capacity provision.

In addition to cost differences the results of our modeling approach also differ in comparison to existing approaches with respect to the geographical distribution of the installed wind power capacity. This is a result of the marginal local contribution of wind power to security of supply, which is reflected in our modeling approach and is often neglected in existing methodologies. To analyze the impact of this ef-

Year	0 %	5 %	10 %	15 %	20 %
2030	2.1 (3 %)	1.5 (3 %)	1.0 (2 %)	0.5 (1 %)	- 0.1 (- 0.2 %)
2050	5.3 (10 %)	3.8 (7 %)	1.9 (4 %)	0.2 (0 %)	- 1.5 (- 3 %)

Table 3.1: Additional yearly costs for firm capacity provision when applying exogenous fixed wind power capacity values of 0 % to 20 % compared to endogenous capacity values. Absolute cost differences are stated in bn EUR.

fect, Figure 3.7(a) shows the geographically differentiated installed wind capacities in 2050 based on endogenous capacity value calculations. Figure 3.7(b) displays the regional differences in installed capacities compared to an equivalent model run with fixed wind power capacity values of 5 %. Green areas on the map in Figure 3.7(b) indicate that more wind power capacities are installed when endogenously calculating the contribution to reliability, red areas on the other hand indicate that less wind power capacities are installed in the respective area. The equivalent comparisons for exogenous capacity values of 0 %, 10 %, 15 % and 20 % are presented in Appendix 3.6.

The results illustrate that there are substantial regional differences between a model run with a constant capacity value of 5 % and our methodology. The reason for the regional shifts in wind power capacity is that when the contribution to security of supply is accounted for, it can be cost optimal to prefer locations with relatively lower total wind power generation, which instead have a higher capacity value. Consequently there is a trade-off between electricity generation and contribution to security of supply of one unit of wind power capacity. Because of the weather dependency of wind power generation this trade-off depends on the wind conditions in a specific region and the correlations with demand and wind power generation at other sites.

It can be seen from Figure 3.7 that there is for example a shift of offshore wind power capacity from the Netherlands to German and Belgian offshore wind regions if the contribution to security of supply is endogenously accounted for. Additionally, the results show that there is less onshore wind power capacity installed in central Germany. Instead more capacity is installed for example in Spain, Romania, Finland and Norway. Consequently, the results suggest that wind power generation is shifted from Germany to other countries in order to spread wind power plants over a wider area, and take advantage of differing wind conditions on a wider geographical scope.

More generally it can be concluded that there are regional as well as technological differences regarding offshore and onshore wind power plants between our method-

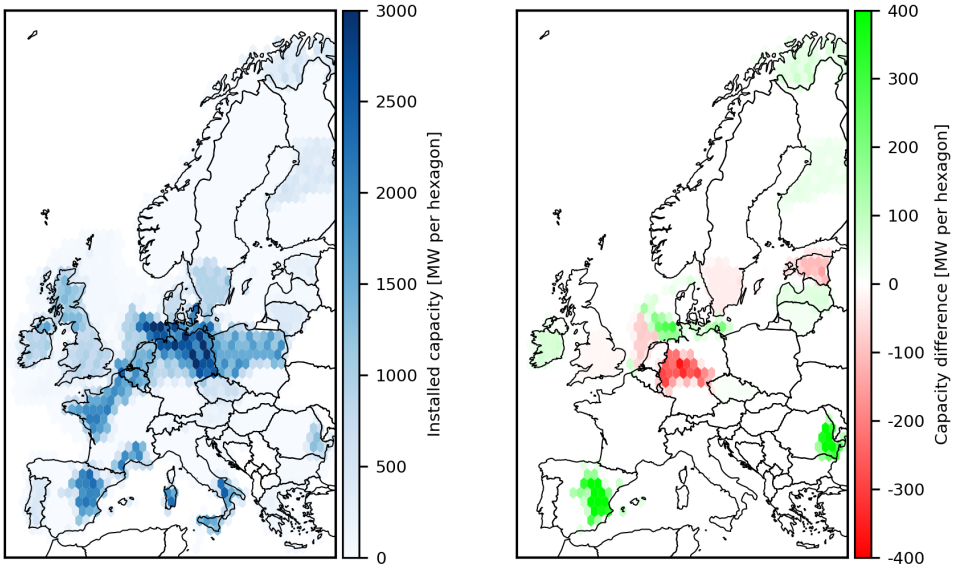

(a) Optimal wind power capacity in 2050 based on endogenous capacity value calculations

(b) Difference in optimal wind power capacity in 2050: Endogenous capacity values vs exogenous capacity values of 5%

Figure 3.7: Allocation effects of endogenizing the capacity value of wind power in investment and dispatch models for the European electricity market.

ological approach and existing modeling approaches. Hence, our results suggest that the contribution to security of supply should be considered in studies that analyze optimal locations of wind power generation in electricity systems based on long-term investment models.

The impact of cross-border cooperation

The previous sections identify substantial cross-border contributions of wind power to security of supply. In order to quantify the benefit of cross-border cooperation with respect to reliability, this section analyzes an additional scenario, in which each country ensures the reliability target within its own jurisdiction. Cross-border contributions to reliability are therefore not considered. The remaining model assumptions are unchanged compared to the results presented in the previous sections.

Figure 3.8 shows the aggregated average capacity value of wind power in Europe without cross-border cooperation, based on the endogenous capacity value framework. The equivalent value for the model runs with cooperation as presented in Figure 3.3(a) is shown as a dashed line for comparison. The results show that there

are substantial gains of cross-border cooperation. The average difference in wind power capacity values amounts to roughly 2 % in 2015. This gap increases over time and amounts to almost 6 % in 2050. The additional benefits over time can be explained by the assumed exogenous grid extensions. Without cooperation, the increased potential for cross-border contributions to reliability enabled by the additional grid capacities remain unused.

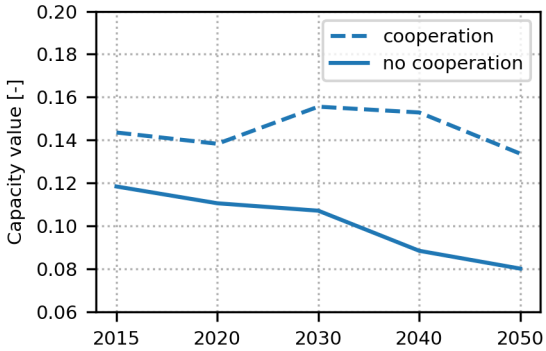

Figure 3.8: Aggregated average capacity value of wind power in Europe with and without cross-border cooperation.

Figure 3.9 shows the difference in firm capacity provision from wind power in 2050 between the model results with and without cross-border cooperation for each country. The results show that the contribution of wind power to reliability decreases in almost all countries. The difference is larger for large and well integrated countries with many European neighbours such as Germany. Additionally, the results show that not only the cross-border contribution of wind power to reliability is reduced to zero without cooperation but that there is also a reduction in the national contribution to reliability. The latter can be explained by the lack of cross-border back-up for wind power generation from dispatchable generation capacities. If wind power cannot be backed up by dispatchable generation from neighboring countries, more national back-up capacities are required, which is reflected in the lower capacity value and firm capacity provision.

In consequence, the yearly costs of firm capacity provision are higher when cross-border contributions to reliability are neglected. The cost difference on a European level amounts to 0.8 and 2.9 bn EUR in 2030 and 2050, respectively, which represents additional costs of 2 % and 6 %.

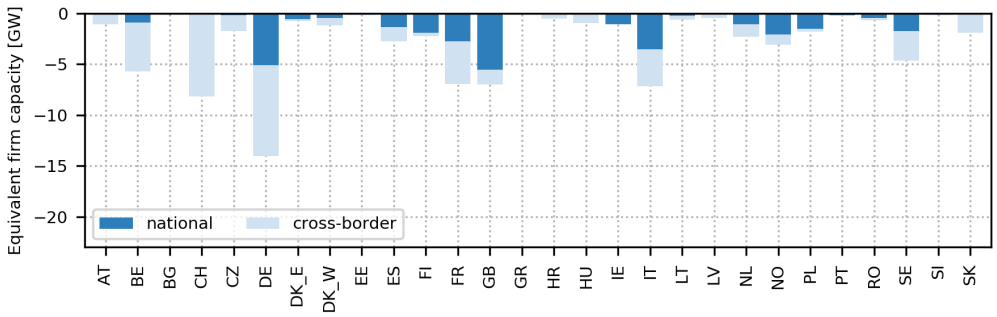

Figure 3.9: Difference in national and cross-border equivalent firm capacity provision of wind power in European countries in 2050: No cooperation vs. cooperation.

3.5 Conclusions

This article analyzes the contribution of wind power generation to security of supply in electricity systems and develops a new methodology to endogenously determine the capacity value of generation capacities based on variable renewable energy sources in large-scale optimization models. Our novel framework allows to account for the non-linear dependency of the capacity value of wind power on the amount and spatial distribution of installed wind capacity, considering cross-border cooperation via interconnectors. Building on that, we quantify differences in system costs and wind power capacity allocation in comparison to existing modeling approaches, which typically assign fixed exogenous capacity values for wind power.

We find, based on a large-scale application of the proposed methodology, that wind power substantially contributes to security of supply in a decarbonized European electricity system with capacity values between 1 % and 40 %. The regional capacity value of wind power depends on the region-specific wind conditions, its correlation to other regions, as well as on the installed wind power capacity and the capacity of interconnections to neighboring markets. Assigning fixed and invariable capacity values therefore results in inefficient levels of required back-up capacities in electricity systems with high shares of variable renewable energy. We find that, for the European electricity system, the additional yearly costs for firm capacity provision when applying exogenous fixed wind power capacity values of 5 % compared to endogenous capacity values amount to 1.5 and 3.8 bn EUR in 2030 and 2050, respectively, which represents additional costs of 3 % and 7 %.

Our results imply that long-term scenarios for electricity systems should account for the contribution of variable renewable energy sources to security of supply. Addi-

tionally our results suggest that capacity mechanisms, which are being implemented in many countries, should allow for participation of generation capacities based on variable renewable energy sources as well as cross-border contributions. However, the assigned capacity values should be determined based on careful assessments of the statistical properties of the variable renewable energy generators and need to be regularly updated in order to account for changes in the system configuration. Finally, our results show that cross-border cooperation and market integration based on increasing interconnections between different countries increases the potential of variable renewable energy sources to contribute to security of supply.

The results of this analysis are subject to model limitations which result from specific assumptions and simplifications. Transmission investment is exogenous in the model. Consequently, possible additional contributions to reliability with optimal transmission investment are not accounted for. Additionally, power flows are modeled based on net transfer capacities between regions without taking into account potential internal transmission constraints within regions, which could limit the contribution of wind power to reliability. Extending the presented model with a physical load flow model as well as allowing for endogenous transmission investment are promising directions for future research. Additionally, the model assumes perfect competition and perfect foresight. Consequently, an analysis of the impact of market imperfections and myopic behaviour on reliabilty could be investigated. Also, the analysis assumes that solar power does not contribute to security of supply. Future work could therefore analyze possible interactions and optimal combinations of wind and solar power with respect to reliability. Finally, the model could be extended with other reliability metrics in order to improve the understanding of security of supply in electricity systems with high shares of generation based on variable renewable energy sources.

Acknowledgments

The authors thank Felix Höffler for his helpful comments, Simeon Hagspiel for fruitful in-depth discussions, Philipp Henckes for the meteorological data, Henrike Sommer for her support, and the participants of the ‘17. Wind Integration Workshop’ (Stockholm, 2018) for valuable input. The work was carried out within the UoC Emerging Group on ‘Energy Transition and Climate Change (ET-CC)’. Funding by the DFG Zukunftskonzept (ZUK 81/1) is gratefully acknowledged.

3.6 Appendix

Nomenclature and abbreviations

Sets	
$i \in \mathbf{I}$	Generation technologies
$m, n \in \mathbf{M}$	Markets
$t \in \mathbf{T}, \mathscr{T}$	Time (**T**: complete data set, $\mathscr{T}$: time slices)
Random variables	
L	Load
X	Availability of existing capacity
Y	Availability of extra capacity
K	Availability of import capacity
Parameters	
$LOLP$	Loss of load probability
$LOLE$	Loss of load expectation
EEU	Expected energy unserved
EFC	Equivalent firm capacity
$\bar{x}$	Nominal capacity of existing generator
x	Availability of existing generator
$\bar{y}$	Nominal capacity of extra generator
v	Capacity value of extra capacity $\bar{y}$
$\bar{k}$	Transmission capacity
η	Transmission / generation efficiency
l	Load
l_{peak}	Peak demand
δ	Fixed costs
γ	Variable costs electricity generation
κ	Fuel-specific emission factor
GHG_{cap}	Greenhouse gas emissions cap
Optimization variables	
$\mathbf{z}$	Overall equivalent firm capacity needed
$\mathbf{z}^y$	Equivalent firm capacity of extra capacity $\bar{y}$
$\mathbf{u}$	Load curtailment
$\mathbf{k}$	Capacity / electricity transmission between markets
$\bar{\mathbf{x}}$	Generation capacity
$\mathbf{g}$	Electricity generation

Table 3.2: Model sets, parameters and variables.

AT	Austria	FI	Finland	NL	Netherlands
BE	Belgium	FR	France	NO	Norway
BG	Bulgaria	GB	Great Britain	PL	Poland
CH	Switzerland	GR	Greece	PT	Portugal
CZ	Czech Republic	HR	Croatia	RO	Romania
DE	Germany	HU	Hungary	SE	Sweden
DK_E	Eastern Denmark	IE	Ireland	SI	Slovenia
DK_W	Western Denmark	IT	Italy	SK	Slovakia
EE	Estonia	LT	Lithuania		
ES	Spain	LV	Latvia		

Table 3.3: Country codes.

a	Years
bn	Billion
CCGT	Combined-cycle gas turbine
CCU	Carbon capture and utilization
CO_2	Carbon dioxide
DSR	Demand side response
ENTSO-E	European Network of Transmission System Operators for Electricity
ERCOT	Electric Reliability Council of Texas
EUR	Euro
FOM	Fixed operation and maintenance
GHG	Greenhouse gas
GW	Gigawatt
LCOE	Levelized costs of electricity
$MtCO_2$	Million tons of CO_2
NTC	Net transmission capacity
OCGT	Open-cycle gas turbine
PV	Photovoltaics
t	Ton
TWh	Terawatt hour
VRE	Variable renewable energy

Table 3.4: Abbreviations.

Additional results

The transition towards a cost-optimal 95 % decarbonization of the European electricity sector is driven by large-scale investments in wind and solar, as shown in Figure 3.10(a).

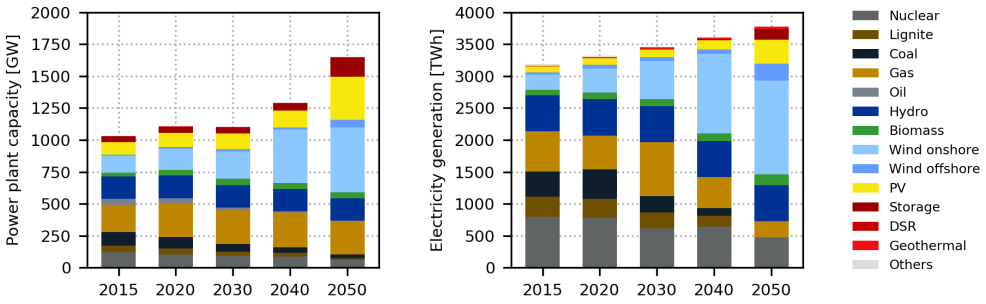

(a) Power plant capacity (b) Electricity generation

Figure 3.10: Cost-optimal development of European power plant capacity and electricity generation for system with endogenous wind power capacity values and 95 % decarbonization.

Flexibility is provided by interconnector capacities, storage, hydro and gas power plants. As this analysis is not a greenfield analysis, the path dependency of investments is considered via the technical lifetime of power plants. Thus, the model can decide to decommission a power plant ahead of its end-of-lifetime, while the annuitized capital costs still incur until the end of the economic lifetime. Figure 3.10(b)

presents the development of electricity generation. In 2050, more than half of electricity generation comes from VRE, followed by hydro, nuclear, gas and biomass.

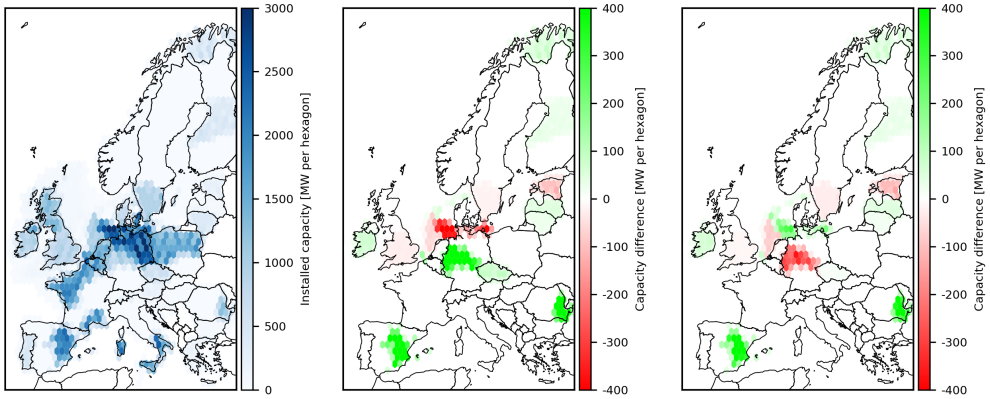

(a) Endogenous (b) 0% (c) 5%

Figure 3.11: Absolute capacity and difference in optimal wind power capacity in 2050: Endogenous capacity values vs exogenous capacity values of 0 % and 5 %, respectively.

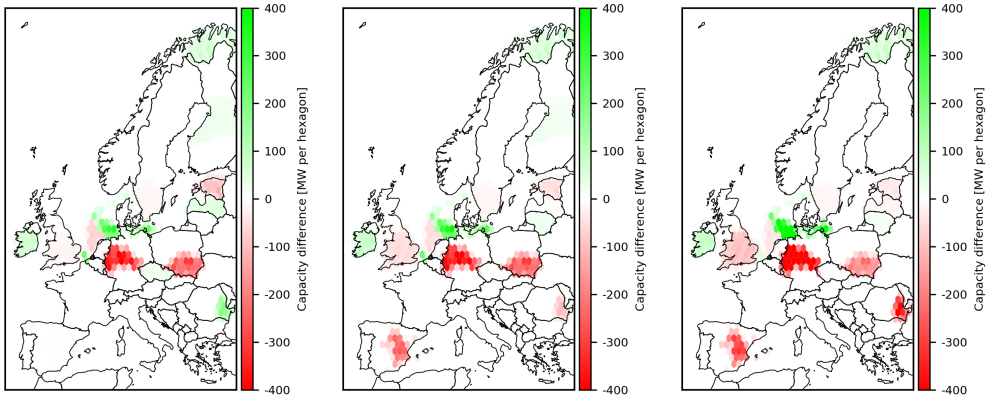

(a) 10% (b) 15% (c) 20%

Figure 3.12: Difference in optimal wind power capacity in 2050: Endogenous capacity values vs exogenous capacity values of 10 %, 15 %, and 20 %, respectively.

Convergence

Figure 3.13 shows total system costs for each step of the iteration for different start values for the capacity value. It can be seen that total system costs converge quickly to very similar values independently of the start value. It is also apparent that

changes in total system costs are negligible after the third iteration. We abort the iteration after the tenth step. The relative change in total system costs between the ninth and the tenth iteration is less than 0.1 %. The results for other start values within the depicted range were merely identical and are therefore omitted in Figure 3.13.

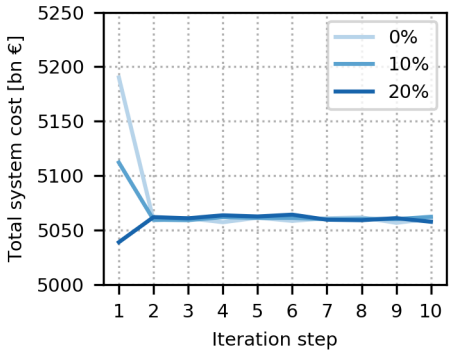

Figure 3.13: Convergence of total system costs in large-scale application for different starting values.

Spatial clustering methodology

The input data for wind and solar power generation is derived from the meteorological reanalyis dataset COSMO-REA6. The data has a high spatial resolution with data points on a 24x24 km grid over whole Europe. In order to keep the electricity market model computationally tractable the spatial resolution has to be reduced. We apply a spatial clustering methodology in order to construct representative regions, which optimally reduce the spatial resolution. Our methodology consists of three basic steps:

1. Derive number of clusters per market and energy source
2. Apply the clustering algorithm
3. Determine regional potential for wind and solar power capacities

In the first step we choose the number of clusters. We use a simple heuristic approach based on the surface area of a country to determine the number of clusters for onshore wind and solar power. The total surface are of each market is divided by 100'000 km^2 and the resulting number is rounded to determine the number of clusters. For offshore wind we choose only one region per market for water depths

below 50 m and one region for water depths between 50 m and 150 m. The results are presented in Table 3.10.

In the second step we apply a k-means clustering algorithm in order to cluster the data points into the number of chosen regions. Wind power and solar power are clustered independently in order to capture the spatial properties of both energy sources. Based on the clustered data points the energy output of one representative region is calculated by averaging over all data points in a cluster. Figure 3.14 shows exemplary the clustering results for onshore wind and solar power in Germany. Each data point is represented by a dot, while the color coding differentiates the resulting clusters.

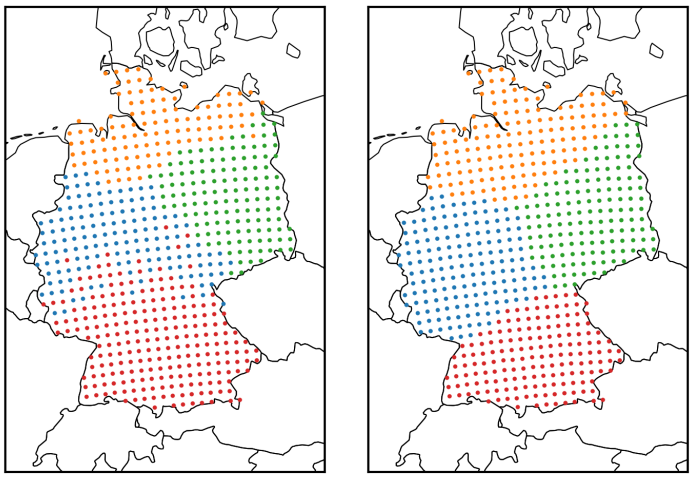

(a) Wind onshore (b) Solar

Figure 3.14: Exemplary results of spatial clustering for onshore wind power (a) and solar power (b) in Germany.

In the third step the potential for installed capacity in each region is calculated for wind and solar power. The calculation is based on the country-level area potentials in Schmidt et al. (2016). Based on the total area potentials we calculate the regional area potentials with the ratio between the number of data points per region and the total data points in the corresponding country, assuming an equal distribution.

Numerical assumptions

Fuel type	2015	2020	2030	2040	2050
Nuclear	3	3	3	3	3
Lignite	2	3	3	3	3
Coal	9	10	11	11	11
Oil	22	33	49	58	58
Natural gas	15	19	25	28	28

Table 3.5: Assumptions on gross fuel prices (EUR/MWh_{th}).

Country	2015	2020	2030	2040	2050	*EEU* (‰)
AT	70	73	77	80	80	0,005
BE	85	87	89	90	90	0,008
BG	33	41	42	44	44	0,011
CH	63	62	58	56	56	0,006
CZ	63	69	71	74	74	0,007
DE	521	565	547	552	552	0,007
DK_E	13	15	17	18	18	0,014
DK_W	20	26	30	32	32	0,014
EE	8	9	10	11	11	0,015
ES	263	268	282	283	283	0,010
FI	82	90	94	96	96	0,007
FR	475	481	467	447	447	0,013
GB	333	328	322	313	313	0,010
GR	51	57	63	70	70	0,013
HR	17	19	22	24	24	0,010
HU	41	43	47	52	52	0,002
IE	27	31	36	38	38	0,010
IT	314	326	362	400	400	0,007
LT	11	12	13	15	15	0,006
LV	7	8	8	9	9	0,008
NL	113	115	119	122	122	0,006
NO	128	136	150	143	143	0,019
PL	151	163	207	253	253	0,006
PT	49	51	53	56	56	0,009
RO	55	58	64	70	70	0,007
SE	136	142	143	142	142	0,008
SI	14	13	17	20	20	0,007
SK	27	29	33	36	36	0,004

Table 3.6: Assumptions on the future development of net electricity demand including network losses (TWh) and the reliability target expected energy unserved *EEU* as share of yearly demand (‰). Electricity demand is based on scenarios *Best Estimate* (2020), *European Commission* (2030), *Global Climate Action* (2040 - 2050) in TYNDP2018 (ENTSO-E (2018)). *EEU* is based on a loss-of-load expectation *LOLE* of 3 h/y.

Technology	2015	2020	2030	2040	2050
Wind onshore	1656	1602	1548	1512	1476
Wind offshore (bottom-fixed, <50 m depth)	3493	3168	2473	2236	2061
Wind offshore (floating, >50 m depth)	3749	3460	2581	2300	2099
Photovoltaics (roof)	1440	1152	972	882	792
Photovoltaics (ground)	1188	936	774	702	630
Biomass (solid)	3298	3297	3295	3293	3287
Biomass (gas)	2826	2826	2826	2826	2826
Geothermal	12752	10504	9500	9035	9026
Hydro (river)	5000	5000	5000	5000	5000
Compressed air storage	1100	1100	1100	1100	1100
Pump storage	2336	1237	1237	1237	1237
Battery	1000	1000	750	650	550
Nuclear	5940	5400	4590	4050	4050
OCGT	450	450	450	450	450
CCGT	1031	900	900	900	900
IGCC	2115	2115	2115	2070	2070
Coal	1800	1800	1800	1800	1800
Coal (advanced)	1980	1980	1980	1980	1980
Lignite	1596	1596	1596	1596	1596

Table 3.7: Assumptions on generation technology investment costs (EUR/kW). Conventional power plants, PV and wind onshore are based on scenario *New Policies* in World Energy Outlook 2017 (IEA (2017b)). Wind offshore is based on Myhr et al. (2014), Heidari (2017), Engel (2014).

Technology	FOM costs (EUR/kW/a)	Net efficiency (-)	Technical lifetime (a)
Wind onshore	13	1	25
Wind offshore (bottom-fixed, <50 m depth)	93	1	25
Wind offshore (floating, >50 m depth)	93	1	25
Photovoltaics (roof)	17	1	25
Photovoltaics (ground)	15	1	25
Biomass (solid)	120	0.30	30
Biomass (gas)	165	0.40	30
Geothermal	300	0.23	30
Hydro (river)	12	1	60
Compressed air storage	9	0.70	40
Pump storage	12	0.76	60
Battery	10	0.90	20
Nuclear	101-156	0.33	60
OCGT	19	0.28-0.40	25
CCGT	24-29	0.39-0.60	30
IGCC	44-80	0.46-0.50	30
Coal	44-60	0.37-0.46	45
Coal (advanced)	64	0.49	45
Lignite	46-53	0.32-0.46	45

Table 3.8: Assumptions on techno-economic parameters of electricity generators, based on scenario *New Policies* in World Energy Outlook 2017 (IEA (2017b)) and Knaut et al. (2016).

	2015	2020	2030	2040	2050
CO_2 quotas	1079	1039	779	425	72

Table 3.9: Assumptions on yearly CO_2 quotas for the European electricity market ($MtCO_2/a$), based on official reduction targets formulated by the European Commission.

	Number of clusters			
Country	**Wind onshore**	**Wind offshore (<50 m depth)**	**Wind offshore (>50 m depth)**	**Solar**
AT	1	0	0	1
BE	1	1	0	1
BG	1	1	1	1
CH	1	0	0	1
CZ	1	0	0	1
DE	4	1	0	4
DK_E	1	1	1	1
DK_W	1	1	1	1
EE	1	1	1	1
ES	5	1	1	5
FI	3	1	1	3
FR	6	1	1	6
GB	2	1	1	2
GR	1	1	1	1
HR	1	1	1	1
HU	1	0	0	1
IE	1	1	1	1
IT	3	1	1	3
LT	1	1	1	1
LV	1	1	1	1
NL	1	1	0	1
NO	4	1	1	4
PL	3	1	1	3
PT	1	1	1	1
RO	2	1	1	2
SE	4	1	1	4
SI	1	0	0	1
SK	1	0	0	1

Table 3.10: Number of spatial clusters for VRE per country.

4 How Does Climate Change Affect Optimal Allocation of Variable Renewable Energy?

Ongoing climate change affects complex and long-lived infrastructures like electricity systems. Particularly for decarbonized electricity systems based on variable renewable energies, there is a variety of impact mechanisms working differently in size and direction. Main impacts for Europe include changes in wind and solar resources, hydro power, cooling water availability for thermoelectric generation and electricity demand. Hence, it is not only important to understand the total effects, i.e., how much welfare may be gained when accounting for climate change impacts in all dimensions, but also to disentangle various effects in terms of their marginal contribution to the potential welfare loss. This paper applies a two-stage modeling framework to assess RCP8.5 climate change impacts on the European electricity system. Thereby, the performance of two electricity system design strategies – one based on no anticipation of climate change and one anticipating impacts of climate change – is studied under a variety of climate change impacts. Impacts on wind and solar resources are found to cause the largest system effects in 2100. Combined climate change impacts increase system costs of a system designed without climate change anticipation due to increased fuel and carbon permit costs. Applying a system design strategy with climate change anticipation increases the cost-optimal share of variable renewable energy based on additional wind offshore capacity in 2100, at a reduction in nuclear, wind onshore and solar PV capacity. Compared to a no anticipation strategy, total system costs are reduced.

4.1 Introduction

The current nationally stated mitigation plans are expected to lead to a global warming of about 3 °C above pre-industrial levels by 2100 (IPCC (2018b)). Increasing the mitigation ambition levels is therefore key for a successful implementation of the central *well below 2 °C*-statement of the Paris Agreement (United Nations (2015)). Scientific evidence indicates that ongoing climate change, particularly when reaching levels beyond 2 °C, will have severe consequences such as increasing surface

temperatures, changes in water and wind availability and a rising frequency of extreme weather events (IPCC (2014b), IPCC (2018b)).

The analysis of climate change scenarios suggests various ways of how changes in climate will affect complex and long-lived infrastructures like electricity systems.[1] Particularly for decarbonized electricity systems based on variable renewable energies (VRE), there are important and ample effects and mechanisms, how a changing climate will affect the (well-)functioning of electricity systems within the next 50 to 100 years.[2] For Europe, which is the focus of this analysis, most important are effects on VRE resources (both availability and gradients), hydro power availability, cooling water availability for thermal power plants and electricity consumption. Each of these effects may work differently in size, direction and transmission mechanism. E.g., periods with low wind speeds are expected to increase, potentially increasing the need for back-up energy (Moemken et al. (2018), Weber et al. (2018)). Low summer river flows with high water temperatures are expected to increase in frequency, affecting cooling water availability of thermoelectric power plants (Vliet et al. (2013), Tobin et al. (2018)). The hydro power potential is expected to experience on average a decrease in Europe due to changed precipitation patterns (Vliet et al. (2013), Schlott et al. (2018)). Furthermore, electricity demand for heating is expected to decrease in northern Europe, while electricity demand for cooling will increase in southern Europe (Eskeland and Mideksa (2010), Wenz et al. (2017)).[3] Hence, it is not only important to understand the total effects, i.e., how much welfare may be gained when accounting for climate change impacts in all dimensions, but also to disentangle various effects in terms of their marginal contribution to the potential welfare loss. This may be particularly relevant when accounting for uncertainties in climate change scenarios and discussing policy reactions and priorities.

In this paper, we will contribute to fill this research gap. Based on a detailed partial equilibrium model for the European electricity sector, we compare the evolution of electricity systems up to 2120, which in the planning, i.e. investment, either neglect climate change, or account for climate change. In the dispatch, of course, both systems have to cope with climate change. The difference between the two invest-

[1] The technical lifetime of certain electricity sector assets like hydro and nuclear power plants, as well as grid infrastructure, spans time frames of 40 up to 80 years.

[2] Cost-optimal decarbonized electricity systems are expected to be largely based on VRE in light of recent VRE cost reductions, particularly for wind and solar PV, in combination with increasing awareness and regulation of environmental externalities (e.g., Ueckerdt et al. (2017), IPCC (2018c), IEA (2017)).

[3] Climate change impacts on biomass yield are not accounted for in this study, as the changes in biomass yield for electricity generation are expected to be small and the overall biomass energy potential in Europe is limited (IEA (2018)).

ment strategies will inform us on the order of magnitude of consequences that are caused when ignoring climate change in electricity system planning. Furthermore, each of the different effects of climate change may vary in their order of magnitude of impact on electricity systems. We will therefore disentangle the different effects by comparing isolated climate change effects to a world without climate change, focusing on an electricity system, which was planned without anticipation of climate change.

The analysis is based on a two-stage modeling framework building on a numerical large-scale partial equilibrium model of the European electricity market. In the first stage, the model is run in a long-term investment planning mode in order to derive the evolution of two cost-optimal power plant capacity mixes from 2015 until the year 2120, based on the two design strategies without and with climate change anticipation. For computational tractability, hereby a reduced temporal resolution based on typical days is applied. In the second stage, the model is run in a high-resolution dispatch mode with fixed power plant capacities from the first stage, representing a full year in hourly resolution. Thereby, the two systems are dispatched for a set of scenarios representing climate change impacts on wind and solar resources, hydro resources, cooling water availability for thermoelectric generation and electricity demand. This setup allows to investigate, on the one hand, the order of magnitude of isolated climate change impacts on an electricity system, which was designed without anticipation of climate change impacts. On the other hand, the performance of the two electricity system design strategies can be analyzed in a scenario representing the best-guess expectation of future climate change impacts, i.e. a scenario, where all climate change impacts occur combined. Variable renewable energy resource availability without and with climate change impacts is represented by a high-resolution dataset based on the EURO-CORDEX project. The analysis builds on one of the official scenarios of the IPCC reports on climate change, namely RCP8.5, which represents a scenario with very high greenhouse gas (GHG) emissions and accordingly drastic climate change. Far-reaching impacts on the worlds population and ecosystems are expected in consequence of a RCP8.5 climate crisis.[4]

[4] RCP8.5 is characterized by an increase in radiative forcing of 8.5 W/m^2 around the year 2100 relative to pre-industrial values. The Representative Concentration Pathways (RCPs) describe different 21st century pathways of GHG emissions and atmospheric concentrations, air pollutant emissions and land use. The last IPCC reports on climate change were based on four RCPs, consisting of a stringent mitigation scenario (RCP2.6), two intermediate scenarios (RCP4.5 and RCP6.0) and one scenario with very high GHG emissions (RCP8.5). Business-as-usual scenarios without additional efforts to constrain emissions lead to pathways ranging between RCP6.0 and RCP8.5 (IPCC (2014b)). Only RCP2.6 is representative of a scenario that aims to keep global warming likely below 2 °C above pre-industrial temperatures, in line with the Paris Agreement (United Nations (2015)).

Our analysis shows that the RCP8.5 climate change impact on wind and solar energy resource availability has the largest consequences for the European electricity system, compared to climate change impacts on hydro power, cooling water availability for thermoelectric generation and electricity demand. All isolated climate change effects on the supply side lead to a reduction in the availability of the respective technology, resulting in compensating electricity generation by other generation technologies. Additionaly, effects on electricity demand also require an increase in generation. A system designed without anticipation of climate change reacts to all isolated climate change effects with increased gas and biomass electricity generation in order to comply with the decarbonization target, however to different extents. The predominant impact of a reduction in VRE availability follows the intuition that systems based on high VRE shares, which are not allowed to adjust their investments, react sensibly – even to small changes in VRE availability. When subject to all climate change effects combined, system costs in 2100 increase by 24 bn EUR, or 12 %, due to increased fuel and carbon permit costs compared to a world without climate change, and marginal electricity generation costs show strong increases of 15 to 75 EUR/MWh. Applying a system design strategy based on climate change anticipation results in a trend towards wind offshore capacity in 2100, while nuclear, wind onshore and solar PV capacities are reduced. Overall, the share of VRE electricity generation is increased. The trend towards wind offshore is driven by a combination of reduced base-load nuclear capacity, cost structures and local capacity factor reductions in wind due to climate change, resulting in a shift in competitiveness towards wind offshore. Compared to a system designed without climate change anticipation, the climate change anticipating system reduces total system costs by 3.6 bn EUR in 2100 in a world with all RCP8.5 climate change impacts combined. Marginal electricity generation costs can thereby be reduced in most countries, with reductions ranging from -12 to -46 EUR/MWh.

Our contribution with respect to the existing literature is to i) analyze major impacts of RCP8.5 climate change on cost-optimal electricity system planning in a consistent manner, taking into account existing generation assets and path dependencies, and ii) to disentangle various climate change impacts on electricity systems and compare their order of magnitude. Tobin et al. (2018) also assess climate change impacts on wind, solar PV, hydro and thermoelectric power generators. Their study focuses on how these single power generators are impacted, applying a consistent modeling approach. However it does not account for system effects between generators in a cost-optimizing framework. Nahmmacher et al. (2016b) analyze, how different power system design strategies are able to deal with shocks on the European

power system, such as heat waves or periods of low wind production. The study investigates short-term shocks, which may be caused by climate change, however the focus does not lie on assessing the impacts of climate change based on a consistent framework within a specific climate change scenario. Wohland et al. (2017) and Weber et al. (2018) focus on back-up energy requirements in the European electricity system under RCP8.5 climate change impacts on wind energy. The studies are based on a back-up energy minimization problem, representing a simplified electricity system without a detailed representation of dispatchable power plant characteristics and climate change impacts other than on wind. They find an increase in long periods of low wind generation and seasonal variability, resulting in increased back-up requirements. Kozarcanin et al. (2018) use a simplified representation of wind, solar and a generic dispatchable power source to analyze climate change impacts on the European electricity system and key metrics such as short-term variability. Complex system interactions are not accounted for. Schlott et al. (2018) apply a detailed greenfield power system investment model to derive the cost-optimal European capacities of power plants and transmission lines under RCP8.5 climate change impacts on wind, solar and hydro power. They find an increase in the share of solar PV in the cost-optimal power system under climate change. The greenfield approach, however, does not take into consideration path dependencies of the power plant mix during the transition towards a decarbonized electricity system.[5] Also, interaction effects between base-load nuclear generation and VRE are not accounted for. Various studies investigate isolated impacts of climate change on VRE generation (e.g., Reyers et al. (2016), Moemken et al. (2018), Tobin et al. (2016), Tobin et al. (2015), Jerez et al. (2015)). However, these studies focus on meteorological aspects and isolated impacts on electricity generation from wind or solar PV, without a detailed representation of the entire electricity system. Additionally, none of the literature mentioned above disentangles and compares the single effects of climate change and assesses the order of magnitude of their impact on the electricity system.

The remainder of the paper is structured as follows. Section 4.2 introduces the methodology. Section 4.3 introduces the scenario framework and data. Section 4.4 discusses the resulting impacts of climate change on electricity systems, based on a large-scale application for the European electricity system. Section 4.5 concludes.

[5] In a greenfield model, the power plant capacity mix in each considered model year is built without consideration of existing capacities from preceeding model years.

4.2 Methodology

Throughout the paper, notation as listed in Table 4.5 is applied. Unless otherwise noted, bold capital letters indicate sets, lowercase letters parameters and bold lowercase letters optimization variables.

4.2.1 Investment and dispatch model

In order to investigate the impacts of climate change on the European electricity system, this analysis applies a partial equilibrium model that determines the cost minimal configuration of the European electricity system, considering investment decisions as well as dispatch of power plants. The investment and dispatch model is based on optimization problem (4.1).[6] The commonly applied assumptions of market clearing under perfect competition, i.e. absence of market distortions, and inelastic demand, e.g. due to the lack of real-time pricing, allows to treat the problem as a cost minimization problem. With the complete time frame being optimized at once, the problem can be interpreted as a social planner problem where a social planner with perfect foresight minimizes total system costs for investment in generation capacity and the operation of generation and transmission between markets.

The objective function (4.1a) minimizes total costs TC over the complete time period, i.e., the sum of the fixed costs of generation capacity $\bar{\mathbf{x}}_{i,m,y}$ and variable costs of generation $\mathbf{g}_{i,m,y,d,h}$ of technology i in market m. The objective function is subject to various constraints: an equilibrium condition (4.1b) for supply and demand, two capacity constraints (4.1c) and (4.1d) to restrict generation and transmission, an electricity trade constraint (4.1e) for consistency, a peak capacity constraint (4.1f) to ensure sufficient firm capacity and a decarbonization constraint (4.1g) to limit

[6] See, e.g., Turvey and Anderson (1977) for a similar formulation of the integrated optimization problem for investment and operation in electricity systems.

carbon emissions for climate change mitigation.[7]

$$\min \quad TC = \sum_{i,m,y} \delta_{i,m,y} \bar{\mathbf{x}}_{i,m,y} + \sum_{i,m,y,d,h} \gamma_{i,m,y,d,h}\, \mathbf{g}_{i,m,y,d,h} \tag{4.1a}$$

$$\text{s.t.} \qquad l_{m,y,d,h} = \sum_{i} \mathbf{g}_{i,m,y,d,h} + \sum_{n} \mathbf{k}_{n,m,y,d,h} \qquad \forall m,y,d,h, m \neq n \tag{4.1b}$$

$$\mathbf{g}_{i,m,y,d,h} \leq x_{i,m,y,d,h} \bar{\mathbf{x}}_{i,m,y} \qquad \forall i,m,y,d,h \tag{4.1c}$$

$$|\mathbf{k}_{m,n,y,d,h}| \leq \bar{k}_{m,n,y} \qquad \forall m,n,y,d,h, m \neq n \tag{4.1d}$$

$$\mathbf{k}_{m,n,y,d,h} = -\mathbf{k}_{n,m,y,d,h} \qquad \forall m,n,y,d,h, m \neq n \tag{4.1e}$$

$$l_{m,y,peak} \leq \sum_{i} v_{i,m} \bar{\mathbf{x}}_{i,m,y} \qquad \forall m \tag{4.1f}$$

$$GHG_{y,cap} \geq \sum_{i,m,d,h} \kappa_i\, \mathbf{g}_{i,m,y,d,h} / \eta_{i,m} \qquad \forall y \tag{4.1g}$$

for technologies $i \in \mathbf{I}$, markets $m,n \in \mathbf{M}$ and time $y,d,h \in \mathbf{Y},\mathbf{D},\mathbf{H}$.

The large-scale model for the European electricity market applied in this analysis follows the same basic model structure as in Problem (4.1), however additional features are included in order to improve the representation of technical properties of electricity systems and politically implied restrictions. Such features include for example capacity investment and decommissioning constraints, ramping and storage constraints, as well as a module for power-to-x processes such as electrolysis, which allows the model to produce carbon-neutral gases for use in the electricity sector in order to further decarbonize it. The model was originally presented in Richter (2011) and has been applied for example in Bertsch et al. (2016b) and Peter and Wagner (2018). An extended version of the model including the power-to-x module is described in Helgeson and Peter (2018). The subsequent analysis covers the European electricity market represented by a total of 27 European countries.[8]

[7] See, e.g., Peter and Wagner (2018) for a more comprehensive description of the constraints.

[8] Austria (AT), Belgium (BE), Bulgaria (BG), Switzerland (CH), Czech Republic (CZ), Germany (DE), Denmark (DK), Estonia (EE), Spain (ES), Finland (FI), France (FR), Great Britain (GB), Greece (GR), Croatia (HR), Hungary (HU), Ireland (IE), Italy (IT), Lithuania (LT), Latvia (LV), Netherlands (NL), Norway (NO), Poland (PL), Portugal (PT), Romania (RO), Sweden (SE), Slovenia (SI), Slovakia (SK).

4.2.2 Performance of investment strategies without and with climate change anticipation

The goal of this analysis is to study the performance of electricity systems designed without and with anticipation of climate change under a variety of possible futures of climate change impacts. Thereby, a two-stage modeling framework is applied, based on a long-term investment planning stage and a high-resolution dispatch stage.

In the first stage, the long-term investment planning model (4.1) is run based on two design strategies, one without climate change anticipation (*No-CC-anticipation*) and one with climate change anticipation (*CC-anticipation*). It covers a time period from 2015 to 2120, applying 10-year time steps from 2020 onwards. Running investment planning models for such large time periods at full temporal resolution results in prohibitively high solving times. Therefore, for computational tractability, in this first stage, the investment and dispatch model applies a reduced temporal resolution based on 16 typical days.[9] In order to represent a full year, the typical days are scaled up by multiplying each typical day with its frequency of occurrence. Each typical day consists of eight time slices representing three consecutive hours.

In the second stage, the dispatch of the two power systems, *No-CC-anticipation* and *CC-anticipation*, is recalculated under a variety of possible climate change futures. As such, the performance of the two design strategies under different climate change impact scenarios can be assessed. In this second stage, the cost-optimal power plant capacities resulting from the two investment planning model runs are fixed, i.e. the capacity variables $\bar{\mathbf{x}}$ are treated as parameters $\bar{x}$:

$$\bar{x}_{i,m,y,dispatch} = \bar{\mathbf{x}}_{i,m,y,invest} \tag{4.2}$$

The dispatch of power plants is then calculated for single years running optimization problem (4.1) with fixed power plant capacities (4.2). Calculating single years without the investment stage allows to apply the full temporal resolution and consequently to consider the full variability and flexibility needs of the power system.

[9] As shown by Nahmmacher et al. (2016b), even less than 10 typical days are sufficient to obtain investment planning results that are similar to results based on a 365-day resolution.

4.2.3 Clustering of variable renewable energy and load data

In order to study power systems with high shares of variable renewable energy, a detailed representation of weather-dependent renewable energy sources is required. However, in order to keep the large-scale investment planning model computationally tractable, the spatial and temporal resolution of wind and solar as well as load data has to be reduced. This analysis applies a two-step clustering approach as described in Peter and Wagner (2018), which will be briefly introduced in the following. A description of the utilized high-resolution data set will be given in Section 4.3.2.

In a first step, the spatial resolution is reduced by clustering the spatially high-resolved wind and solar data into representative wind and solar regions, where the number of regions for wind onshore and solar is chosen based on the surface area of each country. Wind offshore is accounted for by two regions per country, where applicable, with one region with water depths smaller than 50 m for bottom-fixed offshore wind turbines and one region with water depths between 50 m and 150 m for floating offshore wind turbines. Aggregated over Europe, this results in 54 representative regions for wind onshore and solar, respectively, and 41 representative regions for wind offshore.[10] Wind onshore, wind offshore and solar are clustered independently in order to capture the spatial properties of the different energy sources. As clustering method, this analysis applies the k-means clustering algorithm. After the spatial clustering, the time series of the representative regions are calculated by averaging over all data points within the respective cluster. Figure 4.1 shows exemplary spatial clustering results for France, where each data point is represented by a dot and color coding represents the resulting representative regions.

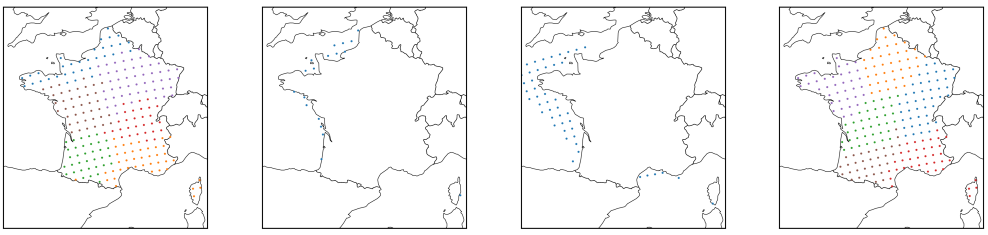

(a) Wind onshore (b) Wind offshore < 50m (c) Wind offshore > 50m (d) Solar

Figure 4.1: Results of spatial clustering for France for different variable renewable energy sources.

[10] See Table 4.12 in Appendix 4.6 for a complete list of the number of representative regions per country and variable renewable energy resource.

In a second step, a temporal clustering is performed in order to identify typical days at full hourly resolution. The goal of the temporal clustering is to reduce the temporal resolution without losing the statistical properties of weather-dependent VRE and load. As input for the temporal clustering, the spatially reduced VRE data, i.e. the time series of the representative regions determined in the first clustering step, and load time series on a country-level are combined as described in Section 4.3.2. This analysis applies a ward clustering algorithm for the temporal clustering and follows the approach presented in Nahmmacher et al. (2016a).

4.3 Scenario definition and data

4.3.1 Scenario definition

The scenarios applied in this study are based on two electricity system design strategies. The *No-CC-anticipation* system is based on a strategy of no climate change impacts anticipation. As such, for the investment planning, the social planner assumes no changes in, e.g. wind resources or cooling water availability due to climate change. The *CC-anticipation* system, on the other hand, foresees and takes into account impacts of climate change when planning power plant capacity investments.[11]

The two system designs are then dispatched under a variety of possible futures. Thereby, a set of seven scenarios is analyzed in order to study the order of magnitude of isolated climate change impacts and compare the performance of the two electricity system designs under all climate change impacts combined (Table 4.1). The first scenario, *No-CC*, represents the *No-CC-anticipation* system dispatched under no climate change impacts. The next four scenarios are defined by the *No-CC-anticipation* system being subject to four isolated impacts of climate change during high-resolution dispatch, namely impacts on variable renewable energy resources (*CC-VRE*), impacts on hydro power (*CC-hydro*), impacts on cooling water availability for thermal power plants (*CC-therm*) and impacts on electricity demand (*CC-eldem*). In the last two scenarios, *CC-all* and *CC-all-anticipation*, the two system designs *No-CC-anticipation* and *CC-anticipation* are dispatched under all climate change impacts combined.

Comparing the five scenarios *CC-VRE*, *CC-hydro*, *CC-therm*, *CC-eldem*, and *CC-all* to scenario *No-CC* then allows to analyze and compare the order of magnitude of the

[11] Note that the impacts of climate change applied in the first stage (investment planning) are assumed to emerge from 2050 onwards.

Scenario name	Investment stage	Dispatch stage
No-CC	No climate change anticipation	No climate change impacts
CC-VRE	No climate change anticipation	Climate change impact on VRE
CC-hydro	No climate change anticipation	Climate change impact on hydro power
CC-therm	No climate change anticipation	Climate change impact on thermoelectric power
CC-eldem	No climate change anticipation	Climate change impact on electricity demand
CC-all	No climate change anticipation	All climate change impacts combined
CC-all-anticipation	Climate change anticipation	All climate change impacts combined

Table 4.1: Scenario definition.

isolated and combined impacts of climate change on the *No-CC-anticipation* system, respectively. Subsequently, a comparison of scenario *CC-all-anticipation* to scenario *CC-all* analyzes the behaviour of the two system designs when dispatched under a future with climate change impacts. Thereby, the performance of the two systems in dealing with climate change impacts can be assessed.

Next to the differences in scenario definition discussed in Table 4.1, all scenarios are based on an identical scenario framework as described in the following. The European electricity sector is subject to a decarbonization of minus 95 % in 2050 compared to 1990, implemented as yearly CO_2 quotas. From 2050 until 2120, the CO_2 quota is kept constant. Additional emission reduction targets for the intermediate years require a 21 % reduction in 2020 compared to 2005 and 43 % reduction in 2030 compared to 2005. For 2040, the emission reduction target is linearly interpolated. The emission reduction targets for 2020, 2030 and 2050 are based on official reduction targets formulated by the European Commission.[12]

Existing capacities in 2015 are taken from a detailed database developed at the Institute of Energy Economics at the University of Cologne, which is mainly based on the Platts WEPP Database (Platts (2016)) and constantly updated. Based on these start values, the model optimizes the European electricity system until the year 2120 in 10-year time steps from 2020 onwards. Investment into nuclear power is only allowed for countries with no existing nuclear phase-out policies. Investments in carbon capture and storage (CCS) technologies are not allowed due to a general lack of social acceptance in European countries. Fuel costs and investment costs for new generation capacities are based on the World Energy Outlook 2017 (IEA (2017b)). Yearly national electricity consumption is assumed to develop according to the ENTSO-E Ten-Year Network Development Plan 2018 (ENTSO-E (2018)) with the values being kept constant from 2040 onwards. Transmission between countries is represented by net transfer capacities (NTC), which are assumed to be extended

[12] See https://ec.europa.eu/clima/policies/strategies for detailed explanations.

according to the ENTSO-E Ten-Year Network Development Plan 2018 (ENTSO-E (2018)). See Appendix 4.6 for a detailed presentation of numerical assumptions.

4.3.2 Data for variable renewable electricity generation and load

Next to the parameters used for scenario definition described in the previous section, a detailed representation of weather-dependent renewable energy sources is required in order to study power systems with high shares of VRE. This analysis applies a dataset for wind and solar resources for the historical 30-year time period (1970 - 1999) based on the EURO-CORDEX project (Jacob et al. (2014)).[13] The original data is resolved on a 0.11°grid (about 12.5 km) in 3-hourly resolution. For computational tractability, every fourth grid point of the original data was considered for this analysis, resulting in a grid of about 50 km in 3-hourly resolution. Wind speeds, which are available at 10 m, are extrapolated via power law to the respective hub height as in Henckes et al. (2019). Subsequently, wind speeds are converted to electricity generation via power curves based on state-of-the-art onshore and offshore wind power plants according to Henckes et al. (2019).[14] Based on this, a consistent hourly[15] 30-year time series of wind power capacity factors over whole Europe is generated for historical climate wind speeds (1970 - 1999).

Solar data is generated based on solar irradiance data of the EURO-CORDEX project for the same 50 km grid over Europe as for wind power generation. The methodology used to convert solar irradiance to electricity is described in detail in Frank et al. (2018) and Henckes et al. (2019). Again, based on this, a consistent hourly 30-year time series of solar power capacity factors over whole Europe is generated for historical climate irradation (1970 - 1999).

Load is assumed to be inelastic except for electricity demand from storage and power-to-x processes, which is part of the integrated optimization and thus endogenously determined. The assumption of inelastic load can be justified by Lijesen (2007), who found that price responsiveness during times of scarcity is low. Load

[13] The standard WMO climate normal is defined as a 30-year average, according to the World Meteorological Organisation (WMO) (Arguez and Vose (2011)). The EURO-CORDEX project provides - next to historical time periods - also data for future climate projections. Such data will be used to estimate impacts of climate change on wind and solar, as described in Section 4.3.3.

[14] This analysis is based on the onshore wind turbine Enercon E-126 EP4 and the offshore wind turbine Vestas V164. Power curves for both turbines were determined based on technical data on the manufacturer websites.

[15] The hourly time series are generated by taking identical values for each 3-hour interval of the original data in 3-hourly resolution.

data is based on hourly national vertical load[16] data for all considered countries for the years 2011 - 2015, taken from ENTSO-E (2016a). It is important to note that such historical load measurements are the result of a functioning electricity market and may therefore include some price responsiveness of consumers or load shedding. Nevertheless, historical load is commonly seen as the best approximation of actual load time series. After normalization, the load data is scaled with the assumed yearly future electricity demand development in order to generate consistent time series.[17]

In order to generate a good representation of the joint probability space of wind, solar and load, each of the five load years in then combined with the 30 years of VRE data, while wind and solar data are kept synchronous.[18] This results in an ensemble of 150 synthetic years of hourly load and VRE data for historical climate data (1970 - 1999).

For the investment planning model, the 150 synthetic years are then used as input for the temporal clustering as described in Section 4.2.3, resulting in one year represented by 16 typical days.

For the high-resolution dispatch calculations, the 150 synthetic years are clustered to one year represented by 365 typical days. In doing so, the high-resolution dispatch can be run with a typical year generated from a large ensemble of data.

4.3.3 Description of climate change impacts

The impacts of climate change and resulting interaction effects within the power system can be isolated and analyzed by comparing the power system dispatch based on future climate projection data to the power system dispatch based on historical data, assuming that historical climate is still prevailing in the future in a world without climate change.

This analysis focuses on climate change scenario RCP8.5 (Meinshausen et al. (2011)), the most extreme scenario used in the latest IPCC reports. The likely range of global

[16] National vertical load = national net electricity consumption + network losses.

[17] By scaling the normalized historical load time series with a future demand development scenario, it is assumed that the temporal structure of electricity demand does not change in the future. Possible changes in the temporal demand structure, e.g. from increasing electrification of the mobility or heat sector, are therefore not accounted for. However, changes in the temporal demand structure from storage and power-to-x processes are endogenously accounted for via the integrated optimization.

[18] Note that hereby, stochastic independence between load and VRE is assumed. Correlations between wind and solar, however, are accounted for via applying synchronous time series.

average temperature increase by the end of century (2081 - 2100) associated with RCP8.5 amounts to 3.2 - 5.4 °C compared to pre-industrial levels (1850 - 1900), resulting in severe climate change impacts (IPCC (2014b)).[19] In combination with the 95 % decarbonization target for the European power sector, the realization of the RCP8.5 climate change scenario is constrained to a scenario of prevalent inaction with respect to decarbonization on continents other than Europe. As such, the underlying scenario of this analysis can be interpreted as an extreme scenario with strong climate action in the European power sector, accompanied with a strong weather-dependency due to VRE, and modest climate action in the rest of the world.

Impact of climate change on wind and solar generation

In order to study the impact of climate change on wind and solar power generation, data representing future changes in wind and solar energy potentials over Europe at a high temporal resolution are required. Such climate change affected weather datasets are, amongst others, available as ensemble members of the EURO-CORDEX project (Jacob et al. (2014)). In addition to the historical 30-year period (1970 - 1999), wind and solar power generation timeseries were calculated for a future 30-year period with RCP8.5 climate projection (2070 - 2099). In order to guarantee consistency, both 30-year periods were calculated using the same GCM-RCM[20] model chain: EC-EARTH (GCM) and RCA4 (RCM) from the EURO-CORDEX project. The original data from the RCM simulations is resolved on a 0.11° grid (about 12.5 km) in 3-hourly resolution. As for the historical data, for computational tractability, every fourth grid point of the original data is considered in this analysis, resulting in a grid of about 50 km in 3-hourly resolution. Wind speeds at 10 m are extrapolated to hub height and converted to electricity analogous to the historical dataset. Combined with the five load years, again 150 synthetic years are used as input for the temporal clustering as described in Section 4.3.2.

The resulting relative change in capacity factors of wind and solar energy due to RCP8.5 climate change in 2100 is shown in Figure 4.2. The general trend of a

[19] Climate change impacts of RCP8.5 include more frequent hot temperature extremes and heat waves, extreme precipitation events, increased ocean acidification and sea level rise, strong reduction in near-surface permafrost and global glacier volume. Associated future risks of a RCP8.5 climate crisis affect food security, poverty, displacement of people, intensify competition for water and exacerbate already existing health problems (IPCC (2014b)).

[20] Generation circulation models / global climate models (GCM) are global numerical climate models on a coarse spatial grid, which replicate large-scale circulation features of the climate. In order to increase the spatial resolution, GCM data are then used to drive regional climate models (RCM), which yield regionally higher resolved data, e.g., for Europe.

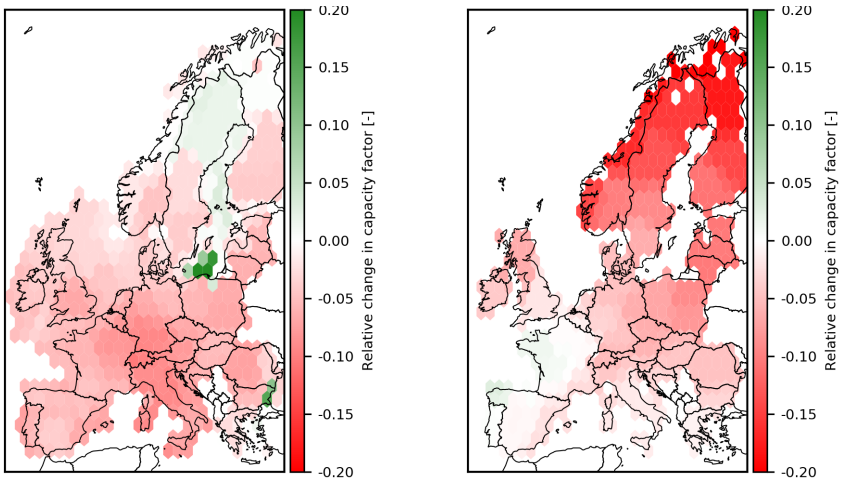

(a) Wind power (b) Solar power

Figure 4.2: Relative change in wind and solar power capacity factor in 2100.

reduction in wind onshore capacity factor of -5 % to -15 % in central and southern Europe, and an increase in capacity factor by 5 % to 15 % in some parts of northern Europe is in line with previous literature (e.g., Moemken et al. (2018)). Changes in solar PV capacity factor include reductions in central and northern Europe from -2 % to -20 % and small increases in southwestern Europe by 2 %, similar to results in, e.g., Jerez et al. (2015).

Impacts of climate change on hydro generation

In order to estimate the impact of climate change scenario RCP8.5 on hydro power potential in Europe, this analysis builds on data provided by Schlott et al. (2018). They use three ensemble members of the EURO-CORDEX project as climate change affected weather datasets for water runoff under RCP8.5. Historical hydro inflow is characterized by major seasonal patterns. For example in Norway, Austria and Italy, one can observe major peaks during late spring due to snow melting and large inflow in autumn with its predominant rainfall. Climate change reduces the size of the spring peaks considerably, while at the beginning and end of the year, inflow increases (Schlott et al. (2018)). In Spain, however, the seasonal inflow pattern looks different: It shows homogeneous amounts during the whole year except for summer, where the inflow is almost inexistent. Climate change exacerbates this pattern in Spain, combined with a considerable overall reduction in total inflow (Schlott et al. (2018)).

Austria	+18.4 | +12.3 %	Germany	-0.6 | -1.7 %	Norway	+2.6 | +21.1 %
Belgium	-0.5 | +1.6 %	Great Brit.	+4.6 | +4.5 %	Poland	+1.8 | +1.0 %
Bulgaria	-18.2 | -17.9 %	Greece	-29.4 | -27.6 %	Portugal	-18.8 | -20.1 %
Croatia	-7.6 | -10.5 %	Hungary	-5.1 | -6.3 %	Romania	-4.2 | -0.2 %
Czech Rep.	+0.7 | +1.9 %	Ireland	-2.1 | -2.6 %	Slovakia	n.a. | +1.3 %
Denmark	n.a. | +0.6 %	Italy	-3.6 | -5.7 %	Slovenia	-3.4 | -4.6 %
Estonia	n.a. | +20.6 %	Latvia	n.a. | +18.2 %	Spain	-23.3 | -24.1 %
Finland	+0.5 | +23.9 %	Lithuania	+23.9 | +24.7 %	Sweden	+1.8 | +25.6 %
France	-7.5 | -9.7 %	Netherlands	n.a. | -2.3 %	Switzerland	+20.5 | +15.3 %

Table 4.2: Changes in availability for hydro potential (Reservoir | Run-of-river), based on Schlott et al. (2018).

In this analysis, country-specific average values of yearly changes in hydro potential from three ensemble members of the EURO-CORDEX project used in Schlott et al. (2018) were applied (Table 4.2). The end-of-century hydro potential changes in European countries range between -29 % and 24 % for reservoir hydro inflow, and between -28 % and 26 % for run-of-river hydro.

Impacts of climate change on thermoelectric generation

Climate change is likely to impact cooling water availability for thermoelectric power plants. In particular coal-fired and nuclear power plants rely on large volumes of cooling water. Compared to other sectors like agriculture, industry or domestic use, the thermoelectric power sector has the largest share in water consumption, accounting for about 43 % of total surface water withdrawal (Vliet et al. (2013)). In recent warm and dry summers (e.g. 2003, 2006, 2009 and 2018), several thermoelectric power plants, in particular nuclear power plants, were forced to reduce electricity generation because of environmental restrictions on cooling water use based on water availability and legal temperature limits (Förster and Lilliestam (2010)). Several studies use simulations of daily river flow and water temperature projections using a physically based hydrological-water temperature modeling framework (e.g., Vliet et al. (2013), Tobin et al. (2018)). Their results show in line that due to climate change, periods with low summer river flows in combination with high water temperatures are expected to occur more frequently in Europe. Low flow values, defined as the 10-percentile of daily river flow, are projected to decline all over Europe except for Scandinavia. Strongest declines are expected in southern and south-eastern European countries like Spain, Italy, Bulgaria, Romania and Greece.

This analysis builds on data from Tobin et al. (2018) to estimate the impacts of climate change on cooling water availability of thermoelectric power plants (Table

Austria	-8.3 %	Germany	-8.3 %	Norway	0.0 %
Belgium	-7.9 %	Great Britain	-8.3 %	Poland	-6.4 %
Bulgaria	-10.7 %	Greece	-10.0 %	Portugal	-0.8 %
Croatia	-8.4 %	Hungary	-5.6 %	Romania	-9.0 %
Czech Republic	-7.3 %	Ireland	-4.0 %	Slovakia	-7.7 %
Denmark	0.0 %	Italy	-8.9 %	Slovenia	-9.4 %
Estonia	-8.4 %	Latvia	-8.8 %	Spain	-10.9 %
Finland	-5.1 %	Lithuania	-8.6 %	Sweden	-5.5 %
France	-8.6 %	Netherlands	-8.4 %	Switzerland	-9.6 %

Table 4.3: Changes in availability in thermoelectric generation, based on Tobin et al. (2018) and Vliet et al. (2013).

4.3).[21] The reductions in thermoelectric power plant availability are imposed on nuclear, lignite and coal power plants.[22] Yearly availability reduction values in European countries range between -10.9 % and 0 %.

Impacts of climate change on electricity demand

Next to electricity supply, climate change is also expected to impact electricity demand due to adaptive responses to a changing environment. Short-term human responses to weather shocks and long-term adaptation to changing climatic conditions will alter electricity consumption in all sectors (Wenz et al. (2017)). Electricity demand for heating is projected to decrease in northern Europe and electricity demand for cooling will increase in southern Europe (Eskeland and Mideksa (2010)). Wenz et al. (2017) statistically estimate country-level dose-response functions between total electricity load and ambient temperature. The dose-response functions are then used to compute national electricity loads for temperatures that lie outside each country's currently observed temperature range. This allows the authors to impose end-of-century climate under RCP8.5 on today's European economies, ceteris paribus, e.g., with respect to the economic structure. They find a significant north-south polarization across Europe with increases in annual electriciy consumption in southern and western Europa and decreases in northern Europe.

In this analysis, data from Wenz et al. (2017) were used to estimate the end-of-

[21] The estimated impacts in Tobin et al. (2018) are discussed to be upper range estimates, as all thermoelectric power plants are assumed to be using river water (see discussion in Tobin et al. (2018)). To account for this and possible adaptive measures to reduce cooling water dependence, a factor accounting for adaptive measures based on Vliet et al. (2013) was applied on the cooling water availability reduction values from Tobin et al. (2018).

[22] Note that in some locations, lignite power plant cooling systems are connected to mine water, which reduces their vulnerability to low river flow occurrences. This does, however, not affect the results of this analysis, as in decarbonized power systems, lignite power plants without carbon capture and storage play no role.

Austria	-1.0 %	Germany	-0.8 %	Norway	-0.3 %
Belgium	-0.7 %	Great Britain	-1.7 %	Poland	-1.1 %
Bulgaria	+5.5 %	Greece	+7.3 %	Portugal	+3.6 %
Croatia	-2.5 %	Hungary	+0.6 %	Romania	+1.6 %
Czech Republic	-1.2 %	Ireland	-1.1 %	Slovakia	-0.8 %
Denmark	-1.4 %	Italy	+1.3 %	Slovenia	+0.4 %
Estonia	-3.0 %	Latvia	-2.4 %	Spain	+5.2 %
Finland	-2.5 %	Lithuania	-1.8 %	Sweden	-3.0 %
France	+0.9 %	Netherlands	-0.4 %	Switzerland	-1.3 %

Table 4.4: Changes in electricity demand, based on Wenz et al. (2017).

century changes in annual electricity consumption under RCP8.5 (Table 4.4). As relative percentage changes are calculated with respect to today's economies, this analysis applies the changes to today's electricity consumption in order to add the absolute change in consumption to the future development of country-level electricity consumption. The end-of-century electricity consumption changes in European countries range between -3 % and 7 %.

4.4 Results

Based on the introduced modeling framework and parametrization, this section assesses the resulting impacts of climate change on the European electricity system. Section 4.4.1 starts with a brief discussion of general trends of the cost-optimal capacity mix towards the end-of-century under a 95 % decarbonization target for the *No-CC-anticipation* system, i.e., a system without climate change anticipation. Based on this and given the assumptions on climate change impacts presented before, the performance of the *No-CC-anticipation* system under various climate change impacts is discussed. By comparing the effects, predominant impacts of climate change on the electricity system can be identified. Section 4.4.2 then discusses the cost-optimal *CC-anticipation* system, which anticipates climate change impacts. The section concludes by discussing allocation effects for wind and solar generation capacities as a consequence of climate change impacts.

4.4.1 Impacts of climate change on a system with no climate change anticipation strategy

The transition towards a cost-optimal 95 % decarbonization of the European electricity sector is driven by large-scale investments in wind and solar, as shown for the *No-CC-anticipation* system in Figure 4.3(a). In 2100, wind onshore capacity

reaches 530 GW, wind offshore 50 GW and solar PV 481 GW. Nuclear power still plays a role in 2100 (79 GW), its cost-optimal capacity is however reduced by 35 % compared to 2020 due to competitive disadvantages. Flexibility is provided by interconnector capacities, storage (116 GW), hydro power (180 GW) and mainly open-cycle gas turbines (343 GW OCGT, 57 GW CCGT). After 2050, the cost-optimal mix of power plants sees only slight changes, mainly driven by the decommissioning of coal and nuclear power plants being replaced by VRE and gas power plants. In 2040, 1 GW of electrolysis starts to feed-in hydrogen into the gas grid for subsequent re-electrification. In 2050, the electrolysis capacity for decarbonized gas production reaches 28 GW, while in 2100, it is slightly reduced to 24 GW as the residual power system is further decarbonized via other technologies. Figure 4.3(b) presents the high-resolution dispatch of the *No-CC-anticipation* system in 2100 for a world without climate change impacts. About 63 % of electricity generation comes from VRE (42 % wind onshore, 6 % wind offshore, 15 % solar PV), 14 % from nuclear and hydro, respectively, 3 % from gas (with 18 % of the gas being decarbonized via hydrogen feed-in) and 2 % from biomass. In 2050, a small amount of lignite and coal capacity is kept online for capacity provision (Figure 4.3(a)), however its electricity generation is phased-out before 2050 due to decarbonization constraints.[23]

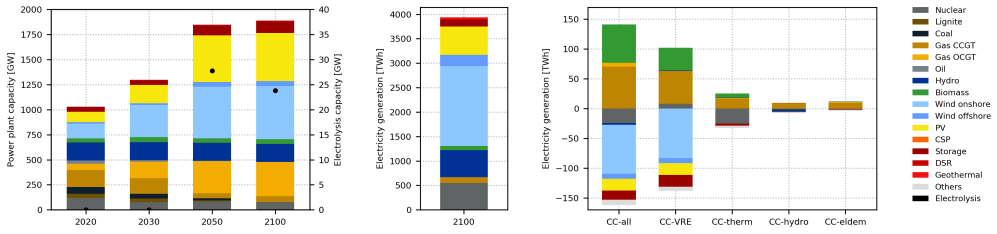

(a) Capacity (b) Generation (c) Generation difference in 2100

Figure 4.3: Power plant/electrolysis capacity, electricity generation in 2100, and difference in electricity generation in 2100 due to climate change impacts (*No-CC-anticipation* system).

In order to study the effects of climate change on the *No-CC-anticipation* system, the system is dispatched under various impacts of climate change as described in Section 4.3.3. Figure 4.3(c) shows the resulting difference in electricity generation compared to the dispatch in a world without climate change. Comparing the order of magnitude of isolated impacts, climate change impacts on wind and solar resources have the largest consequences for electricity generation (*CC-VRE*). The re-

[23] The suitability and economic business case of lignite and coal power plants being used for flexible capacity provision at very low capacity factors is debatable and would need a further in-depth analysis beyond the scope of this work.

duced resource availability of VRE results in reduced electricity generation, mainly from wind onshore, but also wind offshore and solar PV. Given the fixed power plant fleet of the *No-CC-anticipation* system, the lack in electricity generation is offset by increased utilization of generation assets with upwards potential in capacity factor, such as gas and biomass power plants.

The next largest impact on the electricity system, however on a much smaller level, stems from climate change impacts on thermoelectric generation due to changes in cooling water availability (*CC-therm*). Mainly coal-fired and nuclear power plants will be affected due to their large consumption of cooling water. However, in view of the 95 % decarbonization target, in 2100 only nuclear capacity is still part of the cost-optimal power plant mix, whereas coal power plants mostly exit the market until 2050. The reduction in cooling water availability leads to an aggregated reduction in nuclear power generation of 25 TWh (4.6 %) in 2100. The missing generation is mainly compensated by gas generation (partly biogas), combined with some additional biomass generation and a gas fuel-switch from other generation sources to stay within the decarbonization target.

Impacts of climate change on hydro power potential lead to an aggregated reduction in hydro generation of 4 TWh on a European level (*CC-hydro*). On a region-specific scale, however, local climate change impacts on hydro potential are much larger, resulting in changes in hydro generation ranging between -29 % and 24 % for reservoir hydro, and between -28 % and 26 % for run-of-river hydro. The reduction in hydro generation on a European level is mainly compensated by increased gas generation (partly fueled with decarbonized gas from hydrogen feed-in and biogas), and minor shifts with other generation sources to keep the emissions balance.

Impacts of climate change on electricity demand stem from adaptive responses to changing climatic conditions (*CC-eldem*). On a European level, the cumulative change in electricity demand amounts to 8 TWh of additional demand. With heterogenous demand changes in different countries, ranging between -3 % and 7 %, the reaction of the electricity system also differs between countries. As a general trend on a European level, the additional demand is to large parts supplied by additional gas generation, which is partly decarbonized with feed-in hydrogen. To keep the emissions balance, some fuel-switch to gas from other generation with higher emission factors is observed.

All climate change impacts combined lead to cumulative effects on the power system due to decreased VRE, nuclear, hydro and storage generation (*CC-all*). The missing generation is replaced by gas and biomass generation, combined with a fuel-

switch to gas from other generation to comply with the decarbonization target.

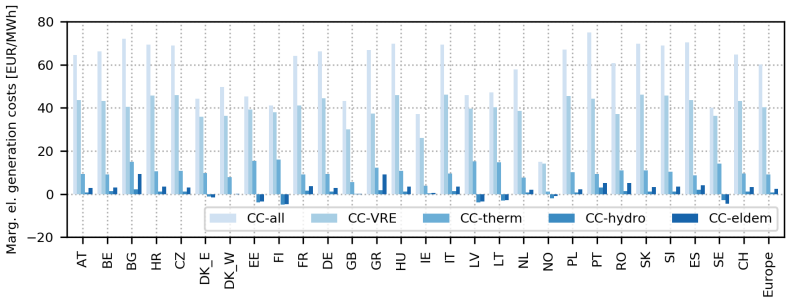

Figure 4.4: Differences in marginal electricity generation costs in 2100 due to climate change impacts (*No-CC-anticipation* system).

The changes in electricity generation mix due to climate change impacts translate into changes in marginal electricity generation costs (Figure 4.4). In line with Figure 4.3(c), the reduction in wind and solar generation (*CC-VRE*) due to climate change have the largest effect on annual mean marginal electricity generation costs, with absolute and relative increases ranging from 14 to 46 EUR/MWh and 43 % to 69 %, respectively. The impact of climate change on thermoelectric generation due to cooling water restrictions (*CC-therm*) also shows an increasing effect on marginal electricity generation costs, however on a much smaller scale with increases ranging from 1 to 16 EUR/MWh (9 % to 43 %). Impacts of climate change on hydro resource potential (*CC-hydro*) shows heterogeneous effects on marginal electricity generation costs, in line with the opposite direction of change. I.e., increasing hydro potential leads to decreasing marginal electricity generation costs. Resulting changes in marginal electricity generation costs range between -5 and 3 EUR/MWh (-9 % to 3 %). Changes in demand due to climate change (*CC-eldem*) also result in heterogeneous changes in marginal electricity generation costs, in line with the sign change compared to the dispatch in a world without climate change. Values range between -5 and 9 EUR/MWh (-8 % to 11 %). All climate change impacts combined (*CC-all*) lead to strong increases in marginal electricity generation costs between 15 and 75 EUR/MWh (100 % to 178 %).

The general trend of higher biomass and gas generation, partly fueled with decarbonized gas from hydrogen feed-in and biogas, combined with a fuel-switch from higher emitting other generation to gas results in higher fuel costs in 2100 (Figure 4.5).

Also, given the fixed decarbonization target and reduced generation from low-carbon technologies, the endogenous prices for carbon permits are bound to in-

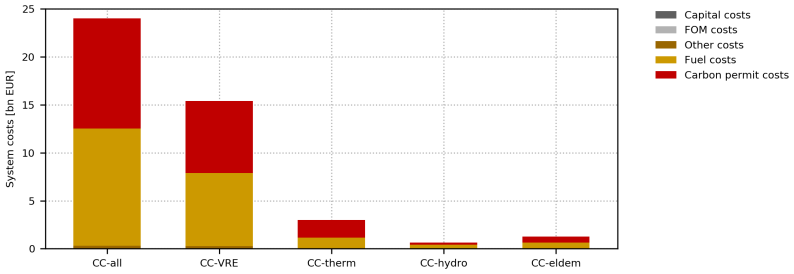

Figure 4.5: Difference in system costs in 2100 due to climate change impacts (*No-CC-anticipation* system).

crease, resulting in higher spendings for carbon permits. Note that, as the power plant fleet is fixed in all scenarios (*No-CC-anticipation* system), capital costs and fixed operation and maintenance (FOM) costs do not change. Absolute and relative aggregated additional system costs over Europe amount to 15.4 bn EUR (8 %) in 2100 for changing wind and solar resources due to climate change (*CC-VRE*), and to 0.6 bn EUR to 3.0 bn EUR (0.3 % to 1.6 %) for changes in thermoelectric cooling water availability (*CC-therm*), hydro potential (*CC-hydro*) and electricity demand (*CC-eldemand*). Combined impacts of climate change on the *No-CC-anticipation* system result in additional costs of 24 bn EUR in 2100, which represents an increase of 12 %.

4.4.2 Impacts of climate change on a system with climate change anticipation strategy

In order to investigate changes in optimal system configuration when anticipating impacts of climate change, the investment planning model is run based on a climate change anticipation strategy, i.e., taking into consideration expected impacts of climate change. Thereby, from 2050 onwards, the social planner sees in perfect foresight what changes to wind, solar and hydro resources are expected to occur, as well as to which extent cooling water will be available and how electricity consumption will evolve under strong RCP8.5 climate change.

Figure 4.6(a) shows the resulting evolution of the cost-optimal European power plant mix for a 95 % decarbonization target with anticipation of climate change impacts. Again, in the long term, the *CC-anticipation* power system is mainly based on wind and solar capacity, while hydro, storage and gas serve as back-up capacity.

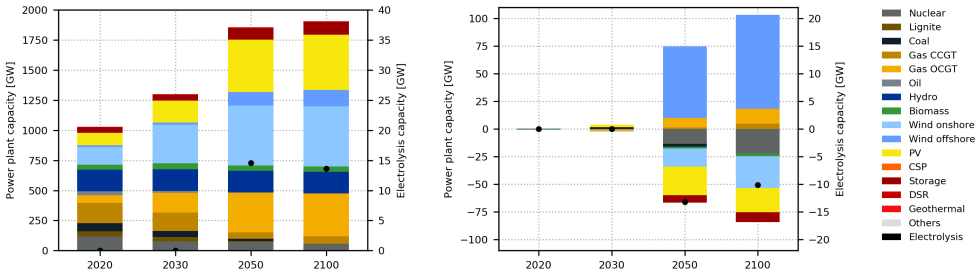

(a) Capacity (b) Capacity difference

Figure 4.6: Power plant/electrolysis capacity (*CC-anticipation* system) and capacity difference compared to *No-CC-anticipation* system.

In contrast to the *No-CC-anticipation* system, the *CC-anticipation* system takes into consideration impacts of climate change. As such, the expected reduced availability of cooling water for nuclear power plants results in a 22 GW reduction in cost-optimal nuclear capacity in Europe in 2100 (Figure 4.6(b)). Also, expected reduced wind onshore and solar resource potentials result in 29 GW less wind onshore and 22 GW less solar PV capacity. At the same time, wind offshore sees a large increase of 85 GW over Europe. Apparently, even though wind offshore wind speeds are also expected to slightly decline in most parts of Europe as a result of climate change (Figure 4.2), the combination of reduced base-load nuclear capacity, cost structures and local capacity factor reductions leads to a shift in competitiveness between wind onshore and offshore. Overall, the *CC-anticipation* system increases its VRE share, compared to the *No-CC-anticipation* system. Due to the reduced variability of the changed mix of VRE towards wind offshore, cost-optimal storage capacity is reduced by 9 GW. Also, 18 GW of additional gas capacities are built (13 GW OCGT, 5 GW CCGT). The expectation of higher marginal electricity generation costs in the *CC-anticipation* system results in a reduction of cost-optimal electrolysis capacity by 10 GW, because the competitiveness of other decarbonization options, such as biogas, is increased compared to the higher power-to-x fuel prices.

Cost-optimal electricity generation of the *CC-anticipation* system under combined climate change impacts in 2100 is characterized by a stronger dominance of VRE electricity generation, accounting for a share of 66 % (Figure 4.7(a)). In line with the difference in installed capacity, electricity generation from wind offshore increases to 15 % of total generation, while the share of wind onshore and nuclear decreases to 38 % and 10 %, respectively.

In order to assess the system performance in a world with climate change, in sce-

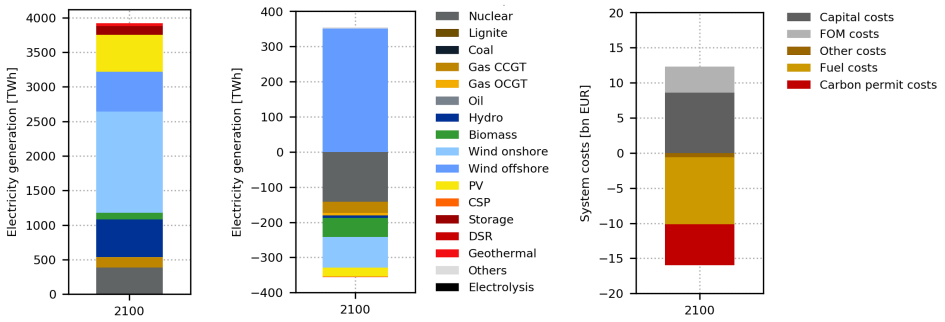

(a) Generation (b) Generation difference (c) System costs / emissions difference

Figure 4.7: Electricity generation in 2100 (*CC-anticipation* system) and difference in generation, system costs and emissions in 2100 compared to *No-CC-anticipation* system, dispatched under combined climate change impacts.

narios *CC-all* and *CC-all-anticipation*, the two strategies *No-CC-anticipation* and *CC-anticipation* are dispatched under all climate change impacts combined. In the *CC-anticipation* system, electricity generation from wind offshore sees a strong increase of 351 TWh compared to the *No-CC-anticipation* system under combined climate change impacts (Figure 4.7(b)). It partly replaces the increased gas and biomass generation being dispatched in the *No-CC-anticipation* system when subject to combined climate change impacts. On the other hand, it compensates for reduced nuclear, hydro, wind onshore and solar PV electricity generation due to their reduced capacity factors and resulting reduced cost-optimal capacities under combined climate change impacts.

Reduced nuclear, gas (partly from power-to-x) and biomass generation translates into reduced fuel costs of -9.5 bn EUR in 2100 (Figure 4.7(c)). As the *CC-anticipation* system is able to optimize its investments in decarbonized technologies, the carbon permit price is reduced compared to the *No-CC-anticipation* system, leading to a reduction in carbon permit costs of -5.8 bn EUR. While the *CC-anticipation* system features increased capital and fixed operation and maintenance costs, mainly driven by wind offshore investments, they are overcompensated by the fuel and carbon permit cost reductions. As a result, the cost-optimal power plant mix of the *CC-anticipation* system outperforms the *No-CC-anticipation* system in terms of total system costs by -3.6 bn EUR in 2100, which represents a reduction of -1.7 %.

As the *CC-anticipation* system is optimized with respect to climate change impacts, its cost-optimal power plant mix leads in most parts of Europe to lower marginal electricity generation costs when dispatched under combined climate change impacts,

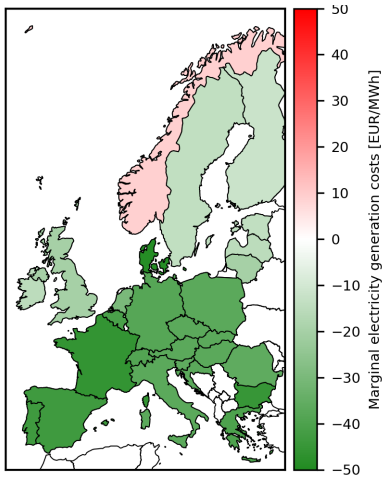

Figure 4.8: Difference in marginal electricity generation costs of the *CC-anticipation* system compared to the *No-CC-anticipation* system, dispatched under combined climate change impacts.

compared to the *No-CC-anticipation* system (Figure 4.8).

This is mainly the result of increased VRE generation in the *CC-anticipation* system compared to increased gas and biomass generation in the *No-CC-anticipation* system, with resulting higher fuel and carbon permit costs to compensate for unforeseen climate change impacts. Interestingly, however, in Norway, a reduction in wind onshore capacity in the *CC-anticipation* system due to lower wind onshore capacity factors leads to an increase in marginal electricity generation costs compared to the *No-CC-anticipation* system. Reductions in marginal electricity generation costs in single countries range from -12 to -46 EUR/MWh, except for Norway with an increase of 9 EUR/MWh. On average, the marginal electricity generation costs in Europe decrease by -34 EUR/MWh.

Allocation effects of climate change anticipation on wind and solar capacity

Optimal allocation of wind onshore, wind offshore and solar PV capacity is influenced by both the impact of climate change on wind and solar resources (Figure 4.2) as well as the configuration of the residual power system. Figure 4.9(a) and 4.9(b) show the optimal allocation of wind onshore and offshore capacity in the *No-CC-anticipation* system and the *CC-anticipation* system, respectively. The resulting allocation effects are depicted in Figure 4.9(c).

Wind onshore capacity is overall reduced by 29 GW over Europe in 2100. Spain and Norway see a reduction in wind onshore capacity of -7 GW and -6 GW, respec-

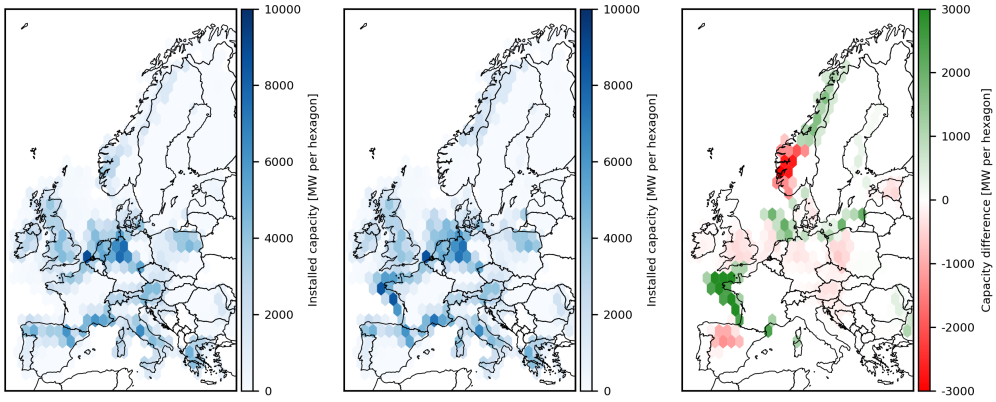

(a) Wind power capacity in 2100: No CC anticipation

(b) Wind power capacity in 2100: CC anticipation

(c) Difference CC anticipation vs no CC anticipation

Figure 4.9: Allocation effects in optimal wind onshore and offshore capacity of the *CC-anticipation* system compared to the *No-CC-anticipation* system in 2100.

tively, while in Norway, there is a shift in optimal capacity allocation from south to the north. Great Britain, Germany, Poland, Austria, Slovenia, and Estonia also face reductions in cost-optimal wind onshore capacity, however at amounts lower than -4 GW. Relative reduction values compared to the total capacity per country range from -3 % to -10 %.

Wind offshore capacity is strongly increased by a total amount of 85 GW in Europe in 2100. The increased offshore wind capacity in the optimal *CC-anticipation* system is mainly located in north-western France (66 GW), the North Sea coast of Germany (10 GW) and Denmark (4 GW), as well as the Baltic Sea coast of Poland (5 GW) and Lithuania (3 GW). The changes in wind offshore capacity allocation is particularly relevant for grid reinforcement planning, due to the high grid connection costs of offshore wind sites and the long lifetime of grid infrastructure.

Changes in cost-optimal solar PV capacity allocation over Europe are depicted in Figure 4.10. Total solar PV capacity is reduced by -22 GW in 2100. Allocation effects of the *CC-anticipation* system compared to the *No-CC-anticipation* system can be observed in southern Germany (-20 GW, -16 %) and western Poland (-2 GW, -2 %).

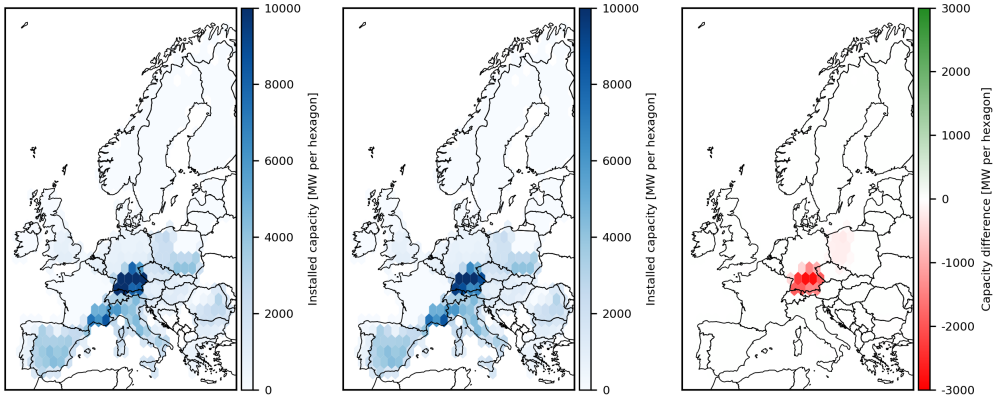

(a) Solar power capacity in 2100: No CC anticipation

(b) Solar power capacity in 2100: CC anticipation

(c) Difference CC anticipation vs no CC anticipation

Figure 4.10: Allocation effects in optimal solar PV capacity of the *CC-anticipation* system compared to the *No-CC-anticipation* system in 2100.

4.5 Conclusions

This article analyzes the impacts of drastic climate change (RCP8.5) on the European electricity system by applying a two-stage modeling framework based on a large-scale partial equilibrium model of the European electricity market. Two electricity systems, which are based on a no climate change anticipation strategy and a climate change anticipation strategy, are dispatched under climate change impacts on wind and solar resources, hydro resources, cooling water availability for thermoelectric generation and electricity demand. Thereby, the order of magnitude of isolated climate change impacts on the no climate change anticipation electricity system is assessed. Building on that, the performance of the two electricity system design strategies is analyzed in a scenario representing the best-guess expectation of future climate change impacts, i.e. a scenario where all climate change impacts are combined.

The analysis shows that the RCP8.5 climate change impact on wind and solar energy resource availability has the largest consequences for the European electricity system, compared to climate change impacts on hydro power, cooling water availability and electricity demand. A system designed without anticipation of climate change impacts reacts to combined climate change impacts with increased gas and biomass electricity generation to compensate for the reduced capacity factors of wind and solar, reduced hydro generation, reduced nuclear generation due to cooling water constraints and increased demand due to climate change. In consequence, system

costs in 2100 increase by 24 bn EUR, or 12 %, due to increased fuel and carbon permit costs. Marginal electricity generation costs show strong absolute and relative increases of 15 to 75 EUR/MWh and 100 % to 178 %, respectively. Applying a system design strategy based on climate change anticipation results in a large increase in cost-optimal wind offshore capacity in 2100 (85 GW), at a reduction of 29 GW wind onshore, 22 GW solar PV and 9 GW storage capacity. Consequently, overall cost-optimal VRE capacity increases. Nuclear capacity is reduced by 22 GW due to lower cooling water availability and resulting competitive disadvantages. The trend towards wind offshore is driven by a combination of reduced base-load nuclear capacity, cost structures and local capacity factor reductions in wind due to climate change, resulting in a shift in competitiveness towards offshore. Compared to a system designed without climate change anticipation, the climate change anticipating system reduces total system costs by 3.6 bn EUR in 2100 in a world with RCP8.5 climate change impacts. Marginal electricity generation costs can thereby be reduced by -12 to -46 EUR/MWh, except for Norway, where reduced wind onshore capacity factors due to climate change lead to an increase in marginal electricity generation costs of 9 EUR/MWh.

Our results imply that impacts of climate change show non-negligible effects on electricity systems with system cost increases up to 12 % when climate change impacts are not anticipated. Ramping up climate ambition to comply with the Paris Agreement and designing mitigation measures to avoid drastic RCP8.5 climate change impacts should therefore be treated with highest priority in order to limit economic damage in a world beyond 1.5 °C global warming, compared to a world with 1.5 °C (Burke et al. (2018), IPCC (2018b)). However, in order to be prepared for futures beyond 2 °C, which are likely from today's perspective, long-term electricity system planning based on energy scenarios from numerical optimization models should account for impacts of climate change. In particular considering the long technical lifetime of certain assets like hydro and nuclear power plants, as well as grid infrastructure, some decisions on the end-of-century electricity system design may have to be taken in the years to come. Thereby, in particular allocation effects in optimal wind onshore and wind offshore capacity should be accounted for. In order to reach cost-optimal allocation as a market outcome, the regulator may design a market environment focusing on transparent price signals, e.g., via nodal pricing. Considering the order of magnitude of isolated climate change impacts, next to impacts on VRE, the regulator is advised to take into consideration constraints in cooling water availability when setting the regulatory framework for cost-optimal power plant investments, including the choice of cooling technology.

In future work, this analysis could be extended to account for different climate change scenarios based on various GCM-RCM model chain combinations to account for the uncertainty of single climate model runs. Furthermore, the effect of increasing the temporal granularity of the impacts on hydro power potential, cooling water availability and electricity consumption could be analyzed. Finally, further research could extend this analysis towards robust decision making considering the uncertainty of different climate change futures.

Acknowledgments

The author thanks Felix Höffler for his helpful comments, Philipp Henckes for the inspiring cooperation and access to the meteorological data, Johannes Wagner for in-depth discussions and Henrike Sommer for her support. The work was carried out within the UoC Emerging Group on 'Energy Transition and Climate Change (ET-CC)'. Funding by the DFG Zukunftskonzept (ZUK 81/1) is gratefully acknowledged.

4.6 Appendix

Sets		
$i \in \mathbf{I}$		Technologies
$m, n \in \mathbf{M}$		Markets
$y \in \mathbf{Y}$		Years
$d \in \mathbf{D}$		Days (**D**: Typical days or all days)
$h \in \mathbf{H}$		Hours (**H**: Reduced hours or all hours)
Parameters		
l	MWh	Exogenous electricity demand
l_{peak}	MWh	Peak electricity demand
x	-	Availability of electricity generator
$\bar{x}$	MW	Electricity generation capacity for dispatch
v	-	Capacity value of electricity generators
$\bar{k}$	MW	Transmission capacity
η	-	Efficiency
δ	EUR/MW	Fixed costs
γ	EUR/MW	Variable costs electricity generation
κ_i	tCO_2eq/MWh	Fuel-specific emission factor
GHG_{cap}	tCO_2eq	Greenhouse gas emissions cap
TC	bn. EUR	Total costs
Variables		
$\bar{\mathbf{x}}$	MW	Electricity generation capacity
$\mathbf{g}$	MWh	Electricity generation
$\mathbf{k}$	MWh	Electricity transmission between markets

Table 4.5: Model sets, parameters and variables.

AT	Austria	FI	Finland	NL	Netherlands
BE	Belgium	FR	France	NO	Norway
BG	Bulgaria	GB	Great Britain	PL	Poland
CH	Switzerland	GR	Greece	PT	Portugal
CZ	Czech Republic	HR	Croatia	RO	Romania
DE	Germany	HU	Hungary	SE	Sweden
DK (East)	Eastern Denmark	IE	Ireland	SI	Slovenia
DK (West)	Western Denmark	IT	Italy	SK	Slovakia
EE	Estonia	LT	Lithuania		
ES	Spain	LV	Latvia		

Table 4.6: Country codes.

a	Years
bn	Billion
CCGT	Combined-cycle gas turbine
CCU	Carbon capture and utilization
CO_2	Carbon dioxide
CSP	Concentrated solar power
DSR	Demand side response
EUR	Euro
FOM	Fixed operation and maintenance
GCM	Generation circulation pathway / global climate model
GHG	Greenhouse gas
GW	Gigawatt
IPCC	Intergovernmental Panel on Climate Change
LCOE	Levelized costs of electricity
NTC	Net transmission capacity
OCGT	Open-cycle gas turbine
PV	Photovoltaics
RCM	Regional climate model
RCP	Representative concentration pathway
t	Ton
TWh	Terawatt hour
VRE	Variable renewable energy
WMO	World Meteorological Organization

Table 4.7: Abbreviations.

Numerical assumptions

Fuel type	**2015**	**2020**	**2030**	**2040**	**2050**	**...**	**2120**
Nuclear	3	3	3	3	3	...	3
Lignite	2	3	3	3	3	...	3
Coal	9	10	11	11	11	...	11
Oil	22	33	49	58	58	...	58
Natural gas	15	19	25	28	28	...	28

Table 4.8: Assumptions on gross fuel prices (EUR/MWh_{th}), based on scenario *New Policies* in World Energy Outlook 2017 (IEA (2017b)).

Technology	2015	2020	2030	2040	2050	...	2120
Wind onshore	1656	1602	1548	1512	1476	...	1476
Wind offshore (bottom-fixed, <50 m depth)	3493	3168	2473	2236	2061	...	2061
Wind offshore (floating, >50 m depth)	3749	3460	2581	2300	2099	...	2099
Photovoltaics (roof)	1440	1152	972	882	792	...	792
Photovoltaics (ground)	1188	936	774	702	630	...	630
CSP	4494	3989	3429	3102	2805	...	2805
Biomass (solid)	3298	3297	3295	3293	3287	...	3287
Biomass (gas)	2826	2826	2826	2826	2826	...	2826
Geothermal	12752	10504	9500	9035	9026	...	9026
Hydro (river)	5000	5000	5000	5000	5000	...	5000
Compressed air storage	1100	1100	1100	1100	1100	...	1100
Pump storage	2336	1237	1237	1237	1237	...	1237
Battery	1000	1000	750	650	550	...	550
Nuclear	5940	5400	4590	4050	4050	...	4050
OCGT	450	450	450	450	450	...	450
CCGT	1031	900	900	900	900	...	900
IGCC	2350	2350	2350	2300	2300	...	2300
Coal	1800	1800	1800	1800	1800	...	1800
Coal (advanced)	1980	1980	1980	1980	1980	...	1980
Lignite	1596	1596	1596	1596	1596	...	1596

Table 4.9: Assumptions on generation technology investment costs (EUR/kW). Conventional power plants, PV and wind onshore are based on scenario *New Policies* in World Energy Outlook 2017 (IEA (2017b)). Wind offshore is based on Myhr et al. (2014), Heidari (2017), Engel (2014).

Technology	FOM costs (EUR/kW/a)	Net efficiency (-)	Technical lifetime (a)
Wind onshore	13	1	25
Wind offshore (bottom-fixed, <50 m depth)	93	1	25
Wind offshore (floating, >50 m depth)	93	1	25
Photovoltaics (roof)	17	1	25
Photovoltaics (ground)	15	1	25
CSP	100	0.37	25
Biomass (solid)	120	0.30	30
Biomass (gas)	165	0.40	30
Geothermal	300	0.23	30
Hydro (river)	12	1	60
Compressed air storage	9	0.70	40
Pump storage	12	0.76	60
Battery	10	0.90	20
Nuclear	101-156	0.33	60
OCGT	19	0.28-0.40	25
CCGT	24-29	0.39-0.60	30
IGCC	44-80	0.46-0.50	30
Coal	44-60	0.37-0.46	45
Coal (advanced)	64	0.49	45
Lignite	46-53	0.32-0.46	45

Table 4.10: Assumptions on techno-economic parameters of electricity generators, based on scenario *New Policies* in World Energy Outlook 2017 (IEA (2017b)) and Knaut et al. (2016).

Country	2015	2020	2030	2040	2050	...	2120
AT	70	73	77	81	81	...	81
BE	85	87	96	92	92	...	92
BG	33	41	34	44	44	...	44
CH	63	62	72	58	58	...	58
CZ	63	69	71	76	76	...	76
DE	521	565	576	576	576	...	576
DK_E	13	15	15	21	21	...	21
DK_W	20	26	24	33	33	...	33
EE	8	9	9	11	11	...	11
ES	263	268	273	290	290	...	290
FI	82	90	90	102	102	...	102
FR	475	481	501	469	469	...	469
GB	333	328	373	341	341	...	341
GR	51	57	55	70	70	...	70
HR	17	19	18	25	25	...	25
HU	41	43	42	52	52	...	52
IE	27	31	30	41	41	...	41
IT	314	326	318	405	405	...	405
LT	11	12	11	15	15	...	15
LV	7	8	9	10	10	...	10
NL	113	115	118	137	137	...	137
NO	128	136	152	148	148	...	148
PL	151	163	185	251	251	...	251
PT	49	51	49	58	58	...	58
RO	55	58	61	73	73	...	73
SE	136	142	160	146	146	...	146
SI	14	13	16	21	21	...	21
SK	27	29	33	36	36	...	36

Table 4.11: Assumptions on the future development of net electricity demand including network losses (TWh), based on scenarios *Best Estimate* (2020), *European Commission* (2030), *Global Climate Action* (2040 - 2120) in TYNDP2018 (ENTSO-E (2018)).

	Number of clusters			
Country	**Wind onshore**	**Wind offshore (<50 m depth)**	**Wind offshore (>50 m depth)**	**Solar**
AT	1	0	0	1
BE	1	1	0	1
BG	1	1	1	1
CH	1	0	0	1
CY	1	0	0	1
CZ	1	0	0	1
DE	4	1	0	4
DK_E	1	1	1	1
DK_W	1	1	1	1
EE	1	1	1	1
ES	5	1	1	5
FI	3	1	1	3
FR	6	1	1	6
GB	2	1	1	2
GR	1	1	1	1
HR	1	1	1	1
HU	1	0	0	1
IE	1	1	1	1
IT	3	1	1	3
LT	1	1	1	1
LU	1	0	0	1
LV	1	1	1	1
NL	1	1	0	1
NO	4	1	1	4
PL	3	1	1	3
PT	1	1	1	1
RO	2	1	1	2
SE	4	1	1	4
SI	1	0	0	1
SK	1	0	0	1

Table 4.12: Number of spatial clusters for VRE per country.

5 The Role of Electricity in Decarbonizing European Road Transport - Development and Assessment of an Integrated Multi-Sectoral Model

Despite regulation efforts, CO_2 emissions from European road transport have continued to rise. Increased use of electricity offers a promising decarbonization option, both to fuel electric vehicles and run power-to-x systems producing synthetic fuels. To understand the economic implications of increased coupling of the road transport and electricity sectors, an integrated multi-sectoral partial-equilibrium investment and dispatch model is developed for the European electricity and road transport sectors, linked by an energy transformation module to endogenously account for, e.g., increasing electricity consumption and flexibility provision from electric vehicles and power-to-x systems. The model is applied to analyze the effects of sector-specific CO_2 reduction targets on the vehicle, electricity and power-to-x technology mix as well as trade flows of power-to-x fuels in European countries from 2020 to 2050. The results show that, by 2050, the fuel shares of electricity and power-to-x fuels in the European road transport sector reach 37 % and 27 %, respectively, creating an additional electricity demand of 1200 TWh in Europe. To assess the added value of the integrated modeling approach, an additional analysis is performed in which all endogenous ties between sectors are removed. The results show that by decoupling the two sectors, the total system costs may be significantly overestimated and the production costs of power-to-x fuels may be inaccurately approximated, which may affect the merit order of decarbonization options.

5.1 Introduction

Preventing severe, pervasive and irreversible impacts of climate change requires rapid emission reduction in all sectors (IPCC (2014b)). However, European road transport emissions have increased by 22 % since 1990, accounting for a share of 21 % of total European greenhouse gas emissions in 2016 (EEA (2018)). European regulation such as fleet targets for the average carbon emission levels for new vehicles is one of the more recent attempts to decarbonize road transport; however, factors such as increasing road transport demand and the countinued adoption of fossil-fueled gasoline and diesel motors have counteracted emission reduction efforts. Diversification of the current fuel and vehicle mix using alternatives such as natural gas, hydrogen, biofuels, synthetic fuels and electricity would offer decarbonization opportunities – yet the cost-optimal pathway to a low-carbon fuel mix remains unclear.

Most recently, electricity has gained attention as an energy carrier capable not only of fueling electric vehicles but also power-to-x (ptx) systems to produce synthetic power-to-x fuels (ptx fuels). More specifically, stand-alone electrolysis or electrolysis coupled with, e.g., methanation or Fischer-Tropsch synthesis can produce zero-carbon and carbon-neutral fuels for the road transport sector.[1] Yet decarbonizing the road transport sector via electricity results in the road transport and electricity sectors being coupled such that supply and demand become linked across sectors, which may have significant impacts on the future energy system. On the one hand, increased electricity consumption from road transport and ptx systems would require additional electricity generation, which must be produced subject to its own emission reduction regulations. In this case, both the marginal cost of electricity generation as well as marginal CO_2 abatement costs of the electricity sector would be influenced by the electricity demand from road transport and ptx systems. On the other hand, linking the road transport and electricity sectors may provide system flexibility since, e.g., electric vehicles or electrolysis may serve as energy storage capacities for the electricity sector. Especially in the case of high variable renewable energy (VRE) deployment, power-to-x systems may consume electricity in hours of high VRE supply and very low or even negative electricity prices as well as may offer ptx fuels to generate electricity in times of poor VRE supply and critical demand.

[1] Zero-carbon fuels refers to fuels with a chemical composition without C-atoms and thus with no carbon emissions associated when burnt. Carbon-neutral fuels, however, generate carbon emissions during combustion, but consist of recycled carbon and thus form part of the carbon cycle (see Section 5.2.1 for a more detailed discussion).

With growing pressure for decarbonization and an increased interest in electrification, it becomes vital to understand the economic implications of coupling the road transport and electricity sectors. One common method to assess long-term market behavior is via numerical optimization models, which assume future developments in, e.g., emissions, electricity demand and technologies. However, many current modeling approaches tend to either focus on a single sector or on the energy system as a whole. As such, they either fall short of accounting for cross-sectoral interdependencies or lack granularity in their representation of technologies regarding, e.g., road transport and energy transformation such as power-to-x. Therefore, the paper at hand seeks to answer the following research questions: i) how can the road transport sector and energy transformation technologies be integrated into an electricity market model?, ii) what are the key interactions between the sectors and technologies, and how may these contribute to decarbonization?, and iii) what is the added value of modeling the electricity and road transport sectors as well as energy transformation processes in an integrated multi-sectoral framework?

Within the scope of this paper, an integrated multi-sectoral partial-equilibrium investment and dispatch model combining the European electricity and road transport sectors is developed. A linear dynamic electricity market optimization model is extended to include both the European road transport sector in a road transport module as well as cross-sectoral conversion technologies such as power-to-x systems, with the x indicating a synthetic gas or fuel, in an energy transformation module. The focus lies not only on creating a detailed technological representation within each module but also on properly accounting for any interconnections between the electricity and road transport sectors as well as energy transformation processes. These include all electricity consumption from electric mobility or from energy transformation as well as ptx fuel flows to the road transport and electricity sectors, both within countries and across borders. Furthermore, the model observes any cross-sectoral emissions, such as upstream emissions in the electricity sector emitted during electricity generation for the road transport sector. Many cross-sectoral technologies such as power-to-x systems may only become competitive if they can be rewarded for their carbon-neutral nature, which is only apparent when considering the complete emissions cycle of the fuel production pathway.

The extended integrated multi-sectoral model is then able to simulate cost-minimal decarbonization pathways for the electricity and road transport sectors in European countries up to 2050. In order to demonstrate the capabilities of the model developed, an exemplary scenario is presented to analyze the effects of sector-specific CO_2

reduction targets on the long-term vehicle, electricity and ptx technology mix in Europe. The model yields the cost-optimal solution, minimizing the total costs of the electricity sector as well as the total costs for the vehicles, fuel use and infrastructure needed to reach the CO_2 reduction goals. The results of the single scenario analysis show that, by 2050, the fuel share of electricity and ptx fuels in the European road transport sector reaches 37 % and 27 %, respectively, creating an additional electricity demand of 1200 TWh in Europe. The scenario results provide a basis for understanding the integrated multi-sectoral model, revealing endogenous marginal costs of electricity generation and sector-specific marginal CO_2 abatement costs as well as cross-border trade flows that reflect the cost-optimal decarbonization pathway under integrated sectors.

In order to understand the added value of building complex integrated models, the second part of the analysis applies the model with decoupled sectors, removing all endogenous ties between the modules and allowing each to be optimized independently of one another. Additional electricity demanded by road transport and energy transformation is therefore ignored by the electricity sector. Electricity prices for the road transport module are defined exogenously. The energy transformation module, which is by definition coupled to the electricity sector, is shut off; however power-to-x fuels can be bought by either the electricity or road transport sector at a fixed price equal to the expected production costs. The results show that by decoupling the two sectors, the total system costs may be significantly overestimated and the production costs of ptx fuels inaccurately approximated, which may affect the merit order of decarbonization options. By comparing the model results, conclusions may be made as to the added value of integrated multi-sectoral modeling and the key discrepancies that may occur when performing single-sector analyses.

This paper is related to two streams of literature. The first relevant stream encompasses research that develops multi-sectoral models covering electricity, road transport and energy transformation. In particular, a large body of literature seeks to extend the MARKAL family of models[2] to include additional sectors and technologies, with a smaller niche addressing electrification of road transport and power-to-x fuels. Dodds and McDowall (2014) and Dodds and Ekins (2014) extend the MARKAL model to simulate the road transport sector in the UK, with a particular focus on hydrogen consumption. Similarly, Börjesson and Ahlgren (2012) develop and integrate

[2]The MARKAL (Market Allocation) family of models, including GMM, TIMES and TIAM, were some of the first energy system models (early contributions include Fishbone and Abilock (1981)). MARKAL and its descendants are widely-applied partial equilibrium, bottom-up, dynamic optimization models that are used to identify the energy system meeting energy service demands with the lowest discounted capital, operating and resource costs (Loulou et al. (2004), Dodds and Ekins (2014)).

a transport module into MARKAL for the Nordic regions in order to asses taxation strategies. Two other MARKAL models, namely TIMES and TIAM, are also often seen in literature on coupling the road transport and electricity sectors. Both Sgobbi et al. (2016) and Thiel et al. (2016) extend the TIMES model developed in Simoes et al. (2013) to simulate road transport in Europe with approximately 50 vehicle technologies, assessing decarbonization with hydrogen and electricity, respectively. Studies by van der Zwaan et al. (2013) and Rösler et al. (2014) build on the TIAM model described in Rösler et al. (2011) to perform an integrated assessment of decarbonizing the global and European road transport sector, comparing endogenous CO_2 prices across sectors. Apart from MARKAL-based analyses, other simulations of the electricity and road transport sectors include papers by Hedenus et al. (2010) and Krishnan et al. (2014), who build on the models GET 7.0 and NETPLAN, respectively, to determine the future vehicle mix and fuel supply under carbon constraints.

Although many of the aforementioned studies use modeling techniques to address similar issues to the study at hand, none of the methodologies were found to implement the same level of temporal, spatial and technological granularity. Often only hydrogen production via electrolysis and the direct use of electricity appear to be coupled to the electricity sector, ignoring the production of other ptx fuels. The possibility to use ptx fuels to decarbonize the electricity sector next to the road transport sector is also not taken into account. Furthermore, the dispatch of ptx technologies is often exogenous, i.e., the utilization rate of, e.g., an electrolysis system is exogenously defined while its investments are endogenous. In the model developed in this paper, ptx systems are exposed to developments in the electricity system at a higher temporal resolution than in the models mentioned. Trade flows of ptx fuels were also found to be possible in only a limited number of cases and are never examined in detail. As such, the study at hand seeks to contribute to the literature on integrated electricity and road transport sector models by accounting for a wide range of ptx applications, optimizing European electricity and ptx fuel production as well as simulating cost-minimizing trade flows according to endogenous market conditions.

The second relevant literature stream focuses on single-sector analyses of the road transport sector and the resulting optimal decarbonization pathways. Many studies assess the penetration of alternative vehicle technologies under certain scenarios (e.g., Pasaoglu et al. (2016), Harrison et al. (2016)). Ou et al. (2013) as well as Gambhir et al. (2015) simulate the Chinese road transport sector up to 2050 to determine total costs under varying penetration levels of electric or hydrogen fuel-

cell vehicles. Applying similar methods to those used in the road transport module developed in this paper, Romejko and Nakano (2017) perform a cost minimization for the Polish road transport sector in order to determine endogenous vehicle investments and carbon emissions up to 2030. However, as the models used are decoupled from the energy system, all three papers must assume exogenous prices for all fuels, including electricity. One aim of the study at hand is to gain understanding as to how exogenous assumptions on cross-sectoral parameters may cause the model to deviate from the cost-optimal solution. The assessment of the added value of coupled models, a step that none of the aforementioned studies perform, is another key contribution of this paper.

The remainder of the paper is organized as follows: In Section 5.2, the methodology behind the coupling of the electricity market, energy transformation and road transport modules as well as behind the individual modules are explained in detail. The scenario framework and results of the integrated model are presented in Section 5.3, and the comparison to a decoupled model is made in Section 5.4. Section 5.5 concludes.[3]

5.2 Methodology

One of the main objectives of the research at hand is to develop a consistent, integrated energy system model. The foundation of the work presented is the electricity market model DIMENSION, which has been used in numerous analyses;[4] yet with increasing electrification in synthetic fuel production and road transport, complex interactions arise that cannot be investigated with a single-sector model. In order to account for these multi-sectoral effects, not only do the energy transformation and road transport modules themselves need to be modeled in detail, it is also critical that any interdependencies with the electricity market are also properly simulated.

The remainder of this section is structured as follows: Section 5.2.1 begins by providing an overview of the model developed in this study as well as identifies the key links connecting the individual modules. The main equations, assumptions and parameters for the energy transformation and road transport modules are then given in Sections 5.2.2 and 5.2.3, respectively. For completeness, a short overview of the electricity market module is also included in Appendix 5.6.

[3] See Appendix 5.6 for a list of abbreviations and nomenclature used throughout this paper.
[4] See, e.g., Jägemann et al. (2013), Knaut et al. (2016) and Peter and Wagner (2018).

5.2.1 Developing an integrated multi-sectoral model

Overview of the model

Figure 5.1 presents an overview of the model developed and shows how the individual modules (electricity market, energy transformation and road transport) are connected on the supply side. A key factor of this analysis is that the entire fuel supply chain, from the primary energy source to final fuel consumed, is taken into account. The different fuel types and their production paths can be seen in Figure 5.1.

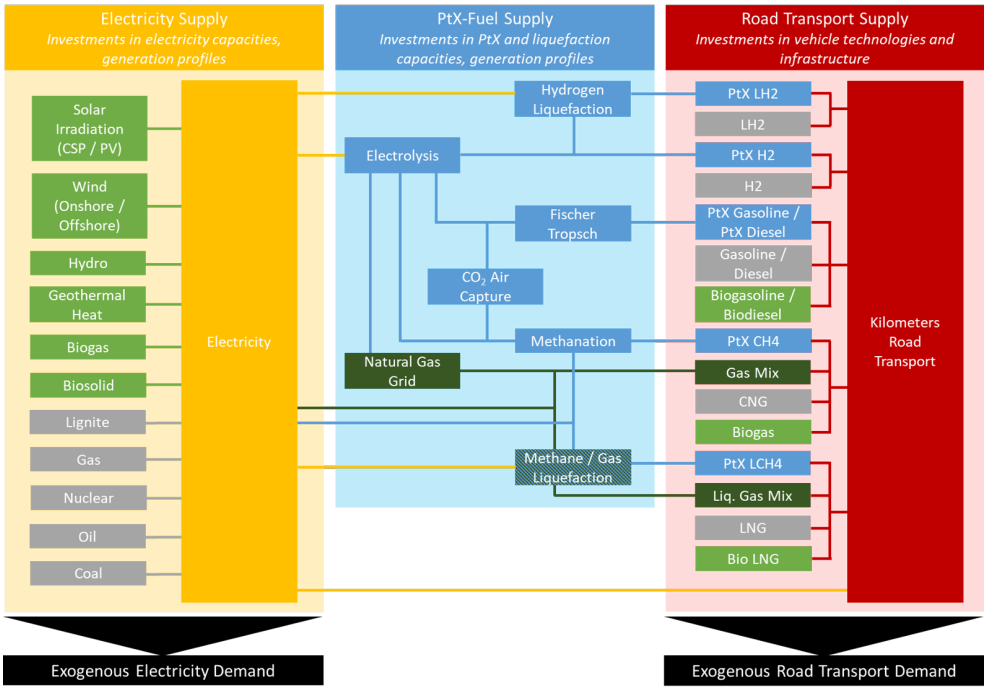

Figure 5.1: Overview of the model developed for this study. The yellow area indicates the electricity market module, the blue area the energy transformation module and the red area the road transport module.

The electricity market module, as shown in the yellow area of Figure 5.1, is responsible for providing the necessary investments to supply electricity to meet both a country-specific exogenous electricity demand[5] (indicated by the black box) as well as any electricity-consuming technologies in both the energy transformation module (the blue area of Figure 5.1) or the road transport module (the red area of Figure 5.1). The yellow lines exiting the yellow area of the electricity market module in-

[5]The electricity market module is also subject to an endogenous electricity demand from, e.g., storage or demand side response (see Appendix 5.6). For simplification, this is excluded from Figure 5.1.

dicate these electricity flows. The green and gray boxes are the renewable/bio and fossil fuels, respectively, that are available to the power plant fleet.[6]

The energy transformation module (the blue area) installs power-to-x as well as liquefaction capacities. The blue boxes in Figure 5.1 show the different ptx processes that are accounted for in the energy transformation module, including electrolysis, CO_2 air capture, methanation, Fischer-Tropsch synthesis as well as hydrogen and methane/gas liquefaction.[7] Endothermic processes such as electrolysis, which splits water into oxygen and hydrogen, and liquefaction require an electricity input from the electricity market module, as indicated by the yellow lines. The blue lines indicate the flow of ptx fuels, which include zero-carbon ptx hydrogen gas (PtX H2) and ptx liquefied hydrogen (PtX LH2) as well as carbon-neutral ptx methane gas (PtX CH4), ptx liquid methane (PtX LCH4) as well as ptx synthetic gasoline (PtX Gasoline) and ptx synthetic diesel (PtX Diesel).[8] The dark green boxes and lines depict the production of a gas mixture (Gas Mix), created by feeding in zero-carbon hydrogen from the electrolysis system into the existing natural gas grid.[9] The resulting gas mixture is equivalent to a low-carbon substitute for fossil natural gas and can also be liquefied via methane/gas liquefaction to provide a low-carbon alternative to fossil liquefied natural gas (Liq. Gas Mix). The energy transformation module is not subject to an exogenous demand but rather optimizes its supply according to the other modules, meaning that ptx fuels can either be supplied back to the electricity market module (i.e., as ptx methane or gas mix for electricity generation) or to the road transport module to be used in a wide range of vehicle technologies.

The road transport module invests in vehicle technologies as well as infrastructure to cover an exogenous demand for road transport (indicated by the black box), varying across countries and years. In the model, the equilibrium condition is defined in annual vehicle kilometers, which in turn defines an energy demand based on the vehicle's motor type and specific fuel consumption. As indicated by the red lines, a single vehicle technology may consume multiple fuel types, as explained in Sec-

[6] Investments in nuclear power are only allowed in countries with no existing nuclear phase-out policies. Investments in carbon capture and storage (CCS) technologies are not allowed due to a general lack of social acceptance in European countries.

[7] Unlike the other processes presented, CO_2 air capture is not modeled as an investment object but rather assumed to be available at a feedstock price equal to the average costs of CO_2 air capture (see Section 5.2.2).

[8] The upstream emissions from the electricity generation used as input for the ptx production processes are accounted for within the electricity market emissions. Therefore, the zero-carbon and carbon-neutral properties hold with respect to the sector in which the fuel is used, irrespective of how the electricity was generated in the first place.

[9] The existing natural gas grid is not modeled as an investment object but rather as an energy constraint (see Section 5.2.2).

tion 5.2.1. In addition to ptx fuels (blue and dark green boxes), the road transport module may also purchase fossil fuels (gray boxes) such as gasoline, diesel, natural gas (CNG), liquefied natural gas (LNG), hydrogen gas (H2) and liquefied hydrogen (LH2) from natural gas reformation as well as biofuels (light green boxes) such as biodiesel, biogasoline, biogas and bio LNG. Fossil fuels and biofuels can be bought from the global commodity market at a price reflecting both the raw fuel and the fuel production costs.[10] Electricity may also be consumed in the road transport module, which is endogenously supplied by the electricity market module.

The integrated multi-sectoral model optimizes the energy transformation and road transport modules simultaneously with the electricity market module to determine the cost-efficient investment and dispatch strategy for meeting electricity and road transport demand of each country. To this end, accumulated discounted total system costs are minimized subject to regulatory conditions as well as technical constraints such as carbon emission reduction targets[11] or energy balance restrictions. The model allows for an integrated analysis yielding a cost-minimal, welfare-optimal solution across multiple coupled sectors. The spatial scope of the model covers 28 countries, including 26 countries of the European Union as well as Norway and Switzerland.[12] The analyzed time period spans 2015 to 2050 in 5-year steps. For computational tractability, the model applies a reduced temporal resolution based on 16 typical days.[13]

Understanding the structure of the electricity market module

The model developed within the scope of this study is an extended version of the dynamic electricity market model DIMENSION, similar to the integrated problem for investment and operation as presented in, e.g., Turvey and Anderson (1977). It may be interpreted as a social planner problem in which the social planner minimizes

[10] Costs for oil refining, natural gas reformation, etc. are added as a price markup to the commodity price. Note that such a marginal cost approach does not take into account any sunk costs such as the investment costs for oil refineries. Biofuels are assumed to be traded on a European market, with prices based on the fossil-based equivalent plus a 20 % markup.

[11] In its current form, the model only considers CO_2 emissions and does not account for other externalities such as air pollution and resulting health damage.

[12] See Table 5.3 in Appendix 5.6 for a complete list of the countries considered.

[13] In order to represent a full year, the typical days are scaled up by multiplying each typical day with its frequency of occurrence. Each typical day consists of four time slices representing six consecutive hours. The authors have chosen this temporal resolution due to restrictions in computational power given the complexity of the multi-sectoral model framework. As shown in Nahmmacher et al. (2016a), a temporal resolution exceeding 48 time slices is assumed to be sufficient to ensure reliable results when using investment models for electricity.

total system costs under perfect foresight for investments in generation capacity and the operation of generation and transmission between markets.[14]

As is often seen in the literature on electricity market modeling, fundamental assumptions are necessary to reduce the complexity of the optimization problem. The model at hand assumes inelastic demand due to, e.g., the lack of real-time pricing as well as market clearing under perfect competition. As such, the problem can be treated as a linear optimization, as shown in Equation (5.1). The objective function (5.1a) minimizes total costs TC, i.e., the sum of the fixed costs of generation capacity $\bar{\mathbf{x}}_{i,m}$ and variable costs of generation $\mathbf{g}_{i,m,t}$ of technology i in market m.[15] Investing in additional generation capacities comes with costs of $\delta_{i,m}$ and generation incurs variable costs of $\gamma_{i,m,t}$.

$$\min \quad TC = \sum_{i,m} \delta_{i,m} \bar{\mathbf{x}}_{i,m} + \sum_{i,m,t} \gamma_{i,m,t} \mathbf{g}_{i,m,t} \tag{5.1a}$$

$$\text{s.t.} \qquad l_{m,t} = \sum_{i} \mathbf{g}_{i,m,t} + \sum_{n} \mathbf{k}_{n,m,t} \qquad \forall m,t,m \neq n \tag{5.1b}$$

$$\mathbf{g}_{i,m,t} \leq x_{i,m,t} \bar{\mathbf{x}}_{i,m} \qquad \forall i,m,t \tag{5.1c}$$

$$|\mathbf{k}_{m,n,t}| \leq \bar{k}_{m,n} \qquad \forall m,n,t,m \neq n \tag{5.1d}$$

$$\mathbf{k}_{m,n,t} = -\mathbf{k}_{n,m,t} \qquad \forall m,n,t,m \neq n \tag{5.1e}$$

$$l_{m,peak} \leq \sum_{i} \nu_{i,m} \bar{\mathbf{x}}_{i,m} \qquad \forall m \tag{5.1f}$$

$$GHG_{cap} \geq \sum_{i,m,t} \kappa_i \, \mathbf{g}_{i,m,t} / \eta_{i,m} \tag{5.1g}$$

for technologies $i \in \mathbf{I}$, markets $m,n \in \mathbf{M}$ and time $t \in \mathbf{T}$.

The cost-minimizing objective function is subject to various constraints: The equilibrium condition (5.1b) ensures that supply, i.e., the sum of generation $\mathbf{g}_{i,m,t}$ and electricity exchanges between markets m and n, $\mathbf{k}_{n,m,t}$ and $\mathbf{k}_{m,n,t}$, equals demand $l_{m,t}$. The two capacity constraints (5.1c) and (5.1d) require that generation and transmission are restricted by installed generation and transmission capacities. Equation (5.1e) states that electricity trades from market m to market n are equal to negative trades from market n to market m. The peak capacity constraint (5.1f) requires

[14] The electricity market model DIMENSION will be referred to as the *electricity market module* henceforth. The reader is referred to Richter (2011), Fürsch et al. (2013) and Jägemann et al. (2013) for more detailed descriptions of the model DIMENSION, which was developed and has been maintained at the Institute of Energy Economics at the University of Cologne (EWI).

[15] See Table 5.2 in Appendix 5.6 for a complete list of model sets, parameters and variables. Unless otherwise noted, bold capital letters indicate sets, lowercase letters parameters and bold lowercase letters for optimization variables.

the sum of generation capacities $\bar{\mathbf{x}}$ weighted by their capacity values[16] $\nu_{i,m}$ is to be greater than or equal to the market-specific annual peak load $l_{m,peak}$. The peak capacity constraint is typically introduced in long-term investment models that are based on a reduced temporal resolution, e.g., a typical-days approach, to ensure security of supply even when only modeling select hours. Finally, the decarbonization constraint (5.1g) requires the sum of greenhouse gas emissions of all technologies in all markets to be lower than a certain greenhouse gas cap. The emissions are calculated by dividing electricity generation $\mathbf{g}_{i,m,t}$ by the technology-specific efficiency $\eta_{i,m}$ to determine the technology's fuel consumption, which is then multiplied with its fuel-specific emission factor κ_i.

Identifying key links between modules

Within the scope of this research, two additional modules were developed and embedded into the optimization problem shown in Equation (5.1): a road transport module simulating the European road transport sector and an energy transformation module simulating conversion technologies, e.g., power-to-x systems providing fuels to the electricity and road transport sectors.

The complexity of a multi-sectoral model lies within the proper representation of interlinkages between the modules.[17] Within the integrated multi-sectoral model, the electricity market module is still represented by Equations (5.1b) - (5.1f), which now, however, only apply to the set of electricity market technologies $i \in \mathbf{I_{el}}$, i.e., a sub-quantity of the entire quantity of technologies $\mathbf{I} = \mathbf{I_{el}} + \mathbf{I_{rt}} + \mathbf{I_{et}}$ comprising all technologies from the electricity market module, the road transport module and the energy transformation module.

The cost-minimizing objective function (5.1a) is still valid; however it now encompasses technologies from all modules, i.e., $i \in \mathbf{I}$, and thereby represents the core of the integrated modeling approach. The fixed costs $\delta_{i,m}$ include the annuity as well as the yearly fixed operation and maintenance costs of power plants, vehicles and infrastructure as well as ptx and liquefaction systems. The variable costs $\gamma_{i,m,t}$ include fuel costs as well as costs for, e.g., CO_2 air capture and fuel distribution (see Sections 5.2.2 and 5.2.3).

One key link between the modules is achieved via modifying the equilibrium con-

[16] In the existing literature, capacity value and capacity credit are often used as synonyms. Throughout this paper, the term capacity value is used.

[17] See Figure 5.8 in Appendix 5.6 for a schematic representation of the key links between the modules.

dition (5.1b) in order to account for the endogenous electricity demand from all modules. In addition to the endogenous electricity demand in the electricity market module, e.g., by storage technologies, both the energy transformation module and the road transport module may demand electricity in order to generate ptx fuels (see Section 5.2.2) or fuel electric vehicles (see Section 5.2.3), which in turn must be supplied by the electricity market module. The modified equilibrium condition then reads

$$l_{m,t} + \sum_{s} \mathbf{ec}_{f,f1,m,s,t}\Big|_{f,f1=elec} = \sum_{i} \mathbf{g}_{i,m,t} + \sum_{n} \mathbf{k}_{m,n,t} \tag{5.2}$$

where the electricity demand has both an exogenous component, $l_{m,t}$, and an endogenous component, represented by the electric energy consumption $\mathbf{ec}_{f,f1,m,s,t}$ for $f1 = f =$ electricity, summed over sectors s.

Another key link between the modules is the endogenous country-specific electricity price. It is implicitly visible to all modules as they are all subject to one common cost-minimizing objective function (5.1a). The endogenous country-specific electricity price is derived from the dual variable of Equation (5.2) and represents the change in total system costs for supplying one additional unit of electricity. The remaining two key links between the modules consist of the endogenous ptx fuels demand and the resulting endogenous ptx fuel price in the energy transformation module: The endogenous ptx fuel demand drives investments in ptx and liquefaction technologies, which in turn determines the implicit ptx fuel prices, discussed in Section 5.2.2.

Introducing substitute fuels

Both the electricity market module and road transport module have a wide range of fuels to choose from when making the investment decision in an electricity generation or vehicle technology. However, some of the fuel choices are substitutes, varying only in, e.g., production costs and upstream carbon emissions. For example, a fuel-cell vehicle running on hydrogen can run both on ptx and fossil-based hydrogen; yet the model must be able to distinguish between the two fuel types as hydrogen from electrolysis differs strongly in terms of production cost and upstream carbon emissions compared to that from natural gas reformation. Moreover, both carbon-based ptx fuels and biofuels are assumed to be carbon neutral, which can only be accounted for if the fuel's production cycle is properly recognized by the model (see

Section 5.2.1).

As a result, the concept of substitute fuels is introduced in order to differentiate fuels by how they are produced while still allowing for fuels to be grouped by their type (Table 5.1).[18] It should be noted that for fuels without multiple substitute fuels (e.g., electricity, coal, lignite), f equals $f1$. For simplification they are omitted from Table 5.1.

Fuel type f	**Substitute fuels** f_1		
Diesel	Diesel	PtX Diesel	Biodiesel
Gasoline	Gasoline	PtX Gasoline	Biogasoline
Gas	CNG	PtX CH4/Gas Mix	Biogas
Liquefied Gas	LNG	PtX LCH4/Liq. Gas Mix	Bio LNG
Hydrogen	H2	PtX H2	
Liquefied Hydrogen	LH2	PtX LH2	

Table 5.1: Fuel types and the corresponding substitute fuels.

By applying the concept of substitute fuels, not only can each sector's endogenous energy consumption $\mathbf{ec}_{f,f1,m,s,t}$ be determined for a certain fuel type f, but the mix of substitute fuels $f1$ can be simultanously derived, taking into account constraints such as decarbonization targets. As such, in terms of the electricity market model given in Equation (5.1), the energy consumption of power plants in the electricity sector is then defined by

$$\sum_{f1} \mathbf{ec}_{f,f1,m,s,t} \Big|_{s=el} = \sum_{i} \mathbf{g}_{i,m,t} / \eta_{i,m} \tag{5.3}$$

For example, the ptx methane consumption of a power plant in the electricity sector $s = el$ of market m is depicted by $\mathbf{ec}_{f,f1,m,s,t}$ with f = gas and $f1$ = ptx methane. The electricity consumption of, e.g., a pump storage is denoted by $f1 = f$ = electricity.

[18] It should be noted that the concept of substitute fuels ignores any differences in the chemical composition of the respective fuels. Substitute fuels are thus treated, economically speaking, as perfect substitutes. This assumption is justified in an economic model as long as the fuel-consuming technologies can interchangeably switch between fuels without affecting their performance.

Accounting for upstream emissions and the carbon cycle

Carbon emissions from combustion processes are based on the carbon content of the respective fuel, i.e., a fuel-specific carbon emission factor κ_{f1}. For non-carbon fuels such as electricity or hydrogen, this value is equal to zero. Fuel-specific upstream carbon emissions, on the other hand, include emissions from fuel extraction and transformation and are accounted for by a fuel-specific upstream carbon emission factor $\kappa_{f1,upstream}$.[19] For fossil fuels and biofuels, this includes carbon emissions generated during fuel production and conditioning at the source, fuel transformation at the source, transformation near market and conditioning and distribution (Edwards et al. (2014)).[20] It should be noted that the upstream emissions of electricity as an input fuel for, e.g., electric vehicles or ptx processes are accounted for in the electricity market module. Thus, the upstream emissions of ptx fuels produced in the energy transformation module consist only of emissions resulting from the distribution of the final fuel from the central ptx system to the consumer. The fuel-specific carbon emission factors and upstream carbon emission factors are shown for each substitute fuel in Table 5.5 of Appendix 5.6.

The carbon emissions $\mathbf{em}_{m,s}$ from sector s in market m are then defined by

$$\mathbf{em}_{m,s} = \sum_{f,f1,t} \mathbf{ec}_{f,f1,m,s,t}(\kappa_{f1} + \kappa_{f1,upstream}) \tag{5.4}$$

In order to account for the carbon cycle of carbon-neutral fuels such as biofuels or ptx fuels (discussed in detail in Section 5.2.2), a carbon capture variable $\mathbf{cpt}_{m,s}$ is introduced and defined as

$$\mathbf{cpt}_{m,s} = \sum_{f,f1,t} \mathbf{ec}_{f,f1,m,s,t}\ \kappa_{f1}\big|_{f1=bio/ptx} \tag{5.5}$$

Thereby, it is assumed that the entire carbon content of the biofuels or ptx fuels, represented by κ_{f1}, is captured from air either by natural carbon bonding via biomass photosynthesis or by a direct air capture process (DAC) (see Section 5.2.2). It thus forms a carbon cycle and the respective fuel can be regarded as carbon neutral.

[19] Note that the carbon emission factor from combustion processes κ_{f1} is equal for fuel f and its substitute fuels $f1$, assuming the fuels are perfect substitutes. The upstream carbon emissions factor $\kappa_{f1,upstream}$ however varies for different substitute fuels $f1$.

[20] Upstream emissions differs from a Life Cycle Analysis (LCA), as it does not consider energy and emissions involved in building facilities and the vehicles, or end of life aspects.

A generalized formulation of the decarbonization constraint (5.1g) in Equation (5.1) reads then as

$$GHG_{cap,s} \geq \sum_{m} (\mathbf{em}_{m,s} - \mathbf{cpt}_{m,s}) \tag{5.6}$$

It should be noted that for carbon-neutral fuels, i.e., biofuels and ptx fuels, the emissions κ_{f1} cancel out in Equation (5.6); however, any upstream emissions based on $\kappa_{f1,upstream}$ do not. Furthermore, the sum on the right hand side of Equation (5.6) has to be adjusted depending on the definition of the decarbonization target, be it a multi-national sectoral target, a national sectoral target, or a national multi-sectoral target.

5.2.2 Simulating energy transformation

The energy transformation module is a tool that was developed to simulate the investment in as well as energy consumption and production volumes of energy conversion technologies in order to serve, among others, the electricity and road transport sectors. Within the scope of this analysis, the module endogenously reacts to developments in the electricity market (i.e., increased VRE production) as well as the demand for ptx fuels in the electricity and road transport modules, which may be necessary to achieve, e.g., decarbonization targets. This section seeks to introduce the conversion technologies considered as well as provide key details on how the ptx fuel supply is modeled. Finally, further explanation on how the conversion technologies are linked to the electricity market module is provided.

Power-to-x, liquefaction and carbon neutrality via CO_2 air capture

The ptx conversion technologies, analogous to the electricity generation technologies, are investment objects with defined techno-economical parameters that vary across vintage classes. These technologies include alkaline and PEM electrolysis, catalytic methanation and Fischer-Tropsch synthesis. Key techno-economic assumptions for each ptx investment object considered in the energy transformation module including investment costs, fixed operation and maintenance costs (FOM), efficiency and technical lifetime can be found in Table 5.6 in Appendix 5.6. Plants to liquefy gaseous hydrogen or natural gas are also taken into account in the energy transformation module. Analogous to ptx systems, liquefaction plants are modeled as

investment objects. The techno-economic assumptions for the liquefaction plants may be found in Table 5.7 in Appendix 5.6.

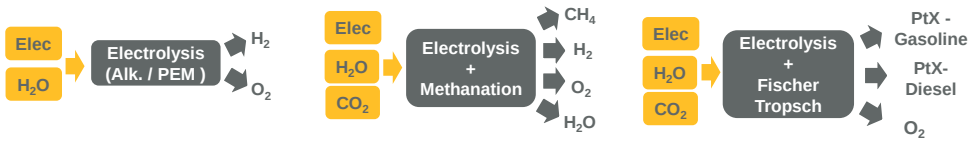

Figure 5.2: Inputs and outputs of ptx processes.

Figure 5.2 gives an overview of the relevant input and outputs for each ptx technology modeled in this analysis. The hydrogen gas produced in electrolysis can either be sold directly or be stored to successively produce methane via catalytic methanation or hydrocarbons via Fischer-Tropsch synthesis. Alternatively, ptx hydrogen may be mixed with natural gas in the existing gas grid infrastructure up to a certain threshold which depends on the design and certification of end appliances. An upper limit of 10 vol-% of the natural gas grid is assumed for hydrogen feed-in.[21] It should be noted that, as shown in Figure 5.2, an electrolysis system produces oxygen as by-product. As such, in addition to selling ptx fuels, the energy transformation module also sells oxygen to an exogenously-defined market at an exogenous price, increasing the profitability of ptx systems.[22] Detailed descriptions of the energy transformation processes can be found in Appendix 5.6.

As previously stated, the ptx fuels produced in the energy transformation module are assumed to be either zero-carbon or carbon neutral. Upstream emissions aside, hydrogen fuel produced from electrolysis is by definition carbon-free as electricity splits water into oxygen and hydrogen. Technologies such as methanation and Fischer-Tropsch synthesis, however, produce carbon-based fuels that, via combustion, will emit carbon dioxide into the atmosphere. Yet these ptx fuel production processes require carbon dioxide together with hydrogen as an input in order to create carbon-based ptx methane or ptx gasoline and ptx diesel (see Figure 5.2). The classification carbon neutral depends on the origin of the carbon fed into the ptx processes. More specifically, if the carbon stems from a fossil-based origin, the eventual release of carbon dioxide during the ptx fuel combustion process cannot be

[21] In the future, it is expected that gas turbines, motors and consumer appliances will be able to function under higher shares of hydrogen gas. However, the authors have chosen 10 vol-% as an average in order to account for a wide range of older and newer technologies. In order to set the limit in the model, the national gas demand is used as a proxy for gas grid size in each respective country.

[22] An oxygen price of 0.07 EUR/cubic meter is assumed based on Brynolf et al. (2018). The country-specific upper limit for oxygen sales is estimated based on industry data for Germany (VCI (2014)) and for the other European countries scaled according to GDP (Eurostat (2017)), whereby only 25 % of a country's oxygen demand is assumed to be able to be provided by electrolysis.

regarded as carbon neutral.[23] If, however, the carbon is based on air capture either from biomass photosynthesis or a technical direct air capture process, the CO_2 is recycled, resulting in a carbon-neutral process being part of a carbon cycle. In this work, it is assumed that the carbon required for ptx fuel production stems from CO_2 extracted from the atmosphere via direct air capture.[24]

Key aspects of modeling the supply of ptx fuels

The equilibrium condition for ptx fuels ensures that the ptx fuel production, $\mathbf{fp}_{f1,i,m,t}$, within each country m in addition to any ptx fuel trade $\mathbf{ft}_{f1,n,m,t}$, i.e., ptx fuels being imported into country m from other EU countries n or from outside of Europe, $\mathbf{ft}_{f1,nonEU,m,t}$, is equal to the amount of ptx energy consumption in country m, $\mathbf{ec}_{f,f1,m,s,t}$, plus ptx fuel exports from country m to country n, $\mathbf{ft}_{f1,m,n,t}$:

$$\sum_i \mathbf{fp}_{f1,i,m,t} + \sum_n \mathbf{ft}_{f1,n,m,t} + \mathbf{ft}_{f1,nonEU,m,t} = \sum_s \mathbf{ec}_{f,f1,m,s,t} + \sum_n \mathbf{ft}_{f1,m,n,t} \tag{5.7}$$

This equilibrium condition holds for all liquid fuels $f1$ produced by ptx technologies i such as ptx gasoline, ptx diesel, ptx liquefied hydrogen, ptx liquid methane and liquefied gas mix.

The gaseous ptx fuels, namely ptx hydrogen, ptx methane and gas mix, are subject to a slightly modified equilibrium condition in order to account for any ptx hydrogen that is injected into the natural gas grid. Similar to Equation (5.7), the equilibrium

[23] Note that carbon from fossil-based carbon capture and utilization (CCU) is, while relieving the first combustion process from its carbon emissions, still fossil-based carbon. Thus, it does not qualify for production of carbon-neutral ptx fuels, as this would entail double counting.

[24] The CO_2 feedstock prices from air capture are assumed to reduce from 300 EUR/tCO_2 in 2020 to 84 EUR/tCO_2 in 2050 (Sanz-Pérez et al. (2016)), as shown in Figure 5.9 in Appendix 5.6.

conditions for gaseous ptx fuels are

$$\sum_i \mathbf{fp}_{PtXH2,i,m,t} + \sum_n \mathbf{ft}_{PtXH2,n,m,t} + \mathbf{ft}_{PtXH2,nonEU,m,t} = \sum_s \mathbf{ec}_{H2,PtXH2,m,s,t} + \sum_n \mathbf{ft}_{PtXH2,m,n,t} + \mathbf{ffi}_{PtXH2,m,t} \quad (5.8)$$

$$\sum_i \mathbf{fp}_{PtXCH4,i,m,t} + \sum_n \mathbf{ft}_{PtXCH4/GasMix,n,m,t} + \mathbf{ft}_{PtXCH4,nonEU,m,t} + \mathbf{ffi}_{PtXH2,m,t} = \sum_s \mathbf{ec}_{Gas,PtXCH4/GasMix,m,s,t} + \sum_n \mathbf{ft}_{PtXCH4/GasMix,m,n,t} \quad (5.9)$$

with the extra variable ptx fuel feed-in $\mathbf{ffi}_{PtXH2,m,t}$ indicating the amount of ptx hydrogen injected into the natural gas grid. In Equation (5.8), the ptx hydrogen into grid contributes to the hydrogen demand, whereas in Equation (5.9) it becomes part of the gas supply. Apart from being fed into the natural gas grid ($\mathbf{ffi}_{PtXH2,m,t}$), ptx hydrogen can be directly used in sectors such as road transport or sent to a liquefaction plant in order to produce ptx liquefied hydrogen ($\mathbf{ec}_{H2,PtXH2,m,s,t}$). Ptx methane, analogous to ptx hydrogen, can be either fed into the natural gas grid or liquefied, represented by each sector's energy consumption ($\mathbf{ec}_{Gas,PtXCH4/GasMix,m,s,t}$).[25]

As shown in Equation (5.7), (5.8) and (5.9), ptx fuels can either be traded between European countries or bought from outside of Europe, e.g., from North Africa. Inner-European import and export volumes via trucks are determined endogenously, being subject to tanker transport costs relative to delivery distance.[26] As the model does not cover investments outside Europe, an exogenous ptx fuel import price is calculated based on the expected production and distribution costs of ptx fuels at a typical location in North Africa.[27] For the recycled carbon supply for ptx diesel, ptx gasoline and ptx methane production outside of Europe, CO_2 air capture is assumed and included in the production costs. Ptx fuels from European production are not permitted to be exported outside Europe.

[25] Note that liquefaction plants use gaseous ptx hydrogen and ptx methane as input, representing an energy consumption of the energy transformation module in Equations (5.8) and (5.9).

[26] The transport costs are derived based on km-specific transport costs and the distance between capital cities as a proxy, see Table 5.8 in Appendix 5.6.

[27] The production costs include the investment and FOM costs of the ptx systems as well as the variable costs, i.e., the electricity price, calculated as the LCOE of a hybrid onshore wind and photovoltaics plant in North Africa.

Linking the energy transformation module to the electricity market and road transport modules

One key link between the energy transformation and electricity market module is the demand of electricity by power-to-x and liquefaction systems to produce gaseous and liquid ptx fuels, determined endogenously. The electric energy consumption $\mathbf{ec}_{f,f1,m,s,t}$ of the energy transformation module is defined as

$$\sum_{f1} \mathbf{ec}_{f,f1,m,s,t} \Big|_{f,f1=elec} = \sum_{i} \mathbf{fp}_{f1,i,m,t} / \eta_{i,m} \tag{5.10}$$

where the factor $\eta_{i,m}$ represents the efficiency of the ptx or liquefaction system, i.e., the ratio of fuel output to electricity input. This equation holds also for methanation and Fischer-Tropsch systems, as they are modeled as integrated systems with integrated efficiencies (see discussion in Appendix 5.6). Equation (5.10) together with Equation (5.2) then defines the link between the electricity market module and the energy transformation module, integrating the endogenous electricity demand. Short-term drops in the electricity price, for example, may cause ptx systems to ramp up their production and, in turn, their electricity demand. On the other hand, deep decarbonization of sectors, e.g., the road transport sector, may drive the demand for ptx fuels upwards, increasing electricity consumption. Greater electricity consumption requires greater investments in generation capacities, raising total system costs of the electricity sector and, therefore, driving the endogenous electricity price upwards.

Analogous to the endogenous electricity price, the endogenous ptx fuel price represents another key link, which is implicitly visible to all modules as they are subject to one common cost-minimizing objective function. More specifically, for every unit of increased ptx fuel consumption in country m or export to another country, an additional unit of ptx fuel has to be produced in country m or imported from another country or from outside of Europe. The resulting increase in total system costs can be understood as the marginal price of that unit of additional fuel production. Thus, the endogenous market-specific ptx fuel price can be derived from the dual variables of the equilibrium conditions (5.7), (5.8) and (5.9) and represents the change in total system costs for supplying one more unit of ptx fuel.

Another key link between the energy transformation module and the electricity market and road transport modules is the endogenous ptx fuel demanded by the

electricity and road transport sectors, defined via the energy consumption $\mathbf{ec}_{f,f1,m,s,t}$ for $f1 =$ ptx fuels as part of the ptx fuel equilibrium conditions (5.7), (5.8) and (5.9). As such, the model has the option to decarbonize the electricity and road transport sectors using, e.g., a carbon-neutral ptx methane gas or a low-carbon natural gas and ptx hydrogen gas mix.

5.2.3 Simulating the European road transport sector

A key contribution of this analysis lies within the detailed modeling of the European road transport sector and the representation of interlinkages with the electricity market and energy transformation modules. The road transport module invests in vehicle technologies as well as infrastructure to cover an exogenous demand for road transport. The choice of vehicle technology, in turn, drives the fuel demand for the road transport sector, being supplied by the electricity market module and the energy transformation module. In the following, the relevant parameters and assumptions as well as equations are presented in detail. Furthermore, the key variables and equations linking the road transport module to the electricity market and the energy transformation module are presented.

Vehicle segments, vehicle technologies, fuels and infrastructure

Modeling the European road transport sector requires a detailed dataset to define parameters, which are categorized according to those that vary across vehicle segment, vehicle technology and fuel type.

The road transport sector is divided into three vehicle segments: private passenger vehicles (PPV), light-duty vehicles (LDV) and heavy-duty vehicles (HDV).[28] Similar to the approach for the electricity sector, technologies are defined for each of these vehicle segments; however, in the case of road transport, technologies can be understood as motor types. The vehicle technologies considered include gasoline motors, gasoline hybrids, diesel motors, diesel hybrids, natural gas motors, natural gas hybrids, battery electric vehicles (BEVs) and fuel-cell electric vehicles (FCVs). Hybrid vehicles (gasoline, diesel, natural gas) are represented by mild hybrids (HEVs) and plug-in hybrids (PHEVs). The existing technology mix in each country for 2015 as well as any recent growth in, e.g., electric vehicles between 2015 and 2017 is defined

[28] Light-duty vehicles are considered to weight less than 3.5 tonnes, heavy-duty vehicles more than 3.5 tonnes. Motorbikes, scooters and bicycles are excluded from this analysis, as are buses.

exogenously.[29] PPVs and LDVs are available for any fuel in Table 5.1 except for liquefied natural gas and liquefied hydrogen, which can solely be consumed by HDVs. HDVs have a variety of liquid fuels available, although gasoline is not assumed to be an option for heavy transport. Similarly, gaseous fuels such as hydrogen and gas are not available for HDVs in the road transport module due to lower energy densities and, as such, lower driving range (DLR et al. (2010), Bünger et al. (2016)).

As in the electricity market module, vintage classes are defined for each vehicle technology such that new investment objects are made available in future years to account for, e.g., cost degressions and technological innovations. One key cost component for vehicles is the investment cost or purchase price, with the values for PPVs, LDVs and HDVs shown in Tables 5.9 - 5.11 in Appendix 5.6. The costs of vehicle technologies vary greatly not only according to the motor type but also across vehicle segments. This also holds true for fuel consumption, with values differing not only between, e.g., a diesel vehicle and a FCV but also between a passenger vehicle and a heavy-duty vehicle (see Tables 5.15 - 5.17 in Appendix 5.6). As a result, under a sector-specific decarbonization target for the road transport sector, different vehicle technologies will compete not only within their segment (e.g., diesel PPV vs. FCV PPV) but also against the CO_2 abatement costs of the other segments (e.g., FCV PPV vs. FCV HDV).

In addition to investments in vehicle technologies, the model also endogenously builds the accompanying refueling or charging station infrastructure, depending on the fuel type. Just as in the other modules, infrastructure is an investment object with capital, FOM and variable costs.[30] Apart from refueling and charging station infrastructure costs, the distribution costs to the refueling or charging station is also taken into account and shown in Table 5.18 in Appendix 5.6.

As explained in Section 5.2.1, substitute fuels are defined as subsets to the fuel types and are priced according to how they were produced. Fossil-based hydrogen, CNG, LNG, gasoline and diesel as well as biogas, bio LNG, biogasoline and biodiesel are assumed to be available at global market prices. The fuel costs reflect not only the raw fuel prices but also additional production costs such as, e.g., natural gas reformation and oil refining. The price for electricity-based fuels, e.g. ptx gas, ptx diesel, etc., as well as the electricity price for BEVs and PHEVs are endogenously determined together with the electricity market and energy transformation modules.

[29] Based on European Commission (2016b), KBA (2017), IEA (2016a), CBS (2015), Statistics Sweden (2017), Statistics Norway (2017), Bundesamt für Statistik (2017), ZSW (2017) and Department of Transport (2017).

[30] Any additions or reinforcements to the electricity grid are not considered in this analysis.

Key aspects of modeling road transport and its infrastructure

The road transport module invests in vehicle technologies as well as infrastructure to cover an exogenous demand for road transport. The underlying equilibrium condition requires the exogenous demand road transport $dr_{m,t}$ to be covered by supply road transport $\mathbf{sr}_{i,m,t}$ summed over all vehicle technologies $i \in \mathbf{I_{rt}}$:

$$dr_{m,t} = \sum_{i} \mathbf{sr}_{i,m,t} \tag{5.11}$$

The demand for road transport $dr_{m,t}$ defines the annual kilometers driven within each vehicle segment in each country up to 2050 (Tables 5.12 - 5.14 in Appendix 5.6). Investments in vehicle technologies therefore supply the kilometers $\mathbf{sr}_{i,m,t}$ needed to serve demand based on a vehicle's annual driving distance, assumed to be 13'800 km for PPVs, 21'800 km for LDVs and 70'000 km for HDVs.[31] A single FCV PPV, for example, can supply 13'800 km of zero-carbon driving to a country's yearly demand for road transport. Large differences in yearly driving distance affect the vehicle lifetime, assumed to be 15 years for PPVs and 10 years for LDVs and HDVs. Such characteristics may influence the results as technologies in one vehicle segment must be replaced more often than others (e.g., FCV HDV vs. FCV PPV). In order to prevent a single technology from dominating the market from one time period to the next, maximum yearly adoption rates are defined, limiting the share of new registrations in the vehicle fleet in a single time period.[32]

Carbon emissions and emission reductions in the road transport sector are accounted for as described in Section 5.2.1. Thereby, both direct and upstream emissions are accounted for via the decarbonization constraint (5.6), which also applies

[31] Assumptions on annual driving distance and vehicle lifetimes are based on EWI et al. (2014), European Commission (2016b), McKinsey (2010), KBA (2017), Rhenus Logistics (2007), Knörr et al. (2012) and Papadimitriou et al. (2013).

[32] The upper bounds for the short term are taken from current data on new vehicle registrations and vary between 1.8 % and 4.8 % per year for a single vehicle technology. For the long term, they are assumed to increase up to 6.6 %. The values are the same across vehicle technologies but vary across vehicle segments due to discrepancies between segment fleet sizes. These maximum adoption rates were set in order to best allow for an exponential deployment curve for new technologies. Note that the condition may become binding under strict decarbonization targets.

to the road transport sector.[33]

Linking the road transport module to the electricity market and energy transformation modules

The fuel demanded, or energy consumed, by the road transport sector is determined endogenously based on the cost-optimal vehicle and infrastructure investments to cover the total demand for road transport per vehicle segment. The energy consumption $\mathbf{ec}_{f,f1,m,s,t}$ by fuel type f for the road transport sector $s = rt$ is determined by the sum over supply road transport divided by the vehicle efficiencies $\eta_{i,m}$ for all vehicles i of the respective fuel type:

$$\sum_{f1} \mathbf{ec}_{f,f1,m,s,t} \Big|_{s=rt} = \sum_{i} \mathbf{sr}_{i,m,t} / \eta_{i,m} \tag{5.12}$$

with vehicle efficiency $\eta_{i,m}$ being the inverse of vehicle fuel consumption and $i \in \mathbf{I}_{rt}$.

One key link between the road transport module and the electricity market module is the direct use of electricity as a fuel for electric vehicles, i.e. PHEVs and BEVs. Combining Equations (5.12) and (5.2) is how the endogenous electricity demanded by electric vehicles, $\mathbf{ec}_{f,f1,m,s,t}$ for $f1 = f =$ electricity, is accounted for in the electricity market module.[34] The endogenous electricity price represents another key link.

The key links between the road transport module and the energy transformation module are represented by the endogenous ptx fuel price and the ptx fuel demand of the road transport sector, i.e. its energy consumption $\mathbf{ec}_{f,f1,m,s,t}$ for $f1 =$ ptx fuels, as defined in Equation (5.12), which directly feeds in the ptx fuel equilibrium conditions (5.7), (5.8) and (5.9). For example, under increased decarbonization targets,

[33] Literature on the road transport sector often uses the concept of well-to-tank (WTT), i.e., the carbon emissions released during fuel production, and tank-to-wheel (TTW) emissions, i.e., the carbon emissions released upon combustion in the vehicle. In this analysis, the fuel-specific upstream carbon emission factor $\kappa_{f1,upstream}$ is analogous to the WTT emission factor in the road transport sector, whereas the fuel-specific carbon emission factor κ_{f1} is analogous to the TTW emission factor from vehicles. The road transport module therefore follows an approach, which is equivalent to a well-to-wheel (WTW) approach.

[34] For electric vehicles, exogenous hourly charging profiles are applied. Three types of charging stations are simulated: private (e.g., households), semi-private (e.g., workplace) and public (fast charging). Private charging is assumed to take place mostly during evenings, whereas semi-public charging occurs primarily in daytime hours on weekdays. Public charging is possible at any hour but assumed to be less common than private and semi-private charging options (see, e.g., BAST (2015) and DLR (2015)). PHEV are assumed to follow the same charging profiles; however, PPVs are assumed to run 67 % and LDVs 50 % electric (see Kelly et al. (2012)).

one option to decarbonize may be to displace carbon-heavy fossil fuels with ptx fuels. The increase in electricity consumption due to ptx fuel production is then accounted for via the energy transformation module and the electricity market module.

5.3 Application of the integrated model

In order to demonstrate the capabilities of the integrated model developed, an exemplary single scenario analysis is performed. The goal is to simulate the future European electricity-, road transport- and ptx-technology mix under sector-specific decarbonization targets and examine the role of electricity in achieving emission reductions. Within this section, first the scenario framework is presented (Section 5.3.1), followed by key results for the road transport sector (Section 5.3.2). The section ends with a discussion on the production of ptx fuels and how equilibrium is reached via the trading of ptx fuels throughout Europe (Section 5.3.3). The results for the European electricity sector are shown in Appendix 5.6.

5.3.1 Scenario framework

The scenario is built on the medium- and long-term CO_2 targets given in the EU's climate strategy (European Commission (2014)). In the electricity market module, a sector-specific European emission reduction target is set to require a decline in emissions by 43 % compared to 2005 by 2030 and 90 % compared to 1990 by 2050. No additional national decarbonization targets for the electricity sectors are introduced. For the road transport sector, the decarbonization targets are set nationally, based on the Effort Sharing Decision of the European Commission for 2030 (European Commission (2016c)), shown in Table 5.19 of Appendix 5.6. The targets for 2050 converge to a 90 % emission reduction compared to 1990, consistent with the electricity sector target.[35] In addition to CO_2 constraints, the modeled scenario inhibits the energy transformation module from importing ptx fuels from outside of Europe.[36] The fuel price assumptions for the scenario are based on a global commodity market at a price reflecting both the raw fuel and the fuel production costs (Figure 5.9 in Appendix 5.6). All other parameters are defined as described in Sec-

[35] See Appendix 5.6 for a detailed description of the CO_2 target definition.

[36] The goal of the analysis is to maximize the endogeneity of the model. Any exogenous decarbonization options such as ptx fuel imports from outside EU at fixed import costs may weaken the effects of the endgenous model output. Therefore, only endogenous investments in ptx and liquefaction capacities within Europe are allowed.

tion 5.2.

5.3.2 Scenario results for the European road transport sector

The vehicle mix cumulated over all European countries is shown in Figure 5.3. The introduction of a country-specific sectoral decarbonization target in road transport drives an almost immediate alteration to the current vehicle mix. Hybrid (HEV) gasoline and diesel engines emerge as a short-term option to replace their fully internal combustion-powered counterparts. Furthermore, vehicles running on natural gas and electricity also show accelerated growth, with varying penetration levels across segments.

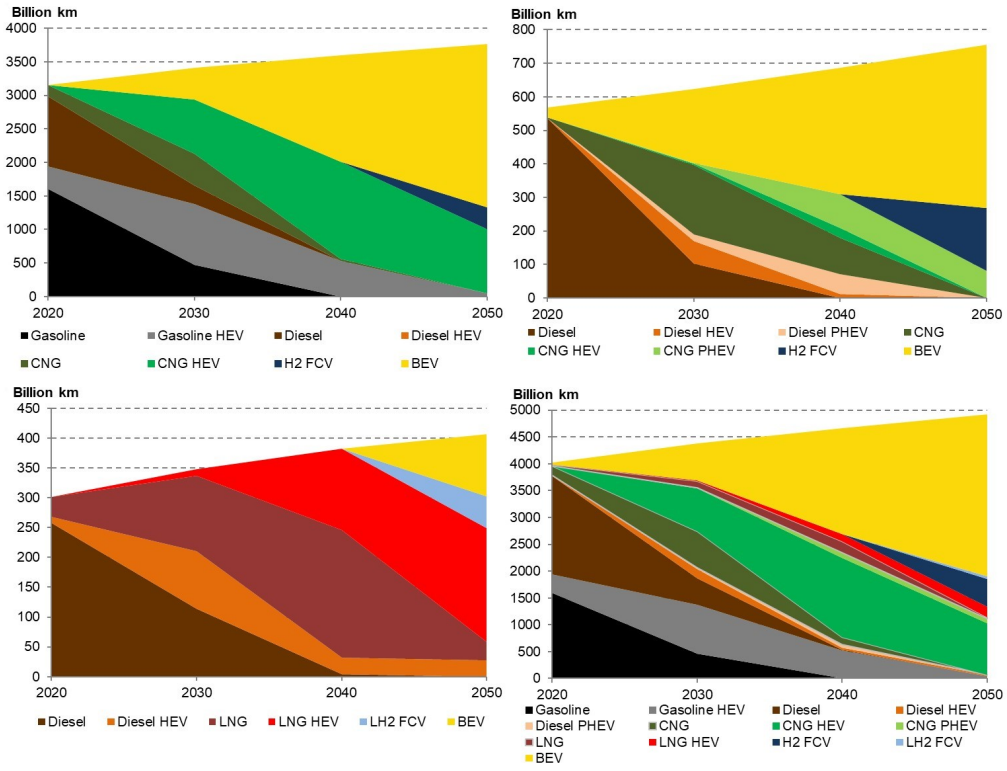

Figure 5.3: EU vehicle mix up to 2050 for PPVs (top left), LDVs (top right), HDVs (bottom left) and all vehicles (bottom right).

For the PPV segment, a mix of hybrid and internal combustion-powered vehicles running on compressed natural gas (CNG) dominate new vehicle investments in the short term. Starting in 2035, the model begins to maximize BEV deployment alongside continued investments in natural gas hybrids. HDVs also use natural gas to jump-start decarbonization, introducing internal combustion-powered trucks in

2020 and hybrid trucks in 2030 that run on liquefied natural gas (LNG) to push out their diesel counterpart; however, diesel HEVs remain in the vehicle mix through 2050. It is not until after 2040 that electric vehicles also begin to break through in the HDV segment, growing quickly to a 25 % share of HDVs by 2050. LDVs, on the other hand, begin to maximize the deployment of electric vehicles early on, reaching upper bound adoption rates already in 2025. Natural gas LDVs help the remaining share to decarbonize, first via internal combustion-powered vehicles and then via plug-in hybrids. Hydrogen FCVs emerge in the LDV segment in 2045 and in the PPV and HDV segments in 2050, as the CO_2 bound becomes more and more restrictive.

Figure 5.4 provides further information about the fuel type consumed by the road transport sector.[37] The amount of fossil gasoline and diesel consumed in the road transport sector decreases by 46 % and 60 %, respectively, between 2020 and 2030. Within this decade, the amount of fossil CNG and LNG, on the other hand, increases ten-fold to account for over 40 % of all fuels consumed in 2030. As the techno-economic characteristics of the vehicles do not drastically differ from one another, the switch from gasoline and diesel to natural gas is driven primarily by comparatively lower well-to-wheel CO_2 emissions as well as cheaper fuel prices. The reduction in non-hybrid gasoline and diesel engines as well as gains in vehicle efficiency drive the total fuel consumption downwards.

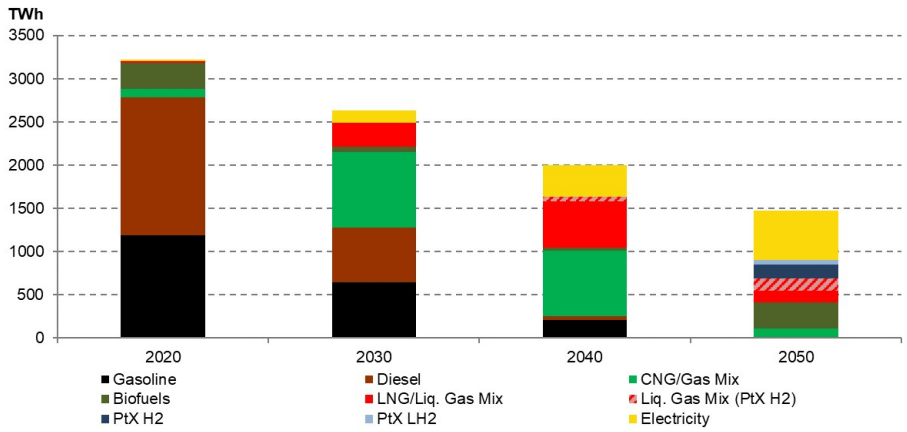

Figure 5.4: Fuel consumption in the road transport sector in Europe in 2020, 2030 and 2050 in the coupled model.

Non-fossil fuels mostly enter the market between 2030 and 2050 as a result of the

[37] The results for the infrastructure follow the developments shown in Figure 5.4, as investments in infrastructure are made independent of vehicle segment and instead serve the total vehicle demand according to fuel type. A detailed discussion of the infrastructure results is omitted from this study as the focus lies primarily on the interdependencies between the modules rather than the individual module results.

long-term country- and sector-specific 90 % CO_2 reduction targets. Most notable is the increase in electricity, accounting for 570 TWh or 37 % of total fuel consumption in the European road transport sector in 2050. Restrictions in new vehicle deployment via maximum adoption rates are binding for BEVs in the PPV and LDV segments relatively early on, which constrains the amount of electricity that can be directly consumed. As such, in order to reach the decarbonization targets, other low-carbon fuels must play a role. In particular, ptx fuels emerge from 2040 onwards, primarily for use in the HDV segment: First as liquefied gas mix and then together with ptx liquefied hydrogen (PtX LH2) and ptx diesel.[38] In fact, in 2050, over 55 % of ptx fuels sold to the European road transport sector is consumed by HDVs. The remaining ptx fuels are in the form of ptx hydrogen gas (PtX H2) and ptx gasoline, consumed by the PPV and LDV segments. In total, the fuel share of ptx fuels in the European road transport sector reaches 27 % by 2050. At this point, fossil as well as biogasoline and biodiesel are completely excluded from the fuel mix. Biogas, on the other hand, makes up a 20 % share of total energy use.

Table 5.20 of Appendix 5.6 shows the corresponding marginal CO_2 abatement costs for the road transport sector in each country for each model year. The countries with higher road transport demand and stricter CO_2 reduction targets in 2030 exhibit non-zero marginal CO_2 abatement costs in all years. A handful of other countries, however, appear to have zero costs for CO_2 abatement in several years up to 2040, i.e., the investments in lower-carbon vehicles and/or fuels are cost-efficient without any price signal from a binding CO_2 constraint. This holds particularly true for countries with higher shares of PPV and LDV demand, as the short-term switch to natural gas and electric cars/vans is cost competitive and thus appears to displace enough carbon emissions to undercut the decarbonization targets. Countries with higher shares of HDV demand, like Belgium, Poland and Spain, reveal some of the highest marginal CO_2 abatement costs in 2040 due to the consumption of liquefied gas mix, which is necessary to reach their sectoral decarbonization target. Because trucks have a higher fuel consumption and longer annual driving distance, the HDV segment in these countries is responsible for a larger share of the emissions. By switching from fossil LNG to low-carbon liquefied gas mix, the model can significantly reduce emissions without a major reinvestment in new vehicle technologies but rather maintaining (and adding to) the existing LNG and LNG hybrid HDV fleet.

[38] The striped areas in Figure 5.4 indicate the share of the gas mix that is decarbonized by ptx hydrogen gas. For example, in 2050, the liquefied gas mix consists of a share of 140 TWh that is decarbonized via ptx hydrogen gas feed-in (red striped area) and a share of 140 TWh liquefied natural gas (red area). For the years without any striped areas, the gas mix is completely fossil. For more information on the assumptions underlying the concept of gas mix, see Appendix 5.6.

By 2050, the country-specific marginal CO_2 abatement costs in the road transport sector in every country reach levels around 500 EUR/tCO_2 as the European-wide production and consumption of ptx fuels in all segments, especially the HDV segment, becomes necessary to reach the 90 % reduction target. Investments in FCV HDVs (with ptx liquefied hydrogen) and BEV HDVs as well as FCVs (with ptx hydrogen gas) in the PPV and LDV segments in 2050 also add to the comparatively high marginal CO_2 abatement costs of the road transport sector.

5.3.3 Supplying ptx fuels in an integrated modeling framework

Decarbonization of the road transport sector appears to create a demand for ptx fuels that must be supplied by either the countries themselves or imported from another European country. As such, a country's electricity market conditions (e.g., endogenous electricity demand, electricity generation mix, NTC constraints) as well as ptx fuel production conditions (e.g., endogenous electricity price, natural gas grid capacities, ptx fuel transport costs) will affect not only how their own road transport sector is decarbonized but whether they supply ptx fuels to or demand ptx fuels from other countries.

A deeper analysis of the ptx investment behavior provides insight into the cost-minimal supply of ptx fuels. Figure 5.12 in Appendix 5.6 shows the development of ptx installed capacities and production across Europe between 2030 and 2050. As can be seen in the figure, investments in ptx first begin to take hold in 2040, with 22 GW electrolysis systems and 400 MW natural gas liquefaction plants. The hydrogen produced from the electrolysis systems (60 TWh) is completely fed into the natural gas grid to produce a low-carbon gas mixture, which is then liquefied (Liq. Gas Mix). The demand for liquefied gas mix in 2040 is driven by the need to decarbonize the fuel consumption in Belgium, Poland and Spain – the three countries with the highest share of HDVs. These three countries both consume their own gas mix production as well as import additional gas mix (via the natural gas grid) and liquefied gas mix (via tankers) to cover their ptx fuel demand. The two largest exporters of gas mix are France and Great Britain, who continue to have significant amounts of nuclear generation in 2040 next to large amounts of VRE. In addition, along with the third largest exporter Germany, these countries profit from large natural gas grid capacities available to feed-in ptx hydrogen gas as well as low transport costs due to the close proximity to the importing countries.

By 2050, the decarbonization targets in the road transport sector have driven every

European country to both produce as well as consume ptx fuels. As shown in Figure 5.12 in Appendix 5.6, 114 GW_{el} of electrolysis systems and 3 GW_{el} of hydrogen and natural gas liquefaction plants are installed across Europe to produce hydrogen gas that is directly consumed (161 TWh_{th}), directly liquefied (56 TWh_{th}) or fed into the natural gas grid (140 TWh_{th}) and eventually liquefied. In addition, 12 GW_{el} of integrated electrolysis/Fischer-Tropsch systems are installed to produce ptx gasoline (16 TWh_{th}) and ptx diesel (33 TWh_{th}).

The ptx-fuel flows in 2050 are shown in Figure 5.5, with red indicating exporting countries and blue importing countries. In addition, Table 5.21 in Appendix 5.6 provides key country-level results for 2040 and 2050 including the marginal costs of electricity generation as well as the average input electricity price for the electrolysis and integrated Fischer-Tropsch systems.[39]

The map on the left-hand side shows the trading of gas mix, i.e., ptx hydrogen gas mixed into the natural gas grid. Although Poland has significantly lower marginal costs of electricity generation than Italy in 2050, the lack of sufficient natural gas grid capacity combined with growing pressure to reduce emissions from its HDV segment result in large import volumes of gas mix. Investing in methanation systems locally, which would be a possible alternative to trading gas mix, does not appear in the cost-optimal solution due to the lower methanation efficiency and resulting higher costs. The model maximizes the feeding-in of ptx hydrogen into the natural gas grid, and, as such, reaches the hydrogen feed-in limit for gas mix in Europe.

As a result, more fuels and/or vehicle technologies to reduce emissions are required to reach the sector-specific decarbonization targets. With the maximum adoption rates for all BEVs, including the HDV segment, have been reached by 2050, the next cost-optimal decarbonization option that emerges in the road transport sector is the consumption of ptx liquefied hydrogen in fuel-cell trucks (FCV HDVs). In fact, all countries invest in FCV HDVs up to their maximum adoption rates during the five-year period between 2045 and 2050, creating a European-wide demand for ptx LH2. As shown in the middle map of Figure 5.5, several countries import significant (>1 TWh_{th}) amounts of ptx LH2 including Czech Republic, Germany, Great Britain, Italy and Poland. The three major exporters include Romania, Sweden and Finland, who not only have significant levels of VRE generation but nuclear generation as well. These effects drive the marginal costs of electricity generation in these

[39] The average input electricity price is calculated for each ptx technology by summing the marginal costs of electricity generation across all hours in which the ptx system produces fuel and then dividing by the respective number of hours. By definition, an average input electricity price only exists if the ptx system is in operation.

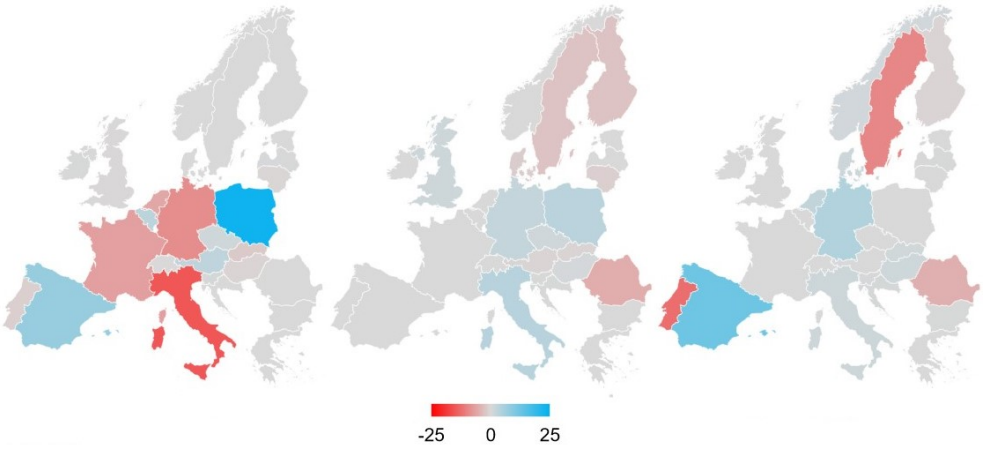

Figure 5.5: Net imports and exports of gas mix (left), ptx liquefied hydrogen (middle) and ptx diesel (right) in TWh_{th}, with positive values in blue indicating net import and negative values in red indicating net export.

countries downwards, lowering the average electricity input price of ptx hydrogen production to 33, 21 and 14 EUR/MWh, respectively (Table 5.21). The liquefaction of hydrogen, in particular, is an energy-intensive process and, as such, requires a large number of hours with very low electricity prices in order to be profitable. Despite the additional costs of transporting LH2, the exporting countries are able to supply the importing countries with ptx LH2 at lower cost than the countries would pay in producing the fuel themselves.

Binding adoption rates also for FCV HDVs however drive the need for an additional decarbonized fuel to enter the market, namely ptx diesel. Analogous to ptx LH2, ptx diesel is produced in select countries with profitable ptx conditions and then exported throughout Europe. The right-hand side of Figure 5.5 shows the corresponding trade flows. Fischer-Tropsch synthesis is, compared to electrolysis, significantly less efficient and, therefore, is only exported by the four countries with the lowest marginal electricity generation costs: Portugal, Sweden, Romania and Finland. As shown in Table 5.21 in Appendix 5.6, the Fischer-Tropsch systems in these countries have an average input electricity price ranging from 47-54 EUR/MWh, similar to their marginal costs of electricity generation. The greatest importer is Spain, who imports over 90 % of its ptx diesel consumption (12 TWh_{th}) from Portugal in order to decarbonize its large HDV fleet. The other producers export small amounts of ptx diesel to fourteen countries across Europe.

Lastly, having exhausted the cost-optimal decarbonization options for the HDV segment, the model chooses to supply the PPV and LDV segments with ptx hydrogen

gas by ramping up investments in fuel-cell vehicles in all countries. Convergence in decarbonization targets to 90 % reduction and similar price-setting abatement technologies result in converging marginal CO_2 abatement costs for the road transport sectors in 2050, as shown in Table 5.20 in Appendix 5.6. Due to very high transport costs of gaseous hydrogen, however, no trading of ptx hydrogen takes place. In other words, all countries supply and consume their own ptx hydrogen, despite significant differences in ptx production costs across countries. The share of ptx hydrogen of total fuel consumption ranges from 3 % (Germany) to 20 % (Ireland); however the maximum adoption rates are never reached. As a by-product of Fischer-Tropsch synthesis, the four exporters of ptx diesel also export small amounts of ptx gasoline for the PPV segments to the neighboring countries with the lowest transport costs, i.e., Spain, Bulgaria, Norway and Denmark.[40]

5.4 Understanding the value of integrated models

Developing and applying an integrated model of this kind can be complex, requiring long computation times and intensive evaluation of the results and their implications. It is not uncommon to question whether such models are more valuable than single-sector or decoupled multi-sectoral models. The model created in this study addresses fundamental economic questions that, given a single market or multiple decoupled markets, could possibly be solved with, e.g., an analytical model. Yet the introduction of multiple coupled markets with integrated demands, substitute fuels across different fuel types, endogenous prices as well as trade possibilities requires that computer-based methods such as linear programming be used to account for the complexity of the coupling of the electricity sector to other sectors.

To provide a quantitative inclination of the added value of the integrated multi-sectoral model at hand, in the following, the results of the integrated model are compared to the results of a model run in which the modules are decoupled and the single sectors optimized independently of one another. In the decoupled model, all endogenous links between the modules are instead fed into the model exogenously. The logic and assumptions behind the exogenous parameters are explained in Section 5.4.1. The results are then compared to the coupled model in Section 5.4.2, with particular focus on key indicators such as CO_2 and electricity prices.

[40] Fischer-Tropsch systems produce a wax (hydrocarbon mixture) that can be upgraded into different fuels. Within the scope of this study, it is assumed that for every unit of ptx diesel, nearly one half unit of ptx gasoline is produced (Becker et al. (2012)). See Appendix 5.6 for more information.

5.4.1 Decoupled versus coupled models

In order to decouple the model, the endogenous links between the electricity market, road transport and energy transformation modules, i.e. the endogenous demands for electricity and ptx fuels, are broken such that each module stands on its own with its own exogenous inputs. As a result, the electricity market module invests in the cost-minimal electricity generation mix in order to cover its own demand, ignoring any additional electricity demand from electric vehicles or ptx technologies, just as in the original DIMENSION model. The road transport module can, nevertheless, invest in electric vehicles, resulting in an electricity demand; however, analogous to the fossil fuels, the module buys the electricity at an exogenous price.[41] The energy transformation module is shut off in order for the electricity and road transport sectors to be independent of one another. Ptx fuels can, however, be bought by the electricity and road transport sectors at an exogenous price, just as is the case with supplying electric vehicles.[42] Gas mix and liquefied gas mix, the result of feeding ptx hydrogen gas into the grid, is not considered in the decoupled case because the link between hydrogen production and gas mix demand cannot be quantified without the energy transformation module. Furthermore, no trading occurs as there is one single European market price for ptx fuels assumed. The exogenous ptx fuel prices as well as the exogenous electricity price for the road transport sector are shown in Figure 5.13 in Appendix 5.6.

5.4.2 Identifying the added value of integrated multi-sectoral models

Figure 5.6 depicts the European electricity demand and electricity generation mix for the coupled and decoupled models in 2050 as well as the developments in marginal electricity generation costs and marginal CO_2 abatement costs in the electricity sector across Europe up to 2050. As expected, the electricity generation levels in the decoupled case are significantly lower (1300 TWh) than in the coupled case, as the additional electricity demand from the road transport and energy transformation modules (1200 TWh), indicated by the striped columns, and additional storage de-

[41] In this analysis, the exogenous electricity price is based on the LCOE of onshore wind generation, accounting for decreasing capital costs and technological improvements (see Figure 5.13 in Appendix 5.6).

[42] The price for ptx fuels is determined according to the production costs, taking into account the annualized investment, variable and fixed costs of different ptx technologies. The electricity price assumptions for the ptx processes are – as for electric vehicles – based on the LCOE of onshore wind. The lack of endogenous information means that the ptx technologies can no longer optimize their electricity consumption according to hourly changes in the electricity price.

mand (100 TWh) is not accounted for.[43] The increase in electricity generation for the additional demand in the coupled model is mainly based on onshore wind and PV due to the identical decarbonization constraint.

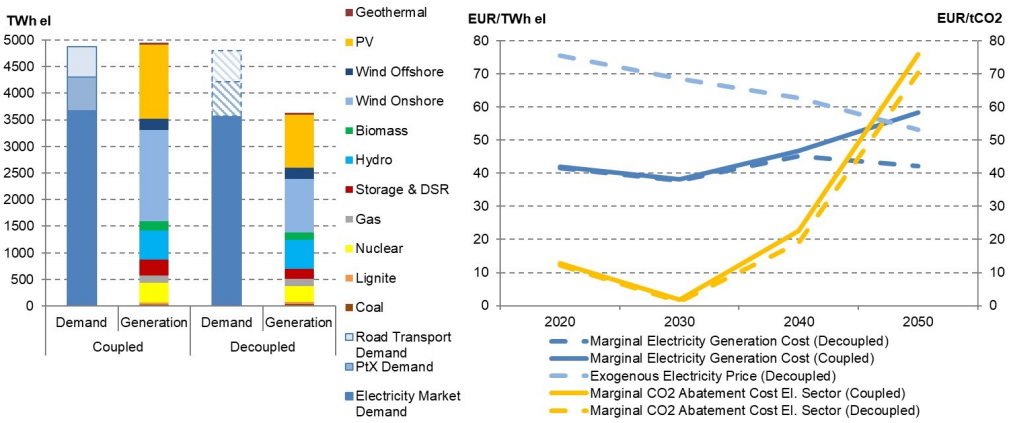

Figure 5.6: Electricity demand by module and electricity generation by fuel type in Europe in 2050 for the coupled and decoupled model (left); Results of average European marginal electricity generation costs and marginal CO_2 abatement costs for the electricity sector in the coupled and decoupled model, including the exogenous electricity price used by the decoupled road transport and energy transformation modules (right).

The prices on the right side of Figure 5.6 also reflect these developments, with the dashed lines indicating the values from the decoupled model. Because the modules are optimized independently of one another, the endogenous electricity price in the decoupled case only reflects the cost of supplying the demand within the electricity market module. While the difference in marginal electricity generation costs is negligible until 2030 due to limited demand increase, from 2040 onwards, the additional electricity demand from the road transport and energy transformation module results in higher marginal electricity generation costs. This is mainly due to fixed decarbonization targets subject to an increasing electricity generation. In 2050, the marginal electricity generation cost delta between the decoupled and coupled model is 16 EUR/MWh on average across all EU countries. The exogenous electricity price assumption for the road transport sector and the ptx fuel production, being based on the LCOE of wind onshore, underestimates the endogenous marginal electricity generation costs of the coupled model by 5 EUR/MWh on average across Europe. Analogous to the marginal electricity generation costs, the marginal CO_2 abatement costs for the electricity sector also begin to diverge from 2030 onwards, reaching a difference of 6 EUR/tCO_2 when comparing the coupled to the decoupled model

[43] Any discrepancy between generation and demand in Figure 5.6 is due to transmission losses.

results.[44]

Comparing the results for the road transport sector, both the vehicle technology mix as well as fuel consumption behavior varies, most notably in the trade-off between ptx and fossil fuels. The results for the coupled and decoupled model in 2040 and 2050 are shown in Figure 5.7. In both models, the adoption rates for BEVs reach their maximum yearly values in the long term, leading the direct electricity consumption to be almost identical in both the coupled and decoupled cases. The same holds true for FCV HDVs and PtX LH2 in 2050. Nevertheless, the rest of the fuels show significant discrepancies between the coupled and decoupled cases beginning in 2040. The lack of available gas mix in the decoupled case makes it more expensive to decarbonize LNG and, in turn, drives a decrease in LNG consumption. As such, compared to the coupled case, HDVs in 2040 are supplied by greater amounts of low-cost fossil diesel, which is then balanced out by a growth in biofuel consumption (biogasoline, biodiesel, biogas).

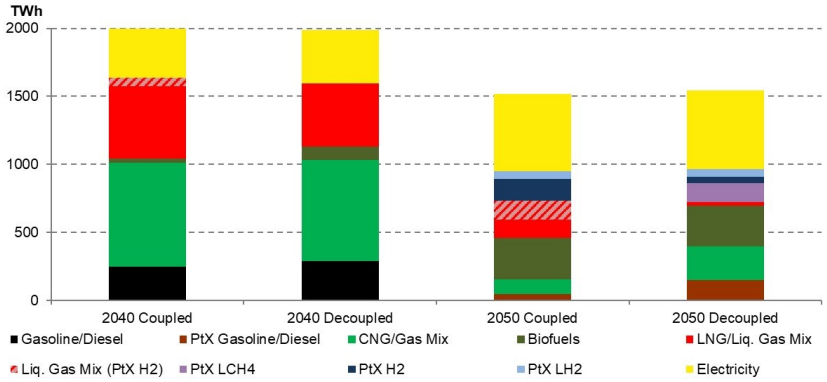

Figure 5.7: Difference in the fuel consumption in the road transport sector in Europe in 2040 and 2050 between the decoupled and the coupled model.

By 2050, carbon-neutral ptx liquid methane (PtX LCH4) displaces much of the fossil LNG at levels equivalent to the decarbonized share of the liquefied gas mix (Liq. Gas Mix (PtX H2)) in the coupled case. Similar to 2040, lower levels of LNG consumption drive higher levels of diesel consumption in the HDV segment, which are, by 2050, entirely made up of carbon-neutral ptx diesel. In the decoupled case, 80 % of all fuel consumption in the HDV segment in 2050 is ptx fuels, compared to the coupled case with 60 %. Given the 90 % decarbonization target in 2050, the

[44] As discussed in Appendix 5.6, the marginal CO_2 abatement costs of the electricity sector sink to 2 EUR/tCO_2 in 2030. Because the model is designed as a social planner problem with perfect foresight, the model anticipates the long-term decarbonization targets with early-on investments in VRE due to limited yearly adoption rates, driving down the marginal CO_2 abatement costs in 2030.

decoupled model reacts to the increased ptx fuel consumption in the HDV segment by avoiding investments in fuel-cell vehicles, driving a 97 % reduction in FCV PPVs and 50 % reduction in FCV LDVs with an accordingly lower ptx hydrogen consumption.

In sum, the total amount of ptx fuel consumption in the road transport sector is 15 TWh_{th} lower in the decoupled case compared to the coupled case, a discrepancy which arises due to the overestimation of ptx fuel costs in the decoupled case. More specifically, the exogenous electricity price used in estimating the production costs of the ptx fuels is a constant value that does not react to hourly changes in electricity market conditions. In the coupled model, however, the ptx systems can reduce their production costs by consuming electricity at times of low marginal costs of electricity generation. In the coupled case, for example, electrolysis operators pay on average across Europe 38 EUR/MWh for their electricity input in 2050 — an average of 15 EUR/MWh less than the exogenous price assumed in the decoupled case (see Table 5.21 in Appendix 5.6). As a result, the production costs of ptx hydrogen are overestimated in the decoupled case. The average EU input electricity price for ptx diesel, on the other hand, only differs by 2 EUR/MWh, which yields similar production costs for ptx diesel across models.

Furthermore, endogenous electricity consumption of the ptx systems yields a significant price spread between the production costs of ptx hydrogen and ptx diesel in the coupled case. The decoupled case, on the other hand, does not take the differences in electricity input prices across ptx systems into account and, as such, exhibits a smaller price spread between ptx hydrogen and ptx diesel. This change in ptx fuel price spreads drives a change in the merit order of decarbonization options: low-cost diesel hybrid (HEV) HDVs fueled with ptx diesel appears to jump ahead of high-cost fuel cell LDVs and PPVs fueled with ptx hydrogen in the decoupled model. Thus, in the decoupled model, decarbonization in the HDV segment is stronger, leaving room for reduced decarbonization in the PPV and LDV segments. The overestimation of ptx production costs and the accompanying change in investment behavior has a direct effect on the marginal CO_2 abatement costs of the road transport sector, with an overestimation of approximately 30 EUR/tCO_2 in the decoupled model (see Table 5.22 in Appendix 5.6).

Overall, the decoupled model overestimates the total system costs in 2050 by 30 billion EUR. The difference in total system costs is a result of the inaccuracy of the estimations for exogenous costs such as electricity and ptx fuel costs compared to the endogenous system costs resulting from the integrated model. In particular, the overestimation of electricity input costs for ptx systems due to a disregard of their

flexibility potential adds to the increase in total system costs of the decoupled model.

5.5 Conclusions

This analysis introduces and assesses an integrated multi-sectoral partial-equilibrium investment and dispatch model to simulate the coupling of the European electricity and road transport sectors. The focus lies not only on depicting a detailed technological representation within each sector but also on properly accounting for any interconnections resulting from electricity consumption from electric mobility or from energy transformation via ptx processes. High technological, spatial and temporal granularity allows for the optimization of European electricity and ptx fuel production as well as the simulation of cost-minimizing trade flows according to endogenous market conditions.

The integrated multi-sectoral model is applied for an exemplary scenario to analyze the effects of sector-specific CO_2 reduction targets (-90 % by 2050 compared to 1990) on the vehicle, electricity and ptx technology mix in European countries from 2020 to 2050. The results show that both electricity and ptx fuels play a key role in decarbonizing the road transport sector, reaching 37 % and 27 % of total fuel consumption in 2050, respectively. The HDV segment, in particular, demands the majority of ptx fuels in Europe, consuming liquefied gas mix, ptx liquefied hydrogen and ptx diesel that is produced primarily in high VRE countries such as Portugal and Sweden. Coupling of the electricity and road transport sectors results in 1200 TWh additional electricity demand in Europe, with average marginal costs of electricity generation across Europe reaching 58 EUR/MWh in 2050.

In order to understand the added value of building complex integrated models, the second part of the analysis examines an identical scenario with decoupled sectors, removing all endogenous ties between sectors and allowing each to be optimized independently of one another. Comparison between the two scenario results confirms that quantitative methods that fail to account for the interdependencies between the electricity and road transport sectors may significantly overestimate the total system costs. The flexibility of ptx systems, in particular, cannot be taken into account once exogenous annual electricity prices are used. As shown in the decoupled model results, ignoring fluctuations in short-term electricity prices may lead to the costs of ptx fuels to be falsely estimated, which may affect the merit order of decarbonization options under strict CO_2 reduction targets and thereby result in substantially different technology choices.

In future work, further detailed scenarios and sensitivity analyses could increase the understanding of the robustness of the presented decarbonization pathway. In particular, the effects of behavioral aspects regarding, e.g., the adoption of new technologies, driving patterns or consumer preferences could be investigated. Furthermore, endogenous charging of electric vehicles may be a promising extension. The model could also be extended to simulate additional modes of transport that may contribute to decarbonization such as, e.g., rail. Although excluded from the discussion, the modeling of the infrastructure for the road transport may be improved to include, e.g., electricity grid investments. Additionally, further research efforts could go into the refining of temporal resolution and technological granularity.

Acknowledgments

The authors would like to thank Simon Paulus for his contributions and Dietmar Lindenberger for the valuable discussions. Special thanks go to Marc Oliver Bettzüge and Felix Höffler for their helpful comments and suggestions. Additionally, the authors would like to thank Joachim Bertsch, Stefan Lorenczik, as well as participants at the 15th IAEE European Conference 2017 for their helpful input and Andreas Fischer for his support. The authors are thankful for support from the participants of the research project 'Virtual Institute - Power to Gas and Heat' (W041A) through the Ministry of Economic Affairs, Innovation, Digitalization and Energy of the State of North Rhine-Westphalia as well as from S. Rabe und G. Unger from CEF NRW. Funding from this research project is also gratefully acknowledged (see Görner and Lindenberger (2018)). Additional funding of the center of excellence 'Virtual Institute - Power to Gas and Heat' (EFRE-0400155) by the 'Operational Program for the promotion of investments in growth and employment for North Rhine-Westphalia from the European fund for regional development' (OP EFRE NRW) through the Ministry of Economic Affairs, Innovation, Digitalization and Energy of the State of North Rhine-Westphalia is gratefully acknowledged.

5.6 Appendix

Nomenclature and abbreviations

Throughout the paper, notation as listed in Table 5.2 is applied. Unless otherwise noted, bold capital letters indicate sets, lowercase letters parameters and bold lowercase letters optimization variables.

Sets		
$f \in \mathbf{F}$		Fuel type ($f1$: Subfuels)
$i \in \mathbf{I}$		Technologies (electricity generators, ptx plants, cars)
$m, n \in \mathbf{M}$		Markets
$s \in \mathbf{S}$		Sector (rt: road transport, el: electricity, et: energy transformation)
$t \in \mathbf{T}$		Time (**T**: time slices)
Parameters		
$l_{m,t}$	MWh	Exogenous electricity demand
l_{peak}	MWh	Peak electricity demand
$dr_{m,t}$	bn. km	Exogenous demand road transport
x	-	Availability of electricity generator
v	-	Capacity value of electricity generators
$\bar{k}$	MW	Transmission capacity
η	-	Efficiency
δ	EUR/MW	Fixed costs
γ	EUR/MW	Variable costs electricity generation
κ_{f1}	tCO_2eq/MWh	Fuel-specific emission factor
$\kappa_{f1,upstream}$	tCO_2eq/MWh	Fuel-specific upstream emission factor
$GHG_{cap,s,t}$	tCO_2eq	Sector-specific greenhouse gas emissions cap
TC	bn. EUR	Total costs
Optimization variables		
$\bar{\mathbf{x}}$	MW	Electricity generation capacity
g	MWh	Electricity generation
k	MWh	Electricity transmission between markets
ec	MWh	Energy consumption
sr	bn. km	Supply road transport
fp	MWh	Fuel production
ft	MWh	Fuel trade
ffi	MWh	Fuel feed-in
em	tCO_2eq	GHG emissions
cpt	tCO_2	CO_2 capture

Table 5.2: Model sets, parameters and variables.

AT	Austria	FI	Finland	NL	Netherlands
BE	Belgium	FR	France	NO	Norway
BG	Bulgaria	GB	Great Britain	PL	Poland
CH	Switzerland	GR	Greece	PT	Portugal
CZ	Czech Republic	HR	Croatia	RO	Romania
DE	Germany	HU	Hungary	SE	Sweden
DK (East)	Eastern Denmark	IE	Ireland	SI	Slovenia
DK (West)	Western Denmark	IT	Italy	SK	Slovakia
EE	Estonia	LT	Lithuania		
ES	Spain	LV	Latvia		

Table 5.3: Country codes.

a	Years
BEV	Battery electric vehicle
bn	Billion
CAES	Compressed air energy storage
CCU	Carbon capture and utilization
CHP	Combined heat and power
CHP	Open cycle gas turbine
CNG	Compressed natural gas
CO_2	Carbon dioxide
cp.	Compared to
CSP	Concentrated solar power
DAC	Direct air capture
DSR	Demand side response
El/el	Electricity / electric
eq	Equivalent
EUR	Euro
FCV	Fuel-cell vehicle
FOM	Fixed operation and maintenance
GW	Gigawatt
H2	Hydrogen
H_2O	Water
HDV	Heavy-duty vehicle
HEV	Hybrid electric vehicle
km	Kilometer
kW_{el} / kW_{th}	Kilowatt (electric / thermal)
kWh_{el} / kWh_{th}	Kilowatt hours (electric / thermal)
LCA	Life cycle analysis
LCOE	Levelized costs of electricity
LDV	Light-duty vehicle
LH2	Liquid hydrogen
Liq	Liquefaction/liquefied
LNG	Liquefied natural gas
m	Million
$MtCO_2$ eq	Million tons carbon dioxide equivalent
MW	Megawatt
NTC	Net transmission capacity
O_2	Oxygen
OCGT	Open-cycle gas turbine
PEM	Polymer electrolyte membrane electrolysis
PHEV	Plug-in hybrid electric vehicle
PPV	Private passenger vehicles
PtX	Power to X (heat, gas, liquid, fuel, chemicals etc.)
PtX H2	Ptx hydrogen gas
PtX LH2	Ptx liquid hydrogen
PtX CH4	Ptx methane gas
PtX LCH4	Ptx liquid methane
PV	Photovoltaics
th	Thermal
t	Ton
TTW	Tank-to-wheel
TW	Terawatt
VRE	Variable renewable energy
WTT	Well-to-tank
WTW	Well-to-wheel

Table 5.4: Abbreviations.

Modeling the European electricity sector

The model covers all 28 countries of the European Union, except for Cyprus and Malta, but includes Norway and Switzerland. Existing electricity generation capacities in 2015 are based on a detailed power plant database developed at the Institute of Energy Economics at the University of Cologne, which is mainly based on the Platts WEPP Database (Platts (2016)) and regularly updated. The investment decisions and generation profiles for a wide range of power plants are optimized endogenously. These include conventional, combined heat and power (CHP), nuclear, onshore and offshore wind turbines, roof and ground photovoltaic (PV) systems, biomass (CHP-) power plants (solid and gas), hydro power plants, geothermal power plants, concentrating solar power (CSP) plants and storage technologies (battery, pump, hydro and compressed air energy (CAES)).[45] Only countries without existing nuclear phase-out policies are allowed to invest in nuclear power plants. Investments in carbon capture and storage (CCS) technologies are not allowed due to a general lack of social acceptance in European countries. Technological improvements in, e.g., efficiency are taken into account using vintage classes. These are then included in the model as an additional technology option that is only available from a certain point in time onwards.

The objective function of the model seeks to minimize the accumulated discounted total system costs.[46] All cost assumptions for technologies listed above are taken from the power plant database at the Institute of Energy Economics at the University of Cologne. Key cost factors are investment, fixed operation and maintenance and variable production costs as well as costs due to ramping thermal power plants. Investment costs occur for new investments in generation and storage units and are annualized with a 7 % interest rate for the depreciation time. The fixed operation and maintenance costs represent staff costs, insurance charges, interest rates and maintenance costs. Variable costs are determined by the fuel price, net efficiency and total generation of each technology. Depending on the ramping profile additional costs for attrition occur. CHP plants can generate income from the heating market, thus reducing the objective value (Jägemann et al. (2013)). The model applies a discount rate of 2.75 % for discounting of future cashflows to the present (net present value).

[45] The use of lignite and biomass sources (solid and gaseous) is restricted by a yearly primary energy potential in MWh per country.

[46] The total system costs do not include investment costs for electricity grid extensions nor operational costs for grid management.

Short-term deployment of renewable technologies is taken into account via minimal deployment targets (based on ENTSO-E (2015a)) for 2020 and remain constant up to 2050.[47]

The model also considers several subregions within the countries, which differ with regard to the hourly electricity feed-in profiles and the achievable full load hours of wind turbines (onshore and offshore) and solar power plants (PV and CSP) per year. Overall, the model distinguishes between 47 onshore wind, 42 offshore wind and 38 solar subregions across Europe. The hourly electricity feed-in of wind and solar power plants per subregion are based on historical hourly wind speed and solar radiation data by EuroWind (2011).[48] The deployment of wind and solar power technologies is restricted by a space potential in km^2 per subregion.

Yearly national electricity consumption is assumed to follow the Ten-Year Network Development Plan (TYNDP) from ENTSO-E (2015b) and the European Commission's e-Highway 2050 Project (European Commission (2015)). It is important that the countries' future electricity consumption, i.e., their exogenous electricity demand, does not assume any additional electricity demand from, e.g., electric vehicles or power-to-x systems. This additional electricity demand is determined endogenously from the energy transformation and road transport modules. Therefore, specific scenarios fitting this criteria were chosen from ENTSO-E (2015b) and European Commission (2015), namely the Small & Local scenario for 2040 and 2050. Hourly electricity demand is based on historical hourly load data from ENTSO-E (ENTSO-E (2012)). Interconnector capacities are taken into account via one node per country. Hence, the model covers 28 countries connected by 65 transmission corridors. Existing and future extensions of net-transfer capacities are exogenously defined and may in some cases limit the power exchange across country borders. This data has been taken from ENTSO-E (2015b), Bundesnetzagentur (2016) and European Commission (2015).

[47] This statement holds true for all technologies with the exception of offshore wind. Expected deployment projections were taken from WindEurope (2017) for 2020 and EWEA (2015) for 2030 and 2050

[48] While the securely available capacity of dispatchable power plants within the peak-demand hour is assumed to correspond to the seasonal availability, the securely available capacity of wind power plants (onshore and offshore) within the peak-demand hour (capacity value or capacity credit) is assumed to amount to 5 %. In contrast, PV systems are assumed to have a capacity value of 0 % due to the assumption that peak demand occurs during evening hours in the winter. A peak-demand constraint ensures enough back-up capacity to meet security of supply requirements given a high share of fluctuating renewables (Jägemann et al. (2013)).

Key links between the modules

Figure 5.8 provides an illustration of the links between the electricity market, the energy transformation and the road transport modules, represented by endogenous demands for electricity and ptx fuels as well as the respective endogenous prices resulting from the integrated optimization.

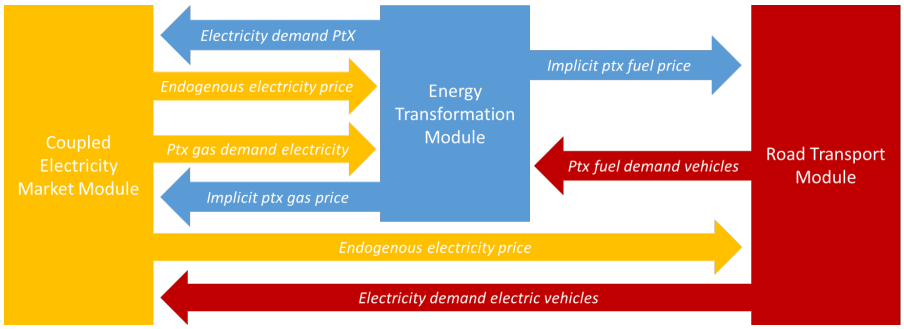

Figure 5.8: Exchange of endogenous information between the modules in the integrated model.

Additional data and assumptions

Substitute Fuel	Direct Emissions (TTW)[49]	Upstream Emissions (WTT)[50]	Description Production Cycle (plus dispensing at retail site)
Diesel	0.268	0.052	Crude oil production, crude refining. distribution
Biodiesel	0.268	0.192	Rape cultivation, rapeseed drying, oil production, biodiesel production, distribution
PtX Diesel	0.268	0.005	Distribution
Gasoline	0.253	0.046	Crude oil production, crude refining, distribution
Biogasoline	0.253	0.191	Wheat cultivation, grain drying, storage and handling, ethanol production, distribution
PtX Gasoline	0.253	0.005	Distribution
CNG	0.204	0.028	NG production, distribution, compression
Biogas (hc)	0.204	0.053	Fermentation, upgrading, compression, distribution
Biogas (lc)	0.204	0.053	Fermentation, upgrading, compression, distribution
PtX CH4	0.204	0.012	Distribution
LNG	0.204	0.053	NG production, liquefaction, loading & unloading terminal, road transport
Bio LNG	0.204	0.077	Fermentation, upgrading, liquefaction, distribution
PtX LCH4	0.204	0.016	Distribution
H2	0.000	0.334	NG production, stream reforming, pipeline, compression
PtX H2	0.000	0.047	Distribution
LH2	0.000	0.423	NG production, stream reforming, liquefaction, road transport
PtX LH2	0.000	0.015	Distribution
Biosolid	0.327	0.028	Wood plantation & chipping
Coal	0.339	0.059	Hard coal provision
Lignite	0.403	0.020	Lignite provision
Nuclear	0.000	<0.001	Uranium ore extraction, fuel production

Table 5.5: Direct and upstream emission factors [tCO_2eq/MWh].

[50]The upstream emission factors are taken from Edwards et al. (2014) and include CO_2 emissions resulting from production and conditioning. Any CO_2 emissions emitted during transportation of the fuel to market is not accounted for in the upstream emission factor.

[50]The direct emissions factors are taken from Department for Business, Energy and Industrial Strategy (2016) and UBA (2017).

Selected data and assumptions used in the energy transformation module

In the following, additional explanations and technical details about the technologies used in the energy transformation module are presented. An electrolysis system uses electricity in an endothermic process to split water into hydrogen and oxygen. Alkaline and PEM electrolysis vary according to their electrolyte solution and electrode composition; however, both operate at temperatures ranging from 50 to 80 degrees Celsius. The hydrogen produced can either be sold directly or be stored to successively produce methane via catalytic methanation, hydrocarbons via Fischer-Tropsch synthesis, or a low-carbon natural gas mixture via feeding into the natural gas grid. During catalytic methanation, carbon dioxide and hydrogen undergo an exothermic reaction at temperatures between 200 and 400 degrees Celsius to yield methane, steam and heat.[51] Fischer-Tropsch synthesis is a more complex process in which carbon monoxide and hydrogen build carbon chains via a series of exothermic reactions followed by an endothermic hydrocracking isometrisation distillation to separate the crude product into usable fuels (e.g., ptx gasoline, ptx diesel). A simplified production ratio of ptx gasoline to ptx diesel of 9.8 : 20.1 is applied in the model (Becker et al. (2012)). CO_2 is used to create the carbon monoxide via reverse CO shift (Schmidt et al. (2016)).

The feed-in of hydrogen into the natural gas grid is modeled with an upper limit of 10 vol-% of natural gas. Note that hereby it is assumed that the changes in the energy density of the gas mix (natural gas / ptx hydrogen gas mix) are negligible, i.e., one MWh of injected ptx hydrogen adds one MWh to the natural gas supply, or, stated differently, it substitutes one MWh of natural gas and thereby reduces the amount of CO_2 emissions from combustion accordingly. Thereby, the model implicitly assumes a certificate market for units of decarbonized gas (i.e., hydrogen feed-in). As such, the energy transformation module can feed-in hydrogen gas up the upper 10 vol-% limit, being based on the natural gas demand of all sectors in each respective country as a proxy. The certificate market for decarbonized gas allows the road transport module to buy decarbonized gas. Note that thereby the total amount of decarbonized gas consumed in the road transport sector may exceed 10 vol-% of the total gas consumption of the road transport, as the feed-in limit is defined on total gas demand of all sectors and not of the road transport sector alone. In a model covering multiple sectors, the single sectors thereby compete for low-cost decarbonized gas via hydrogen feed-in on the certificate market.

[51] As the heating sector is not accounted for in this analysis, efficiency gains due to the recycling of the heat generated by methanation is not considered.

For every mole of hydrogen produced, an electrolysis system produces a half-mole of oxygen that can be sold to, e.g. the industry or services sectors. The amount of oxygen produced is determined stoichiometrically based on the amount of ptx hydrogen produced by electrolysis, which is driven not only by the endogenous hydrogen demand but from the need for ptx hydrogen in the methanation or Fischer-Tropsch processes as well. To determine the amount of oxygen produced, octane was assumed for gasoline and hexadecane for diesel.

Table 5.6 gives an overview of the key assumptions made for each ptx investment object considered in the energy transformation module with regard to investment costs, FOM costs, efficiency and technical lifetime. It should be noted that only integrated systems are considered for methanation and Fischer-Tropsch systems, meaning that all investments in methanation and Fischer-Tropsch technologies include the simultaneous investment in a PEM electrolysis to produce the ptx hydrogen required in the subsequent methanation or Fischer-Tropsch processes. Therefore, the techno-economical parameters, e.g., investment costs, for methanation and Fischer-Tropsch systems in Table 5.6 are for integrated, as opposed to stand-alone, systems. This is especially important when considering the efficiencies, which are always defined with respect to the electricity input of the integrated system, i.e., the amount of fuel output relative to the amount of electricity input.[52] The FOM costs also include the stack replacement costs of the electrolysis system, calculated based on the assumptions in Grahn (2017).

Conversion systems to liquefy gaseous hydrogen or natural gas are also taken into account in the energy transformation module. Because liquefaction plants also consume electricity, they are modeled analogous to ptx systems as investment objects. Unlike the integrated ptx systems, liquefaction plants are assumed to be stand-alone systems. The techno-economic assumptions for the liquefaction plants are in Table 5.7.

[52] PEM electrolysis in integrated systems is also allowed to produce ptx hydrogen in stand-alone mode.

		2020	2030	2050	Main sources
Investment costs [EUR/(kW_el)]	Alkaline Electrolysis	833	500	383	Henning and Palzer (2015), FfE (2016), Elsner and Sauer (2015), Schiebahn et al. (2015)
	PEM Electrolysis	980	545	484	Elsner and Sauer (2015), Schmidt et al. (2016)
	Methanation (coupled with a PEM electrolysis)	1317	845	717	Grahn (2017), Brynolf et al. (2018), Tremel et al. (2015)
	Fischer-Tropsch (coupled with a PEM electrolysis)	1887	1152	917	Grahn (2017), Brynolf et al. (2018), Tremel et al. (2015), Smejkal et al. (2014)
FOM costs (including stack replacement costs for electrolysis) [EUR/(kW*a)]	Alkaline Electrolysis	40	21	16	Schmidt et al. (2016), Grahn (2017)
	PEM Electrolysis	50	23	18	Schmidt et al. (2016), Grahn (2017)
	Methanation (coupled with a PEM electrolysis)	63	35	28	Schmidt et al. (2016), Grahn (2017)
	Fischer-Tropsch (coupled with a PEM electrolysis)	83	46	37	Schmidt et al. (2016), Grahn (2017)
Efficiency [MWh_th/MWh_el]	Alkaline Electrolysis	0.67	0.70	0.70	FfE (2016), Elsner and Sauer (2015), Schiebahn et al. (2015)
	PEM Electrolysis	0.65	0.67	0.71	Schmidt et al. (2016)
	Methanation (coupled with a PEM electrolysis)	0.48	0.50	0.54	Schmidt et al. (2016), Grahn (2017), Brynolf et al. (2018), Tremel et al. (2015)
	Fischer-Tropsch (coupled with a PEM electrolysis)	0.45	0.47	0.51	Schmidt et al. (2016), Grahn (2017), Brynolf et al. (2018), Tremel et al. (2015)
Technical Lifetime [a]	Alkaline Electrolysis	15	20	25	Henning and Palzer (2015), FfE (2016), Elsner and Sauer (2015), Schiebahn et al. (2015)
	PEM Electrolysis	15	20	25	FfE (2016), Elsner and Sauer (2015), Schiebahn et al. (2015)
	Methanation (coupled with a PEM electrolysis)	15	20	25	Elsner and Sauer (2015), Brynolf et al. (2018), Parra and Patel (2016)
	Fischer-Tropsch (coupled with a PEM electrolysis)	15	20	25	Brynolf et al. (2018), Becker et al. (2012)
Interest rate [%]	All	7	7	7	Kost et al. (2018)

Table 5.6: Assumptions on PtX costs.

Hydrogen Liquefaction	**Efficiency (MWh_fuel/MWh_el)**	3.53	Amos (1998), Krewitt and Schmid (2005),U.S. Department of Energy (2009)
	Technical Lifetime (a)	25	Krewitt and Schmid (2005)
	Invest Costs 2020/2030/2050 (EUR/kW_el)	1588 / 761 / 622	Pfennig et al. (2017)
	FOM Costs (EUR/kW_el*a)	91	Krewitt and Schmid (2005)
	Interest Rate (%)	7	Fraunhofer 2018
Methane/ Natural Gas Liquefaction	**Efficiency (MWh_fuel/MWh_el)**	17.37	Franco and Casarosa (2014)
	Technical Lifetime (a)	20	Schmidt et al. (2016)
	Invest Costs 2020/2030/2050 (EUR/kW_el)	5466 / 5286 /4927	Schmidt et al. (2016), Songhurst (2014)
	FOM Costs (EUR/kW_el*a)	211	Schmidt et al. (2016)
	Interest Rate (%)	7	Kost et al. (2018)

Table 5.7: Assumptions on liquefaction costs.

Fuel transport costs between markets [EUR/MWh/km]	
PtX Gasoline/PtX Diesel	0.010
Gas Mix/PtX CH4	0.002
Liq. Gas Mix/PtX LCH4	0.015
PtX H2	0.090
PtX LH2	0.020

Table 5.8: Ptx fuel transport costs between markets[53]

Selected data and assumptions used in the road transport module

In the following, additional details about the technologies used in the road transport module are presented.

	2015	2020	2030	2040	2050
Gasoline	22'475	22'573	22'769	22'769	22'769
Diesel	24'275	24'373	24'569	24'569	24'569
Gasoline HEV	23'890	23'752	23'476	23'123	22'769
Diesel HEV	25'803	25'646	25'332	24'951	24'569
Gasoline PHEV	31'774	30'125	26'829	26'110	25'371
Diesel PHEV	34'318	32'529	28'950	28'174	27'377
CNG	24'729	24'631	24'436	24'363	24'289
CNG HEV	26'286	25'922	25'195	24'742	24'289
CNG PHEV	34'960	32'905	28'793	27'979	27'146
H2 FCV	66'746	54'892	31'184	27'990	24'796
BEV	34'900	31'042	27'581	26'114	24'646

Table 5.9: PPV Vehicle Cost [EUR/vehicle][54]

	2015	2020	2030	2040	2050
Diesel	26'003	26'585	27'748	27'748	27'748
Diesel HEV	31'156	30'966	30'498	29'123	27'748
Diesel PHEV	41'437	38'523	32'696	31'820	30'920
CNG	28'955	28'841	28'612	28'526	28'440
CNG HEV	34'692	33'594	31'448	29'940	28'440
CNG PHEV	46'141	41'999	33'714	32'761	31'785
BEV	41'021	36'967	32'100	30'392	28'684
H2 FCV	78'452	64'519	36'653	32'899	29'145

Table 5.10: LDV Vehicle Cost [EUR/vehicle][55]

[53] Based on Balat (2008), Dodds and McDowall (2014), IEA (2013), Yang and Ogden (2007).

[54] Own calculations based on Wietschel et al. (2010), Fraunhofer IWES et al. (2015), Henning and Palzer (2015), ADAC (2015), Arndt et al. (2016), IEA (2017a) and Özdemir (2011).

[55] Own calculations based on Wietschel et al. (2010), Fraunhofer IWES et al. (2015), Henning and Palzer (2015), ADAC (2015), Arndt et al. (2016), IEA (2017a) and Özdemir (2011).

[56] Own calculations based on Wietschel et al. (2010), Fraunhofer IWES et al. (2015), Henning and Palzer (2015), ADAC (2015), Arndt et al. (2016), IEA (2017a) and Özdemir (2011).

	2015	2020	2030	2040	2050
Diesel	108'157	109'959	113'565	113'565	113'565
Diesel HEV	144'209	143'332	140'757	138'181	135'196
LNG	130'689	130'046	128'758	127'471	126'183
LNG HEV	174'253	170'819	163'952	157'085	150'218
BEV	441'640	397'219	250'000	180'000	130'689
LH2 FCV	441'640	397'219	308'376	219'533	130'689

Table 5.11: HDV Vehicle Cost [EUR/vehicle][56]

	2015	2020	2030	2040	2050
AT	65	67	71	76	80
BE	76	82	89	95	101
BG	34	35	37	39	40
HR	19	21	23	24	26
CZ	48	52	60	68	75
DK (East)	16	17	18	18	19
DK (West)	18	20	21	22	22
EE	8	8	9	9	10
FI	48	48	50	51	52
FR	453	480	507	533	550
DE	621	626	651	663	671
GB	417	444	483	513	540
GR	58	59	60	62	63
HU	29	32	36	41	45
IE	31	34	41	45	48
IT	342	358	379	387	407
LV	9	10	10	11	11
LT	17	18	19	19	20
NL	104	108	114	120	125
NO	33	34	36	37	39
PL	112	128	149	167	179
PT	56	57	64	68	72
RO	42	46	57	67	74
SK	14	17	22	24	26
SI	16	17	19	20	21
ES	192	201	231	257	278
SE	77	79	86	91	95
CH	59	61	65	69	74

Table 5.12: PPV Road Transport Demand [Billion km][57]

[57] Own calculations based on European Commission (2016b) and EWI et al. (2014).

	2015	2020	2030	2040	2050
AT	11	12	14	16	18
BE	13	14	16	17	19
BG	3	3	3	3	3
HR	4	5	5	6	6
CZ	9	9	11	12	13
DK (East)	5	5	6	7	8
DK (West)	6	6	6	7	8
EE	1	1	1	1	1
FI	5	6	6	6	7
FR	118	125	140	156	174
DE	44	46	51	57	62
GB	73	75	81	87	94
GR	14	15	17	18	20
HU	9	9	10	11	12
IE	16	16	18	20	21
IT	85	87	92	96	101
LV	1	1	2	2	2
LT	2	2	3	3	3
NL	21	22	23	25	28
NO	9	10	11	12	13
PL	21	23	30	38	48
PT	21	21	22	23	24
RO	7	7	8	9	10
SK	4	4	5	5	6
SI	3	3	4	4	5
ES	22	23	24	26	28
SE	12	12	13	14	15
CH	4	5	5	5	6

Table 5.13: LDV Road Transport Demand [Billion km][58]

[58] Own calculations based on European Commission (2016b) and EWI et al. (2014).

	2015	2020	2030	2040	2050
AT	4	4	5	6	6
BE	11	12	15	17	18
BG	1	1	1	2	2
HR	1	1	2	2	2
CZ	5	6	6	7	8
DK (East)	1	2	2	2	2
DK (West)	2	2	2	3	3
EE	0	0	0	0	0
FI	2	3	3	3	3
FR	30	34	42	47	50
DE	53	59	67	70	72
GB	33	34	38	41	44
GR	4	5	5	5	6
HU	3	3	4	4	4
IE	1	2	2	3	3
IT	20	22	24	26	28
LV	1	1	1	1	1
LT	1	1	1	1	1
NL	7	8	8	9	9
NO	2	3	3	3	3
PL	25	28	35	40	43
PT	1	2	2	2	2
RO	3	4	5	6	6
SK	2	2	3	3	3
SI	1	1	2	2	2
ES	51	55	63	70	75
SE	3	3	3	4	4
CH	4	5	5	5	6

Table 5.14: HDV Road Transport Demand [Billion km][59]

[59] Own calculations based on European Commission (2016b) and EWI et al. (2014).

	2015	2020	2030	2040	2050
Gasoline	0.71	0.60	0.55	0.53	0.53
Diesel	0.66	0.54	0.46	0.42	0.42
Gasoline HEV	0.46	0.43	0.40	0.36	0.34
Diesel HEV	0.43	0.40	0.37	0.36	0.34
Gasoline PHEV	0.37	0.33	0.29	0.28	0.28
Diesel PHEV	0.35	0.31	0.26	0.24	0.24
CNG	0.70	0.61	0.58	0.55	0.53
CNG HEV	0.53	0.44	0.39	0.37	0.37
CNG PHEV	0.36	0.33	0.30	0.28	0.28
H2 FCV	0.34	0.32	0.28	0.26	0.24
H2 Hybrid FCV	0.34	0.32	0.28	0.26	0.24
H2 PHEV FCV	0.25	0.24	0.21	0.20	0.19
H2 ICE	0.45	0.44	0.41	0.40	0.38
BEV	0.20	0.19	0.16	0.15	0.15

Table 5.15: PPV Fuel Consumption [kWh/km][60]

	2015	2020	2030	2040	2050
Diesel	1.01	0.86	0.77	0.75	0.71
Diesel HEV	0.81	0.69	0.61	0.60	0.57
Diesel PHEV	0.54	0.49	0.42	0.40	0.38
CNG	1.25	1.22	1.17	1.08	1.03
CNG HEV	1.00	0.98	0.94	0.86	0.82
CNG PHEV	0.62	0.60	0.56	0.51	0.49
LNG	1.25	1.22	1.17	1.08	1.03
LNG HEV	1.00	0.98	0.94	0.86	0.82
BEV	0.31	0.30	0.25	0.23	0.22
H2 FCV	0.61	0.52	0.46	0.45	0.43
LH2 FCV	0.61	0.52	0.46	0.45	0.43

Table 5.16: LDV Fuel Consumption [kWh/km][61]

[60] Own calculations based on EWI et al. (2014), Dodds and McDowall (2014), Dodds and Ekins (2014), DLR et al. (2012), dena and LBST (2017), PLANCO Consulting and Gewässerkunde (bfg) and Papadimitriou et al. (2013).

[61] Own calculations based on EWI et al. (2014), Dodds and McDowall (2014), Dodds and Ekins (2014), DLR et al. (2012), dena and LBST (2017), PLANCO Consulting and Gewässerkunde (bfg) and Papadimitriou et al. (2013).

	2015	2020	2030	2040	2050
Diesel	2.45	2.30	2.10	1.90	1.77
Diesel HEV	1.72	1.61	1.47	1.33	1.24
CNG	2.54	2.36	1.97	1.88	1.79
CNG HEV	1.78	1.65	1.38	1.31	1.25
LNG	2.54	2.36	1.97	1.88	1.79
LNG HEV	1.78	1.65	1.38	1.31	1.25
BEV	0.80	0.80	0.80	0.80	0.80
H2 FCV	1.47	1.38	1.26	1.14	1.06
LH2 FCV	1.47	1.38	1.26	1.14	1.06

Table 5.17: HDV Fuel Consumption [kWh/km][62]

Supporting information scenario framework

The CO_2 constraint in the electricity market module covers cumulative emissions from electricity generation across all European countries, regardless of the sector that uses the electricity. In the scenario at hand, the aim is to reduce not only the direct emissions from, e.g., the burning of fossil fuels but the upstream emissions as well. Within the electricity market module, upstream emissions may result from, e.g., coal mining or biofuel production. Historical data on European greenhouse gas emissions is taken from the European Environmental Agency (EEA (2017)).[63] For 2020, an emission reduction of 24 % compared to 2005 emission levels is set for the European electricity sector.[64] Furthermore, the scenario requires that emissions decline by 43 % compared to 2005 emission levels by 2030 and 90 % compared to 1990 by 2050. All percent values are based on official reduction targets formulated by European Commission (2014).

For the road transport sector, the CO_2 constraint is implemented as a percentage reduction of CO_2-equivalent emissions emitted not for Europe as a whole, but rather for each individual European country. Whereas policies to decarbonize the electricity sector tend to be regulated on the European level (e.g., via instruments such as the EU-ETS), the road transport sector is assumed in this scenario to be overseen nationally. The decarbonization target for the road transport sector applies to both the TTW and the WTT emissions. Historical emissions data is based on the EEA (2017) and UBA (2017).[65] National reduction targets for the road transport sec-

[62] Own calculations based on EWI et al. (2014), Dodds and McDowall (2014), Dodds and Ekins (2014), DLR et al. (2012), dena and LBST (2017), PLANCO Consulting and Gewässerkunde (bfg) and Papadimitriou et al. (2013).

[63] Historical values were adjusted to account for upstream emissions.

[64] The European 2020 Climate & Energy Package outlines a 21 % reduction relative to 2005 emission levels European Commission (2014). However, latest developments and discussions have shown that this target is likely to be surpassed and was therefore adjusted accordingly in the model.

[65] Historical values were adjusted to account for the WTT emissions.

	Fuel Type	2015	2050	Sources
Investment Cost [EUR/kW]	Gasoline/Diesel	10	10	**Krewitt and Schmid (2005), Mariani (2016), Schmidt et al. (2016)**
	Gas	65	30	
	Liquefied Gas	40	20	
	H2	350	100	
	LH2	280	100	
	Electricity	550	350	
Interest Rate [%]	All	10	10	**Platts (2016)**
Lifetime [a]	All	25	25	**IEA (2013)**
FOM Cost [% of investment cost]	Gasoline/Diesel	3.2	3.2	**Schmidt et al. (2016)**
	Gas	0.4	0.4	
	Liquefied Gas	3.2	3.2	
	H2	2.9	2.9	
	LH2	2.9	2.9	
	Electricity	1.0	1.0	
Variable Cost [EUR/MWh]	Gasoline/Diesel	0.05	0.05	**IEA (2013)**
	Gas	11	7	
	Liquefied Gas	5	5	
	H2	15	15	
	LH2	5	5	
	Electricity	0.1	0.1	
Full Load Hours	All	2000	2000	**IEA (2013)**
Fuel Distribution Costs to Refueling/Charging Station [EUR/MWh]	Gasoline/Diesel	1.0	1.0	**Balat (2008), Dodds and McDowall (2014), IEA (2013), Yang and Ogden (2007)**
	Gas	1.0	1.0	
	Liquefied Gas	2.3	2.3	
	H2	13.2	13.2	
	LH2	3.0	3.0	
	Electricity	6.7	6.7	

Table 5.18: Techno-economic assumptions for refueling/charging stations as well as fuel distribution costs to refueling/charging stations as used in the road transport module.

tor are based on the Effort Sharing Decision of the European Commission for 2020 European Commission (2009) and 2030 European Commission (2016c) for each European member state and can be found in Table 5.19. For 2050, CO_2 emissions in the transportation sector are to be reduced by 90 % compared to 1990 values in every country, consistent with the electricity sector target. The energy transformation module is not subject to a CO_2 reduction target. The produced zero-carbon and carbon-neutral ptx fuels, however, contribute to the targets imposed on the electricity and road transport sectors, depending on the sector in which the fuels are consumed.

	2020		2030	
	$MtCO_2$	Target (cp. 2015)	$MtCO_2$	Target (cp. 2005)
AT	19.1	-5%	13.9	-36%
BE	25.4	-10%	18.0	-35%
BG	9.0	4%	7.4	0%
HR	6.5	4%	5.5	-7%
CZ	17.6	5%	13.8	-14%
DK (East)	5.1	-13%	3.8	-39%
DK (West)	6.0	-13%	4.4	-39%
EE	2.2	2%	1.7	-13%
FI	12.1	-8%	9.0	-39%
FR	143.8	-7%	100.8	-37%
DE	170.4	-7%	113.2	-38%
GB	126.0	-6%	89.5	-37%
GR	20.4	2%	20.4	-16%
HU	12.1	10%	9.9	-7%
IE	10.9	-13%	9.4	-30%
IT	108.0	-3%	86.8	-33%
LV	2.8	5%	2.5	-6%
LT	2.6	-44%	3.5	-9%
NL	29.9	-10%	23.4	-36%
NO	10.7	-7%	6.8	-38%
PL	48.4	3%	34.7	-7%
PT	19.7	3%	18.4	-17%
RO	14.5	10%	10.7	-2%
SK	6.1	6%	5.5	-12%
SI	5.1	1%	3.6	-15%
ES	82.2	-4%	75.0	-26%
SE	19.7	-8%	14.4	-40%
CH	15.6	-7%	10.7	-38%

Table 5.19: Decarbonization targets for the road transport sector, based on the EU Effort Sharing CO_2 Targets.

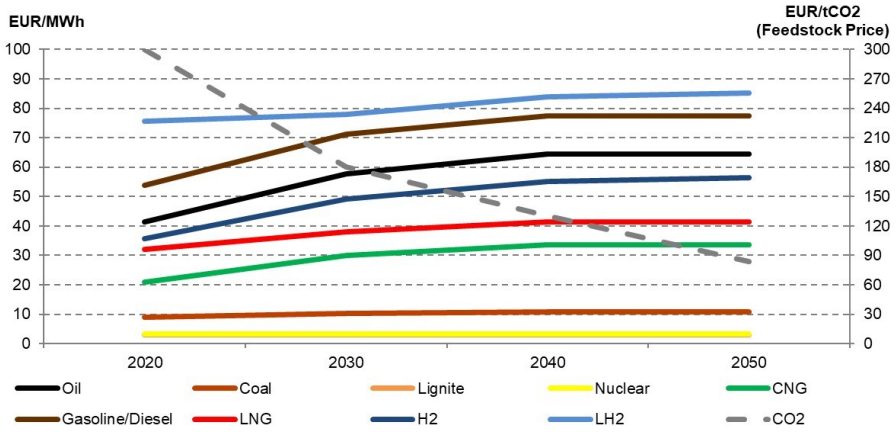

Figure 5.9: Assumptions on fossil fuel and CO_2 feedstock (from direct air capture) price developments based on IEA (2016b), DLR et al. (2014), Krewitt and Schmid (2005), EIA (2015), Henderson (2016) and Schmidt et al. (2016). Fossil fuel prices include any production costs (e.g., oil refining or methane reformation) and exclude taxes and fees.

Additional European road transport results

The marginal CO_2 abatement costs for single countries are shown in Table 5.20.

	2015	2020	2030	2040	2050
AT	0	147	0	114	496
BE	0	175	112	121	497
BG	0	0	0	0	496
HR	0	0	0	42	496
CZ	0	0	0	130	501
DK (East)	0	175	100	116	496
DK (West)	0	175	96	116	496
EE	0	0	0	0	469
FI	0	175	0	0	470
FR	0	175	73	59	496
DE	0	168	70	92	499
GB	0	168	80	88	496
GR	0	0	0	0	496
HU	0	0	0	35	496
IE	0	175	0	63	499
IT	0	0	0	0	496
LV	0	0	0	0	495
LT	0	903	0	0	481
NL	0	175	0	46	496
NO	0	114	25	6	496
PL	0	129	110	137	501
PT	0	0	0	0	496
RO	0	0	0	111	496
SK	0	0	0	57	497
SI	0	0	40	130	498
ES	0	168	0	124	501
SE	0	175	0	0	488
CH	0	175	75	105	496

Table 5.20: Marginal CO_2 Abatement Costs, Road Transport Sector [EUR/tCO2].

Developments in the European electricity sector

One of the main objectives of the research at hand is to develop a consistent, integrated multi-sectoral energy system model that can be used to understand the cross-sectoral effects under the increased electrification of fuel production and road transport. The scenario results for the European road transport sector shown in Section 5.3.2 reveal that both electric vehicles and ptx fuels will play an important role in reaching the sector-specific decarbonization targets. Because of the endogenous nature of the model presented, the consequences of these changes in fuel consumption patterns in the electricity sector can be quantified.

Figure 5.10 shows the results of the electricity capacities and generation in Europe in 2020, 2030 and 2050. The overall installed capacity in Europe more than doubles, from 1160 GW in 2020 to 2660 GW in 2050. Declining costs as well as the sector-specific European CO_2 target drives the investments in renewable energy, which ultimately dominate the electricity mix. For the European conventional power plant fleet, decarbonization drives a switch from coal- to gas-fired power plants. In 2050 there is a large share of open-cycle gas turbines (OCGT) which serve as backup capacities, offering security of supply under high penetration of VRE. The net electricity generation in Europe rises from 3600 TWh in 2020 to 4950 TWh in 2050. Renewable energy resources comprise 54 % in 2030 and 88 % in 2050 of all European electricity produced. Wind power yields the largest share with 40 % in 2050, followed by PV with a share of 30 % of total electricity generation in 2050.

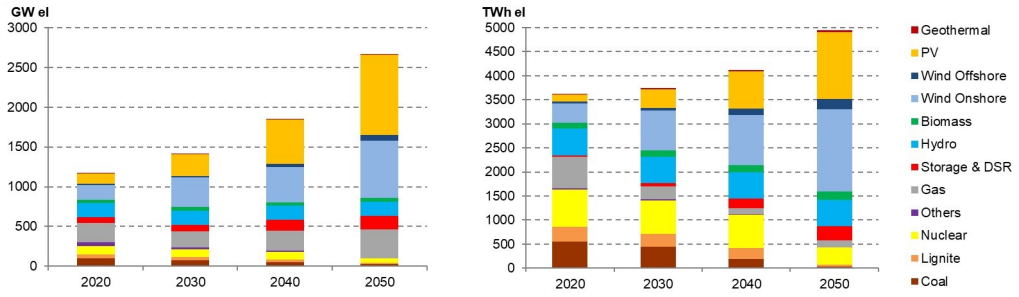

Figure 5.10: Installed electricity capacity (left) and generation (right) in Europe in 2020, 2030 and 2050 in the coupled model.

The developments in the European road transport sector described in Section 5.3.2 drive a significant increase in electricity demand over time. As such, the investments in electricity capacities between 2030 and 2050 shown in Figure 5.10 are made, in part, to generate electricity to serve the additional electricity demand from road

transport and ptx processes. As shown in Figure 5.11, the exogenous demand before ptx and electric mobility decreases over time due to, among others, efficiency improvements. Nevertheless, electrolysis, integrated Fischer-Tropsch and liquefaction systems, accounting for nearly 130 GW_{el} in 2050, demand an additional 630 TWh of electricity to serve fuel-cell and natural gas PPVs, LDVs and HDVs. An additional 570 TWh of electricity is consumed directly by BEVs. As a result, the European electricity demand is increased by nearly 33 % in 2050, from 3675 TWh to 4870 TWh.

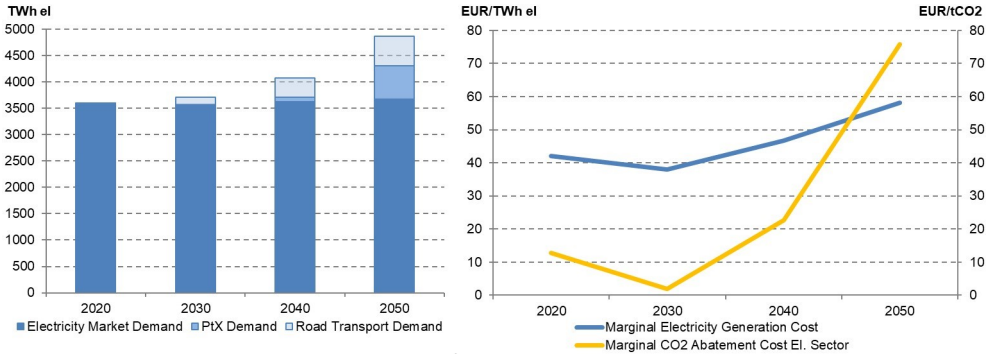

Figure 5.11: Electricity consumed by the exogenous electricity demand as well as the endogenous ptx and road transport demand in Europe in 2020, 2030 and 2050 in the coupled model (left); Results of the marginal electricity generation costs (weighted-average across all EU countries) and marginal CO_2 abatement costs for the electricity sector in the coupled model (right).

The average short-term marginal costs of electricity generation across all European countries are shown in Figure 5.11. The average European marginal costs of electricity generation increases from 38 EUR/MWh in 2030 to 58 EUR/MWh by 2050. Increasing investments in VRE, which are needed to achieve the sector-specific decarbonization target, require investments in flexible backup capacities to ensure security of supply. Also, changes in variable costs of price-setting power plants due increasing fuel price projections or fuel switches may increase average marginal electricity generation costs. Countries with lower marginal costs tend to build VRE capacity for export into other EU countries. In 2050, large NTC capacities allow the electricity prices across Europe to converge, as electricity imports and exports are often unrestricted until equilibrium is reached. Finland, for example, exhibits the lowest marginal costs of electricity generation at 50 EUR/MWh and Italy the highest at 67 EUR/MWh in 2050 (Table 5.21).

The marginal CO_2 abatement costs in the European electricity sector, driven by the sector-specific European-wide decarbonization target of -90 % compared to 1990, are also shown in Figure 5.11. Between 2020 and 2030, Europe relies on low-cost

decarbonization options such as a gradual switch from coal to gas and renewable expansion at cost-efficient locations. In particular, because the model is designed as a social planner problem with perfect foresight, it anticipates the 2050 emissions target. Restrictions on yearly capacity additions increase investments in low-emission generation capacities ahead of time, causing a gradual decrease in the marginal CO_2 abatement costs. By 2030, the marginal CO_2 abatement costs sink to 2 EUR/tCO_2, as investments in VRE have relaxed the CO_2 constraint. After 2030, the decarbonization target becomes more restrictive, pushing the CO_2 price to reach just over 75 EUR/tCO_2 by 2050. Because of the consistent, integrated nature of the model, the marginal costs of electricity generation as well as the marginal CO_2 abatement costs of the electricity sector properly account for the endogenous demand from electric vehicles and ptx systems. As such, the electricity sector enables not only the decarbonization of itself but also of major parts of the road transport sector, both via the increased electrification and ptx fuel production.

Developments in energy transformation technologies

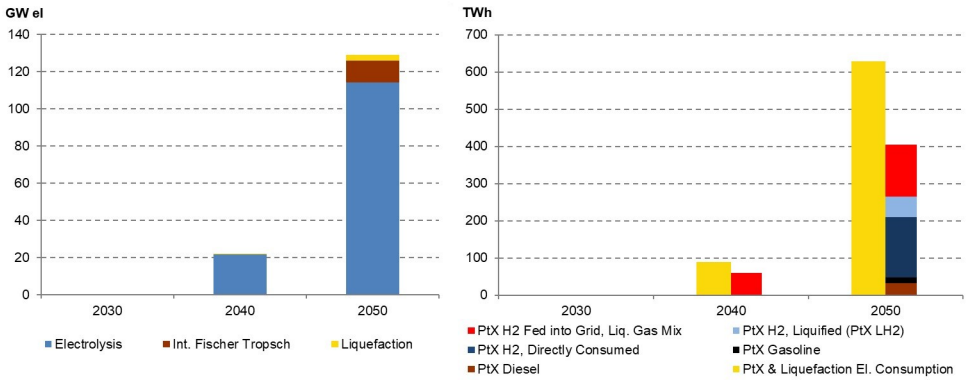

Figure 5.12: Installed capacities (left) as well as electricity consumption and fuel production (right) of ptx and liquefaction technologies in Europe between 2030 and 2050.

	2040		2050		
	Marginal Costs Electricity Generation	**Input Price Electricity, Electrolysis**	**Marginal Costs Electricity Generation**	**Input Price Electricity, Electrolysis**	**Input Price Electricity, Fischer-Tropsch**
AT	53	-	62	42	-
BE	56	40	60	38	-
BG	44	36	54	29	55
HR	51	-	64	50	-
CZ	49	41	65	53	-
DK (East)	52	37	57	43	-
DK (West)	51	34	57	42	-
EE	45	34	56	26	-
FI	39	22	50	14	47
FR	45	33	59	46	-
DE	53	39	59	44	-
GB	47	27	59	41	-
GR	49	-	62	47	-
HU	49	40	61	45	-
IE	42	20	57	37	-
IT	55	-	67	50	-
LV	45	36	57	28	-
LT	44	36	57	30	-
NL	55	39	60	41	-
NO	33	7	54	26	-
PL	46	40	59	41	-
PT	36	15	51	20	50
RO	41	31	52	33	54
SK	48	41	62	46	-
SI	51	41	64	50	-
ES	40	24	54	30	51
SE	36	13	51	21	47
CH	53	-	62	46	-
EU	**47**	**31**	**58**	**38**	**51**

Table 5.21: Results of the yearly average marginal electricity generation costs and endogenous PtX input electricity prices in 2040 and 2050.

Supplementary assumptions and results of the decoupled model: Exogenous parameters

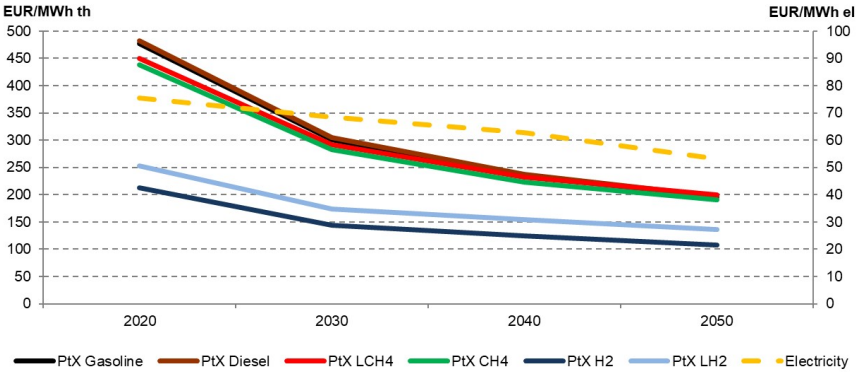

Figure 5.13: Exogenous ptx fuel and electricity prices assumed in the decoupled model.

Supplementary results of the decoupled model: Selected delta comparisons

	2015	2020	2030	2040	2050
AT	0	17	0	-40	27
BE	0	-6	0	65	27
BG	0	0	0	0	27
HR	0	0	0	-42	27
CZ	0	0	0	-8	23
DK (East)	0	-6	7	-27	27
DK (West)	0	-6	12	-26	27
EE	0	0	0	0	55
FI	0	-6	11	70	54
FR	0	-6	19	10	27
DE	0	-4	36	-22	25
GB	0	2	13	-10	27
GR	0	0	0	0	27
HU	0	0	0	-35	27
IE	0	-6	0	11	25
IT	0	0	0	0	27
LV	0	0	0	0	29
LT	0	5	0	0	42
NL	0	-6	0	24	27
NO	0	56	83	84	27
PL	0	12	2	49	32
PT	0	0	0	0	27
RO	0	0	0	10	27
SK	0	0	0	-41	27
SI	0	0	13	-9	25
ES	0	-4	0	19	27
SE	0	-6	11	70	36
CH	0	-6	18	-15	27

Table 5.22: Delta Marginal CO_2 Abatement Costs, Road Transport Sector (decoupled minus coupled) [EUR/tCO2].

Bibliography

Abel, G. J., Brottrager, M., Crespo Cuaresma, J., Muttarak, R., Jan. 2019. Climate, conflict and forced migration. Global Environmental Change 54, 239–249.
URL http://www.sciencedirect.com/science/article/pii/S0959378018301596

ADAC, 2015. ADAC Autokosten 2015 - Kostenübersicht für über 1.800 aktuelle Neuwagen-Modelle. Tech. rep., Allgemeiner Deutscher Automobil-Club e.V. (ADAC).

Allan, R. N., Billinton, 1996. Reliability Evaluation of Power Systems. Springer US.
URL //www.springer.com/la/book/9780306452598

Amelin, M., May 2009. Comparison of Capacity Credit Calculation Methods for Conventional Power Plants and Wind Power. IEEE Transactions on Power Systems 24 (2), 685–691.

Amos, W. A., 1998. Costs of Storing and Transporting Hydrogen. Tech. rep., National Renewable Energy Laboratory.

Arguez, A., Vose, S. R., 2011. The Definition of the Standard WMO Climate Normal - The Key to Deriving Alternative Climate Normals. American Meteorological Society.
URL https://journals.ametsoc.org/doi/pdf/10.1175/2010BAMS2955.1

Arndt, W.-H., Döge, N., Stefanie, M., 2016. Elektrifizierungspotential kommerzieller Kraftfahrzeug-Flotten im Wirtschaftsverkehr als dezentrale Energie-Ressource in städtischen Verteilnetzen. Tech. rep., Technische Universität Berlin.

Balat, M., Aug. 2008. Potential importance of hydrogen as a future solution to environmental and transportation problems. International Journal of Hydrogen Energy 33 (15), 4013–4029.
URL http://www.sciencedirect.com/science/article/pii/S0360319908005272

BAST, 2015. Verkehrsmengendaten an Dauerzählstellen - Kurzinfo. Tech. rep., Bundesanstalt für Straßenwesen (BAST).
URL http://2015.bmvi-data-run.de/datensaetze/dateien/Dauerzaehlstellen.pdf

Becker, W. L., Braun, R. J., Penev, M., Beccali, M., 2012. Production of Fischer-Tropsch liquid fuels from high temperature solid oxide co-electrolysis units. Energy 47, 99–115.

Bertsch, J., Growitsch, C., Lorenczik, S., Nagl, S., 2016a. Flexibility in Europe's power sector - An additional requirement or an automatic complement? Energy Economics.
URL http://www.sciencedirect.com/science/article/pii/S0140988314002679

Bertsch, J., Hagspiel, S., Just, L., Dec. 2016b. Congestion management in power systems. Journal of Regulatory Economics 50 (3), 290–327.
URL https://link.springer.com/article/10.1007/s11149-016-9310-x

Billinton, R., 1970. Power System Reliability Evaluation. Taylor & Francis.

Bünger, U., Landinger, H., Weindorf, W., Wurster, R., Zerhusen, J., Zittel, W., 2016. Vergleich von CNG und LNG zum Einsatz in Lkw im Fernverkehr: Eine Expertise für die Open Grid Europe GmbH - Abschlussbericht. Tech. rep., Ludwig-Bölkow-Systemtechnik GmbH (LBST).
URL http://www.lbst.de/ressources/docs2016/1605_CNG_LNG_Endbericht_public.pdf

Bollmeyer, C., Keller, J. D., Ohlwein, C., Wahl, S., Crewell, Friederichs, P., Hense, A., Keune, J., Kneifel, S., Pscheidt, I., Redl, S., Steinke, S., 2014. Towards a high-resolution regional reanalysis for the European CORDEX domain. Quarterly Journal of the Royal Meteorological Society 141 (686), 1–15.
URL https://rmets.onlinelibrary.wiley.com/doi/abs/10.1002/qj.2486

Börjesson, M., Ahlgren, E. O., 2012. Assessment of transport fuel taxation strategies through integration of road transport in an energy system model - the case of Sweden. International Journal of Energy Research 36, 648–669.

Brynolf, S., Taljegard, M., Grahn, M., Hansson, J., 2018. Electrofuels for the transport sector: A review of production costs. Renewable and Sustainable Energy Reviews 81(2), 1887–1905.

Bundesamt für Statistik, 2017. Strassenfahrzeuge - Bestand, Motorisierungsgrad. Bundesamt für Statistik.
URL https://www.bfs.admin.ch/bfs/de/home/statistiken/mobilitaet-verkehr/verkehrsinfrastruktur-fahrzeuge/fahrzeuge/strassenfahrzeuge-bestand-motorisierungsgrad.html

Bundesnetzagentur, 2016. Genehmigung des Szenariorahmens für die Netzentwicklungspläne Strom: 2017-2030. Tech. rep., Bundesnetzagentur für Elektrizität, Gas, Telekommunikation, Post und Eisenbahnen.

Burke, M., Davis, W. M., Diffenbaugh, N. S., May 2018. Large potential reduction in economic damages under UN mitigation targets. Nature 557 (7706), 549–553.
URL https://www.nature.com/articles/s41586-018-0071-9

Burke, M., Hsiang, S. M., Miguel, E., Aug. 2015. Climate and Conflict. Annual Review of Economics 7 (1), 577–617.
URL https://www.annualreviews.org/doi/10.1146/annurev-economics-080614-115430

Byers, C., Levin, T., Botterud, A., Jan. 2018. Capacity market design and renewable energy: Performance incentives, qualifying capacity, and demand curves. The Electricity Journal 31 (1), 65–74.
URL http://www.sciencedirect.com/science/article/pii/S1040619017303330

CBS, 2015. Transport and mobility 2015. Tech. rep., Statistics Netherlands (CBS).
URL http://download.cbs.nl/pdf/2015-transport-and-mobility.pdf

Cepeda, M., Saguan, M., Finon, D., Pignon, V., 2009. Generation adequacy and transmission interconnection in regional electricity markets. Energy Policy 37 (12), 5612 – 5622.
URL http://www.sciencedirect.com/science/article/pii/S0301421509006120

Cramton, P., MacKay, D. J., Ockenfels, A., Stoft, S., 2017. Global Carbon Pricing: The Path to Climate Cooperation. MIT Press.

Cramton, P., Ockenfels, A., Stoft, S., 2013. Capacity Market Fundamentals. Economics of Energy & Environmental Policy 2 (2), 27–46.
URL http://www.jstor.org/stable/26189455

dena, 2010. Kurzanalyse der Kraftwerksplanung in Deutschland bis 2020 (Aktualisierung).
URL https://shop.dena.de/sortiment/detail/produkt/studie-kurzanalyse-der-kraftwerksplanung-in-deutschland-bis-2020-aktualisierung/

dena, LBST, 2017. E-FUELS STUDY: The potential of electricity-based fuels for low-emission transport in the EU - An expertise by LBST and dena. Tech. rep., Deutsche Energie - Agentur GmbH (dena).
URL https://shop.dena.de/fileadmin/denashop/media/Downloads_Dateien/

verkehr/9219_E-FUELS-STUDY_The_potential_of_electricity_based_fuels_for_low_emission_transport_in_the_EU.pdf

Department for Business, Energy and Industrial Strategy, 2016. Greenhouse gas reporting - Conversion factors 2016. Department for Business, Energy and Industrial Strategy.
URL https://www.gov.uk/government/publications/greenhouse-gas-reporting-conversion-factors-2016

Department of Transport, 2017. Car statistics tables, produced by Department for Transport. Department of Transport.
URL https://www.gov.uk/government/statistical-data-sets/veh02-licensed-cars

DLR, 2015. Erstnutzer von Elektrofahrzeugen in Deutschland - Nutzerprofile, Anschaffung, Fahrzeugnutzung. Tech. rep., Deutsches Zentrum für Luft- und Raumfahrt (DLR).
URL http://www.dlr.de/vf/Portaldata/12/Resources/dokumente/projekte/pakt2/Ergebnisbericht_E-Nutzer_2015.pdf

DLR, Fraunhofer IWES, IFNE, 2012. Langfristszenarien und Strategien für den Ausbau der erneuerbaren Energien in Deutschland bei Berücksichtigung der Entwicklung in Europa und global. Tech. rep., Bundesministerium für Umwelt, Naturschutz, Bau und Reaktorsicherheit (BMU).
URL http://www.fvee.de/fileadmin/publikationen/Politische_Papiere_anderer/12.03.29.BMU_Leitstudie2011/BMU_Leitstudie2011.pdf

DLR, IFEU, LBST, DBFZ, 2014. Power-to-Gas (PtG) im Verkehr Aktueller Stand und Entwicklungsperspektiven. Tech. rep., Bundesministeriums für Verkehr und digitale Infrastruktur (BMVI).
URL http://www.lbst.de/download/2014/mks-kurzstudie-ptg.pdf

DLR, Shell, HWWI, 2010. Shell LKW-Studie. Tech. rep., DLR.
URL http://www.dlr.de/Portaldata/1/Resources/portal_news/newsarchiv2010_3/Shell_Lkw_Studie_FIN_17042010.pdf

Dodds, P. E., Ekins, P., 2014. A portfolio of powertrains for the UK: An energy systems analysis. International Journal of Hydrogen Energy 39, 13941–13953.

Dodds, P. E., McDowall, W., 2014. Methodologies for representing the road transport sector in energy system models. International Journal of Hydrogen Energy 39, 2345–2358.

Edwards, R., Larivé, J.-F., Rickeard, D., Weindorf, W., 2014. Well-to-wheels analysis of future automotive fuels and powertrains in the European context. Tech. rep., JRC, CONCAWE, EUCAR.
URL https://iet.jrc.ec.europa.eu/about-jec/sites/iet.jrc.ec.europa.eu.about-jec/files/documents/report_2014/wtt_report_v4a.pdf

EEA, 2017. Greenhouse gas emissions by source sector. European Environment Agency.
URL http://appsso.eurostat.ec.europa.eu/nui/show.do?dataset=env_air_gge&lang=en

EEA, 2018. EEA Greenhouse Gas Data Viewer.
URL https://www.eea.europa.eu/data-and-maps/data/data-viewers/greenhouse-gases-viewer

EIA, 2015. Annual Energy Outlook 2015 - with projections to 2040. Tech. rep., Energy Information Administration, US Department of Energy.
URL https://www.eia.gov/outlooks/aeo/pdf/0383(2015).pdf

Elsner, P., Sauer, D. U., 2015. Energiespeicher: Technologiesteckbrief zur Analyse 'Flexibilitätskonzepte für die Stromversorgung 2050'. Tech. rep., Fraunhofer-Institut für Chemische Technologie.

Engel, P., 2014. Optimal Design of Offshore Wind Energy Converters for increased Security of Supply. Dissertation.

ENTSO-E, 2012. Hourly load levels for european countries.
URL https://www.entsoe.eu/resources/data-portal/consumption/

ENTSO-E, 2015a. Scenario Outlook & Adequacy Forecast. Tech. rep., European Network of Transmission System Operators for Electricity.

ENTSO-E, 2015b. TYNDP 2016: Scenario Development Report: European Network of Transmission System Operators for Electricity. Tech. rep., European Network of Transmission System Operators for Electricity.

ENTSO-E, 2016a. Hourly load levels for European countries. Https://www.entsoe.eu/data/data-portal/.

ENTSO-E, 2016b. Net generation capacities for european countries.
URL https://www.entsoe.eu/data/statistics/Pages/ngc.aspx

ENTSO-E, 2016c. Ten-Year Network Development Plan 2016.
URL http://tyndp.entsoe.eu/reference/#downloads

ENTSO-E, 2017. Winter outlook 2017/2018, summer review 2017.
URL https://www.entsoe.eu/publications/system-development-reports/outlook-reports/Pages/default.aspx

ENTSO-E, 2018. Ten-Year Network Development Plan 2018.
URL http://tyndp.entsoe.eu/tyndp2018/

Eskeland, G. S., Mideksa, T. K., 2010. Electricity demand in a changing climate. Mitigation and Adaptation Strategies for Global Change 15 (8), 877–897.
URL https://link.springer.com/article/10.1007/s11027-010-9246-x

ETSO, 2011. Definitions of transfer capacities in liberalised electricity markets - final report.

European Commission, 2009. Effort Sharing Decision of the European Parliament and of the Council. European Commission.

European Commission, 2014. 2030 Climate and Energy Policy Framework. European Commission.

European Commission, 2015. Europe's future secure and sustainable electricity infrastructure: e-Highway2050 project results. European Commission.

European Commission, 2016a. Commission staff working document - accompanying the document Interim Report of the Sector Inquiry on Capacity Mechanisms C(2016) 2107 final.
URL http://ec.europa.eu/competition/sectors/energy/capacity_mechanisms_swd_en.pdf

European Commission, 2016b. EU Reference Scenario 2016: Energy, Transport and GHG emissions: Trends to 2050. European Commission.
URL https://ec.europa.eu/energy/sites/ener/files/documents/20160713%20draft_publication_REF2016_v13.pdf

European Commission, 2016c. Proposal for a regulation on the internal market for electricity (recast) - COM(2016)861.
URL https://ec.europa.eu/energy/sites/ener/files/documents/1_en_act_part1_v9.pdf

Eurostat, 2017. GDP and main components (output, expenditure and income). Eurostat.
URL http://appsso.eurostat.ec.europa.eu/nui/show.do?dataset=nama_10_gdp&lang=en

EWEA, 2015. Wind energy scenarios for 2030. Tech. rep., European Wind Energy Association (EWEA).
URL https://www.ewea.org/fileadmin/files/library/publications/reports/EWEA-Wind-energy-scenarios-2030.pdf

EWI, GWS, Prognos, 2014. Entwicklung der Energiemärkte - Energiereferenzprognose. Tech. rep., Bundesministerium für Wirtschaft und Energie (BMWi).
URL https://www.bmwi.de/Redaktion/DE/Publikationen/Studien/entwicklung-der-energiemaerkte-energiereferenzprognose-endbericht.pdf?__blob=publicationFile&v=7

FAZ, Nov. 2018. Prognosesenkung: Aktienkurs von Covestro unter Druck. Frankfurter Allgemeine Zeitung.
URL http://www.faz.net/1.5900245

Feng, S., Krueger, A. B., Oppenheimer, M., Aug. 2010. Linkages among climate change, crop yields and Mexico-US cross-border migration. Proceedings of the National Academy of Sciences 107 (32), 14257–14262.
URL https://www.pnas.org/content/107/32/14257

FfE, 2016. Verbundforschungsvorhaben Merit Order der Energiespeicherung im Jahr 2030 - Teil 2: Technoökonomische Analyse Funktionaler Energiespeicher. Tech. rep., Forschungsstelle für Energiewirtschaft e. V. (FfE).
URL https://www.ffe.de/images/stories/Themen/414_MOS/20160728_MOS_Speichertechnologien.pdf

Fishbone, L. G., Abilock, H., 1981. Markal, a linear-programming model for energy systems analysis: Technical description of the bnl version. International Journal of Energy Research 5(4), 353–375.

Franco, A., Casarosa, C., 2014. Thermodynamic and heat transfer analysis of LNG energy recovery for power production. Journal of Physics: Conference Series 547.

Frank, C. W., Wahl, S., Keller, J. D., Pospichal, B., Hense, A., Crewell, S., 2018. Bias correction of a novel European reanalysis data set for solar energy applications. Solar Energy 164, 12–24.
URL http://www.sciencedirect.com/science/article/pii/S0038092X18301294

Fraunhofer IWES, Fraunhofer IBP, IFEU, Stiftung Umweltenergierecht, 2015. Interaktion EE-Strom, Wärme und Verkehr - Analyse der Interaktion zwischen den Sektoren Strom, Wärme/Kälte und Verkehr in Deutschland in Hinblick auf steigende Anteile fluktuierender Erneuerbarer Energien im Strombereich unter Berücksichtigung der europäischen Entwicklung. Tech. rep., Fraunhofer-Institut für Windenergie und Energiesystemtechnik (Fraunhofer IWES), Kassel.
URL https://www.iee.fraunhofer.de/content/dam/iwes-neu/energiesystemtechnik/de/Dokumente/Veroeffentlichungen/2015/Interaktion_EEStrom_Waerme_Verkehr_Endbericht.pdf

Fürsch, M., Hagspiel, S., Jägemann, C., Nagl, S., Lindenberger, D., Tröster, E., 2013. The role of grid extensions in a cost-efficient transformation of the European electricity system until 2050. Applied Energy 104 (Supplement C), 642–652.
URL http://www.sciencedirect.com/science/article/pii/S0306261912008537

Förster, H., Lilliestam, J., 2010. Modeling thermoelectric power generation in view of climate change. Regional Environmental Change 10 (4), 327–338.
URL https://doi.org/10.1007/s10113-009-0104-x

Gambhir, A., Tse, L. K. C., Tong, D., Martinez-Botas, R., 2015. Reducing China's road transport sector CO2 emissions to 2050: Technologies, costs and decomposition analysis. Applied Energy 157, 905–917.

Grahn, M., 2017. Hydrogen: An overview of production pathways and possible usage in the transport sector. Chalmers University of Technology.
URL http://www.ht.energy.lth.se/fileadmin/ht/Kurser/MVKF25/Guest_Lecture_1.pdf

Grave, K., Paulus, M., Lindenberger, D., 2012. A method for estimating security of electricity supply from intermittent sources: Scenarios for Germany until 2030. Energy Policy 46, 193–202.
URL http://www.sciencedirect.com/science/article/pii/S0301421512002558

Görner, K., Lindenberger, D., 2018. Virtuelles Institut Strom zu Gas und Wärme - Flexibilisierungsoptionen im Strom-Gas-Wärme-System. Abschlussbericht, Virtuelles Institut Strom zu Gas und Wärme.
URL http://strom-zu-gas-und-waerme.de/aktuelles/

Hagspiel, S., 2017. Reliable Electricity: The Effects of System Integration and Cooperative Measures to Make it Work. EWI Working Paper No 17/13.
URL http://www.ewi.uni-koeln.de/fileadmin/user_upload/Publikationen/

Working_Paper/EWI_WP_17-13_Reliable_Electricity_The_Effects_of_System_Integration.pdf

Hagspiel, S., 2018. Reliability with interdependent suppliers. European Journal of Operational Research 268 (1), 161–173.
URL http://www.sciencedirect.com/science/article/pii/S0377221718300146

Hagspiel, S., Jägemann, C., Lindenberger, D., Brown, T., Cherevatskiy, S., Tröster, E., Mar. 2014. Cost-optimal power system extension under flow-based market coupling. Energy 66, 654–666.
URL http://www.sciencedirect.com/science/article/pii/S0360544214000322

Hagspiel, S., Knaut, A., Peter, J., 2017. Reliability in Multi-regional Power Systems - Capacity Adequacy and the Role of Interconnectors. EWI Working Paper No 17/07.
URL http://www.ewi.uni-koeln.de/fileadmin/user_upload/Publikationen/Working_Paper/EWI_WP_17-07_Reliability_in_multi-regional_power_systems.pdf

Hagspiel, S., Knaut, A., Peter, J., 2018. Reliability in Multi-regional Power Systems: Capacity Adequacy and the Role of Interconnectors. The Energy Journal 39 (5).
URL http://www.iaee.org/en/publications/ejarticle.aspx?id=3181

Hardin, G., 1968. The Tragedy of the Commons. Science 162 (3859), 1243–1248.
URL http://science.sciencemag.org/content/162/3859/1243

Harrison, G., Krause, J., Thiel, C., 2016. Transitions and impacts of passenger car powertrain technologies in European member states. Transportation Research Procedia 14, 2620–2629.

Hasche, B., Keane, A., O'Malley, M., 2011. Capacity Value of Wind Power, Calculation, and Data Requirements: the Irish Power System Case. IEEE Transactions on Power Systems 26 (1), 420–430.

Hauer, M. E., Evans, J. M., Mishra, D. R., 2016. Millions projected to be at risk from sea-level rise in the continental United States. Nature Climate Change 6 (7), 691–695.
URL https://www.nature.com/articles/nclimate2961

Hedenus, F., Karlsson, S., Azar, C., Sprei, F., 2010. Cost-effective energy carriers for transport - The role of the energy supply system in a carbon-constrained world. International Journal of Hydrogen Energy 35 (10), 4638 – 4651, novel Hydrogen

Production Technologies and ApplicationsNovel Hydrogen Production Technologies and Applications.
URL http://www.sciencedirect.com/science/article/pii/S0360319910003460

Heidari, S., 2017. Economic modelling of floating offshore wind power - Calculation of levelized cost of energy. School of Business, Society and Engineering Västeras.
URL https://mdh.diva-portal.org/smash/get/diva2:1128321/FULLTEXT01.pdf

Helgeson, B., Peter, J., 2018. The Role of Electricity in Decarbonizing European Road Transport - Development and Assessment of an Integrated Multi-Sectoral Model. EWI Working Paper No 19/01.
URL http://www.ewi.uni-koeln.de/fileadmin/user_upload/Publikationen/Working_Paper/EWI_WP_19-01_The_Role_of_Electricity_in_Decarbonizing_European_Road_Transport.pdf

Henckes, P., Frank, C., Küchler, N., Peter, J., Wagner, J., 2019. Uncertainty Estimation of Investment Planning Models Under High Shares of Renewables Using Reanalysis Data. EWI Working Paper forthcoming.

Henckes, P., Knaut, A., Obermüller, F., Frank, C., 2018. The benefit of long-term high resolution wind data for electricity system analysis. Energy 143 (Supplement C), 934–942.
URL http://www.sciencedirect.com/science/article/pii/S0360544217317280

Henderson, J., 2016. Gazprom - Is 2016 the Year for a Change of Pricing Strategy in Europe? Tech. rep., The Oxford Intitute for Energy Studies, University of Oxford.
URL https://www.oxfordenergy.org/wpcms/wp-content/uploads/2016/02/Gazprom-Is-2016-the-Year-for-a-Change-of-Pricing-Strategy-in-Europe.pdf

Henning, H.-M., Palzer, A., 2015. Was kostet die Energiewende? - Wege zur Transformation des deutschen Energiesystems bis 2050. Tech. rep., Fraunhofer Institut für Solare Energiesysteme (ISE).
URL https://www.fraunhofer.de/content/dam/zv/de/Forschungsfelder/Energie-Rohstoffe/Fraunhofer-ISE_Transformation-Energiesystem-Deutschland_final_19_11%20(1).pdf

Hobbs, B. F., Bothwell, C., 2017. Crediting Wind and Solar Renewables in Electricity Capacity Markets: The Effects of Alternative Definitions upon Market Efficiency. The Energy Journal 38 (SI).
URL http://www.iaee.org/en/publications/ejarticle.aspx?id=2910

IEA, 2013. Production costs of Alternative Transportation Fuels - Influence of Crude Oil Price and Technology Maturity. International Energy Agency (IEA), Paris.
URL https://www.iea.org/publications/freepublications/publication/FeaturedInsights_AlternativeFuel_FINAL.pdf

IEA, 2014. The Power of Transformation: Wind, Sun and the Economics of Flexible Power Systems. International Energy Agency (IEA), Paris.
URL https://doi.org/10.1787/9789264208032-en.

IEA, 2016a. Global EV Outlook 2016 - Beyond one million electric cars. International Energy Agency (IEA).
URL http://www.iea.org/publications/freepublications/publication/Global_EV_Outlook_2016.pdf

IEA, 2016b. World Energy Outlook 2016. International Energy Agency (IEA), Paris.
URL https://www.iea.org/newsroom/news/2016/november/world-energy-outlook-2016.html

IEA, 2017. Energy Technology Perspectives 2017. International Energy Agency (IEA), Paris, https://doi.org/10.1787/energy_tech-2017-en.
URL https://www.oecd-ilibrary.org/content/publication/energy_tech-2017-en

IEA, 2017a. The Future of Trucks - Implications for energy and the environment. International Energy Agency (IEA), Paris.
URL https://www.iea.org/publications/freepublications/publication/TheFutureofTrucksImplicationsforEnergyandtheEnvironment.pdf

IEA, 2017b. World Energy Outlook 2017. International Energy Agency (IEA), Paris, https://doi.org/10.1787/weo-2017-en.
URL https://www.oecd-ilibrary.org/content/publication/weo-2017-en

IEA, 2018. World Energy Outlook 2018. International Energy Agency (IEA), Paris, https://doi.org/10.1787/weo-2018-en.
URL https://www.oecd-ilibrary.org/content/publication/weo-2018-en

IPCC, 2014a. Climate Change 2014: AR5 Summary for Policymakers.
URL https://www.ipcc.ch/site/assets/uploads/2018/02/AR5_SYR_FINAL_SPM.pdf

IPCC, 2014b. Climate Change 2014: Synthesis Report. Contribution of Working Groups I, II and III to the Fifth Assessment Report of the Intergovernmental Panel on Climate Change. Intergovernmental Panel on Climate Change, Geneva.

URL https://www.ipcc.ch/pdf/assessment-report/ar5/syr/AR5_SYR_FINAL_SPM.pdf

IPCC, 2018a. Global Warming of 1.5 °C - IPCC Special Report, Chapter 2. Intergovernmental Panel on Climate Change.
URL https://report.ipcc.ch/sr15/pdf/sr15_chapter2.pdf

IPCC, 2018b. Global Warming of 1.5 °C - IPCC Special Report, Summary for Policymaker. Intergovernmental Panel on Climate Change, Geneva.
URL http://report.ipcc.ch/sr15/pdf/sr15_spm_final.pdf

IPCC, 2018c. Global Warming of 1.5 °C - IPCC Special Report, Technical Summary. Intergovernmental Panel on Climate Change, Geneva.
URL https://report.ipcc.ch/sr15/index.html

IRENA, 2017. Planning for the renewable future - Long-term modelling and tools to expand variable renewable power in emerging economies.
URL http://www.irena.org/DocumentDownloads/Publications/IRENA_Planning_for_the_Renewable_Future_2017.pdf

Jacob, D., Petersen, J., Eggert, B., Alias, A., Christensen, O. B., Bouwer, L. M., Braun, A., Colette, A., Déqué, M., Georgievski, G., Georgopoulou, E., Gobiet, A., Menut, L., Nikulin, G., Haensler, A., Hempelmann, N., Jones, C., Keuler, K., Kovats, S., Kröner, N., Kotlarski, S., Kriegsmann, A., Martin, E., van Meijgaard, E., Moseley, C., Pfeifer, S., Preuschmann, S., Radermacher, C., Radtke, K., Rechid, D., Rounsevell, M., Samuelsson, P., Somot, S., Soussana, J.-F., Teichmann, C., Valentini, R., Vautard, R., Weber, B., Yiou, P., 2014. EURO-CORDEX: new high-resolution climate change projections for European impact research. Regional Environmental Change 14 (2), 563–578.
URL https://doi.org/10.1007/s10113-013-0499-2

Jerez, S., Tobin, I., Vautard, R., Montávez, J. P., López-Romero, J. M., Thais, F., Bartok, B., Christensen, O. B., Colette, A., Déqué, M., Nikulin, G., Kotlarski, S., Meijgaard, E. v., Teichmann, C., Wild, M., Dec. 2015. The impact of climate change on photovoltaic power generation in Europe. Nature Communications 6, 10014.
URL https://www.nature.com/articles/ncomms10014

Jägemann, C., Fürsch, M., Hagspiel, S., Nagl, S., 2013. Decarbonizing Europe's power sector by 2050 - Analyzing the economic implications of alternative decarbonization pathways. Energy Economics 40, 622 – 636.
URL http://www.sciencedirect.com/science/article/pii/S0140988313001928

Jonas, H., 1973. Technology and responsibility: Reflections on the new tasks of ethics. Social Research 40 (1), 31–54.
URL https://www.jstor.org/stable/40970125

Joskow, P., 2008. Lessons learned from electricity market liberalization. The Energy Journal 29 (SPEC. ISS.), 9–42.

KBA, 2017. Bestand an Pkw am 1. Januar 2016 nach ausgewählten Kraftstoffarten. Kraftfahrt-Bundesamt.
URL https://www.kba.de/DE/Statistik/Fahrzeuge/Bestand/Umwelt/2016/2016_b_umwelt_dusl.html?nn=1609370

Keane, A., Milligan, M., Dent, C. J., Hasche, B., D'Annunzio, C., Dragoon, K., Holttinen, H., Samaan, N., Soder, L., O'Malley, M., 2011. Capacity Value of Wind Power. IEEE Transactions on Power Systems 26 (2), 564–572.

Kelly, J. C., MacDonald, J. S., Keoleian, G. A., 2012. Time-dependent plug-in hybrid electric vehicle charging based on national driving patterns and demographics. Applied Energy 94, 395–405.

Kharin, V. V., Flato, G. M., Zhang, X., Gillett, N. P., Zwiers, F., Anderson, K. J., 2018. Risks from Climate Extremes Change Differently from 1.5°C to 2.0°C Depending on Rarity. Earth's Future 6 (5), 704–715.
URL https://agupubs.onlinelibrary.wiley.com/doi/abs/10.1002/2018EF000813

Knaut, A., Tode, C., Lindenberger, D., Malischek, R., Paulus, S., Wagner, J., May 2016. The reference forecast of the German energy transition - An outlook on electricity markets. Energy Policy 92, 477–491.
URL http://www.sciencedirect.com/science/article/pii/S0301421516300519

Knörr, W., Heidt, C., Schacht, A., 2012. Aktualisierung 'Daten- und Rechenmodell: Energieverbrauch und Schadstoffemissionen des motorisierten Verkehrs in Deutschland 1960-2030' (TREMOD) für die Emissionsberichterstattung 2013 (Berichtsperiode 1990-2011). Tech. rep., Institut für Energie- und Umweltforschung Heidelberg (IFEU).

Kost, C., Shammugam, S., Jülch, V., Nguyen, H.-T., Schlegl, T., 2018. Stromgestehungskosten Erneuerbare Energien - März 2018. Fraunhofer Institut für Solare Energiesysteme (ISE), Fraunhofer Institut für Solare Energiesysteme (ISE).
URL https://www.ise.fraunhofer.de/content/dam/ise/de/documents/publications/studies/DE2018_ISE_Studie_Stromgestehungskosten_Erneuerbare_Energien.pdf

Kozarcanin, S., Liu, H., Andresen, G. B., 2018. Climate change impacts on large-scale electricity system design decisions for the 21st Century. Preprint (arXiv)ArXiv: 1805.01364.
URL http://arxiv.org/abs/1805.01364

Krewitt, W., Schmid, S., 2005. CASCADE Mints - WP 1.5 Common Infromation Database: D 1.1 Fuel Cell Technologies and Hydrogen Production/Distribution Options. Tech. rep., Deutsches Zentrum für Luft- und Raumfahrt (DLR).
URL http://www.dlr.de/fk/Portaldata/40/Resources/dokumente/publikationen/2005-09-02_CASCADE_D1.1_fin.pdf

Krishnan, V., Gonzalez-Marciaga, L., McCalley, J., 2014. A planning model to assess hydrogen as an alternative fuel for national light-duty vehicle portfolio. Energy 73, 943–957.

Lijesen, M. G., 2007. The real-time price elasticity of electricity. Energy Economics 29 (2), 249–258.
URL http://www.sciencedirect.com/science/article/pii/S0140988306001010

Loulou, R., Goldstein, G., Noble, K., 2004. Documentation for the MARKAL Family of Models. Part I: Standard MARKAL, Energy Technology Systems Analysis Programme.

Madaeni, S. H., Sioshansi, R., Denholm, P., 2013. Comparing Capacity Value Estimation Techniques for Photovoltaic Solar Power. IEEE Journal of Photovoltaics 3 (1), 407–415.

Mann, M. E., Rahmstorf, S., Kornhuber, K., Steinman, B. A., Miller, S. K., Coumou, D., 2017. Influence of Anthropogenic Climate Change on Planetary Wave Resonance and Extreme Weather Events. Scientific Reports 7, 45242.
URL http://dx.doi.org/10.1038/srep45242

Mariani, F., 2016. Cost analysis of LNG refuelling stations - LNG Blue Corridors Project by European Commission. European Commission.
URL http://lngbc.eu/system/files/deliverable_attachments/LNG_BC_D%203%208%20Cost%20analysis%20of%20LNG%20refuelling%20stations.pdf

McKinsey, 2010. A portfolio of power-trains for Europe: a fact-based analysis - The role of Battery Electric Vehicles, Plug-in Hybrids and Fuel Cell Electric Vehicles. Tech. rep., McKinsey.
URL http://www.eesi.org/files/europe_vehicles.pdf

Meinshausen, M., Smith, S. J., Calvin, K., Daniel, J. S., Kainuma, M. L. T., Lamarque, J.-F., Matsumoto, K., Montzka, S. A., Raper, S. C. B., Riahi, K., Thomson, A., Velders, G. J. M., van Vuuren, D. P., 2011. The RCP greenhouse gas concentrations and their extensions from 1765 to 2300. Climatic Change 109 (1), 213.
URL https://doi.org/10.1007/s10584-011-0156-z

Milligan, M., Frew, B., Ibanez, E., Kiviluoma, J., Holttinen, H., Söder, L., 2017. Capacity value assessments of wind power. Wiley Interdisciplinary Reviews: Energy and Environment 6 (1), e226.
URL https://onlinelibrary.wiley.com/doi/abs/10.1002/wene.226

Moemken, J., Reyers, M., Feldmann, H., Pinto, J. G., 2018. Future Changes of Wind Speed and Wind Energy Potentials in EURO-CORDEX Ensemble Simulations. Journal of Geophysical Research: Atmospheres 123 (12), 6373–6389.
URL https://agupubs.onlinelibrary.wiley.com/doi/abs/10.1029/2018JD028473

Myhr, A., Bjerkseter, C., Ågotnes, A., Nygaard, T. A., 2014. Levelised cost of energy for offshore floating wind turbines in a life cycle perspective. Renewable Energy 66, 714–728.
URL http://www.sciencedirect.com/science/article/pii/S0960148114000469

Nahmmacher, P., Schmid, E., Hirth, L., Knopf, B., 2016a. Carpe diem: A novel approach to select representative days for long-term power system modeling. Energy 112 (Supplement C), 430–442.
URL http://www.sciencedirect.com/science/article/pii/S0360544216308556

Nahmmacher, P., Schmid, E., Pahle, M., Knopf, B., 2016b. Strategies against shocks in power systems - An analysis for the case of Europe. Energy Economics 59, 455 – 465.
URL http://www.sciencedirect.com/science/article/pii/S0140988316302365

Newbery, D., 2015. Security of supply, capacity auctions and interconnectors. Energy Policy Research Group, University of Cambridge, EPRG Working Paper 1508.
URL http://www.eprg.group.cam.ac.uk/wp-content/uploads/2015/03/EPRG-WP-1508.pdf

Newbery, D., 2016. Missing money and missing markets: Reliability, capacity auctions and interconnectors. Energy Policy 94, 401–410.
URL http://www.sciencedirect.com/science/article/pii/S0301421515301555

Obama, B., 2014. Remarks by the President at U.N. Climate Change Summit 2014.
URL https://obamawhitehouse.archives.gov/the-press-office/2014/09/23/remarks-president-un-climate-change-summit

Ou, X., Zhang, Q., Zhang, X., Zhang, X., 2013. China's New Energy Passenger Vehicle Development-Scenario Analysis Based on Life Time Cost Modelling. Low Carbon Economy 4 (2), 71–79.

Papadimitriou, G., Ntziachristos, L., Wüthrich, P., Notter, B., Keller, M., Fridell, E., Winnes, H., Styhre, L., Sjödin, A., 2013. Transport data collection supporting the quantitative analysis of measures relating to transport and climate change. Tech. rep., EMISIA, INFRAS, IVL.
URL http://emisia.com/sites/default/files/TRACCS_Final.pdf

Parra, D., Patel, M. K., 2016. Techno-economic implications of the electrolyser technology and size for power-to-gas systems. International Journal of Hydrogen Energy 41 (6), 3748–3761.

Pasaoglu, G., Harrison, G., Jones, L., Hill, A., Beaudet, A., Thiel, C., 2016. A system dynamics based market agent model simulating future powertrain technology transition: Scenarios in the EU light duty vehicle road transport sector. Technological Forecasting & Social Change 104, 133–146.

Pentalateral Energy Forum, 2018. Generation Adequacy Assessment 2018.
URL https://www.bmwi.de/Redaktion/DE/Downloads/P-R/plef-sg2-generation-adequacy-assessment-2018.pdf?__blob=publicationFile&v=4

Peter, J., 2019. How Does Climate Change Affect Optimal Allocation of Variable Renewable Energy? EWI Working Paper No 19/03.
URL http://www.ewi.uni-koeln.de/fileadmin/user_upload/Publikationen/Working_Paper/EWI_WP_19-03_How_Does_Climate_Change_Affect_Optimal_Allocation_of_VRE.pdf

Peter, J., Wagner, J., 2018. Optimal Allocation of Variable Renewable Energy Considering Contributions to Security of Supply. EWI Working Paper No 18/02.
URL https://www.ewi.uni-koeln.de/fileadmin/user_upload/Publikationen/Working_Paper/EWI_WP_18-02_Optimal_allocation_of_variable_renewable_energy_considering_contributions_to_security_of_supply.pdf

Pfennig, M., Gerhardt, N., Pape, C., Böttger, D., 2017. Mittel- und langfristige Potenziale von PtL- und H2- Importen aus internationalen EE-Vorzugsregionen. Tech.

rep., Fraunhofer-Institut für Windenergie und Energiesystemtechnik (Fraunhofer IWES).

PLANCO Consulting, Gewässerkunde (bfg), B. f., 2007. Verkehrswirtschaftlicher und ökologischer Vergleich der Verkehrsträger Straße, Bahn und Wasserstraße - Zusammenfassung der Untersuchungsergebnisse. Tech. rep., Wasser- und Schiffahrtsdirektion Ost.
URL http://www.wsd-ost.wsv.de/service/Downloads/Verkehrstraegervergleich_Kurzfassung.pdf

Platts, 2016. UDI World Electric Power Plants Data Base (WEPP).
URL https://www.spglobal.com/platts/en/products-services/electric-power/world-electric-power-plants-database

Reyers, M., Moemken, J., Pinto, J. G., 2016. Future changes of wind energy potentials over Europe in a large CMIP5 multi-model ensemble. International Journal of Climatology 36 (2), 783–796.
URL https://rmets.onlinelibrary.wiley.com/doi/abs/10.1002/joc.4382

Rhenus Logistics, 2007. LKW-Maut in Deutschland. Tech. rep., Rhenus AG & Co. KG.

Richter, J., 2011. DIMENSION - A Dispatch and Investment Model for European Electricity Markets. EWI Working Paper No 11/03.
URL http://www.ewi.uni-koeln.de/fileadmin/user_upload/Publikationen/Working_Paper/EWI_WP_11-03_DIMENSION.pdf

Romejko, K., Nakano, M., 2017. Portfolio analysis of alternative fuel vehicles considering technological advancement, energy security and policy. Journal of Cleaner Production 142, 39–49.
URL http://www.sciencedirect.com/science/article/pii/S0959652616313701

Rösler, H., Bruggink, J. J. C., Keppo, I. J., 2011. Design of a European sustainable hydrogen model - Model structure and data sources. Tech. rep., Energy research Centre of the Netherlands (ECN).

Rösler, H., Van der Zwaan, B., Keppo, I., Bruggink, J., 2014. Electricity versus hydrogen for passenger cars under stringent climate change control. Sustainable Energy Technologies and Assessments 5, 106–118.

Sanz-Pérez, E. S., Murdock, C. R., Didas, S. A., Jones, C. W., 2016. Direct Capture of CO2 from Ambient Air. Chemical Reviews 116 (19), 11840–11876.
URL https://doi.org/10.1021/acs.chemrev.6b00173

Schiebahn, S., Grube, T., Robinius, M., Tietze, V., Kumar, B., Stolten, D., 2015. Power to gas: Technological overview, systems analysis and economic assessment for a case study in Germany. International Journal of Hydrogen Energy 40, 4285–4294.

Schleussner, C.-F., Donges, J. F., Donner, R. V., Schellnhuber, H. J., 2016. Armed-conflict risks enhanced by climate-related disasters in ethnically fractionalized countries. Proceedings of the National Academy of Sciences 113 (33), 9216–9221.
URL http://www.pnas.org/content/113/33/9216.abstract

Schlott, M., Kies, A., Brown, T., Schramm, S., Greiner, M., 2018. The impact of climate change on a cost-optimal highly renewable European electricity network. Applied Energy 230, 1645–1659.
URL http://www.sciencedirect.com/science/article/pii/S0306261918313953

Schmidt, P. R., Zittel, W., Weindorf, W., Raksha, T., 2016. Renewables in Transport 2050 - Empowering a sustainable mobility future with zero emission fuels from renewable electricity. Tech. rep., Ludwig-Bölkow-Systemtechnik GmbH, Munich/Frankfurt a.M., Germany.
URL http://www.lbst.de/news/2016_docs/FVV_H1086_Renewables-in-Transport-2050-Kraftstoffstudie_II.pdf

Schuerch, M., Spencer, T., Temmerman, S., Kirwan, M. L., Wolff, C., Lincke, D., McOwen, C. J., Pickering, M. D., Reef, R., Vafeidis, A. T., Hinkel, J., Nicholls, R. J., Brown, S., 2018. Future response of global coastal wetlands to sea-level rise. Nature 561 (7722), 231.
URL https://www.nature.com/articles/s41586-018-0476-5

Sgobbi, A., Nijs, W., De Miglio, R., Chiodi, A., Gargiulo, M., Thiel, C., 2016. How far away is hydrogen? Its role in the medium and long-term decarbonisation of the European energy system. International Journal of Hydrogen Energy 41, 19–35.

Simoes, S., Nijs, W., Ruiz, P., Sgobbi, A., Radu, D., Bolat, P., Thiel, C., Peteves, S., 2013. The JRC-EU-TIMES model. JRC.
URL http://publications.jrc.ec.europa.eu/repository/bitstream/JRC85804/jrc_times_%20eu_overview_online.pdf

Smejkal, Q., Rodemerck, U., Wagner, E., Baerns, M., 2014. Economic Assessment of the Hydrogenation of CO2 to Liquid Fuels and C2 to C4 Petrochemical Feedstock. Chemie Ingenieur Technik 86, 679–86.

Songhurst, B., 2014. LNG Plant Cost Escalation. Tech. rep., The Oxford Intitute for Energy Studies, University of Oxford.

SPIEGEL, Nov. 2018. Wassermangel im Rhein: BASF muss Milliardenanlage stilllegen. Spiegel Online.
URL http://www.spiegel.de/wirtschaft/unternehmen/basf-stoppt-tdi-produktion-in-ludwigshafen-wegen-niedrigswasser-a-1240547.html

Statistics Norway, 2017. Registered vehicles. Statistics Norway.
URL https://www.ssb.no/en/bilreg

Statistics Sweden, 2017. Registered vehicles. Statistics Sweden.
URL http://www.scb.se/tk1001-EN

Telson, M. L., 1975. The Economics of Alternative Levels of Reliability for Electric Power Generation Systems. The Bell Journal of Economics 6 (2), 679–694.
URL http://www.jstor.org/stable/3003250

Thiel, C., Nijs, W., Simoes, S., Schmidt, J., van Zyl, A., Schmid, E., 2016. The impact of the EU car CO2 regulation on the energy system and the role of electro-mobility to achieve transport decarbonisation. Energy Policy 96, 153–166.

Tobin, I., Greuell, W., Jerez, S., Ludwig, F., Vautard, R., Vliet, M. T. H. v., Bréon, F.-M., 2018. Vulnerabilities and resilience of European power generation to 1.5 °C, 2 °C and 3 °C warming. Environmental Research Letters 13 (4), 044024.
URL http://stacks.iop.org/1748-9326/13/i=4/a=044024

Tobin, I., Jerez, S., Vautard, R., Thais, F., Meijgaard, E. v., Prein, A., Michel Déqué, Kotlarski, S., Maule, C. F., Nikulin, G., Noël, T., Teichmann, C., 2016. Climate change impacts on the power generation potential of a European mid-century wind farms scenario. Environmental Research Letters 11 (3), 034013.
URL http://stacks.iop.org/1748-9326/11/i=3/a=034013

Tobin, I., Vautard, R., Balog, I., Bréon, F.-M., Jerez, S., Ruti, P. M., Thais, F., Vrac, M., Yiou, P., 2015. Assessing climate change impacts on European wind energy from ENSEMBLES high-resolution climate projections. Climatic Change 128 (1-2), 99–112.
URL https://link.springer.com/article/10.1007/s10584-014-1291-0

Tremel, A., Wasserscheid, P., Baldauf, M., Hammer, T., 2015. Techno-economic analysis for the synthesis of liquid and gaseous fuels based on hydrogen production via electrolysis. International Journal of Hydrogen Energy 40, 11457–11464.

Turvey, R., Anderson, D., 1977. Electricity economics: essays and case studies. World Bank.

UBA, 2017. Nationale Trendtabellen für die deutsche Berichterstattung atmosphärischer Emissionen 1990 - 2015. Umweltbundesamt.
URL https://www.umweltbundesamt.de/themen/klima-energie/treibhausgas-emissionen

Ueckerdt, F., Pietzcker, R., Scholz, Y., Stetter, D., Giannousakis, A., Luderer, G., 2017. Decarbonizing global power supply under region-specific consideration of challenges and options of integrating variable renewables in the REMIND model. Energy Economics 64, 665–684.
URL http://www.sciencedirect.com/science/article/pii/S014098831630130X

United Nations, 2015. Paris Agreement. United Nations Framework Convention on Climate Change.
URL https://unfccc.int/sites/default/files/english_paris_agreement.pdf

U.S. Department of Energy, 2009. Energy requirements for hydrogen gas compression and liquefaction as related to vehicle storage needs. Tech. rep., U.S. Department of Energy.

van der Zwaan, B., Keppo, I., Johnsson, F., 2013. How to decarbonize the transport sector? Energy Policy 61, 562–573.
URL http://www.sciencedirect.com/science/article/pii/S0301421513004734

VCI, 2014. Chemiewirtschaft in Zahlen 2014. Tech. rep., Verband der Chemischen Industrie e. V.
URL https://www.vci.de/vci/downloads-vci/publikation/chiz-historisch/chemiewirtschaft-in-zahlen-2014.pdf

VGB and Eurelectric, 2012. Availability of Thermal Power Plants 2002 - 2011, Edition 2012.

Vliet, M. T. H. v., Vögele, S., Rübbelke, D., 2013. Water constraints on European power supply under climate change: impacts on electricity prices. Environmental Research Letters 8 (3), 035010.
URL http://stacks.iop.org/1748-9326/8/i=3/a=035010

Voorspools, K. R., D'haeseleer, W. D., 2006. An analytical formula for the capacity credit of wind power. Renewable Energy 31 (1), 45 – 54.
URL http://www.sciencedirect.com/science/article/pii/S0960148105000716

Weber, J., Wohland, J., Reyers, M., Moemken, J., Hoppe, C., Pinto, J. G., Witthaut, D., 2018. Impact of climate change on backup energy and storage needs in wind-dominated power systems in Europe. PLOS ONE 13 (8), e0201457.
URL https://journals.plos.org/plosone/article?id=10.1371/journal.pone.0201457

Welsch, M., Howells, M., Hesamzadeh, M. R., Ó Gallachóir, B., Deane, P., Strachan, N., Bazilian, M., Kammen, D. M., Jones, L., Strbac, G., Rogner, H., 2015. Supporting security and adequacy in future energy systems: The need to enhance long-term energy system models to better treat issues related to variability. International Journal of Energy Research 39 (3), 377–396.
URL http://onlinelibrary.wiley.com/doi/10.1002/er.3250/abstract

Wenz, L., Levermann, A., Auffhammer, M., 2017. North-south polarization of European electricity consumption under future warming. Proceedings of the National Academy of Sciences 114 (38), E7910–E7918.
URL http://www.pnas.org/content/114/38/E7910

Wietschel, M., Bünger, U., Weindorf, W., 2010. Vergleich von Strom und Wasserstoff als CO2-freie Endenergieträger. Tech. rep., Ludwig-Bölkow-Systemtechnik GmbH (LBST), Fraunhofer-Institut für System- und Innovationsforschung (ISI).

Wijkman, M., 1982. Managing the Global Commons. International Organization 36 (3), 511–536.
URL https://www.jstor.org/stable/2706543

WindEurope, 2017. The European offshore wind industry - Key trends and statistics 2016. Tech. rep., WindEurope.
URL https://windeurope.org/wp-content/uploads/files/about-wind/statistics/WindEurope-Annual-Offshore-Statistics-2016.pdf

Wohland, J., Reyers, M., Weber, J., Witthaut, D., 2017. More homogeneous wind conditions under strong climate change decrease the potential for inter-state balancing of electricity in Europe. Earth System Dynamics 8 (4), 1047–1060.
URL https://www.earth-syst-dynam.net/8/1047/2017/esd-8-1047-2017.html

World Bank, 2018. State and Trends of Carbon Pricing 2018. World Bank, Washington, DC.
URL https://openknowledge.worldbank.org/handle/10986/29687

Yang, C., Ogden, J., 2007. Determining the lowest-cost hydrogen delivery mode. International Journal of Hydrogen Energy 32, 268–286.

Zachary, S., Dent, C. J., 2012. Probability theory of capacity value of additional generation. Proceedings of the Institution of Mechanical Engineers, Part O: Journal of Risk and Reliability 226 (1), 33–43.
URL https://doi.org/10.1177/1748006X11418288

Özdemir, E. D., 2011. The Future Role of Alternative Powertrains and Fuels in the German Transport Sector - A model based scenario analysis with respect to technical, economic and environmental aspects with a focus on road transport. PhD Thesis, Institut für Energiewirtschaft und Rationelle Energieanwendung (IER), Universität Stuttgart.

ZSW, 2017. Datenservice - Elektromobilität. ZSW.
URL https://www.zsw-bw.de/mediathek/datenservice.html#c6700